TECHNICAL BULLETIN

VOL. 6

ECONOMIC COMMISSION FOR ASIA AND THE FAR EAST COMMITTEE FOR CO-ORDINATION OF JOINT PROSPECTING FOR MINERAL RESOURCES IN ASIAN OFFSHORE AREAS (CCOP)

July, 1 9 7 2

ECONOMIC COMMISSION FOR ASIA
AND THE FAR EAST

COMMITTEE FOR CO-ORDINATION OF JOINT PROSPECTING FOR MINERAL RESOURCES IN ASIAN OFFSHORE AREAS (CCOP)

TECHNICAL BULLETIN VOL. 6

CCOP Technical Bulletin Volume 5 (Special Volume—Detrital Heavy Minerals)は特別号としてCCOPの技術事務局により印刷されたので，部数の関係で日本国内の配付は制限されました。

CCOP Technical Bulletin Volume 5 (Special Volume—Detrital Heavy Minerals) was printed in 1971 by the Technical Secretariat of CCOP as an irregular volume.

As for the distribution of Volume 5, please contact with:
Technical Secretariat of CCOP, United Nations ECAFE,
Sala Santitham, Bangkok-2, Thailand.

ECONOMIC COMMISSION FOR ASIA
AND THE FAR EAST

COMMITTEE FOR CO-ORDINATION OF JOINT PROSPECTING FOR MINERAL RESOURCES IN ASIAN OFFSHORE AREAS (CCOP)

TECHNICAL BULLETIN

VOL. 6

July, 1 9 7 2

All communications relating to this and other publications of CCOP should be addressed to: Technical Secretariat of CCOP, United Nations ECAFE, Sala Santitham, Bangkok-2, Thailand.

For citation purpose, this publication should be referred to as: United Nations ECAFE, *CCOP Tech. Bull.*, vol. 6.

Printed by the Geological Survey of Japan as a contribution to the work of the Committee
135, Hisamoto, Takatsu-ku, Kawasaki-shi, Japan
Cable: GEOLSURV TOKYO

Komiyama Printing Co., Ltd.
78 Tenjin-cho, Shinjuku-ku, Tokyo
Japan, 1972

PREFACE

The Committee for Co-ordination of Joint Prospecting for Mineral Resources in Asian Offshore Areas (referred to briefly as the Co-ordinating Committee for Offshore Prospecting, and abbreviated to CCOP) is an intergovernmental body established under the sponsorship of the United Nations Economic Commission for Asia and the Far East (ECAFE). The steps leading to its establishment are outlined in the reports of its first session (paragraphs 1–5) and second session (paragraphs 1, 2); its terms of reference are contained in appendix II of the report of its first session.

At the eighteenth session of the ECAFE Committee on Industry and Natural Resources, held at Bangkok in February 1966, Japan, the Republic of Korea, the Philippines and Taiwan (China) affirmed their readiness to join in the establishment of the Co-ordinating Committee. At the invitation of the Government of the Philippines, the first session of CCOP, attended by representatives of those countries and professional staff of the ECAFE secretariat, was held at the University of the Philippines, Quezon City, from 27 May to 2 June 1966.

Since that time, seven more sessions of CCOP have been held (second session at Tokyo, 29 October to 7 November 1966; third at Seoul, 24 June to 4 July 1967; fourth at Taipei, 6–16 November 1967; fifth at Tokyo, 10–19 June 1968; sixth at Bangkok, 13–27 May 1969; seventh at Saigon, 12–23 May 1970; and eighth at Manila, 6–16 July 1971) together with meetings of its Technical Advisory Group at each of those sessions; the ninth session of CCOP is planned to be held in Indonesia during September-October 1972. At its fourth session, the Governments of the Republic of Viet-Nam and Thailand were welcomed as full members and Malaysia was represented by an observer. At the fifth session, both Indonesia and Malaysia were represented by observers. At the sixth session, the Khmer Republic and Malaysia were welcomed as full members while Indonesia was represented by a group of observers. At the seventh session Indonesia joined as a full member, thus completing the membership in CCOP of nine ECAFE member countries which have substantial areas of offshore territory in eastern Asia.

During the course of these meetings the Committee decided that technical studies relating to marine geology and offshore prospecting for mineral resources, particularly in the offshore areas of the member countries of CCOP, together with preliminary accounts and detailed reports of the results of offshore surveys conducted through the medium of CCOP, should be published in a series of Technical Bulletins, separately from the reports of the Committee's sessions. The Committee was glad to accept the offer of the Government of Japan to print one volume of the Technical Bulletin annually and the first four volumes, together with volume 6, have been printed by the Geological Survey of Japan as a contribution to the activities of the Committee.

A special fifth volume, containing reports on investigations of coastal and inland placers of detrital heavy minerals in the CCOP member countries, together with articles relating to the occurrence of detrital heavy minerals in offshore areas, was prepared and printed by the Technical Secretariat of CCOP in accordance with the request of the Committee at its sixth (report, para. 63) and seventh (report, para. 102) sessions; funds

accruing from the sale of CCOP publications were used for the printing of volume 5.

The technical Bulletins and the printed reports of the sessions of CCOP, including technical documentation, are distributed to the appropriate organizations and authorities concerned in the member countries of CCOP, and copies of the Technical Bulletins are sent without charge to more than three hundred selected reference libraries in other countries of the world. Enquiries concerning the publications of CCOP may be directed to the Technical Secretariat of CCOP, United Nations ECAFE, Sala Santitham, Bangkok-2, Thailand. The contents of volumes 1, 2, 3, 4 and 5 of the Technical Bulletin series are listed on page six to xi, at the end of this volume.

FOREWORD

The progress of the geoscience of the seas in recent years is indeed remarkable, and to-day all fields of geoscience ranging from metallogeny, volcanology, to earthquake studies are pursued with at least some reference to island arcs, deep trenches, ocean-floor spreading and other phases of problems which must be investigated with submarine geoscientific methods. Various submarine mineral resources are, of course, being sought after with great zeal and many important developments have been made in this respect.

Therefore, international co-operation in this field is most worthwhile and it is with great admiration that I have been watching the activities of the Committee for Co-ordination of Joint Prospecting for Mineral Resources in Asian Offshore Areas (CCOP). The contribution of the activities of CCOP to the development of the region is such that mineral resources of the continental shelf areas of the region cannot be considered without reference to the work undertaken by CCOP. Many new developments have taken place during the past year including the success in obtaining financial support from the United Nations Development Programme. It is, however, the technical, scientific achievements and their economic implications which were so impressive that the establishment of a certain "CCOP on land" is being discussed. The Geological Survey of Japan is considering the establishment of a new section concerned with problems of marine geoscience and I am expecting that international co-operation in this field will become more active.

Thus, it is with great honour and pleasure to present the sixth volume of the Technical Bulletin of CCOP, and I would like to express my respect and gratitude to the authors, the staff of the ECAFE Secretariat, and the Editor-in-Chief, Dr. Sano for their efforts in bringing out this volume.

Isamu Kobayashi
Director,
Geological Survey of Japan

NOTE BY THE EDITOR

It is a great pleasure for the editor to present Volume 6 of the CCOP Technical Bulletin to the Committee for Co-ordination of Joint Prospecting for Mineral Resources in Asian Offshore Areas (CCOP). Most of the articles included in this volume are the reports of the co-ordinated survey projects of the Committee or the results of research made in relation to those projects. In addition to the reports of the survey projects carried out under the Work Programme of the Committee, the editor would be glad to receive more articles as contributions to the future volumes from geoscientists and engineers of the Asian countries.

The editor feels that discussions on the technical contents of the articles appearing in the Technical Bulletins are highly desirable for the advancement and promotion of marine geologic and geophysical studies in the region. If the readers wish to comment or raise questions regarding them, the editor will willingly act as intermediary and forward them to the contributors, who alone are responsible for the statements made and opinions expressed in their respective articles.

At its eighth session held at Manila in July 1971, the Committee decided that, in connection with its long range programme, the activities of the Committee should be extended to the continental slopes, rises, seamounts, and shoal areas in the adjoining oceanic basins, beyond the continental shelves of the member countries. Articles concerning research and exploration in the oceanic area of the region will therefore be incorporated in future issues and articles concerning the geologic framework of the continental margin will be particularly welcomed.

As the objective of the CCOP Technical Bulletin is to provide a medium for publication of scientific data relating to the marine shelves and adjoining oceanic areas of eastern Asia, which may have bearing on their mineral potentials, the editor feels that contributions should be considered for publication from all sources, irrespective of whether or not they may be connected with the United Nations or its subsidary bodies. In view of past experiences, the editor wishes to propose at the next session of the Committee, to be held in Indonesia during September-October 1972, that the dead-line date for submission of manuscripts for the next regular volume be set at the end of November 1972.

The editor expresses his gratitude to Mr. Leo W. Stach, Chief of the Mineral Resources Development Section, United Nations Economic Commission for Asia and the Far East, and acting as Co-ordinator of CCOP, for his kind co-operation and valuable suggestions concerning the editing of this volume. His sincere thanks are extended to the Director of the Geological Survey of Japan for the printing of this volume as one of the regular Technical Bulletins, as well as to the members concerned of the Geological Survey for their co-operation in completing this volume.

January 1972

Shun-ichi Sano
Editor-in-Chief

TECHNICAL BULLETIN, VOLUME 6

CONTENTS

Blank page

Page blanche

I. MARINE GEOPHYSICAL SURVEYS IN THE NORTHERN PART OF THE YELLOW SEA

(Project CCOP–I/ROK. 9b)

By

J. H. Koo

Geological Survey of Korea
Seoul, Republic of Korea

(with table I–1; and figures I–1 to I–9)

ABSTRACT

Shipborne sonic and magnetic surveys were carried out by Korean geophysicists during October and November 1970 aboard the vessel "Taeyang 118" in the northern part of the Yellow Sea adjoining the Republic of Korea. On the basis of the submarine geologic structure revealed by this survey, the area surveyed can be divided into two parts, an inner zone and an outer zone, separated along the meridian of longitude 125°30′E. In the inner zone, east of longitude 126°00′E, the geology appears to be similar to that of the adjoining land area, but the geology of the outer zone, west of longitude 125°30′E, is notably different. In the near-shore area, east of longitude 126°00′E, the variation of magnetic intensity is very strong and irregular but, west of longitude 125°30′E, it becomes smoother, indicating either deep magnetic basement or weakly magnetic basement. The sonic profiles revealed the submarine topography and the thickness of unconsolidated as well as consolidated sediments. The average thickness of unconsolidated sediments, probably all of Recent age, about 20 m throughout the area surveyed; in the near-shore area they rest directly on the basement. Consolidated sediments, probably of Neogene age, underlie the Recent unconsolidated sediments west of longitude 126°00′E and a shallow sedimentary basin, with a maximum thickness of about 100 m of sediments, is present farther west to about longitude 125°30′E. In the inner zone, the reflecting layer below the sediments seems to be the basement, which extends to maximum depths of about 150 m, but in the outer zone the basement surface appears to be much deeper, and too deep to be reached by the sonic energy source used, which gave a maximum penetration of about 300 m. Some reflecting layers below the recent sediments in the outer zone appear to be acoustic layers within the Neogene sediments and one of them may represent the boundary between Paleogene and Neogene sediments. A big magnetic anomaly of 1,800 gammas was found south of Ul-do; this may be caused by a dyke containing a large amount of magnetite. The results of this survey suggest that future exploration for placer deposits of heavy minerals in this area should be limited to the near-shore area east of longitude 126°00′E.

INTRODUCTION

Geophysical exploration of the continental shelf surrounding the Korean peninsula has been carried out with assistance provided through the medium of CCOP. Especially in 1969, the U.S. Naval Oceanographic Office, through its Project MAGNET, conducted an aeromagnetic survey covering most of the Korean continental shelf as a contribution to the CCOP work programme (Project CCOP-1/ROK. 2), the final report of which was published in CCOP Technical Bulletin, volume 4. As a result, an outline of the submarine geologic structure of the continental shelf was obtained.

The present report covers the results of geophysical exploration conducted in 1970 by sonic and magnetic profiling over the area included within latitude 36°N to 37°N and longitude 124°30'E to the coast line. Airgun equipment purchased recently by the Geological Survey of Korea was used for the sonic profiling. Shipborne magnetic and sonic profiling were undertaken during the periods 1 to 11 October and 6 to 25 November 1970 using the vessel "Taeyang 118". The total length of traverses was about 1,300 line-km, conducted over an area of about 18,000 sq km.

PROSPECTING METHODS AND DATA COMPILATION

Continuous seismic and magnetic profiling were carried out simultaneously and automatically recorded along E–W traverse lines spaced about 18 km apart.

The seismic reflection records were obtained with an OST-119T recorder. An airgun with pressure of 2,000 psi and triggered every four seconds was towed 5 metres behind the ship, submerged at a depth of 0.5 to 1 metre below the water surface. The hydrophone receiver system consisted of a single channel streamer cable 7.6 metres long, containing 5 pressure-sensitive hydrophones, and the detector head was towed at 55 m behind the ship. The distance between the airgun and streamer cable was therefore about 50 m. The echoes received from the sea-bottom and the underlying reflecting horizons were fed into band pass filters with a frequency range of 80–640HZ and then amplified. The recorder was adjusted to receive signals from depths down to about 360 m; occasionally the depth range was changed to detect reflections down to about 1,800 m, but none could be detected below 360 m. A Varian proton magnetometer was used to record the total magnetic intensity and the speed of the recording paper was set at one inch per minute. Navigation was done by means of radar, Loran and sextant. Positioning near the shore and islands was made every ten minutes by sextant but, farther offshore and during darkness, positioning was made every 30 minutes by Loran or radar. The accuracy of positioning is considered to be within ± 2 km.

For compilation of the data, a traverse map (Fig. I-1) was compiled and the measurements obtained were plotted along the traverse lines. Analog records of magnetic intensity were digitized at 20-gamma intervals and magnetic profiles were made along every traverse line; from these, an isomagnetic intensity map was drawn over the whole of the area investigated. After eliminating various noises contained in the sonic signals,

the depths to various reflectors were determined. From these data, a bathymetric map (Fig. I-2), magnetic profiles (Fig. I-3), geologic profiles from seismic reflection data (Fig. I-4), isomagnetic intensity map (Fig. I-5), residual magnetic profiles of the inner zone (Fig. I-6) and an isopach map of the sedimentary section in the inner zone (Fig. I-7) were prepared.

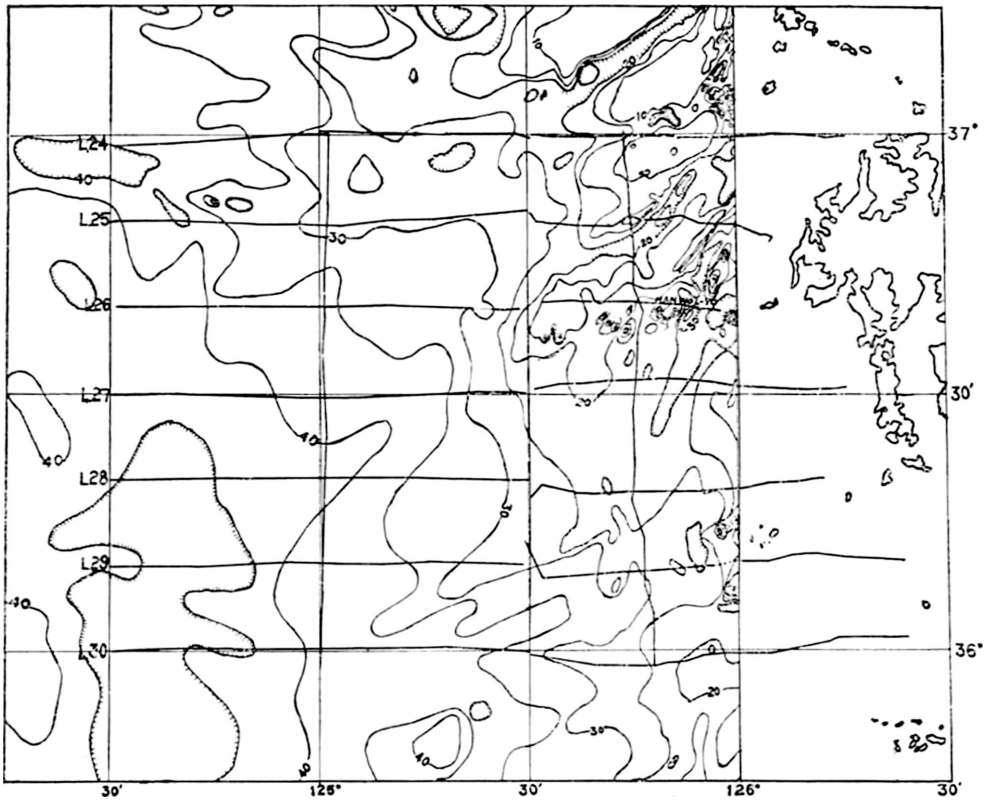

Figure I-1. Location map of geophysical traverses (L-24 to L-30) in the northern part of the Yellow Sea; bathymetric contours in fathoms; contour interval, 5 fathoms.

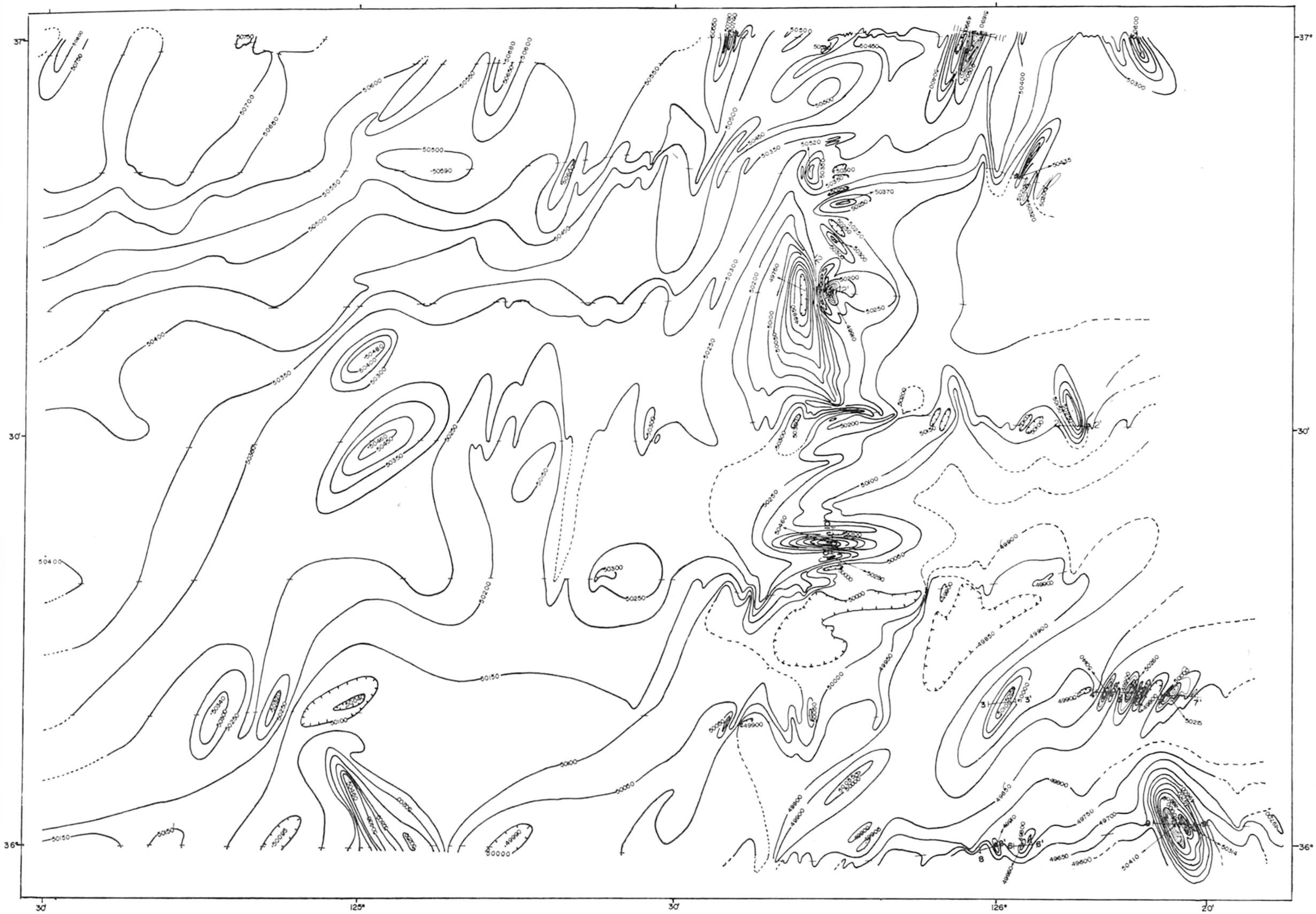

Figure I-5. Iso-magnetic intensity map of the northern part of the Yellow Sea, based on magnetic data along traverse lines L-24 to L-30.

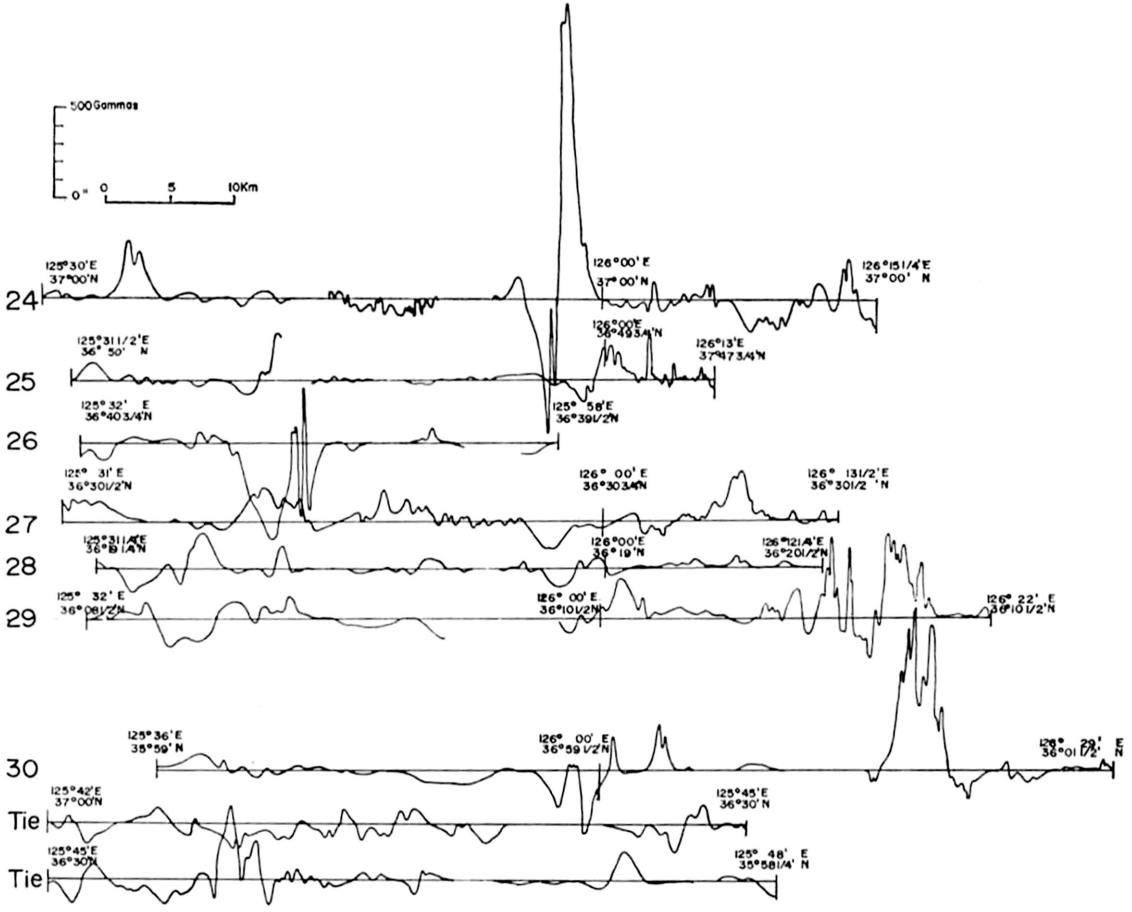

Figure 1-6. Residual magnetic profiles in the "inner zone" of the northern part of the Yellow Sea, along traverse lines L-24 to L-30.

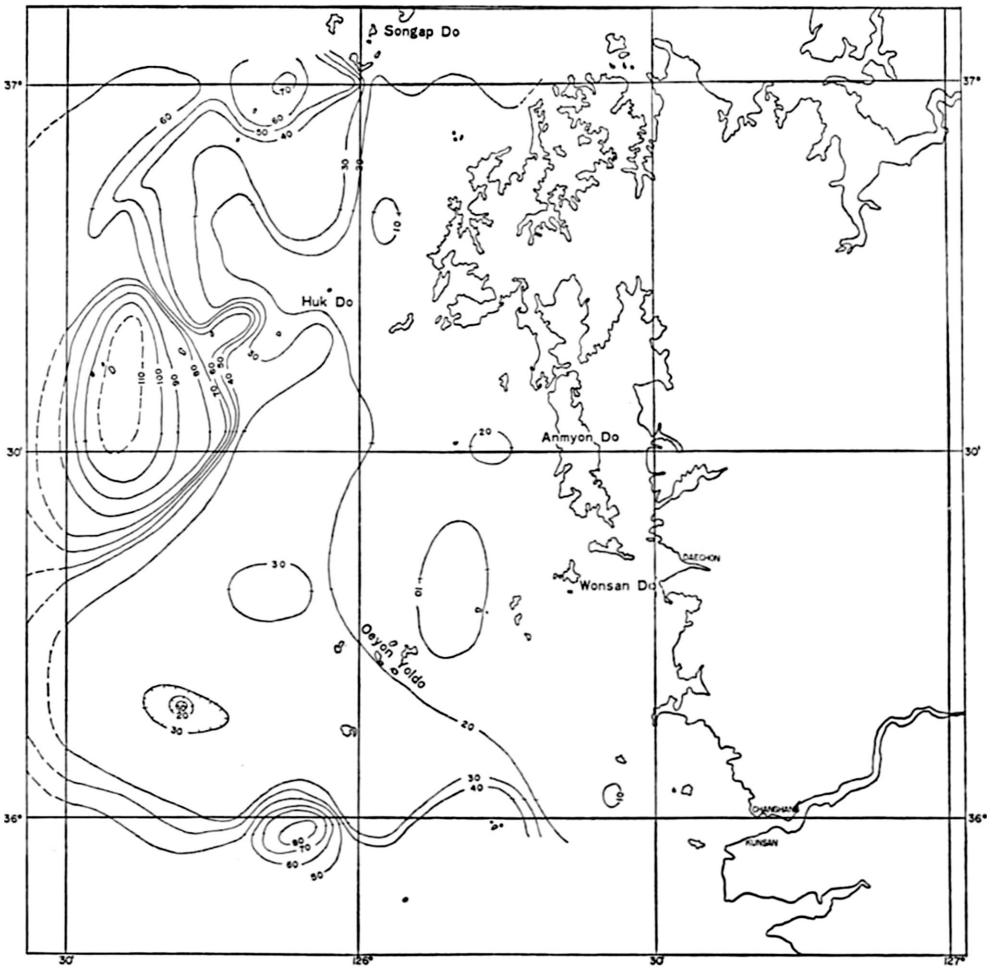

Figure I-7. Isopach map of the sedimentary section between the sea floor and the basement in the "inner zone" of the northern part of the Yellow Sea; contour interval, 10 metres.

OUTLINE OF GEOLOGY

The coastal area between latitudes 36 and 37°N (Fig. I-8) consists largely of Precambrian granite-gneiss and metasediments of the Yeonchun System, small basin-type non-marine sedimentary rocks of the Taedong System and Kyongsang System, and Jurassic intrusive granite in the northern part of the area. The granite is distributed from northeast to southwest so that it could be expected to have a seaward extension. The sedimentary rocks of the Kyongsang System are partly exposed on land, but neither these nor those of the Taedong System are expected to extend into the adjoining offshore area. The absence of the Taedong Formation in the off-lying islands strongly supports

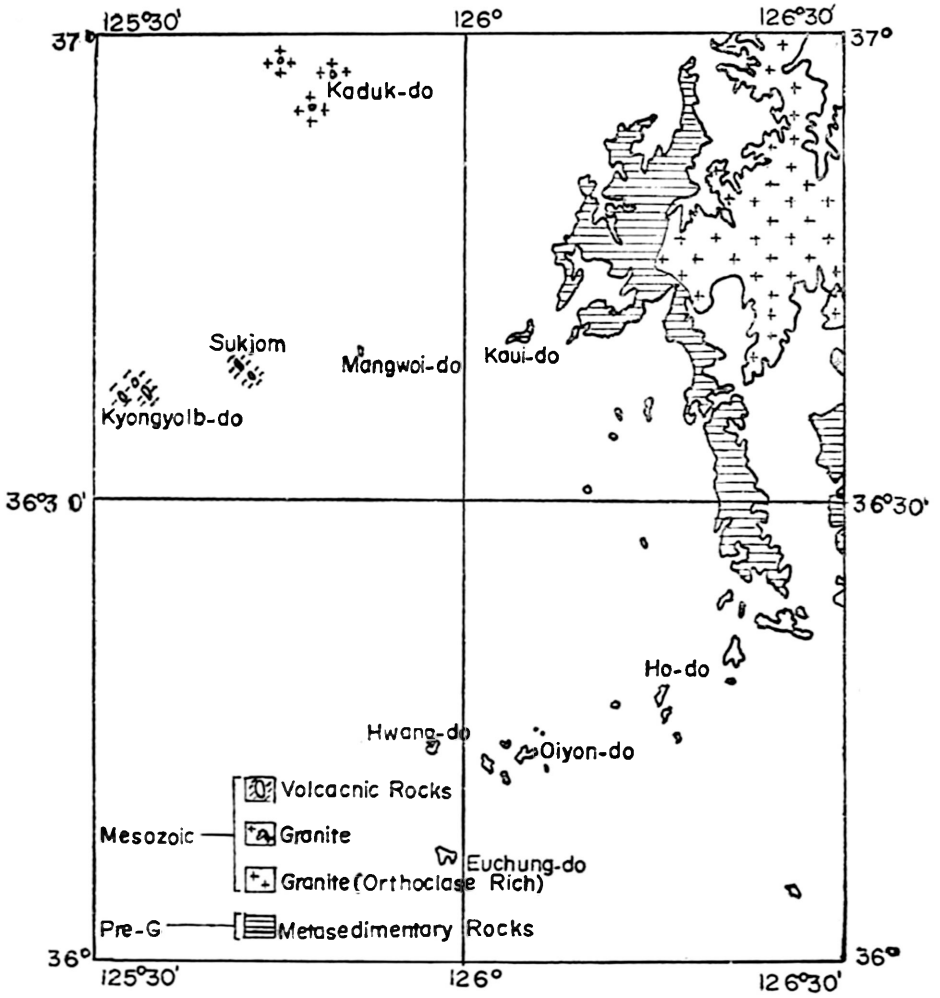

Figure I-8. Geologic sketch map of islands and adjoining coastal area in the northern part of the Yellow Sea.

this; the Taedong sedimentary rocks are more widely disturbed than those of the Kyongsang System and, in the whole of the western coastal area, the Taedong Formation is only found in the region north of Kunsan.

Anmyon-do (island, see Fig. I-7) is wholly composed of rocks of the Yeonchun System and the islands located around the Taean district can be classified into three types according to their geologic features, as follows:

(1) The islands adjacent to the land, namely, Mokgae-do, Kua-do, Ulmi-do, Samseom, Tokki-seom, Nachi-do, Cheongjok-do, and others, are entirely composed of quartzite belonging to the Yeonchun System, but others such as Kaui-do and Heuk-do consist of sericite-schist and banded granite-gneiss as well as quartzite. The geology of this area is, therefore, similar to that of the adjoining land.

(2) Kadeuk-do, Taeryung-do, Mokduk-do and others located in the northwestern part of the area surveyed consist of granite, which is possibly the same as the Jurassic granite on the nearby land area.

(3) The group of islands including Tongkyukyulbi-do, Seokyukyulbi-do, Sukseom and Ube-do are quite different from the others and are composed of volcanic rocks such as dacite, dacite breccia and dacite porphyry, which seem to be generally correlated on a lithologic basis with the Kyongsang System.

With regard to rock magnetism, the Precambrian granite-gneiss and Cretaceous granite are both non-magnetic or weakly magnetic and their magnetic intensities generally range from 1 to 10 gammas; however, in a few places, the intensity is higher, ranging up to 200 gammas. The Taedong sedimentary rocks are non-magnetic, but the volcanic rocks are strongly magnetic.

GEOPHYSICAL RESULTS

Sonic survey

From the seismic records, definite reflecting layers were identified after elimination of multiple reflections, water bubble effect, direct waves, and other noises. However, in many of the record sections it was difficult to identify reflection signals, probably due to the very slight difference of acoustic impedance between adjacent layers. No reflecting layers could be found on the records below 300 m depth from the water surface because the source of energy was not great enough to detect layers below that depth.

Three main reflecting horizons could be distinguished: the uppermost (SB) indicates the sea floor; the B horizon appears occasionally but in some record sections it is believed to mark the boundary between the deeper consolidated sediments and the unconsolidated sediments of Recent age overlying them; the C horizon appears faintly and discontinuously below the B horizon and it seems to represent the top of the igneous basement in the inner zone. In the outer zone, other weak reflectors, horizons D and E, appear below horizon C and it is therefore likely that, in the outer zone, it is caused by the difference of acoustic impedance in Neogene sediments rather than the surface of the basement.

As shown in Fig. I-7, the thickness of sediments between the sea bottom and basement in the inner zone could be determined, but not in the outer zone because the basement surface was too deep to be reached by the energy source. For calculating the thickness of the sediments, an acoustic velocity of 1,500 m per second was used for all media in this area; consequently, the water depth would be quite accurate but the thickness of sediments would be greater than shown because the actual velocity of the seismic waves in the sediments would be more than 1,500 m/sec. The vertical exaggeration of the seismic profiles in Fig. I-4 is about 1:100 and the slopes shown in the profiles, therefore, appear very much steeper than is actually the case.

Magnetic survey

Although the traverses were not always perpendicular to the strike of magnetic bodies, the compilation of the magnetic profiles was made by subtracting the regional

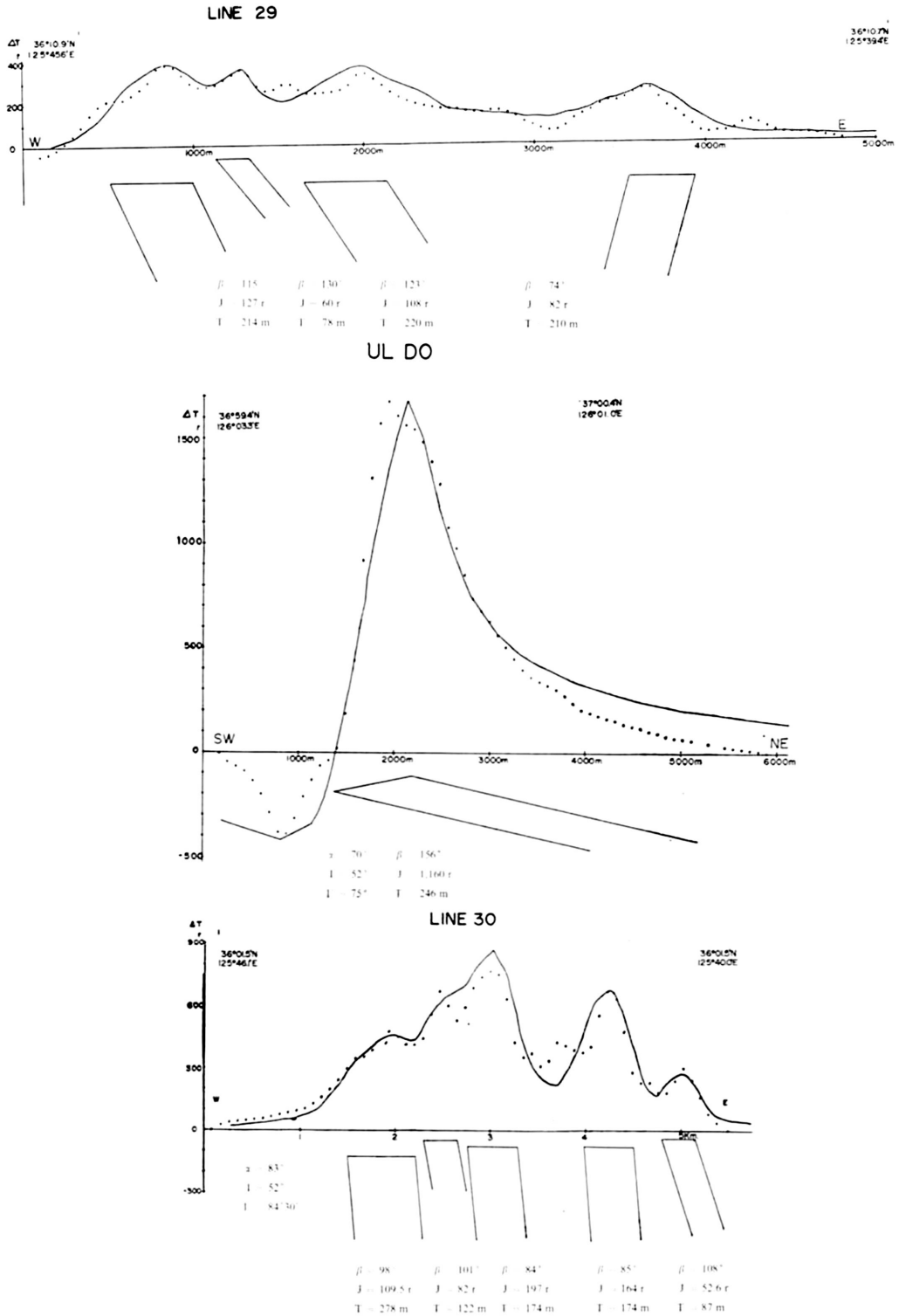

Figure I-9 Two-dimensional interpretation of strong magnetic anomalies in the vicinity of Ul-do, northern part of the Yellow Sea.

magnetic intensities from the measured values. For the interpretation of the magnetic data, the two-dimensional method (Bosum, 1965) was applied. According to the appropriate two-dimensional models, theoretical magnetic values were computed. The computed values were compared with the measured values and the difference between them was adjusted to the minimum by changing the models. The results are shown in Fig. I-9 and Table I-1. All the two-dimensional magnetic bodies were interpreted as intrusive dykes, as shown in Fig. I-4.

Table I-1. Results of two-dimensional interpretation of magnetic anomalies in the northern part of the Yellow Sea, based on the model of an infinite dyke. Locations of the anomalies are shown in Fig. I-5.

No. of anomaly	Depth (m) to top of dyke	Magnetic value (gammas)	Dip of dyke
1	36	51	61°NW
2	652	85	49°E
3	362	48	61°E
4	54	57	76°E
5	1) 114	31	79.3°W
	2) 53	50	79.3°W
	3) 62	110	55°E
	4) 26	17	87°E
6	1) 71	59	87.3°W
	2) 163	65	52°E
7	1) 215	127	65°E (line 29)
	2) 78	61	60°E
	3) 220	107	57°E
	4) 210	82	74°W
8	74	38	78°E
9	1) 278	110	85°E (line 30)
	2) 122	82	79°E
	3) 174	197	84°E
	4) 174	164	85°E
	5) 87	53	72°E
10	210	164	50°N
11	246	1,160	12°NE (Ul-do)
12	1) 148	157	34°W
	2) 39	248	82.5°E

GEOLOGIC INTERPRETATION

Based on the thickness of the sediments and the depth to the surface of basement, the area surveyed can be divided into an inner zone, extending westward from the coast line to 125°30′E, and an outer zone extending between 125°30′E and 124°30′E.

Inner zone

The inner zone, adjoining the land area, has a smooth bottom topography and the water depths range from 20 to 60 m (see Fig. I-2). Between Kaui-do and Huk-do, a

narrow submarine channel 60 m deep is developed, which trends NNE–SSW. The thickness of Recent sediments is usually about 10 to 20 m but strong under-water currents prevent deposition of sediments in the bottom of the channel. Magnetic intensities in this area vary considerably and the basement occurs at shallow depths.

The inner zone can be broadly divided into two parts at 126°00′E; to the east of this boundary, large variation of the magnetic intensities and shallow depths to basement, 26 to 52 m according to two-dimensional interpretation, are characteristic features (see Table I-1 and Fig. I-4). Considering the geology of the land and islands, the magnetic anomalies are attributed to igneous intrusives as the granite and meta-sediments are mostly non-magnetic. No consolidated sediments could be identified in this area and the basement, which has irregular topographic relief, directly underlies the Recent unconsolidated sediments. In these respects, the geology is similar to that of the adjoining land and this area would, therefore, be a favorable target for future exploration of placer deposits.

To the west of 126°00′E and extending to 125°30′E a minor sedimentary basin is present which contains up to 110 m thickness of sediments; in the southern part of this area there is also a smaller basin with sediments up to 80 m thick.

Outer zone

In the outer zone, between 125°30′E and 124°30′E, the topography of the sea floor is very smooth and the water depth increases gradually towards the west, from about 50 to 80 m. The magnetic intensity shows little variation, indicating that either deep magnetic basement or non-magnetic basement is present. If the basement is non-magnetic, its depth cannot be calculated. In the sonic records, some reflecting horizons which do not appear in the inner zone are found below the C horizon, but it is difficult to interpret their geologic significance from the records alone. However, taking into account the results obtained by K. O. Emery *et alia* (1969) from project CCOP-1/IZ. 3 and by Bosum *et alia* (1971) from project CCOP-1/ROK. 2, it would appear that the C horizon in the outer zone is an acoustic reflecting horizon within the Neogene sediments, as would also be the case with horizons D and E (see Fig. I-4). Because of the small amount of energy available for the airgun (2,000 psi in 10 cubic inches), it was not possible to detect the deeper basement which, according to Emery's results (1969, Fig. 12, profile 1) would be at a depth of about 400 m, or more, between longitudes 124°30′E and 125°00′E.

CONCLUSIONS

(1) Throughout the area the topography of the sea floor is generally smooth and the water depth increases gradually westwards from about 20 to 80 m, except in the area between Kaui-do and Huk-do where a channel trending NNE–SSW extends to depths of more than 60 m.

(2) The thickness of Recent sediments is about 20 m except at the bottom of the submarine channel between Kaui-do and Huk-do where little or no Recent sediments are present due to scouring by tidal currents.

(3) Based on the results of magnetic and sonic survey, the area surveyed can be divided into an inner zone and an outer zone, each with its own characteristic geologic features, the boundary between them being at 125°30′E longitude.

(4) The inner zone can also be divided into two areas with the boundary at 126°00′E. East of this boundary, the magnetic intensity varies considerably and the basement is present directly beneath the Recent sediments, similar to the situation on the adjoining land. A small shallow sedimentary basin, containing a maximum thickness of about 100 m of sediments, probably of Tertiary age, was found in the western part of the inner zone.

(5) In the outer zone, west of longitude 125°30′E, the magnetic intensity shows little variation, probably due to the presence of either non-magnetic basement or deeply seated basement. On the basis of evidence from other sources, the C horizon corresponds to the basement surface in the inner zone but, in the outer zone, it appears to be an acoustic reflector within the Neogene sediments, similar to the D and E horizons below it.

(6) A strong magnetic anomaly, the amplitude of which is more than 1,800 gammas, was detected southwest of Ul-do. It seems to be caused by a dyke containing a considerable amount of magnetite.

(7) The area east of 126°00′E would appear to be the most favourable target area to conduct exploration for placer deposits.

REFERENCES

Bosum W., E. G. Kind, and J. H. Koo, 1971, Aeromagnetic survey of offshore areas adjoining the Korean peninsula: United Nations ECAFE, *CCOP Tech. Bull.*, vol. 4, p. 1–21, figs. 1–11, table 1, 2.

———1965, Diagrams for the computation of magnetic field components, for their transformation into one another and for their upward continuation (two-dimensional case): *Z. Geophys., Wurzburg*, vol. 32 (1966), no. 1, p. 1–25.

Emery K. O., *et alia*, 1969, Geological structure and some water characteristics of the East China Sea and the Yellow Sea: United Nations ECAFE, *CCOP Tech. Bull.*, vol. 2, p. 3–43, figs. 1–17.

Geological Survey of Korea, Outline of the geology of Korea.

Volume 6 United Nations ECAFE, CCOP TECHNICAL BULLETIN July 1972

II. A FORAMINIFERAL STUDY OF THE BOTTOM SEDIMENTS OFF THE SOUTHEASTERN COAST OF KOREA

(Project CCOP-1/ROK. 4)

By

Bong Kyun Kim and Jong Hwan Han
Department of Geology, Seoul National University,
Seoul, Republic of Korea

(with tables II-1 to II-3; figures II-1 to II-6; and plates II-1 to II-4)

ABSTRACT

The areas off the southern and eastern coasts of Korea, situated within latitudes 37°30′N and 33°22′N and longitudes 127°00′E and 130°30′E, have been investigated. A total of 120 bottom samples were taken from 120 sites in the area and 21 of these were studied; from them, 23 species belonging to 9 genera of planktonic foraminifers and 196 species belonging to 80 genera of benthonic forms were identified. The foraminiferal assemblages on the continental shelf and the slope show remarkable differences according to depth. Furthermore, cold water species influenced by the Liman current predominate in the eastern sea (Japan Sea) and warm water species influenced by the Kuroshio current in the southern sea (Korea Strait), while a mixed assemblage is present in the vicinity of Yonil Bay. In the area studied, the bottom sediments become coarser away from the coast but, in the vicinity of Tsushima Island, they become finer again.

INTRODUCTION

The samples for this study were taken during September 1968 to November 1969 by members of the research staff of the Fisheries Research and Development Agency, Pusan, Republic of Korea. The writers received 120 samples from the Agency and the foraminiferal assemblages of 21 of them were determined.

The area investigated covered both the neritic and bathyal zones off the eastern coast and the neritic zone off the southern coast. In general, the character of the foraminiferal assemblages in the recent marine sediments off the Korean coast reflects the influence and original paths of the currents in the sea. It is useful, therefore, to study the characteristics of the foraminiferal assemblages in the sediments deposited on the sea floor in this area.

A few reports on the quantitative distribution and taxonomic description of foraminifers of the East Sea (Japan Sea) and the southern coast of Korea have been pub-

lished but precise and comprehensive knowledge of the distribution of foraminifers, particularly in the bathyal zone, has not been adequate. The principal purposes of the present study were to determine the distribution of foraminiferal assemblages in the neritic and bathyal zones off the southeastern coast of Korea and their relation to the oceanographic conditions in this area.

ACKNOWLEDGMENTS

The writers have profited from discussions with Professor Chang Hi Cheong of the Seoul National University. The authors wish to thank Mr. Chong Soo Kim, Chief of the Marine Geology Division, and Mr. Eui Kyu Yoo of the Paleontology section, Geological Survey of Korea, for their helpful and significant suggestions. Thanks are due to Mr. Chong Soo Huh, Chief of the Oceanographic Section of the Fisheries Research and Development Agency, Pusan, Republic of Korea, for his kindness in providing the dredged samples.

METHODS OF STUDY

The sampling tool used was an S. K.-type dredge, suitable for use where the bottom

Table II-1. Locations of sample sites, depths of samples and character of bottom sediments, off the southeastern coast of Korea.

Station	Location	Depth (metres)	Bottom sediments
Eastern coast			
C12-1	About 10 km SE of Chukpyon	About 30 m	Mud
C11-3	About 30 km SE of Chukpyon	About 150 m	Mud
C10-1	About 5 km E of Uljin	About 80 m	Mud
C7-3	About 25 km NE of Chuksan	About 150 m	M. sand
C5-6	About 60 km E of Chuksan	About 1,500 m	Mud
C3-1	About 30 km SE of Chuksan	About 90 m	Mud
C1-1	About 10 km of Janggigap	About 100 m	Mud
209-4	35° 47.3′N; 129° 32.8′E	62 m	Mud
209-6	35° 41.3′N; 129° 49.0′E	About 220 m	S. mud
209-7	35° 36.8′N; 130° 00.3′E	250 m	Sand
209-8	35° 30.8′N; 130° 16.9′E	About 200 m	Sand
Korea strait and southern coast			
A1-1	About 10 km SE of Ulgi	106 m	Mud
A1-4	About 40 km SE of Ulgi	149 m	S. mud
A3-1	About 10 km SE of Zachon	73 m	Mud
A3-5	About 50 km SE of Zachon	150 m	S. mud
02	34° 57.6′N; 129° 11.2′E	96 m	S. mud
07	34° 29.6′N; 128° 41.2′E	69 m	S. mud
09	34° 15.3′N; 128° 58.0′E	110 m	M. sand
16	34° 31.0′N; 128° 12.2′E	48 m	Mud
23	33° 37.3′N; 128° 09.2′E	72 m	S. mud
31	34° 06.7′N; 127° 26.8′E	41 m	S. mud

sediments consist of sand or coarse sand. The deepest sampling site, about 1,500 m, was at station C5–6 off Chuksan (Fig. II-1).

The bottom samples did not undergo any special treatment but were just dried in their natural condition. Portions of 21 of the samples, weighing 30 grams, were washed over a 200-mesh sieve and then dried and weighed again. The foraminiferal tests were separated from sediment by flotation using carbon tetrachloride and other heavy tests

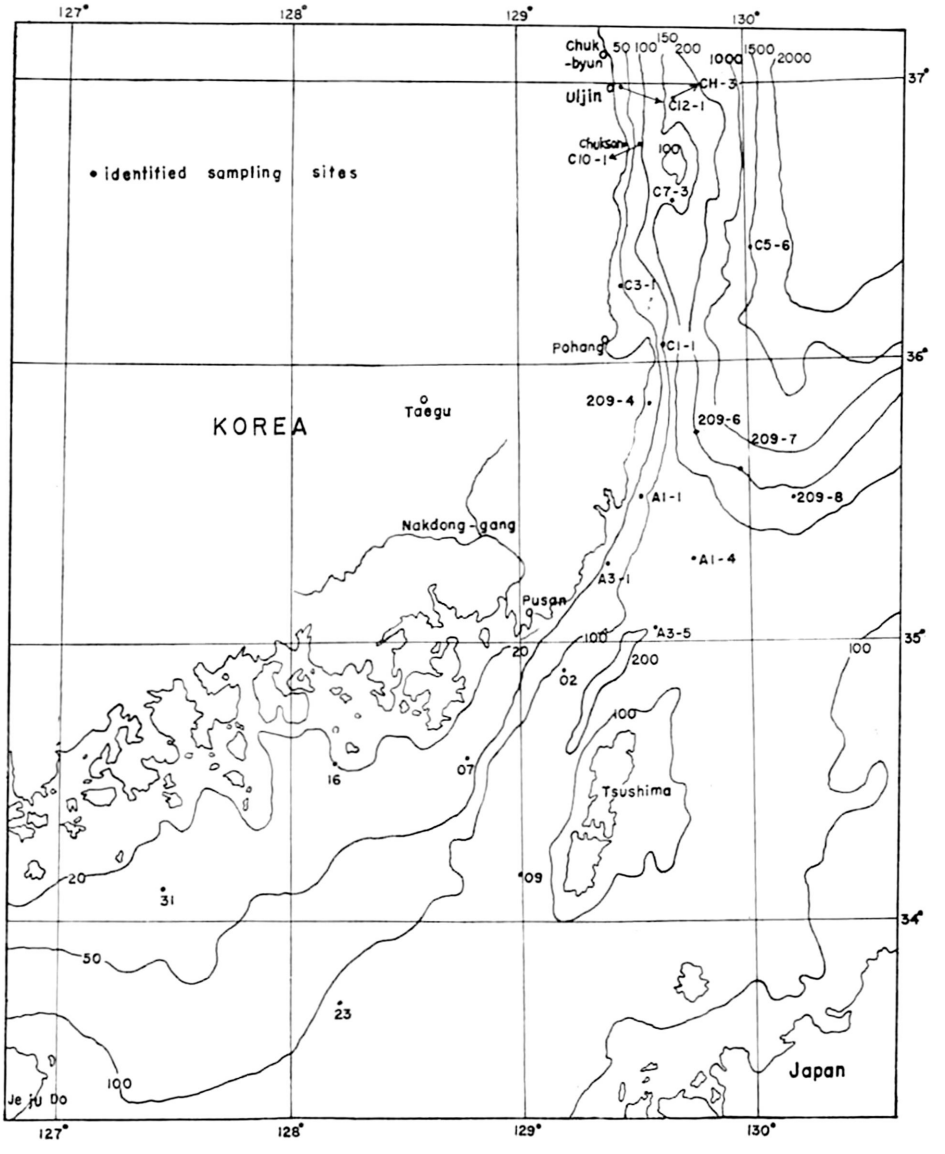

Figure II-1. Topography of the sea floor off the southeastern coast of Korea.

were picked out from the residue and counted by random sampling; from these, the frequency composition of the assemblages was determined.

GENERAL OCEANOGRAPHIC AND GEOLOGIC DATA

Topography of the sea floor

The east coast is characterized by a narrow shelf which descends steeply into the East (Japan) Sea. To the south, the shelf becomes broader and occupies the whole of Korea Strait and its margin extends eastwards across the northern end of the strait to the west coast of Honshu, Japan. There are a few shallow depressions on the shelf and an elongated S-shaped depression more than 200 m deep is developed to west and north of the northern end of Tsushima Island.

Bottom sediments and submarine geology

The bottom sediments can be classified into four groups, namely: sand, muddy sand, sandy mud and mud; they are distributed in broad curved belts as shown in Fig. II-2. The area adjoining the south and east coasts, and extending into the East Sea northwards from Yonil Bay, is covered by dark green mud. Farther away from the coast, and southward from Yonil Bay, sandy muds and sands are successively developed

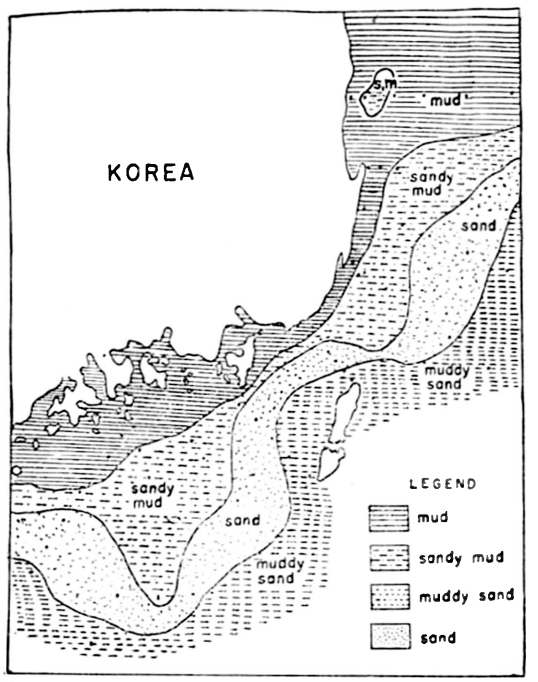

Figure II-2. Map showing the zonal distribution of sea-floor sediments off the southeastern coast of Korea.

to the vicinity of Tsushima Island, where they pass into greenish muddy sands. The coarser bottom sediments off the east coast are developed on the steep continental slope.

According to the report published by the Geological Survey of Korea in 1968, the shelf along the east coast consists of Tertiary sediments up to about 800 m thick, cut by a number of faults trending north-south and generally in the form of a homocline dipping towards the East Sea; these are connected with the small embayments of Tertiary sediments on the adjoining land in the vicinity of Yonil Bay and elsewhere. On the other hand, the shelf area adjoining the southeastern coast is continuous with the Mesozoic sediments of the Kyongsang System on land, intruded in places by Cretaceous granites, but the area around Tsushima Island probably consists of the Paleogene deposits.

Oceanography

The dominant currents in the area are the Tsushima branch of the Kuroshio Current, flowing from south to north along Korea Strait into the East Sea, and the East Korea Cold Current, an extension of the Liman Current, which originates in the East Sea and flows down from the northern coast to Korea Strait. The Kuroshio carries warm water of high salinity from the equatorial regions northwards into the colder water at higher latitudes. This warm current turns eastwards in the vicinity of latitude 38°N, regardless of the change of season; it flows along the channel in the vicinity of longitudes 131° and 132°E and then turns to the west in the region of the Janggigap. The change in direction of the current may be caused by the coastal cold water mass moving down from north to south (Chang Gi Lee and Tae Bong Cheong, 1968). The cold water mass flowing from the north forms an undercurrent beneath the warmer water and causes the development of stratified water layers (see Fig. II-3). The upwelling of the cold

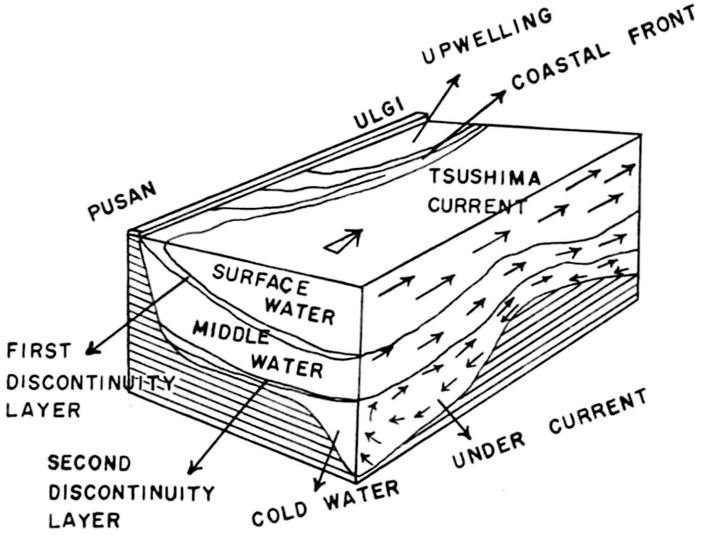

Figure II-3. Schematic representation of the currents and water masses in the eastern part of Korea Strait (Du Byung Lim and Sun Duck Chang, 1969).

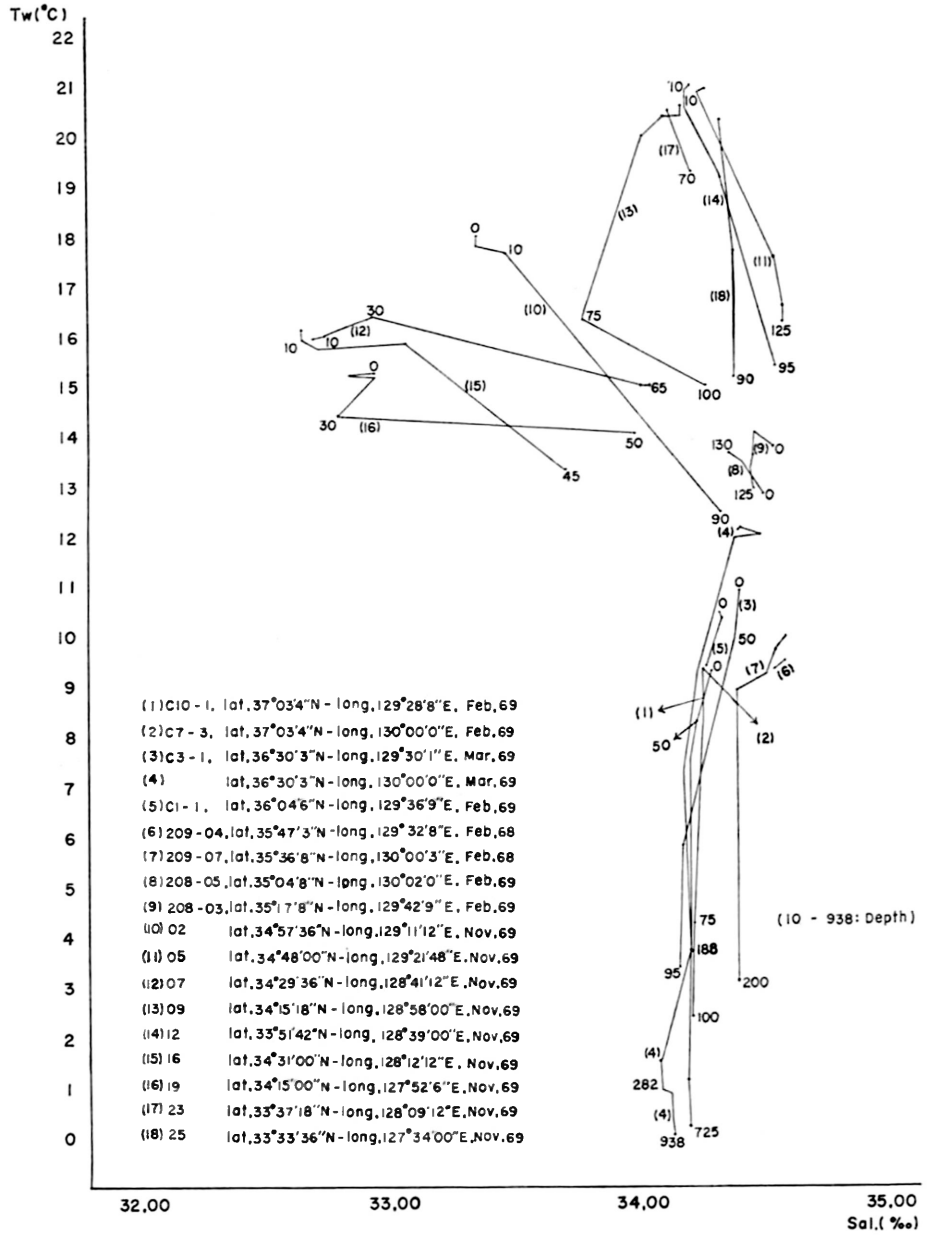

Figure II-4. Temperature-salinity relations of the sea water off the southeastern coast of Korea.

water mass along the southeast coast is caused by interchange currents. According to Defant (1961), in a strait which has interchange currents, the boundary layer between the two currents usually slopes longitudinally and transversely, and becomes steeper where the current is faster and the strait is wider. The upwelling phenomenon and opposite currents are good indications that the cold water forms an undercurrent (Du Byung Lim and Sun Duck Chang, 1969).

The volume of the warm Tsushima Current flowing through Korea Strait varies seasonally with a prominent annual change from 0.33 × $10^6 m^3$/sec in winter and spring to 2.21 × $10^6 m^3$/sec in summer and autumn. On the other hand, the southward flow of the cold Liman counter current varies irregularly from 0.01 × $10^6 m^3$/sec to 0.26 × $10^6 m^3$/sec (Suk-U Yi, 1966).

The surface temperature of the sea in Korea Strait ranges from 9.1° to 20.4°C and the temperature near the bottom, from 0.1° to 19.3°C. The salt content of the sea water ranges from 32,600 to 34,600 parts per million. The changes of temperature and salinity in Korea Strait vary according to the distance from the contact of the currents. On the continental slope off the southeastern part of Korea, no notable difference was found in temperature and salinity at stations C10–1, C7–3, C3–1, C1–1, 209–04, 209–07, 208–05, 208–03 (see Fig. II-4).

DISTRIBUTION OF FORAMINIFERA

General distribution

Although the range in depth of the area investigated is comparatively small, the variations in temperature and salinity of the sea water are probably the main factors responsible for the large number of species of planktonic and benthonic foraminifers amounting to 219, recorded in the samples from the area studied, which includes both the shelf, subject to wave and current action, and the continental slope. These variations in environment influence the distribution of the faunal assemblages in the bottom sediments. As shown in Fig. II-5, a zonal distribution of the planktonic foraminifers is evident, and the percentage of planktonic forms increases with depth and distance from the coast towards the southeast, except that, in the vicinity of Tsushima Island, the proportion decreases to 40–60 per cent; in the near-shore zone and at the higher latitudes north of Yonil Bay the planktonic tests constitute from 0 to 20 per cent of the assemblages. The distribution pattern of the planktonic foraminifers as shown in Fig. II-5 is probably related to the warm, higher salinity Kuroshio Current coming from the Indo-Pacific region.

Hyaline tests comprise more than 80 per cent of the foraminiferal assemblages, with the genera *Fissurina*, *Cassidulina* and *Globocassidulina* dominant in the northern part and *Ammonia*, *Poroeponides*, *Anomalina*, and *Elphidium* in the southern part. Arenaceous foraminifera are absent near the shore and do not exceed 10 per cent of the assemblages except at station 209–8, in the deeper part of the East (Japan) Sea (see Fig. II-5). The porcellanous population, consisting mostly of *Quinqueloculina*, *Massilina*, *Triloculina* and *Miliolinella*, is limited to the shelf area of Korea Strait, away from the shore, and a

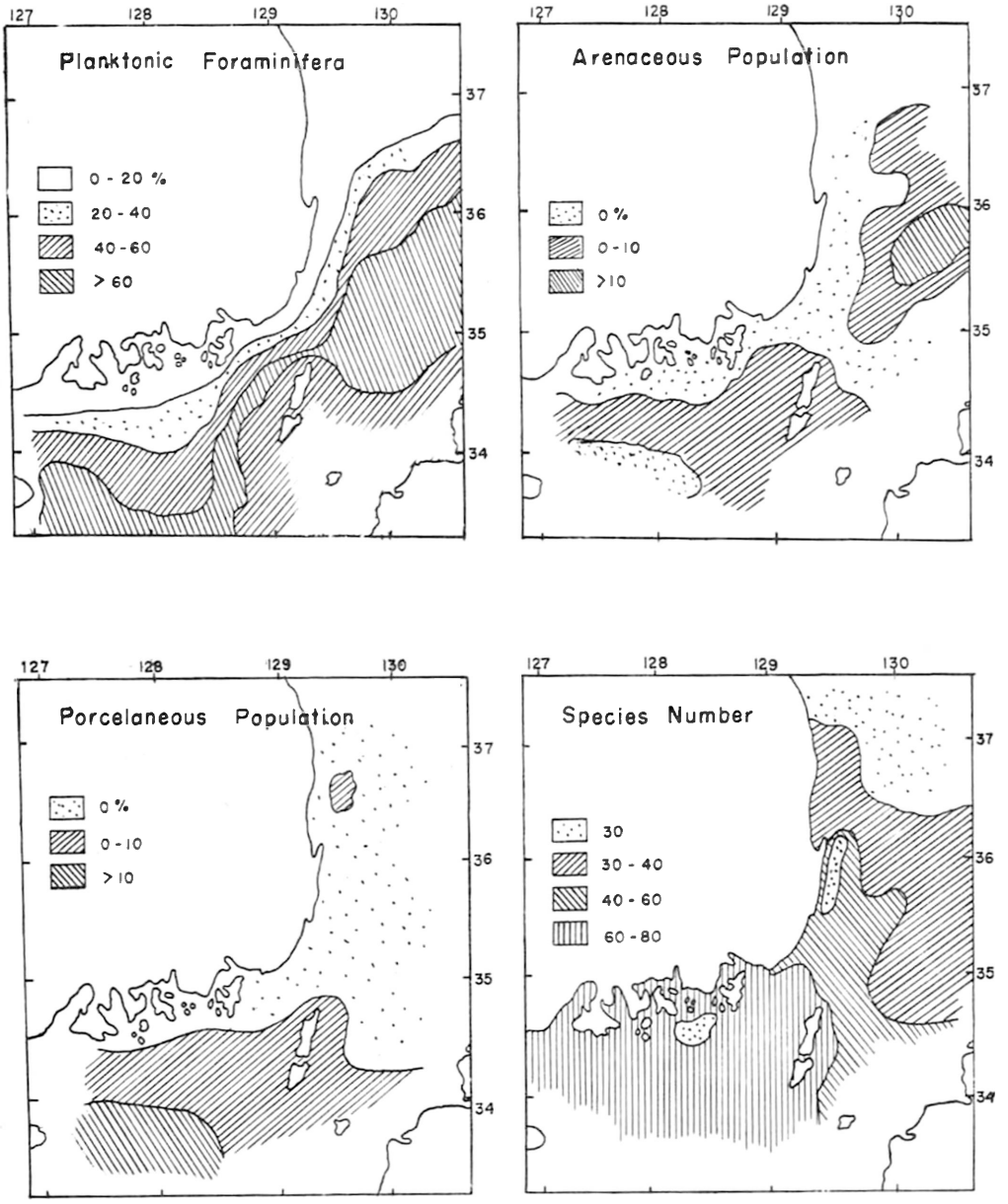

Figure II-5. Areal distribution of planktonic foraminifers, arenaceous and porcellanous populations, and species numbers.

small area north of Yonil Bay; it exceeds 10 per cent of the total assemblage only in the west central part of Korea Strait.

An inverse relationship exists between the distribution of the hyaline population and the arenaceous-porcellanous population off the southern coast, as indicated by Polski (1959). In the areas where the hyaline species are more than 80 per cent, the numbers of arenaceous and porcellanous foraminifers increase. In the areas of higher latitudes north of Yonil Bay, where the cold bottom current penetrates, planktonic foraminifers comprise less than 20 per cent of the total assemblages.

According to the oceanographic data, upwelling of the cold water mass takes place when the cold water mass meets the warm current. In the samples from stations A1–1, A3–1, and C1–1, from the shelf close to the east coast, a typical cold water species, *Globigerina pachyderma* is abundant, while warm water species such as *Globoquadrina dutertrei* are also found commonly; this indicates a mixed ecologic environment.

The East (Japan) Sea

Four major types of assemblages, shown as facies I to IV in Table II-2, are recognized in the East Sea. Facies I corresponds to the neritic zone and Facies II may correspond to the upper bathyal zone. Species in Facies I and II are mostly inhabitants of the arctic and subarctic regions or other cold water regions; they include: *Buccella inusitata* Anderson, *Globocassidulina japonica* (Asano and Nakamura), *Cassidulina yabei* Asano and Nakamura, *Cassidulina norcrossi* Cushman, *Cribrostomoides crassimargo* (Norman), *Haplophragmoides bradyi* (Robertson), *Trifarina kokozuraensis* (Asano) and *Globigerina pachyderma* (Ehrenberg).

Facies III corresponds to the bathyal zone and is characterized by the presence of *Reophax* and *Elphidium advenum*. This facies is found only at station 209–7 where the

Table II-2. Types of foraminiferal assemblages in the East (Japan) Sea.

Facies	Dominant species	Station and depth range
I	*Cassidulina norcrossi* Cushman (predominant) *Uvigerina peregrina dirupta* Todd *Uvigerina akitaensis* Asano *Trifarina kokozuraensis* (Asano)	C10–1 About 80 m
II	*Globocassidulina setanaensis* (Asano & Nakamura) *Globocassidulina japonica* (Asano & Nakamura) *Uvigerina akitaensis* Asano *Trifarina kokozuraensis* (Asano)	About 130 m C7–3
III	*Elphidium advenum* (Cushman) *Globocassidulina japonica* (Asano & Nakamura) *Cassidulina yabei* Asano & Nakamura *Reophax excentricus* Cushman *Reophax curtus* Cushman	209–7 About 250 m
IV	*Cassidulina yabei* Asano & Nakamura *Karreriella baccata japonica* Asano	209–8 About 200 m

bottom sediment is mainly coarse sand, at a water depth of 250 m and temperature of 2.03 C; the salinity at 200 m was 34.120 ppm. *Globigerina pachyderma* was also dominant at this station and others less common are *Elphidium crispum Elphidium subarcticum* and *Hanzawaia nipponica. Reophax excentricus* and *Reophax curtus* have been recorded from Hakada Bay, Japan, from a depth of 250 m.

Facies IV is characterized by the presence of *Karreriella baccata japonica.* This form, together with *Cassidulina yabei,* constitutes about 25 per cent of all foraminiferal tests in this area; this facies corresponds to the bathyal zone. *Bulimina marginata* and *Bolivina robusta* are generally most common at depths ranging from 100 to 150 m. A well-defined facies boundary is found between 200 m and 300 m in depth throughout the area. The annual variations of temperature and salinity are slight at the maximum depths, where the *Uvigerina akitaensis-Trifarina kokozuraensis* assemblage occurs. *Hanzawaia nipponica, Cibicides aknerianus, Cibicides lobatulus, Cassidulina yabei* and the *Cassidulina-Cibicides* assemblages in the outer neritic zone are also inferred to be related to sandy bottom.

Korea Strait

The general oceanographic conditions and the faunal assemblages found in the sediments are rather similar throughout the area, but the upwelling along the northern coast of Korea Strait is worthy of notice. It is necessary to count all the benthonic and planktonic specimens in a sample to get an adequate number for statistical analysis, but this procedure may not be sufficient as the distribution of the various forms cannot be given with accuracy except in the case of the more common and persistent ones.

According to K. Asano (1957), the planktonic species of *Globigerinoides* from Korea Strait are generally very variable in form and it is often difficult to differentiate

Table II-3. Percentages of benthonic foraminifers at stations off the eastern coast of Korea.

Species \ Stations	C12-1	C10-1	C7-3	C5-6	C3-1	C1-1	209-7	209-6	209-8
Ammonia takanabensis	5.0		0.8	0.8	0.7		0.8		
Bulimina exilis					1.8				
Bulimina exilis tenuata		2.7			3.8	2.0			
Bulimina marginata		2.5	0.3		1.1				
Cassidulina norcrossi	2.5	48.0	0.8	5.3	41.8	31.0		4.0	
Cassidulina yabei				3.8			7.3	2.8	12.0
Cibicides cf. *refulgens*	20.0			0.8			3	0.5	
Elphidium advenum							10.0		5.6
Elphidium clavatum						0.5		1.5	
Fissurina marginata	2.5	2.0	0.3	6.3	7.3	0.7		1.0	
Florilus labradoricum		1.3		0.8					
Globocassidulina japonica			5.6	6.8			9.6	16.0	
Globocassidulina setanaensis			12.0	6.0					
Globocassidulina subglobosa	7.5		5.0	4.5	2.7	0.9	1.7	3.0	2.0
Karreriella baccata japonica			1.6	2.3			3.3	5.0	10.0
Reophax (all species)							12.0		
Trifarina kokozuraensis		5.3	6.3	8.3	3.6	9.5		24.0	
Uvigerina akitaensis		8.8	6.3	1.5	27.3	34.0		31.0	0.8
Uvigerina peregrina dirupta	2.5	9.6	5.6		9.0	8.2		5.3	0.8

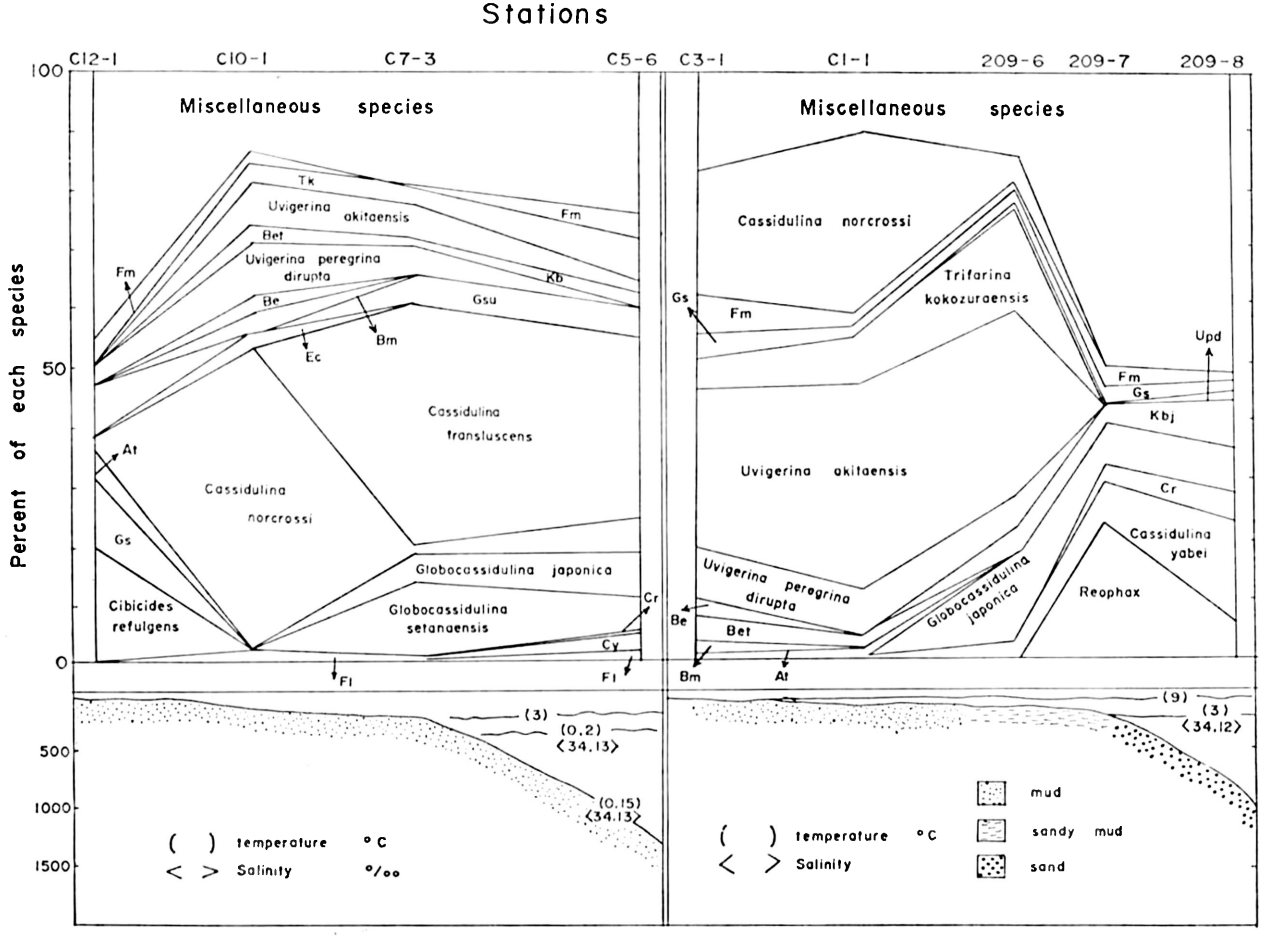

Figure II-6. Frequency distribution of benthonic foraminifers off the eastern coast of Korea. Fl: *Florilus labradoricum;* Cy: *Cassidulina yabei;* Cr: *Cibicides* cf. *refulgens;* At: *Ammonia takanabensis;* Fm: *Fissurina marginata;* Gsu: *Globocassidulina subglobosa;* Tk: *Trifarina kokozuraensis;* Kb: *Karreriella baccata japonica;* Be: *Bulimina exilis;* and Bet: *Bulimina exilis tenuata.*

Table II-4. Assemblages of foraminifera off the southeastern coast of Korea.

Genus & Species	Eastern coast											The Korea Strait & southern coast									
	C12 -1	C11 -3	C10 -1	C7 -3	C5 -6	C3 -1	C1 -1	209 -4	209 -6	207 -7	209 -8	A1 -1	A1 -4	A3 -1	A3 -5	S 2	S 7	S 9	S 16	S 23	S 31
Benthonic Foraminifera																					
Alveophragmium scitulum (Brady)								•		/											
A. sp.								•		•											
Ammonia indopacifica (Cushman)																	/				/
A. inflata (Seguenza)											/	•				•		/		•	×
A. japonica (Hada)											/				•	•	•	•		•	/
A. ketienziensis angulata (Kuwano)										•	•	×	/			/	/	/		•	
A. takanabensis (Ishizaki)	•			•	•	•		/		/		×		○	×	○	○	×	○	○	○
Amphycoryna paucicoluta (Cushman)																	•				
A. scalaris (Batsch)												/	/	/		/	○	○	○		
A. scalaris sagamiensis (Asano)														/			×	×	×		
Anomalina glabrata Cushman															/		•	/	/	×	×
Astrononion umbilicatulum Uchio		•						•				×		/		×	×	/	○	○	•
Baggina philippinensis (Cushman)																					/
Bolivina decussata Brady		•	•																		
B. robusta Brady	•	•	/			•		/			•	○		×	○	○	○	○	×	×	×
B. seminuda Cushman														•							
B. spinescens Cushman			•									×		•	×	/					
B. substriatula Asano		•	•									×			×	×	/	/	×	×	×
Buccella frigida (Cushman)	•		/			/	•			•		/	•	•	•	○	○	/	○	×	×
B. inusitata Anderson			/						•	/			•						•	•	/
B. ? *makiyamae* Chiji									•	•	/		×		/	×	•	•			
B. sp.													•								
Bulimina aculeata d'Orbigny				•		•															
B. exilis Brady			•			/		×				○		•		•					
B. exilis tenuata (Cushman)		•	/			×	/														
B. marginata d'Orbigny		/	/	•		/		×				○	•	×	○	×	•	○	×	/	
Buliminella elegantissima (d'Orbigny)			/																		
Cancris auricularis (Fichtel & Moll)											•	/				•	×	•	/	/	×
C. peroblongus (Cushman)																				•	/
Cassidella sp.																/	•				
Cassidulina norcrossi Cushman	•	○	○	•	/	○	○			/											
C. sublimbata Asano & Nakamura				•							×	/		×							
C. translucens Cushman & Hughes				○						/	/										
C. yabei Asano & Nakamura					/				•	/	×	×		×		•					
Cibicides aknerianus (d'Orbigny)			×	•	/		/			×	/						×	×		•	
C. lobatulus (Walker & Jacob)										•	•			○		/	/	•			/
C. pseudoungerianus (Cushman)		/								/	/	○			×	/	○	○	○	○	/
C. cf. *refulgens* (Montfort)	/	•			•			•	•	×	/										
C. subpraecintus (Asano)				/					×	×	/			×		/	•	×	×	×	×
C. tenuimargo (Brady)										•							/	/		•	×
Clavulina yabei Asano																	•			×	×
Cribrostomoides crassimargo (Norman)	•			•		•															
C. sp.						•	•														
Cruciloculina asanoi Loeblich & Tappan										•											
Cyclammina orbicularis Brady		•																			
C. sp.							•														
Dentalina emaciata Reuss							•					/									
D. fusiformis (d'Orbigny)												/									
D. cf. *roemeri* Neugeboren										•			•		•	/					
D. setanaensis Asano			•																		
Discorbinella bertheloti (d'Orbigny)																		/		/	/
Dyocibicides sp.										•										•	
Elphidium advenum (Cushman)	•		•			•	•	/		○		×	/			○	○	×	○	×	○
E. clavatum Cushman		•	/				•	○	•			○	/			•	/	/	○		/
E. crispum (Linnaeus)											/		/						/		/
E. sp. A											•								/		
E. jenseni Cushman	•								•	/	•		/							/	/
E. kusiroense Asano										/									•		
E. subarcticum Cushman	•									×									•		
E. subincertum Asano									•									/	×	•	
E. sp. B											•										
Epistominella japonica Asano	•								•										/		×
E. naraensis (Kuwano)						•	•	○						×		/		•	○		
Eponides haidingeri (d'Orbigny)											•		•	•	×		○	○	○	○	○
E. umbonatus (Reuss)											•			•	/			•	•		
E. sp.																/				×	×
Fissurina circulo-costa Asano				•														•		/	•
F. lacunata (Burrow & Holland)										•								•			
F. lucida Williamson		•																			
F. marginata (Montagu)	•	/	/	•	/	·	•	•	•	•		○		•	•	·	·	·	×	×	/
F. cf. *orbignyana* (Seguenza)		•	•	•					/			○			×	×	•	×	×	×	•
Florilus labradoricum (Dawson)		•	/		•			×				○		○	○	×	×	×			
Gaudryina robusta Cushman																/				×	×
G. triangularis Cushman																	•			×	×
Globobulimina auriculata (Bailey)		•	/		·	/			•			×	•		/			×			
G. turgida (Bailey)				•				•				×	/	×	×			×		•	
Globocassidulina delicata Cushman									•												
G. japonica Asano & Nakamura			•	×	/			×	○	×			•								
G. setanaensis Asano & Nakamura		•		×	/																

Table II-4. (*Cont.*)

Genus & Species	Eastern coast											The Korea Strait & southern coast									
	C12 -1	C11 -3	C10 -1	C7 -3	C5 -6	C3 -1	C1 -1	209 -4	209 -6	207 -7	209 -8	A1 -1	A1 -4	A3 -1	A3 -5	S 2	S 7	S 9	S 16	S 23	S 31
G. subglobosa Brady	·	·	·	/	/	/	·	/	/	/	/	/			·	×	·	/		/	
G. subglobosa parva Asano & Nakamura		·	·																		
Guttulina austriaca d'Orbigny										·			·								
G. orientalis Cushman & Ozawa										·											
G. kishinouyi Cushman & Ozawa											·		/								
G. yabei Cushman & Ozawa				·														·			·
G. yamazakii Cushman & Ozawa											·		/								
Gyroidina nipponica Ishizaki												×		/	·	/	/	○		×	×
Hanzawaia nipponica Asano				·	·			·		×	/	×	/	○	○	○	×	×	○	○	○
H. sp.			·																		
Haplophragmoides bradyi (Robertson)	·		·		·																
H. sp.			·													·	/				
Hoeglundina elegans (d'Orbigny)															/	·	/			/	/
Hyalinea balthica (Schröter)	·	·													×	·	·			×	
Karreriella baccata japonica Asano				/	·				/	×	×		×								
Lagena apiopleura Loeblich & Tappan				/					/						·	/					/
L. elongata (Ehrenberg)																·		·		·	/
L. flatulenta Loeblich & Tappan														·					/		
L. gracillis Williamson			·															·		·	·
L. gracillima (Seguenza)														·	·	·	·	/			
L. laevis (Montagu)					·	·															
L. striata d'Orbigny		·	·		·					·										·	
L. subamphora Asano				·	·					·										·	
L. substriata Williamson	·						·					×			·			·			·
L. sulcata spicata Cushman & McCulloch			·	·		·					·	×	·	/	·	×	/	×	○	/	/
Lenticulina calcar (Linne)								·												·	·
L. depressus Asano								;							/	/	×	×		×	×
L. kamakuraensis Asano															·						
L. lucidus (Cushman)								·						○	×	○	○	○	○	○	○
L. nicobarensis (Schwager)					·	·					·		/	·		/					×
L. orbicularis (d'Orbigny)															/	×	×	×		○	×
L. sp. (1)														·	/			·			
L. sp. (2)																				·	/
Marginulina glabra d'Orbigny												/								·	·
M. sp.												/									·
Massilina sp.															×	·	×	/		·	·
Melonis nicobarense (Cushman)		·	/		·									·	×	×	·	×		·	
Miliolinella circularis (Bornemann)																				·	·
Nodosaria catenulata Brady															·	·					
N. japonica Cushman														·		/	×	×		/	
N. pyrula d'Orbigny															·						
N. semirogosa d'Orbigny																				·	·
N. vertebralis (Batsch)														·		·	·	×		×	×
Nonionella stella Cushman & Moyer			·			/						○	/	/	·		·	×	×		
Oolina hexagona (Williamson)	·											/									
O. melo (d'Orbigny)			·	·								/				/	·			/	·
O. striatopuncata (Parker & Jones)				·																	
Opthalmidium tenuimargo (Cushman)															·	·		·			
Patellinella hanzawai Asano															·						
P. tricarinella (Reuss)																		·		·	
Planulina wuellerstorfi (Schwager)												○		/	/	/				/	×
P. sp.												/			·						
Polymorphina charlottensis Cushman										·			·								
Poroeponides cribrorepandus Asano & Uchio																					/
Pseudoglandulina laevigata (d'Orbigny)															·	/				·	
Pseudonodosaria sp.											·										
Pseudononion japonicum Asano								·		·	·	·	/	×		/	×	/		/	·
Pseudopolymorphina hanzawaia Cushman & Ozawa											·										
Pseudorotalia gaimardii (d'Orbigny)											·			×	/	×	○	○	○	○	○
Pullenia apertula Cushman													·								
P. bulloides (d'Orbigny)						·		·				×		/		×	/	/			
P. quinqueloba (Reuss)			·															/			
Pyrgo fornasinii Cushman & Parr				·														/		×	×
P. sp.																			·		
Quinqueloculina akneriana d'Orbigny																					/
Q. bicostata d'Orbigny															/	/		/		/	·
Q. contorta d'Orbigny																				·	
Q. costata d'Orbigny																				/	
Q. elongata Natland			·		·											·		/		/	·
Q. lamarckiana d'Orbigny				·										·	/	×	×	×		×	×
Q. sagamiensis Asano																				·	
Q. seminula (Linnaeus)				/	·		/						·						/		
Q. sp. (1)																				/	/
Q. sp. (2)																				/	/
Rectobolivina bifrons (Brady)													·								
Reophax curtus Cushman									·	×										·	
R. excentricus Cushman										×											
R. subfusiformis Earland						·															
R. sp.						·			·	×			·			·	·	·		/	
Reussila aculeata Cushman								·										/			

Table II-4. (*Cont.*)

Genus & Species	Eastern coast											The Korea Strait & southern coast									
	C12 -1	C11 -3	C10 -1	C7 -3	C5 -6	C3 -1	C1 -1	209 -4	209 -6	207 -7	209 -8	A1 -1	A1 -4	A3 -1	A3 -5	S 2	S 7	S 9	S 16	S 23	S 31
R. pacifica Cushman & Mc Culloch												/						•			
Rhabdammina sp.																•					
Rosalina australis (Parr)										/			•								•
R. bradyi (Cushman)											•		/								/
R. orbicularis (Terquem)											•				•						
R. vilardeboana d'Orbigny														/	•	×	×			×	
Rotalia sp.																			/		/
Saccammina sp.						•										/					
Saracenaria angularis Natland																/					/
S. latifrons (Brady)												×		•	•		•				
Sigmoidella pacifica (Cushman & Ozawa)										•	•		/								
Sigmoilina sigmoidea compressa Cushman										•											
Sigmomorphina kagaensis Cushman & Ozawa																	/				
Siphogenerina raphanus (Parker & Jones)						•								×							/
Spiroloculina communis Cushman & Todd																				×	/
S. manifesta Cushman & Todd																					/
Textularia agglutinans d'Orbigny																				×	/
T. abbreviata d'Orbigny															•	/					/
T. rugosa (Reuss)																			/	/	×
T. stricta Cushman																	•			×	/
T. sp. (1)																/	•			•	/
T. sp. (2)																					/
Trifarina kokozuraensis Asano		×	×	×	/	×	×		×			/									
Triloculina tricarinata d'Orbigny																				•	/
T. trigonula (Lamarck)																/	•	×		×	×
Trochammina inflata (Montagu)	•		•			×	/														
T. pacifica Cushman				•																	
T. sp.	•					/	•														
Uvigerina aculeata d'Orbigny						•															
U. akitaensis Asano		×	×	×	•	○	○		×		•	○	×	•				/			
U. peregrina dirupta Todd	•	×	×	×		×	×	•	/		•	/									
U. peregrina shiwoensis Asano			/	•		•	•														
U. proboscidea Schwager									•												
U. proboscidea vadescens Cushman		•										○		•	○	○	•	○			
U. pseudoampullacea Asano						•															
Valvulineria sadonica Asano					•										•	•					
V. sp.															•	•					
Planktonic Foraminifera																					
Globigerina apertura Cushman										•			×		×	×	/	×			
G. bulloides d'Orbigny			•	•						•		○	/	×	○	○	×	○	/	/	/
G. falconensis Blow		•	/					/			•	○				•	/	○	/	/	/
G. pachyderma (Ehrenberg)	/	×	/	×	○	/	○	•	/	○	○	×	○	•	/						
Globigerinita glutinata (Egger)											•		/								
G. uvula (Ehrenberg)												•		•							
Globigerinoides bolli Blow												•			•			•			
G. conglobatus (Brady)										•	•		×	/	/			×			/
G. elongatus (d'Orbigny)													/		•			•			
G. immaturus Leroy											•			•	/	/		×		×	/
G. obliquus (Bolli)												/									
G. ruber ruber (d'Orbigny)											•		×	/	○	×	/	×	×	×	×
G. sacculifer (Brady)										•		×				×	×	•	×		
G. trilobatus (Reuss)											•	○				×	×	•	×	×	
Globoquadrina dutertrei (d'Orbigny)				•	/	•	•			•	×	×	○	×	○	○	○	○		○	○
Globorotalia menardii (d'Orbigny)										/	/	×	×		•	/	•	○			
Hastigerina siphonifera (d'Orbigny)										/	/		×		/	/					
Orbulina universa d'Orbigny											•			•	/	/	/	/	×	/	
Pulleniatina obliquiloculata (Parker & Jones)		•					•	•		/	×	×	○	/	○	○	○	○		○	○
Turborotalia acostaensis (Blow)						•					×		×			•					
T. inflata (d'Orbigny)										/	•	×	○	/	○	×	•	×		×	/
T. subcretacea (Lomnicki)											/	×	×		/	/		×		×	•

○: abundant (more than 100 individuals), ×: common (20–100 individuals), /: few (5–20 individuals), •: rare (less than 5 individuals)

species clearly because of their variability. As all degrees of variation can be found at a single station, the variation does not seem to be related to ecologic differences. Warm water species such as *Globorotalia menardii* and *Pulleniatina obliquiloculata* occur in abundance off the southeastern coast (Stations 209–7 and 209–8) and in the southern part of the East Sea due to the influence of the Kuroshio Current. Cold water species such as *Globigerina pachyderma* are also found in abundance in Korea Strait (Station A-14) as a result of the southward extension of the Liman Current. The warm water species *Globorotalia menardii* and *Pulleniatina obliquiloculata*, and others, also occur commonly in Korea Strait.

The Tsushima branch of the Kuroshio Current brings warm water of relatively high salinity through Korea Strait into the East Sea, together with the species typical of warm water. In the East Sea, the cold Liman Current from the north passes along the east coast and turns back into the central part of the East Sea, carrying with it species typical of high latitudes.

Planktonic species dominantly found in the warm Kuroshio Current are: *Globorotalia menardii* (d'Orbigny), *Pulleniatina obliquiloculata* (Parker & Jones), *Globigerinoides conglobatus* (Brady), *Globigerinoides sacculifer* (Brady) and *Globoquadrina dutertrei* (d'Orbigny). Planktonic species dominantly found in the East Korea Cold Current is *Globigerina pachyderma* (Ehrenberg). Other planktonic species including *Globigerina bulloides* d'Orbigny, *Turborotalia subcretacea* (Lomnicki), *Orbulina universa* d'Orbigny, *Globigerinoides trilobatus* (Reuss), *Globigerinoides ruber ruber* (d'Orbigny), *Hastigerina siphonifera* (d'Orbigny) and so on are dominant species in this area (the Korea Strait).

According to Wallen (1958) and Polski (1959), the planktonic species *Globigerina bulloides* d'Orbigny, *Globoquadrina dutertrei* (d'Orbigny) and others, are restricted to waters colder than those of the Indo-Pacific area of the south Asiatic region. An increase in the number of small, presumably juvenile, forms is also noted in the colder northern waters as compared with the Indo-Pacific region.

A considerable number of benthonic foraminifers have been identified. The more common warm shallow water species are as follows: *Pseudorotalia gaimardii* (d'Orbigny), *Textularia agglutinans* Asano, *Textularia abbreviata* d'Orbigny, *Gaudryina robusta* Cushman, *Spiroloculina communis* Cushman & Todd, *Guttulina kishinouyi* Cushman and Ozawa and *Planulina wuellerstorfi* (Schwager).

Close to the north coast of Korea Strait, upwelling has resulted in the concentration of a cold water faunal assemblage in a narrow belt along the coast; a typical assemblage is found at station A1–1, at a depth of less than 50 m, characterized by the following dominant cold water species: *Globigerina pachyderma* (Ehrenberg), *Uvigerina akitaensis* Asano, *Nonionella stella* Cushman and Moyer and *Elphidium clavatum* Cushman.

CONCLUSIONS

1. The bottom sediments off the southeastern coast of Korea are muddy near the coast and grade successively to the southeast into belts of sandy mud, sand and muddy sand.

2. The foraminiferal population increases towards the south and it contains a considerable amount of juvenile and dwarf planktonic tests off the southern coast.

3. The warm and shallow water species become more common towards the south.

4. Arenaceous foraminifers comprise about 15 per cent of the tests at station 209–7, where the bottom sediments consist are sand and coarse sand.

5. A total of 23 species belonging to 9 genera of planktonic foraminifers and 196 species belonging to 80 genera of benthonic forms were identified.

6. Station A1–1 is in a zone of upwelling and the foraminiferal assemblage shows mixed ecologic features.

REFERENCES

Asano, K., 1950, Some Lituolidae from the Tertiary of Japan: *Contrib. Cushman Found. Foram. Res.*, vol. 1, parts 3 and 4.

Asano, K., 1950–1952, Illustrated Catalogue of Japanese Tertiary Smaller Foraminifera, pts. 1–15, and suppl. 1.

Asano, K., 1956(a), The foraminifera from the adjacent seas of Japan, collected by the S. S. Soyo-Maru, 1922–1930, part 1–Nodosariidae: *Sci. Repts. Tohoku Univ., Sendai, Japan, Second Ser.* (*Geology*), vol. 27, p. 1–55, pls. 1–6.

Asano, K., 1956(b), *idem*, part 2–Miliolidae: *Ibid.*, p. 57–83, pls. 2–9.

Asano, K., 1957, *idem*, part 3–Planktonic foraminifera: *Ibid.*, vol. 28, p. 1–52, pls. 1, 2.

Asano, K., 1958, *idem*, part 4–Buliminidae: *Ibid.*, vol. 29, p. 1–41, pls. 1–7.

Asano, K., 1960, *idem*, part 5–Nonionidae: *Ibid.*, Spec. vol. 41, p. 189–201, pls. 21, 22.

Bandy, Orville L., 1960, Planktonic foraminiferal criteria for paleo-climatic zonation: *Ibid.*, Spec. vol. 4, p. 1–8, 2 text-figs.

Bolli, H. M., Loeblich, A. R. and Tappan, H., 1957, Planktonic foraminiferal families Hantkeninidae, Orbulinidae, Globorotaliidae and Globotruncanidae: *U.S. Nat. Mus., Bull.*, no. 215, p. 3–50, pls. 1–11, text-figs. 1–9.

Bradshaw, I. S., 1960, Ecology of living planktonic foraminifera in the north and equatorial Pacific Ocean: *Contrib. Cushman Found. Foram. Res.*, vol. X, pt. 2, p. 25–64.

Crespin, Irene, 1960, Some Recent foraminifera from Vestfold Hills, Antarctic: *Sci. Repts. Tohoku Univ., Sendai, Japan, Second Ser.* (Geology), Spec. vol. 4, p. 19–31, pls. 1–3, 1 text-fig.

Cushman, J. A., 1921, Foraminifera of the Philippine and adjacent seas: *U.S. Nat. Mus. Bull.*, 100, vol. 4, p. 1–608, pls. 1–100, text-figs. 1–52.

Cushman, J. A. and McCulloch, Irene, 1939, A report on some arenaceous foraminifera: Allan Hancock Pacific Expeditions, vol. 6, no. 1, p. 1–113, pls. 1–12.

Cushman, J. A. and McCulloch, Irene, 1942, Some Virgulininae in the collections of the Allan Hancock Foundation: Allan Hancock Pacific Expeditions, vol. 6, no. 4, p. 179–230, pls. 21–28.

Cushman, J. A. and McCulloch, Irene, 1948, The species of *Bulimina* and related genera in the collections of the Allan Hancock Foundation: Allan Hancock Pacific Expeditions, vol. 6, no. 5, p. 231–294, pls. 29–32.

Geological Survey of Korea, 1968, The outline of the submarine geology of continental shelf off Korea.

Ishiwada, Y., 1964, Benthonic foraminifera off the Pacific Coast of Japan referred to biostratigraphy of the Kazusa Group: *Rept. Geol. Surv. Japan*, no. 205, p. 1–43, pls. 1–8.

Kim, B. K., 1965, The stratigraphic and paleontologic study on the Tertiary (Miocene) of the Pohang Area: *Seoul Nat. Univ. Jour., Sci. and Technol. Ser.*, vol. 15, p. 32–121, pls. 1–9.

Kim, B. K., 1970, A stratigraphic and paleontological study of the Sinyangri Formation in the vicinity of Sinyangri and Gosanri, the Jeju Island: *Jour. Geol. Soc. Korea*, vol. 5, no. 2, p. 103–121.

Kim, B. K., Kim, S. W. and Kim, J. J., 1970, Foraminifera in the bottom sediments off the southwestern coast of Korea: United Nations ECAFE, *CCOP Tech. Bull.*, vol. 3, p. 147–156, pls. IX–1 ~ IX–3.

Lalicker, C. G. and McCulloch, Irene, 1940, Some Textulariidae of the Pacific Ocean: Allan Hancock Pacific Expeditions, vol. 6, no. 2, p. 115–143, pls. 13–16.

Lee, C. K. and Bong, J. H., 1968, On the Current of the Korean Eastern Sea: Fisheries Research and Development Agency, Republic of Korea.

Lim, D. B. and Chang, S. D., 1969, On the cold water mass in the Korea Strait: *Journ. Oceanogr. Soc. Korea.*

Matoba, Y., 1967, Younger Cenozoic foraminiferal assemblages from the Choshi District, Chiba Prefecture: *Sci. Rep. Tohoku Univ., Second Ser. (Geology)*, vol. 38, no. 2, p. 221–263, 8 text-figs, pls. 25–30.

Matsunaga, Takashi, 1963, Benthonic smaller foraminifera from the oil fields of northern Japan: *Sci. Repts. Tohoku Univ., Sendai, Japan, Second Ser. (Geology)*, vol. 35, no. 2, p. 67–122, pls. 1–52.

Moore, R. C., 1964, Treatise on Invertebrate Paleontology (c) Protista: *Geol. Soc. America*, Univ. Kansas Press, U.S.A.

Murata, Shigeo, 1960, Foraminifera from the Sakasegawa Group in the north coastal district of the Amakusa-Shimoshima, Kumamoto Pref., Kyushu: *Bull. Kyushu Inst. Technol.*, no. 6, p. 35–42.

Parker, Frances L., 1960, Living planktonic foraminifera from the equatorial and south Pacific: *Sci. Repts. Tohoku Univ., Sendai, Japan, Second Ser. (Geology)*, Spec. vol. 4, p. 71–82, 20 text-figs.

Parker, F. L., 1962, Planktonic foraminifera species in Pacific sediments: *Micropal.*, vol. 8, no. 2, p. 219–254, pls. 1–10.

Phleger, Fred B., 1960, Foraminiferal populations in Laguna Madre, Texas: *Sci. Repts. Tohoku Univ., Sendai, Japan, Second Ser. (Geology)*, Spec. vol. 4, p. 83–91, 9 text-figs.

Polski, W., 1959, Foraminiferal biofacies off the north Asiatic coast: *Jour. Paleont.*, vol. 33, p. 569–587.

Uchio, Takayasu, 1962, Influence of the River Shinano on foraminifera and sediment grain size distributions: *Publ. Seto Marine Biol. Lab.*, vol. X, no. 2.

Uchio, Takayasu, 1967, Foraminiferal assemblages in the vicinity of the Seto Marine Biological Laboratory, Shirahama-cho, Wakayama-ken, Japan: *Publ. Seto Marine Biol. Lab.*, vol. XV, no. 5.

Vilks, G., 1969, Recent foraminifera in the Canadian Arctic: *Micropal.*, vol. 15, no. 1, p. 35–60.

Yoo, E. K., 1970, Recent distribution of *Globigerina pachyderma* (Ehrenberg) and interpretation of Upper Cenozoic climatological changes: *Jour. Geol. Soc. Korea*, vol. 6, no. 2, p. 119–127.

EXPLANATION OF PLATE II-1

Figures

1. *Reophax excentricus* Cushman. ×23. Hypotype (DGSU coll. cat. 00183)
2. *Reophax curtus* Cushman. ×25. Hypotype (DGSU coll. cat. 00184)
3. a–b. *Textularia abbreviata* d'Orbigny. ×33. Hypotype (DGSU coll. cat. 00185)
4. a–b. *Textularia pacifica* Cushman. ×23. Hypotype (DGSU coll. cat. 00186)
5. a–b. *Karreriella baccata japonica* Asano. ×23. Hypotype (DGSU coll. cat. 00187)
6. a–b. *Textularia rugosa* (Reuss). ×36. Hypotype (DGSU coll. cat. 00188)
7. a–b. *Textularia agglutinans* d'Orbigny. ×36. Hypotype (DGSU coll. cat. 00189)
8. a–b. *Textularia stricta* Cushman. ×21. Hypotype (DGSU coll. cat. 00190)
9. a–c. *Textularia* sp. ×35. Hypotype (DGSU coll. cat. 00191)
10. a–c. *Quinqueloculina akneriana* d'Orbigny. ×45. Hypotype (PGSU coll. cat. 00192)
11. a–c. *Quinqueloculina bicostata* d'Orbigny. ×25. Hypotype (DGSU coll. cat. 00193)
12. a–c. *Quinqueloculina costata* d'Orbigny. ×25. Hypotype (DGSU coll. cat. 00194)

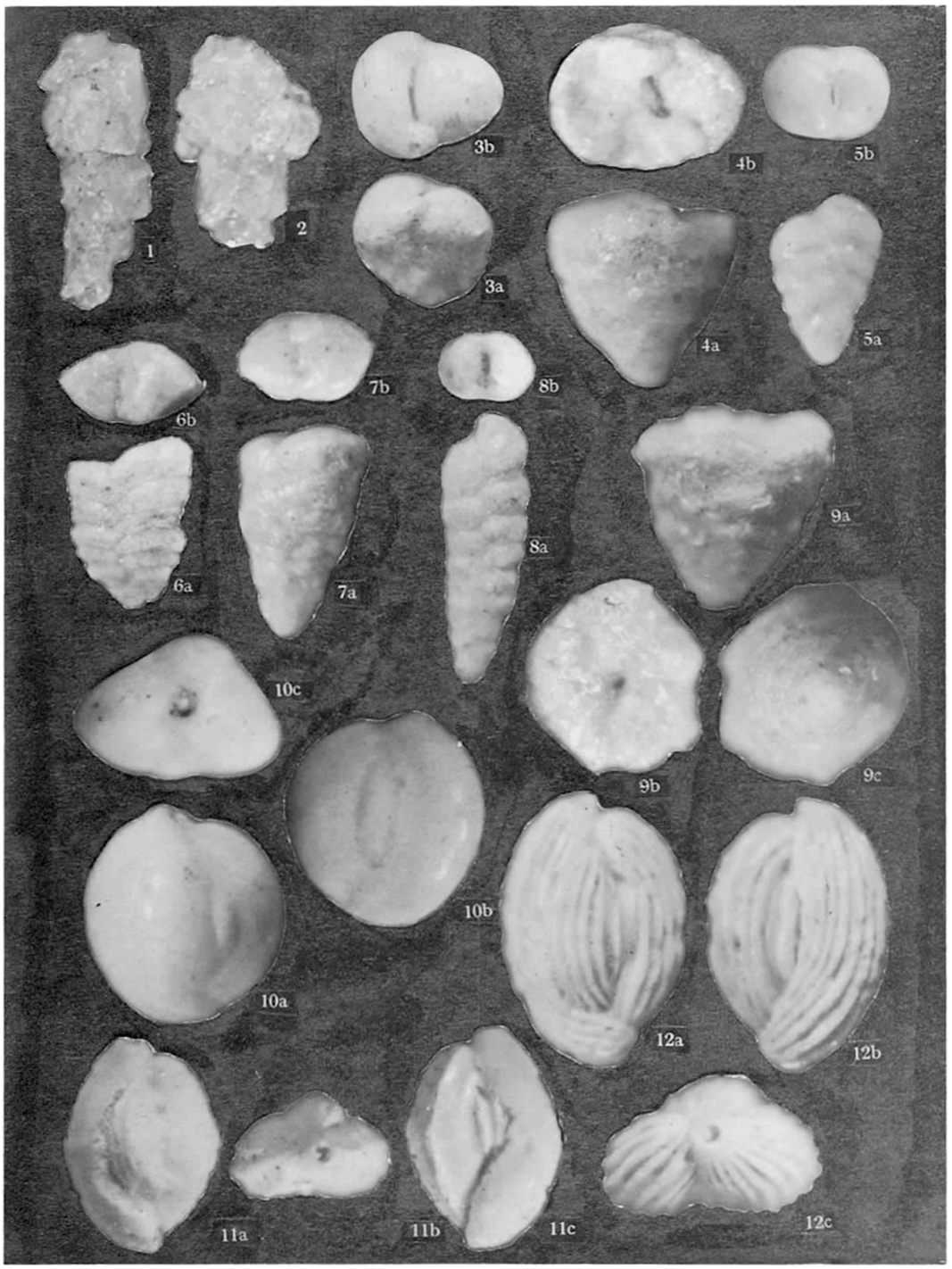

Kim and Han: Foraminifera offshore from southeastern coast of Korea

EXPLANATION OF PLATE II-2

Figures

1. a–b. *Saracenaria latifrons* (Brady). ×51. Hypotype (DGSU coll. cat. 00195)
2. *Amphycoryna scalaris sagamiensis* (Asano). ×30. Hypotype (DGSU coll. cat. 00196)
3. *Lagena elongata* d'Orbigny. ×39. Hypotype (DGSU coll. cat. 00197)
4. a–b. *Lenticulina lucidus* (Cushman). ×36. Hypotype (DGSU coll. cat. 00198)
5. *Dentalina emaciata* Reuss. ×18. Hypotype (DGSU. coll. cat. 00199)
6. a–c. *Cruciloculina asanoi* Loeblich & Tappan. ×29. Hypotype (DGSU coll. cat. 00200)
7. a–b. *Lenticulina* sp. ×18. Hypotype (DGSU coll. cat. 00201)
8. a–b. *Pyrgo fornasinii* Cushman & Parr. ×27. Hypotype (DGSU coll. cat. 00202)
9. *Guttulina yabei* Cushman & Ozawa. ×26. Hypotype (DGSU coll. cat. 00203)
10. a–b. *Lenticulina nikobarensis* Schwager. ×26. Hypotype (DGSU coll. cat. 00204)
11. a–b. *Lenticulina depressus* Asano. ×18. Hypotype (DGSU coll. cat. 00205)
12. a–b. *Nonionella stella* Cushman & Moyer. ×89. Hypotype (DGSU coll. cat. 00206)
13. *Trifarina kokozuraensis* (Asano). ×63. Hypotype (DGSU coll. cat. 00207)
14. a–b. *Rosalina bradyi* (Cushman). ×75. Hypotype (DGSU coll. cat. 00208)
15. *Uvigerina akitaensis* Asano. ×56. Hypotype (DGSU coll. cat. 00209)

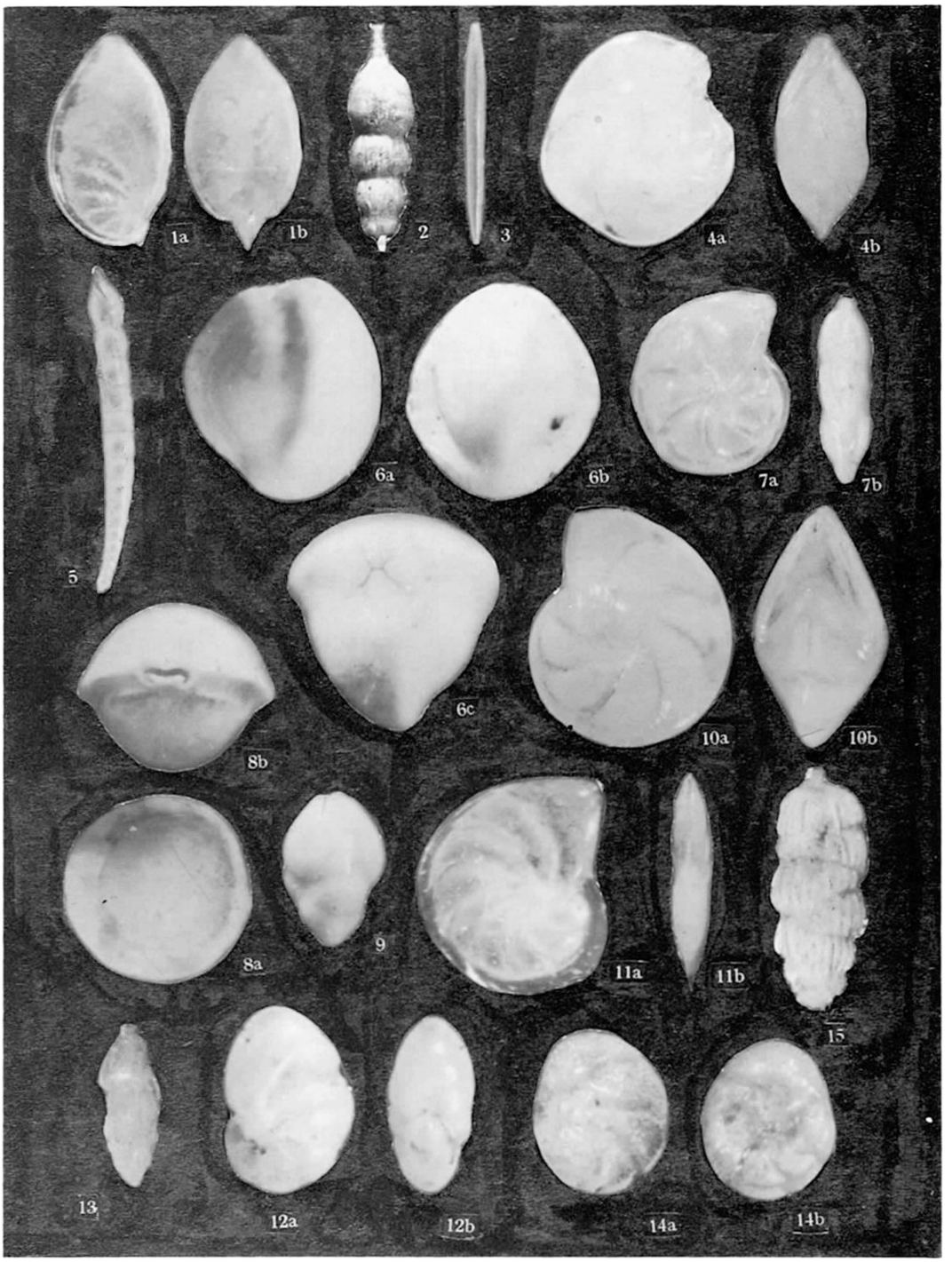

Kim and Han: Foraminifera offshore from southeastern coast of Korea

EXPLANATION OF PLATE II–3

Figures

1.a–c. *Discorbinella bertheloti* (d'Orbigny). ×43. Hypotype (DGSU coll. cat. 00210)

2.a–c. *Ammonia takanabensis* (Ishizaki). ×57. Hypotype (DGSU coll. cat. 00211)

3.a–c. *Pseudorotalia gaimardii* (d'Orbigny). ×36. Hypotype (DGSU coll. cat. 00212)

4.a–b. *Globocassidulina subglobosa* (Brady). ×38. Hypotype (DGSU coll. cat. 00213)

5.a–c. *Ammonia indopacifica* (Cushman). ×20. Hypotype (DGSU coll. cat. 00214)

6.a–b. *Globocassidulina japonica* (Asano & Nakamura). ×30. Hypotype (DGSU coll. cat. 00215)

7.a–c. *Planulina wuellerstorfi* (Schwager). ×32. Hypotype (DGSU coll. cat. 00216)

8.a–b. *Pullenia bulloides* (d'Orbigny). ×59. Hypotype (DGSU coll. cat. 00217)

9.a–b. *Rosalina vilardeboana* d'Orbigny. ×55. Hypotype (DGSU coll. cat. 00218)

10.a–b. *Cassidulina sublimbata* Asano & Nakamura. ×49. Hypotype (DGSU coll. cat. 00219)

11.a–b. *Cassidulina yabei* Asano & Nakamura. ×67. Hypotype (DGSU coll. cat. 00220)

12.a–b. *Hyalinea balthica* (Schroeter). ×56. Hypotype (DGSU coll. cat. 00221)

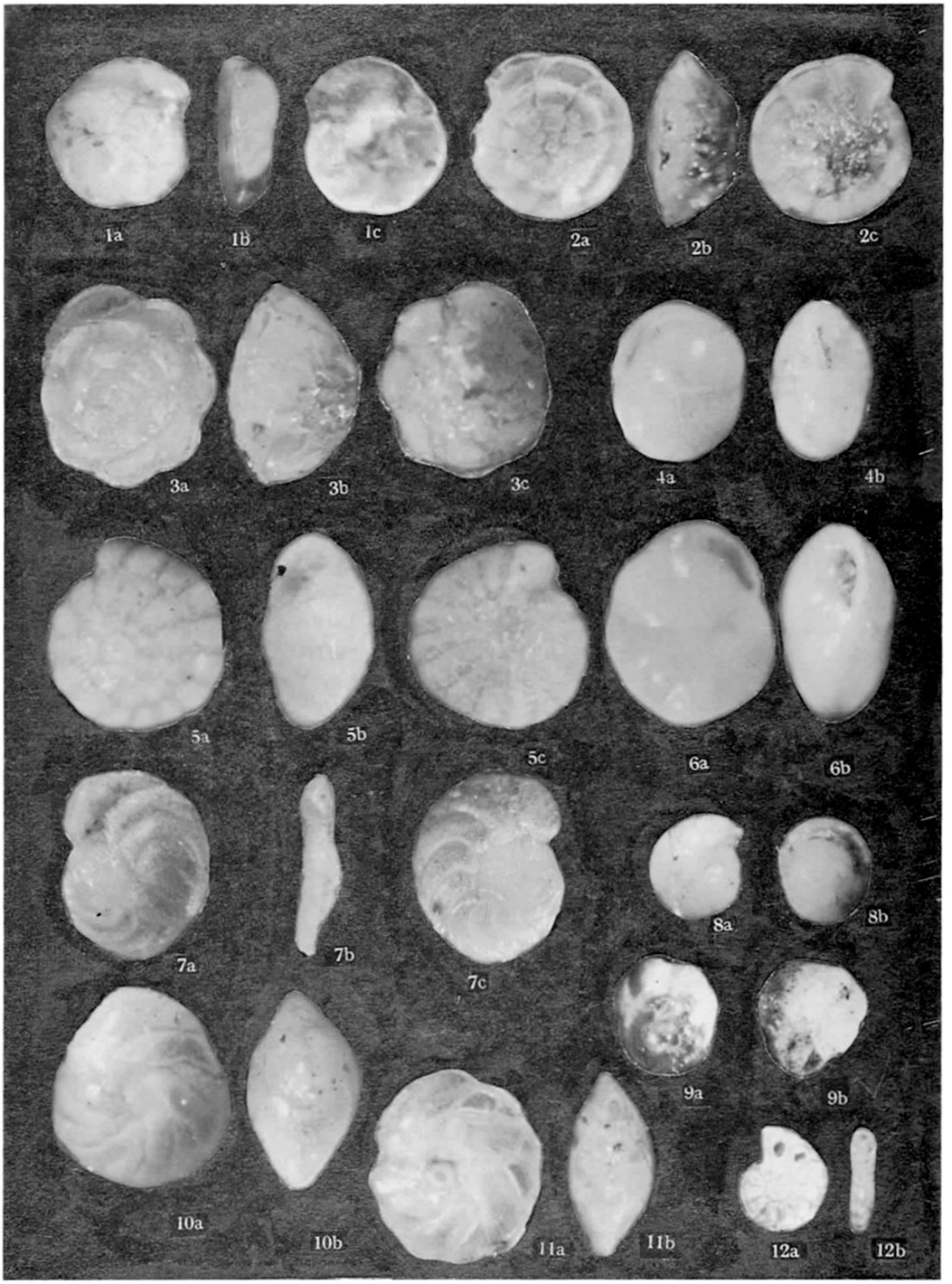

Kim and Han: Foraminifera offshore from southeastern coast of Korea

EXPLANATION OF PLATE II–4

Figures

1. *Orbulina universa* d'Orbigny. ×42. Hypotype (DGSU coll. cat. 00222)
2. a–c. *Globigerina bulloides* d'Orbigny. ×56. Hypotype (DGSU coll. cat. 00223)
3. a–c. *Globigerinoides immaturus* LeRoy. ×44. Hypotype (DGSU coll. cat. 00224)
4. a–c. *Globigerinoides conglobatus* (Brady). ×42. Hypotype (DGSU coll. cat. 00225)
5. a–c. *Globoquadrina dutertrei* (d'Orbigny). ×44. Hypotype (DGSU coll. cat. 00226)
6. a–b. *Globorotalia menardii* (d'Orbigny). ×30. Hypotype (DGSU coll. cat. 00227)
7. a–c. *Turborotalia inflata* d'Orbigny. ×57. Hypotype (DGSU coll. cat. 00228)
8. a–c. *Globigerinoides ruber ruber* d'Orbigny. ×75. Hypotype (DGSU coll. cat. 00229)
9. a–c. *Turborotalia acostaensis* Blow. ×69. Hypotype (DGSU coll. cat. 00230)
10. *Pulleniatina obliquiloculata* (Parker & Jones). ×63. Hypotype (DGSU coll. cat. 00231)
11. a–b. *Hastigerina siphonifera* (d'Orbigny). ×50. Hypotype (DGSU coll. cat. 00232)
12. a–b. *Globigerina pachyderma* (Ehrenberg). ×70. Hypotype (DGSU coll. cat. 00233, 00234)

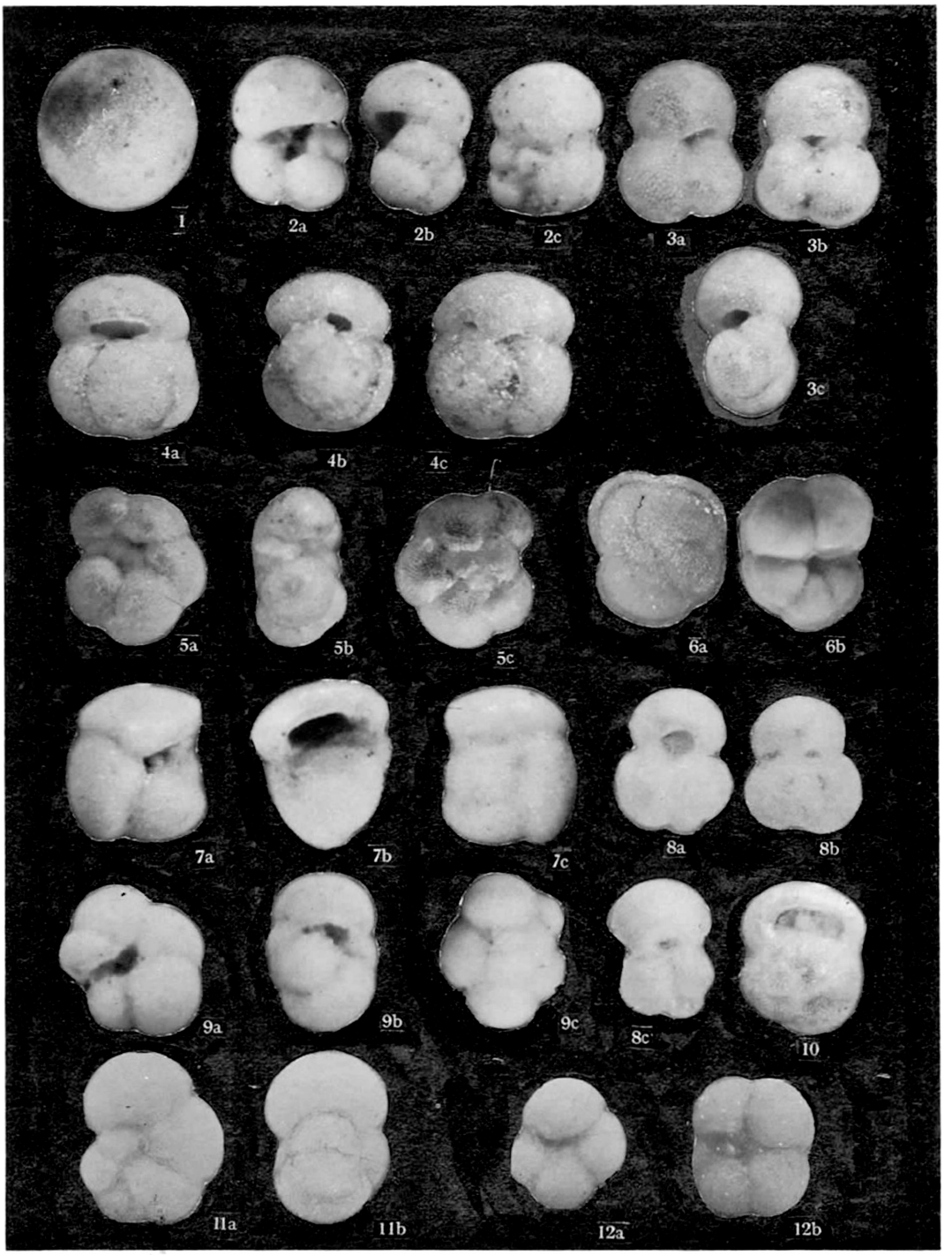

Kim and Han: Foraminifera offshore from southeastern coast of Korea

Blank page

Page blanche

Volume 6 United Nations ECAFE, CCOP TECHNICAL BULLETIN July 1972

III. DISTRIBUTION OF PLANKTONIC FORAMINIFERS IN THE SURFACE SEDIMENTS OF TAIWAN STRAIT

(Project CCOP-1/ROC.3)

By

Tunyow Huang

Chinese Petroleum Corporation, Miaoli, Taiwan, China; and
National Taiwan University, Taipei, Taiwan, China

(with table III-1, figures III-1 to III-40, and plates III-1 to III-3)

ABSTRACT

The assemblages of planktonic foraminifers in 90 bottom samples from Taiwan Strait have been analyzed; of these 18 were short gravity cores and 72 were snapper samples taken with a special tool. The data concerning temperature and salinity conditions were obtained on cruises made during the years 1962 to 1970.

The distribution of planktonic foraminifers in the sediments of Taiwan Strait is controlled by a number of physical and biological variables that may affect the growth of the species. The introduction of large volumes of fresh water in the coastal areas of western Taiwan results in a lowering of surface salinity and the exclusion of planktonic foraminifers. On the other hand, large numbers of planktonic foraminifers are found in the shallow basin in the middle of the strait.

Twenty-seven species of planktonic foraminifers are recorded. The presence of cool-water species in the assemblage is regarded as being due to the influence of the China Coastal Stream flowing from the north, while the warm-water species have been brought from the tropics by the Kuroshio Current. The presence of some poorly preserved specimens indicates a mixing of planktonic assemblages from different sources.

The geographic distribution of the planktonic forms and their relative abundance are discussed. The distribution patterns, foraminiferal dominance, associated diversity, and biological indicators are analyzed and described. The diversity is highest in the deeper portions of the strait and the major patterns of distribution are greatly influenced by the currents and the submarine topography.

INTRODUCTION

This is one of a series of papers describing and interpreting various aspects of the oceanography and sedimentology of Taiwan Strait. Studies to determine the patterns of distribution of Recent planktonic foraminifers in the oceans of the world have been

carried out by many authors. Although the broad patterns are now known, much more detailed work still remains to be done, especially on the ecophenotypic variation within species that takes place in response to changing physical conditions which vary with latitude, among other factors. It is well known that species of planktonic foraminifers are restricted to, and characteristic of, waters of certain temperature limits and that their relative and absolute abundances change with changing characteristics of the water mass. Because of this, planktonic foraminifers are being increasingly utilized for studies of past climatic and oceanographic conditions, especially for those of the Neogene.

The writer analyzed the distribution patterns and the variability of the species diversities in marginal sea areas, taking the environments of Taiwan Strait as an example. This information should be of use in determining more precisely the paleo-oceanographic and paleoclimatological changes during Cenozoic time in Taiwan. The area investigated is an ideal location for such a study because of the presence of warm- and cool-water masses in this marginal sea area.

This study is based on 90 surface sediment samples collected between latitudes 22°N and 26°N and longitudes 118°E and 122°E (Huang, 1971, Fig. II-1). Of these, 18 are short gravity cores and 72 are snapper samples taken with a special tool (Huang, 1971); consequently, there was no mixing of sediments as is usual for dredged samples.

Only the foraminifers from the upper 2 cm of each core were examined, but the snapper samples may also have included slightly deeper layers of the sea floor. The samples were taken in depths ranging from 3 to 200 m; their locations are shown on a map in an earlier publication (Huang, 1971, Fig. II-1). All samples collected from depths shallower than 200 m (Huang, 1971, Figs. II-1 and II-2) contained about 30 per cent of planktonic foraminifers (Huang, 1971, Fig. II-22). All samples were weighed dry and washed on a 74-mesh Tyler screen. A modified Phleger splitter was used to obtain representative fractions of each concentrate for percentage counts.

PREVIOUS STUDIES

A large amount of literature has accumulated in recent years concerning the distribution, ecology, and morphologic variation of recent planktonic foraminifers. The waters of the Pacific and Atlantic Oceans have been investigated most thoroughly.

The earliest contributions on the planktonic foraminifers of the Asiatic shelf were made by Waller and Polski (1959); they showed the broad patterns of distribution of planktonic foraminifers over the Asiatic shelf, based on the study of 300 samples of surface sediments, and they showed the distribution of faunal groups in relation to temperature ranges and latitude.

Cheng and Cheng (1964), studied the living planktonic foraminifers from the northern part of the South China Sea; they observed the seasonal variations in some planktonic foraminifers and concluded that the degree of salinity has a great influence upon planktonic foraminifers.

DESCRIPTION OF THE AREA

Hydrographic conditions which influence the distribution of planktonic foraminifers have been described by various authors for the greater part of the area, and were summarized by the writer in a previous paper (1971). Some important factors affecting the distribution of the planktonic foraminifers are discussed and the following information is added:

Climate

The air temperature of Taiwan Strait is mainly influenced by that of the adjoining continent, where it is high in the summer and low in winter. On the Penghu Islands, the average temperature is 28.1 °C in July and 15.9 °C in January and February; the annual range is therefore about 12 °C.

The high Central Range of Taiwan has a notable effect on the rainfall; it produces a rain shadow area over western Taiwan and Taiwan Strait, and the annual precipitation at Penghu is the lowest recorded for this area.

The runoff of river water greatly dilutes the sea water along the western coast. Flow measurements of the 19 major rivers were given by Huang (1971, Fig. II-4), and the annual flows and months of largest flow for the 15 rivers flowing into Taiwan Strait are listed in Table III-1; the total annual flow of these rivers is 36.54 × $10^9 m^3$ (Chu, 1971). According to the observations made at rainfall stations distributed all over Taiwan, the total annual rainfall is about 92.330 × $10^9 m^3$ but not all of it is included in the runoff of the rivers (total of 54.74 × $10^9 m^3$ for the 19 major rivers of Taiwan).

The wind in the strait is generally NNE, but north in June and July and SSW in

Table III-1. Annual flows of the fifteen major rivers flowing into Taiwan Strait from western Taiwan.

Name of river	Month of largest flow	Annual flow (cubic metres)
Tan-sui-ho	September	4.66 × 10^9
Tou-chien-chi	"	0.65 × 10^9
Hou-long-chi	"	0.87 × 10^9
Ta-an-chi	"	1.68 × 10^9
Ta-chia-chi	"	2.75 × 10^9
Wu-chi	"	6.38 × 10^9
Cho-shui-chi	"	6.18 × 10^9
Pei-kang-chi	August	0.80 × 10^9
Pu-tsu-chi	"	0.50 × 10^9
Pa-chang-chi	"	0.47 × 10^9
Chi-shui-chi	"	0.32 × 10^9
Tzen-wen-chi	"	2.40 × 10^9
Zeh-zon-chi	"	0.45 × 10^9
Kao-pin-chi	"	7.66 × 10^9
Lin-pien-chi	September	0.77 × 10^9
	Total	36.54 × 10^9

August. The wind in winter is very strong, with the mean velocity reaching 9.1 m/sec in December, and there are 20.8 days of storm with winds exceeding a mean velocity of 15 m/sec. The wind velocity is low in summer except during typhoons.

Currents

The most up-to-date surface current maps of Taiwan Strait and adjacent seas are those published by the U.S. Naval Hydrographic Office (1964) and the Naval Hydrographic Office of China (1962). Three major currents affect the area: the Kuroshio Current, the China Coastal Stream, and drift due to the monsoon in the South China Sea.

The strong warm Kuroshio Current comes from the southeast and passes along the east coast of Taiwan to the north, and a branch of it enters the South China Sea through the Bashi Channel. This branch joins the surface drift produced by the prevailing northeast wind of the monsoon in winter and flows towards the southwest; in summer time, however, as the prevailing wind in the South China Sea is from the southeast, the branch of the Kuroshio is diverted by the surface drift caused by the southwest monsoon and it then flows northeastwards through Taiwan Strait and joins the main stream of the Kuroshio again in the East China Sea.

The cool China Coastal Stream comes from the north and flows along the coast of the mainland side of Taiwan Strait to the South China Sea. In winter the northeast wind prevails and the coastal current flows through the strait to the South China Sea; however, during summer, when the southwest monsoon is prevailing, this current cannot enter the strait.

The surface drift due to the monsoon in the South China Sea flows towards the southwest in winter and towards the northeast in summer.

Vertical water movements

On the photograph taken by Astronauts Young and Collins, NASA, on 20 July 1966, two areas of upwelling are clearly shown. One is in a long-known fishing region west of the Tainan coastal plain and the other was first observed by the astronauts in an area off the east coast near Taitung.

The zones of upwelling are distinguished by the steepening of the thermocline, decrease in temperature, and increase in the concentration of phosphate at the depth of 100 m (Oceanographic Data Report of CSK, nos. 1–4, 1966–1970). The phenomenon of upwelling off the southwest coast of Taiwan from Tungkang to Tainan is not as clearly marked as in the area off the southeast coast.

Surface temperature

On the basis of latitude, half of the strait belongs to the subtropical zone and half to the tropical zone. Climatologically, however, the whole of the strait is influenced greatly by both the continent and the ocean and the effects of the monsoon prevail throughout.

The high temperature Kuroshio Current comes from the tropics and the China Coastal Stream has its origin in the seas to the north; the sea water in the strait is therefore warmer in summer and cooler in winter. The variation of surface water tempera-

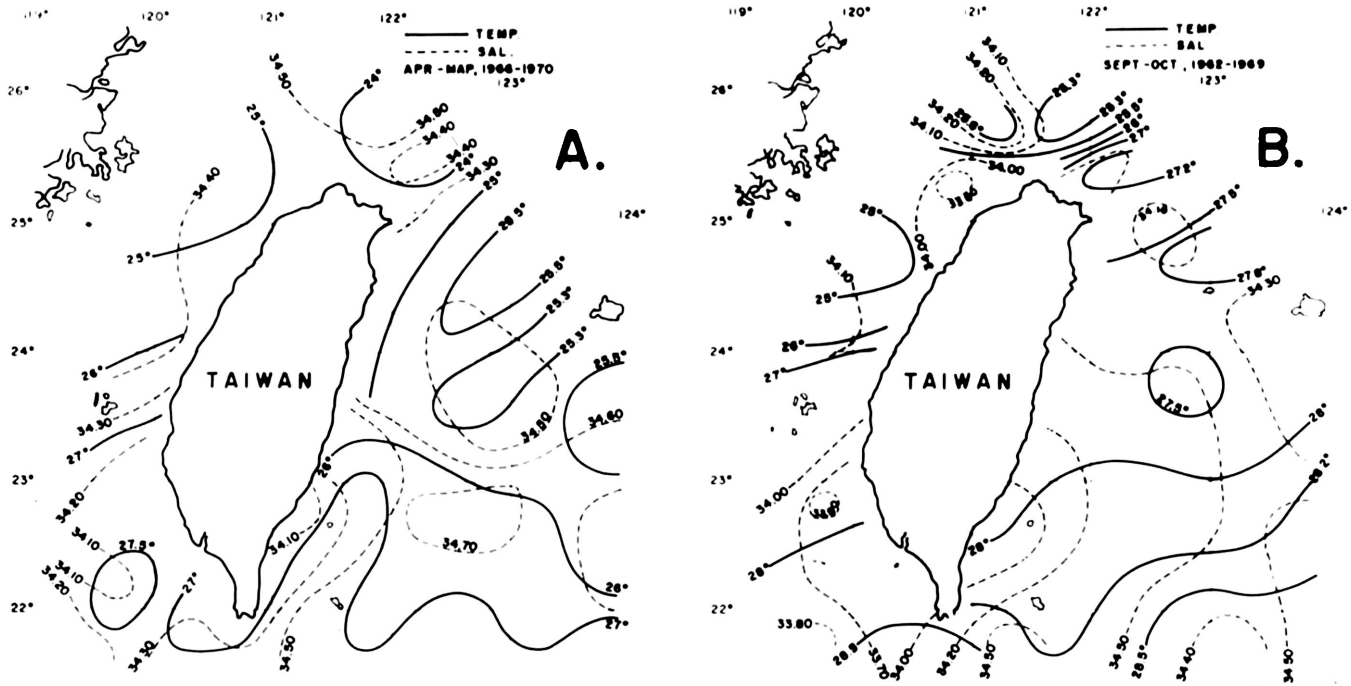

Figure III-1. Temperature and salinity of surface waters surrounding Taiwan; A, April–May 1966 to 1970; B, September–October 1862 to 1969.

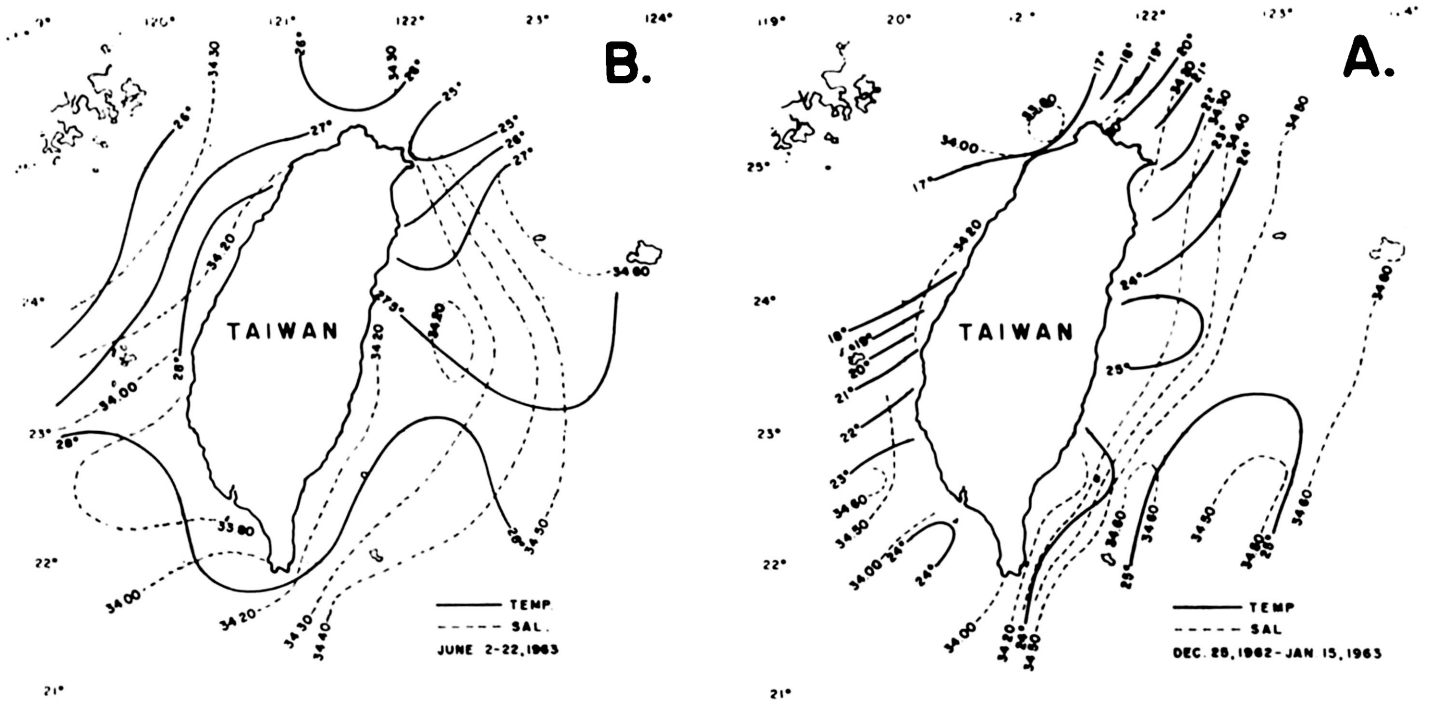

Figure III-2. Temperature and salinity of surface waters surrounding Taiwan; A, 25 Dec. 1962 to 15 Jan. 1963; B, 2–22 June 1963.

ture from the coast of the mainland across Taiwan Strait is quite large; for example, in February, it is 12 °C near Amoy, on the mainland, and 23 °C near the southern tip of Taiwan. In August, however, only the isotherm of 28 °C crosses the strait from northeast to southwest.

All the water temperature records fall within a range suitable for the existence of both tropical and temperate water species of foraminifers. According to data obtained by the R/V "Vang Ming" in December 1962 and January 1963, the temperature ranges from 17 °C in the area northwest of Taiwan to 24 °C in the area to the southwest of Taiwan (Fig. III-1). The mean value of the temperature for the months of April and May, according to data collected on cruises during the years 1966 to 1970, ranges from 25 °C in the north part of the strait to 27.5 °C in the southern part (Fig. III-2A). In September and October, the mean values in the years 1962 to 1969 ranged from 25 °C in the northern part of Taiwan Strait to 28 °C in the southern part (Fig. III-2B).

Surface salinity

Surface isohaline maps (see Fig. III-1 and III-2) were compiled by Chu (1961). The salinity distribution in Taiwan Strait is influenced by the different currents as well as the precipitation and river runoff in this area, but the seasonal variation of salinity is not as great as that of the temperature. The salinity in the Taiwan Strait is usually a little above 34,000 parts per million (ppm) but along the coast of the mainland it can be somewhat lower than 33,000 ppm.

According to data obtained by the R/V "Yang Ming", the salinity in December 1962 and January 1963 was 33,800 ppm in the strait and 34,600 ppm in the Pacific Ocean (Fig. III-1). The mean value of the salinity in Taiwan Strait during April and May, according to data collected on cruises during the years 1966 to 1970, is lowest (34,100 ppm) in the area offshore from southwestern Taiwan (Fig. III-2). During September and October, the mean value of the lowest salinity for the years 1962 to 1969 (33,800 ppm) is also in the offshore area southwest of Taiwan (Fig. III-2).

The salinity of the China Coastal Stream is usually between 31,000 and 33,000 ppm but it can be much lower off the estuaries during the rainy season, and the surface layer may have a much lower salinity than the main body of the current.

Oxygen content and pH

The distribution of dissolved oxygen in sea water is influenced by temperature, current flow, and biological activities. The distribution of O_2 during April and May, according to the mean values determined on cruises during 1966 to 1970 (Fig. III-3B), and for September and October for the years 1962 to 1969 (Fig. III-3A) shows that the value of O_2 content is higher (4.6 m*l*/*l*) in the northern part of the strait and becomes lower (4.3 m*l*/*l*) to the south. These values are only for the surface water layers and they are slightly less at depth. The distribution of pH value varies only slightly in the surface waters of the strait, ranging from 8.25 to 8.35 (Fig. III-3).

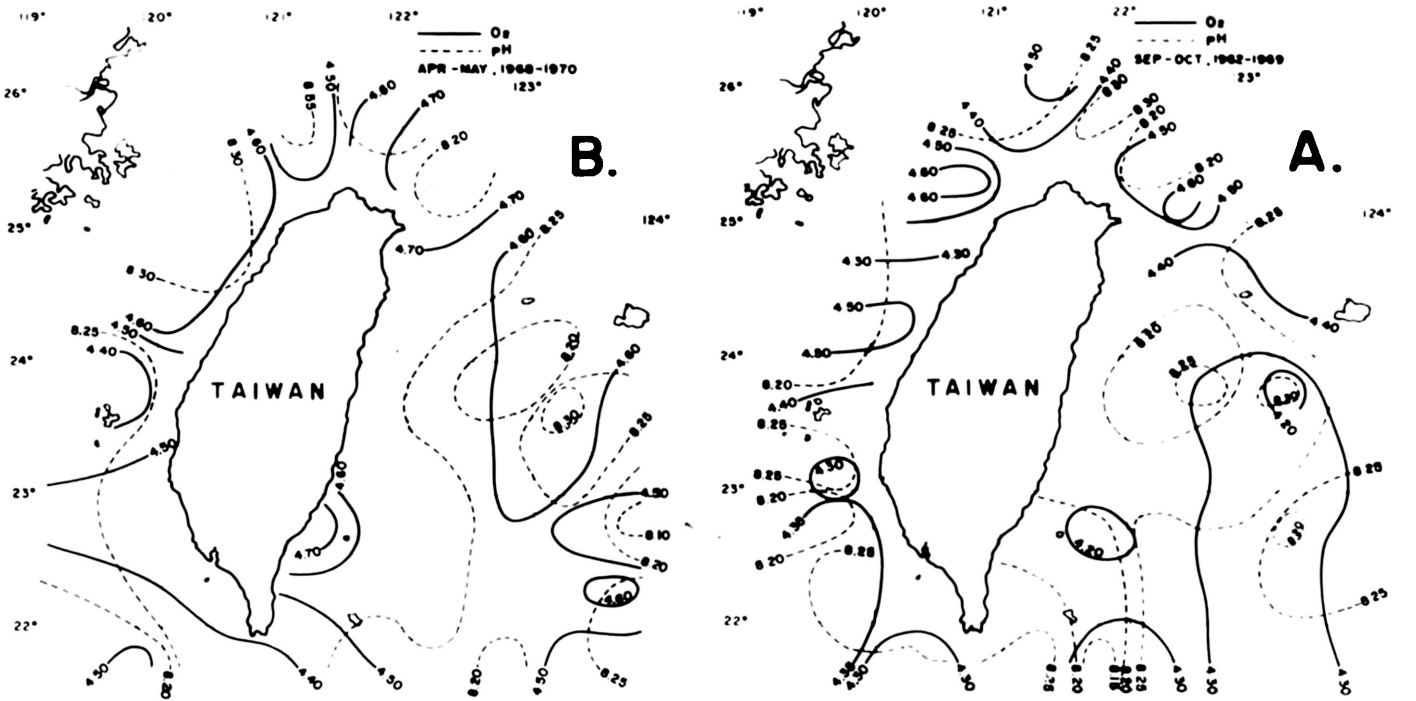

Figure III-3. Oxygen content and pH of surface waters surrounding Taiwan; A, September–October 1962 to 1969; B, April–May 1966 to 1970.

ZOOPLANKTON

It is well known that the quantity of plankton in different areas of tropical regions depends on the supply of nutrients to the upper waters; the distribution of different groups of organisms in these areas therefore varies greatly, depending on their place in the food chain. The present state of knowledge of the trophic position of foraminifers in communities inhabiting a number of distinctive marine environments has been discussed by Lipps and Valentine (1970). Knowledge of the distribution of the biomass and the abundance of zooplankton in the waters surrounding Taiwan is useful for an understanding of the occurrence of planktonic foraminifers in Taiwan Strait.

The distribution of zooplankton in the waters surrounding Taiwan is shown in Fig. III-4. According to Tan (1971) and Tseng (1971), the zooplankton biomass in the waters surrounding Taiwan was found to be smaller in comparison with that of the North Pacific region and the volume of the biomass varied considerably between April (160.39 g/100 m^3) and September (122.64 g/100 m^3). It is comparatively richer in the northeastern and northwestern offshore areas of Taiwan, as well as in the zones of upwelling, and poor in the area southeast of Taiwan. In general, the plankton biomass and the abundance of zooplankton coincide with the regions of upwelling, both to the southeast and southwest of Taiwan.

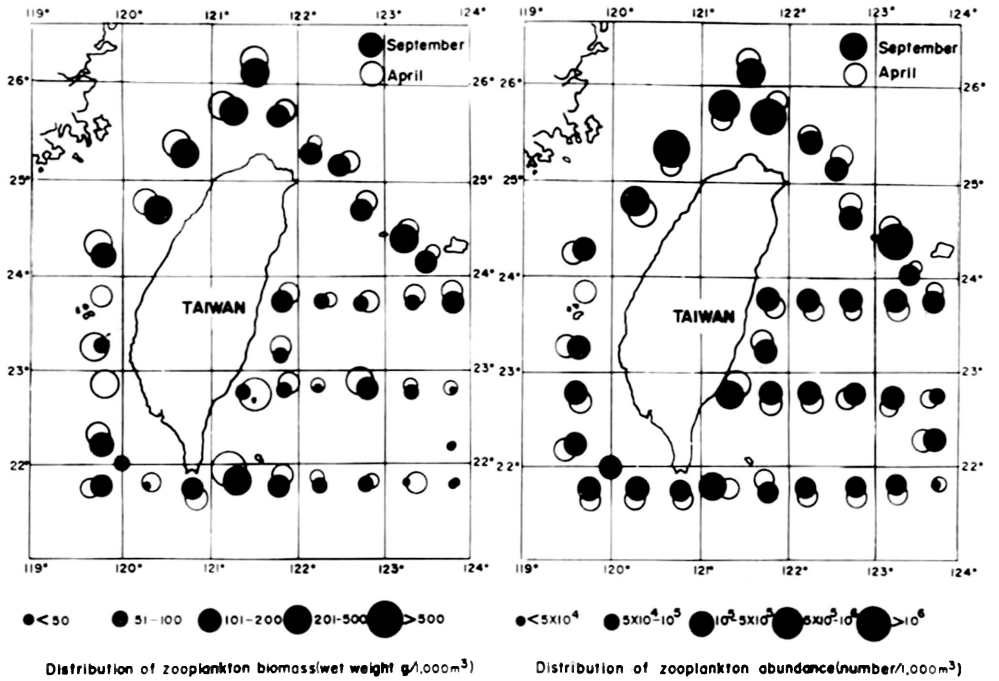

Figure III-4. Distribution of the zooplankton biomass in the waters surrounding Taiwan during the months of September and April, in terms of unit volume (wet weight) and numbers of specimens per unit volume.

The abundance of individuals of zooplankton per 1,000 m^3 fluctuates greatly in the area north of Taiwan, between April (76,480/1,000 m^3 and 129,438/1,000 m^3) and September (509,827/1,000 m^3 and 1,105,443/1,000 m^3). Zooplankton are abundant in the sea off northwestern Taiwan, perhaps because the area is affected by pollutants and is nutrient-rich. A large amount of fouling organisms from some big rivers of the mainland in the north supply food for the zooplankton and stimulate their production: the planktonic foraminifers therefore may also benefit from this.

GENERAL DISTRIBUTION PATTERNS

The planktonic foraminifers of Taiwan Strait, of which 27 species and sub-species have been recognized, consist mostly of forms typically found in shallow tropical waters. Only two species (*Globigerina borealis* and *G. bulloides*) are usually found in cooler water and the tests of most of the species in the sediments of Taiwan Strait are of smaller size and thinner those found in tropical waters.

The distribution of planktonic foraminifers in the sediments of Taiwan Strait is significantly affected by a combination of physical, chemical, and biological variables that determine the variations in the environment. Foremost among these is the large volume of fresh water flowing into the sea off the western coast of Taiwan from many large rivers. During the rainy season, the amount of fresh water flowing into the sea is greatly increased and the salinity becomes notably lower. As planktonic foraminifers are stenohaline, the numbers of planktonic forms in the sediments near the shore zone are much lower than elsewhere and the tests are generally not as well developed as in areas of higher salinity. This illustrates the value of making plots of planktonic foraminiferal numbers as they provide an indication of euryhaline conditions and the courses of currents.

The high planktonic foraminiferal numbers in the middle portion of the strait are due to slower rates of deposition of sediments, and may also be connected with the topographic depression in this area. The pattern of distribution of planktonic foraminifers is shown in Figures II-9 and II-10 of a previous paper by the writer (1971) in terms of numbers of planktonic foraminifers in unit volumes of sediment and as percentages of planktonic foraminifers in relation to the total foraminiferal population. The numbers and percentages of planktonic foraminifers are closely related to submarine topography (Huang, 1971, Fig. II-2) and current action (Huang, 1971, Fig. II-6). Large quantities (high percentages) of planktonic foraminifers are present in the Penghu Channel and the Chilung Channel areas (Huang, 1971, Fig. II-3) and small quantities (low percentages) of planktonic foraminifers are present north of the Taiwan Bank and in the near-shore zone.

It is worthy of note that the areas of low percentages and low numbers of specimens of planktonic foraminifers in the strait correspond approximately to the areas of high concentrations of suspended sediment (more than 10 mg/*l*, Emery, *et al.*, 1969, Fig. 8) and high percentages of yellow colouration of the water (Emery, *et al.*, 1969, Fig. 6) in the near-shore zone of western Taiwan. The areas of highest concentration of planktonic forms in the waters around Taiwan also correspond to those of the planktonic biomass (Fig. III-4).

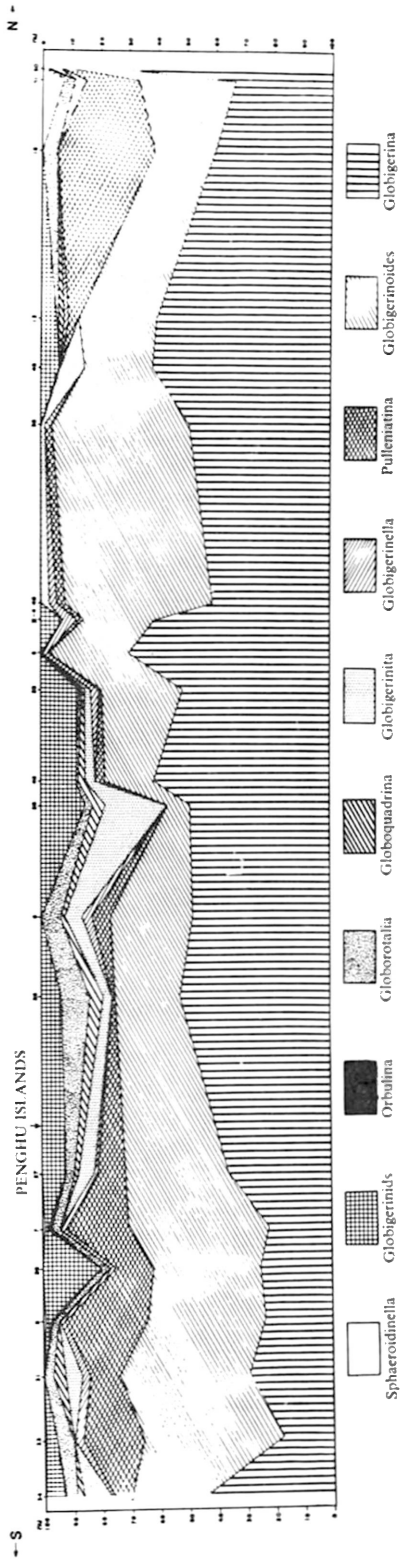

Figure III-5. Profile south to north through Taiwan Strait of the genera of planktonic foraminifers in terms of relative abundance.

The relative frequency distribution of each planktonic foraminiferal genus along S–N profiles is shown in Fig. III-5, to illustrate the inter-relationships among them. In general, the distribution of the major groups is greatly influenced by the high temperature Kuroshio Current and the low temperature China Coastal Stream. The distribution patterns of each species of planktonic foraminifers are shown in terms of relative abundance (percentage of the total number of planktonic tests) in Fig. III-12 to III-39.

MULTIVARIATE ANALYSES

Multivariate analyses (Fig. III-6) of a three-component system of selected dominant planktonic foraminiferal species or species groups reflect the distribution of the water masses or currents, as shown in Fig. III-40. The forms selected for the three-component system were *Globigerina bulloides*, *Neogloboquadrina dutertrei humerosa* and *Globigerinoides trilobus-sacculifer* (*G. sacculifer* and *G. trilobus* are taken together because of their similar temperature and depth range (see Hecht and Savin, 1971) as these are dominant planktonic forms in Taiwan Strait. The first of these is abundant in cold-temperate water; the second species is common at intermediate depths in temperate warm water; and both species of the third component are characteristic shallow tropical species. Multivariate analysis of the dead planktonic foraminiferal populations of these three

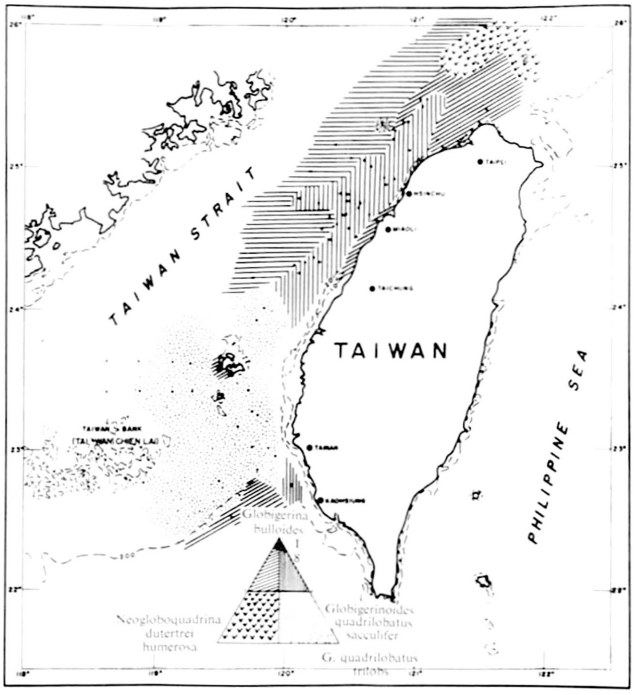

Figure III-6. Relationships in Taiwan Strait of *Globigerina bulloides*, *Neogloboquadrina dutertrei humerosa*, and *Globigerinoides quadrilobatus sacculifer* (including *G. g. trilobus*) as a three-component trigonal system.

components shows that *Globigerina bulloides* is dominant in the Matsu Basin, *Neogloboquadrina dutertrei humerosa* to the north of the Chilung Channel, *Globigerinoides trilobus-sacculifer* over the Taichung Bank and in the southern part of the strait (Fig. III-6). Based on this analysis, the distribution patterns of warm and cold fauna on the floor of the strait is seen to be quite similar to that of the currents or water masses in the area (Huang, 1971).

DIVERSITY RELATIONSHIPS

For the diversity (Berger and Parker, 1970) of the planktonic foraminiferal assemblages on the sea floor of Taiwan Strait, the species diversity (Ds), species dominance (Dd), Simpson's diversity (Dp), and Shannon's diversity (Dh) were used to obtain the diversity distribution and the relationships among these four diversity indices, as shown in Fig. III-7.

Species diversity and compound diversity are only moderately well correlated (Fig. III-7A and C), whereas a good correlation exists between dominance and compound diversity. Once the proportions of the most abundant species in a sample have been determined, the distribution of the measures of compound diversity, notably of Dp, becomes rather narrowly circumscribed. However, no biological significance can be assigned to such regularities that arise from definitions.

Each diversity index (Ds, Dd, Dp, and Dh) is also plotted in relation to geographic distribution (Figs. III-8 to III-11). In general, the diversity observations are highest in the deeper portions of the strait.

BIOLOGICAL INDICATORS

The distribution of planktonic foraminiferal tests in marine sediments generally reflects their living patterns within given water masses. Because of this, the distribution of fossil planktonic foraminiferal tests in marine sediments is being used increasingly for reconstruction of paleo-oceanographic conditions. The organisms that are used to identify different water masses are termed biological indicators and the best of these are the planktonic forms because they have no movement of their own and are closely confined to the waters in which they live. Foraminiferal indicators were used for the first time by Boltovskoy (1959) to determine the limits of ocean currents.

Planktonic foraminifers are known to be sensitive to ecologic changes and they occur abundantly and are widely distributed throughout the world. It follows therefore that, because their distribution depends on the distribution of different current system and a number of species can be used as good biological indicators, some attempt could be made to define the limits of ocean currents with their help. Boltovskoy (1959) has observed that there is a good correspondence in the distribution of the faunas living in the water masses and the dead assemblages in surface sediments on the sea bottom. Because of this, the analysis of the distribution of the planktonic foraminifers in the surface sediments of Taiwan Strait has been used to determine the pattern of water movements in the

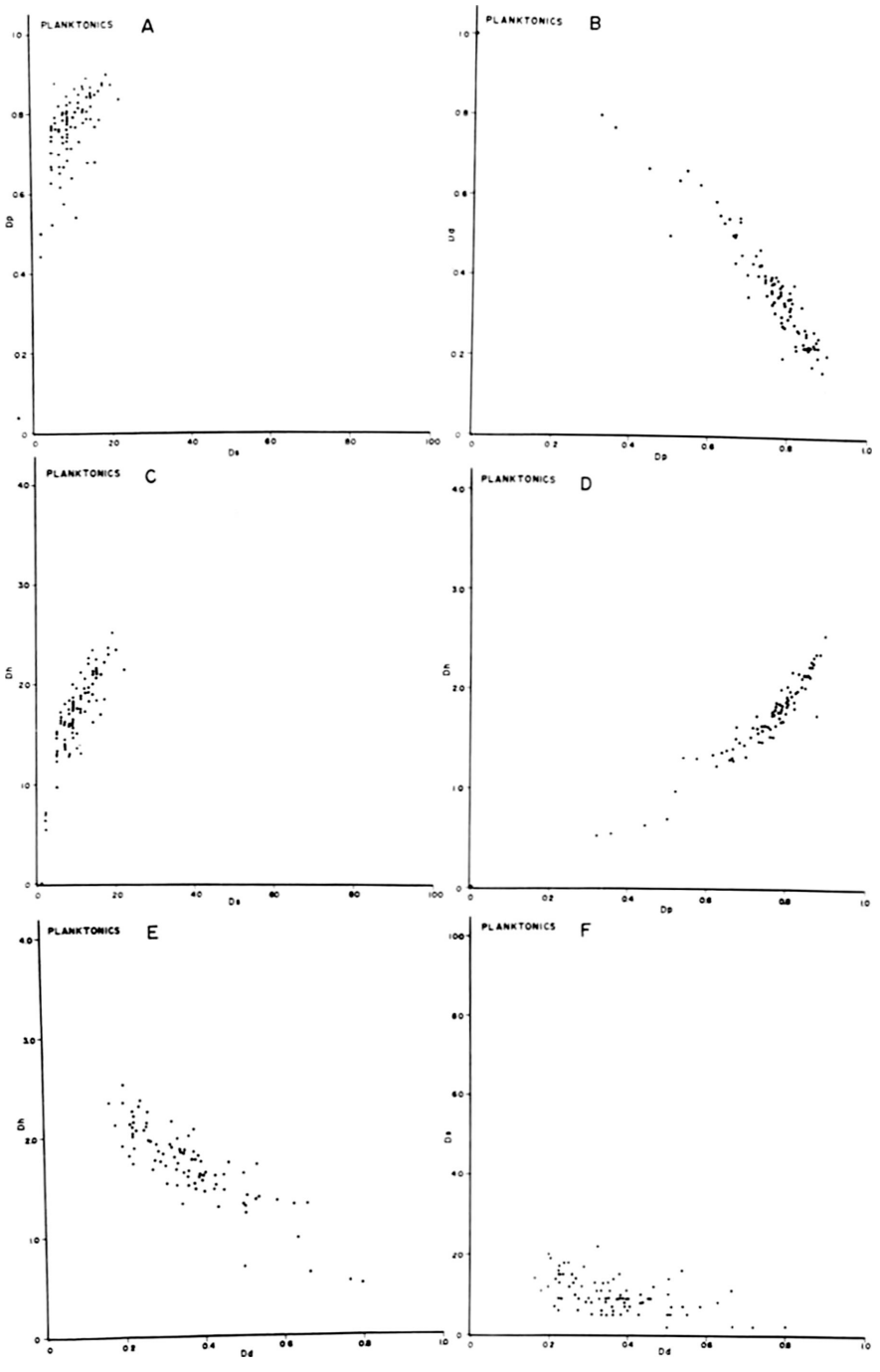

Figure III-7. Relationship between various deversity indices in planktonic foraminiferal assemblages from surface sediments in Taiwan Strait.

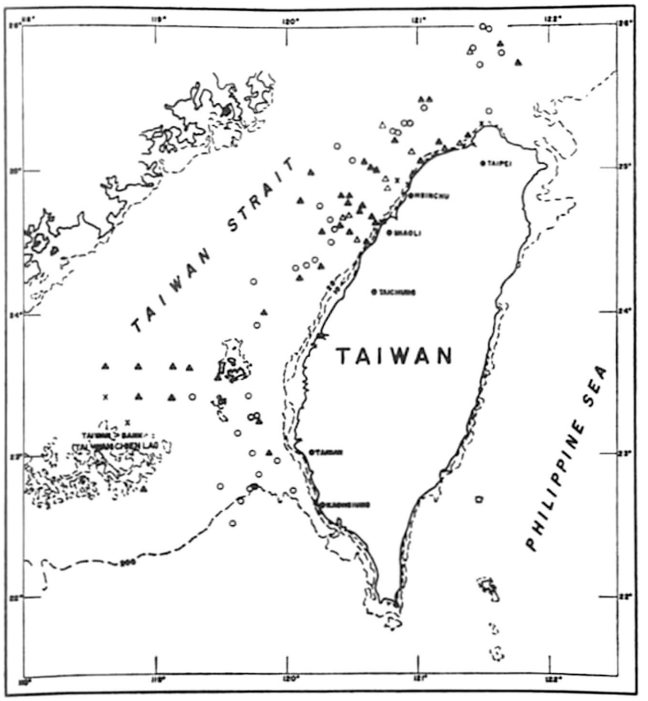

Figure III-8. Distribution patterns of species diversity (Ds) for planktonic foraminifers in Taiwan Strait.

× 1–2
△ 3–5
▲ 6–10
○ 11–20
● 21–25

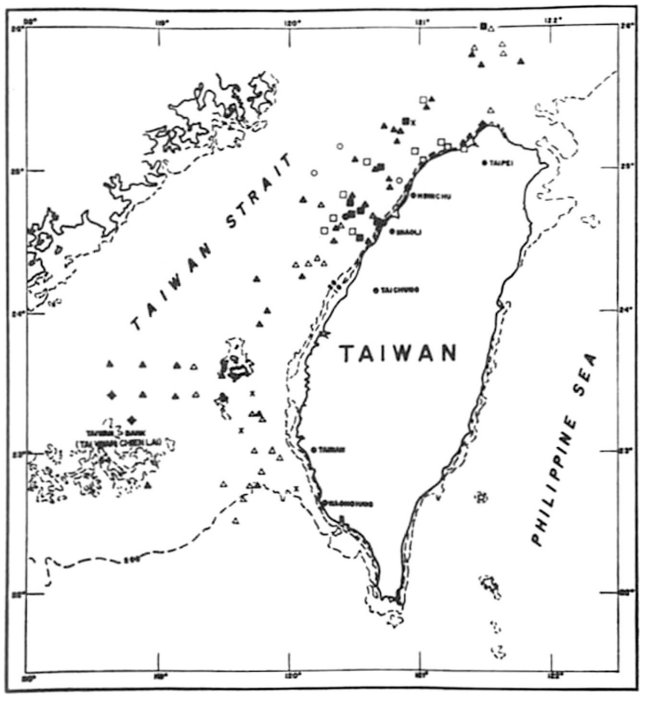

Figure III-9. Distribution patterns of diversity (species dominance, Dd) for planktonic foraminifers in Taiwan Strait.

× 0–2
△ 2–3
▲ 3–4
□ 4–5
■ 5–6
○ 6–7
● 7–8
◆ 8–9

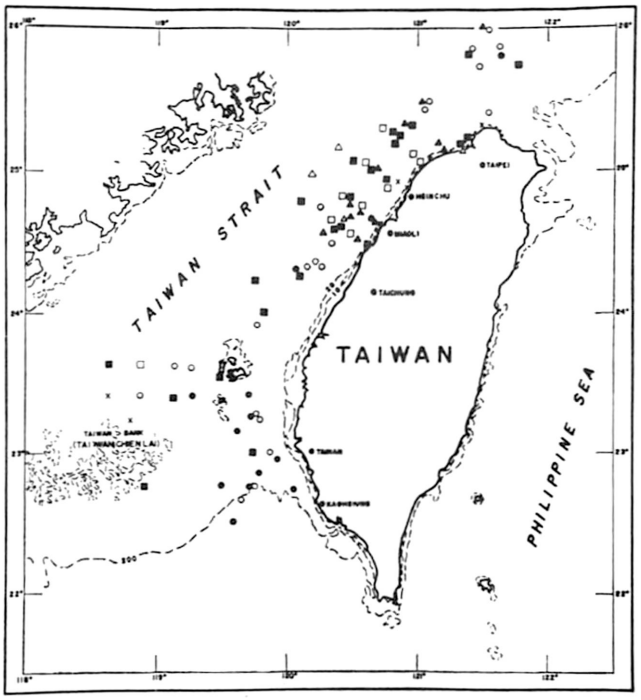

Figure III-10. Distribution patterns of diversity (Simpson's diversity, Dp) for planktonic foraminifers in Taiwan Strait.

- × 0–0.50
- △ 0.50–0.60
- ▲ 0.60–0.70
- □ 0.70–0.75
- ■ 0.75–0.80
- ○ 0.80–0.85
- ● 0.85–0.90

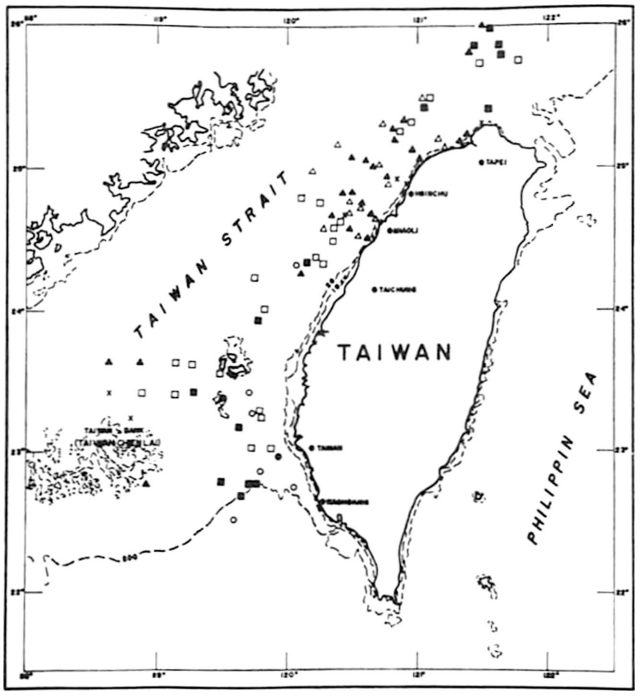

Figure III-11. Distribution patterns of diversity (Shannon's diversity, Dh) for planktonic foraminifers in Taiwan Strait.

- × 0–1.00
- △ $1.00 \leq H < 1.50$
- ▲ $1.50 \leq H < 1.75$
- □ $1.75 \leq H < 2.00$
- ■ $2.00 \leq H < 2.25$
- ○ $2.25 \leq H < 2.50$
- ● $2.50 \leq H < 3.00$

strait. The current patterns of Taiwan Strait (Huang, 1971, Fig. II-6) reflected by the analysis of the distribution patterns of the respective planktonic species are reasonably clear or readily amenable to interpretation.

The distribution of *Globorotalia cultrata menardii* indicates that the Kuroshio Current extends up to latitude 38° N (Asano, 1957) along the east coast of Japan, and that it turns to the east and becomes mixed with waters of other origins. Branches of the Kuroshio Current extend into Taiwan Strait around both the north and south ends of Taiwan (Fig. III-40).

The presence of *Globigerina bulloides* in large quantity in the northern half of the strait and in smaller quantity in the southern half (Fig. III-12) indicates that cool water masses extend into the strait from the north.

Globorotalia menardii tumida has been found in Taiwan Strait and it is assumed that the specimens of this species are not brought into the strait by the Kuroshio Current in the winter time, because this species was found only in the winter material of the Atlantic Ocean by Boltovskoy (1968).

Although *Globigerina borealis* (= *G. pachyderma*) is generally considered to be characteristic of high latitudes, it is interesting to note that the studies of Ericson (1959), Bandy (1960) and others on the coiling characteristics of this species have made it possible to divide the Recent populations of *G. borealis* into two categories: the sinistrally-coiled, cool-water type and the dextrally-coiled, warm-water type; the former is confined to high latitudes and the latter is abundant in temperate waters of mid-latitudes but sometimes extends also to low latitudes. In the samples from Taiwan Strait, all the specimens of *G. borealis* are dextrally coiled and, in this respect, fit the latter category. Additional evidence for their being warm-water types is furnished by the wall of their tests which is invariably thinner and lacks the calcareous thickening considered typical of cool-water forms. Populations of *G. borealis* with thinner tests, reflecting the effect of warmer temperatures, have also often been noted by other workers (Parker, 1962; Saito, 1963).

The occurrence of dextrally-coiled *G. borealis* in association with *G. bulloides* in significant numbers therefore indicates the existence of mid-latitude faunal elements in the assemblage under review. However, it can also be concluded that some cool-water elements have been introduced into the area by a current flowing southwards along the coast of the continent from the mid-latitudes, carrying with it elements of the northern cool-water fauna.

DISTRIBUTION OF INDIVIDUAL SPECIES

All of the 27 species of planktonic foraminifers found in the bottom sediments of Taiwan Strait are well known and they are not described again here. Only the original references are listed, and most of them are illustrated in the plates accompanying this paper. The distribution of each species is discussed below and their distribution and the frequency data obtained from analyses of all the samples are shown in Figs. III-12 to III-39. With the exception of two species characteristic of a cool-water temperate zone habitat (*Globigerina borealis* and *G. bulloides*), all of the other planktonic foraminifers found in the area are typical of tropical shallow waters.

Family HANTKENINIDAE Cushman, 1927

Genus *Hastigerina* Thomson, 1876

Hastigerina siphonifera (d'Orbigny) = *Globigerina siphonifera* d'Orbigny, 1839, *in* de la Sagra, Hist. Phys. Pol. Nat. Cuba, "Foraminiféres", p. 83, pl. 4, figs. 15-18; see Banner and Blow, 1960, Micropaleont., vol. 6, no. 1, p. 22, text-figs. 2 (lectotype), 3.

(Plate III-2, figs. 7-10; plate III-3, figs. 24, 25)

This species is rare (less than 10%), but persistent, in surface sediments throughout the strait (Fig. III-12). The great majority of the specimens are young and small-sized. *H. siphonifera* (in Taiwan Strait) may be divided into two groups, as in Parker's (1962) description: one having compressed chambers and reaching an involute form; and the other with the specimens rarely becoming completely planispiral and the chambers increasing more slowly in size. Both forms are commonly found in each sample. The maximum diameter is about 0.65 mm.

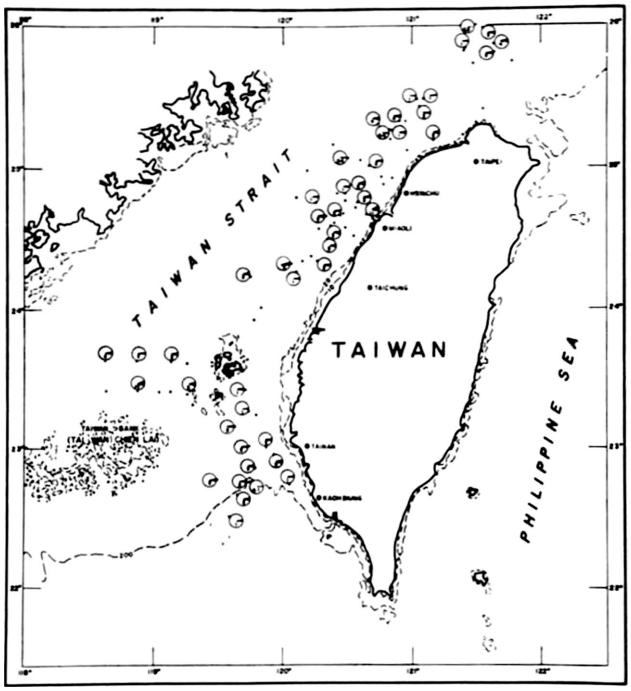

Figure III-12. Geographic distribution of *Hastigerina siphonifera* and its percentage of the total planktonic foraminiferal fauna at stations in Taiwan Strait.

Hastigerina pelagica (d'Orbigny) = *Nonionina pelagica* d'Orbigny, 1839; see Banner and Blow, 1960, Micropaleont., vol. 6, no. 1, p. 20-21, text-fig. 1.

(Plate III-3, figs. 15, 16)

This species was represented by ten specimens found only at station 15 (Fig. III-13)

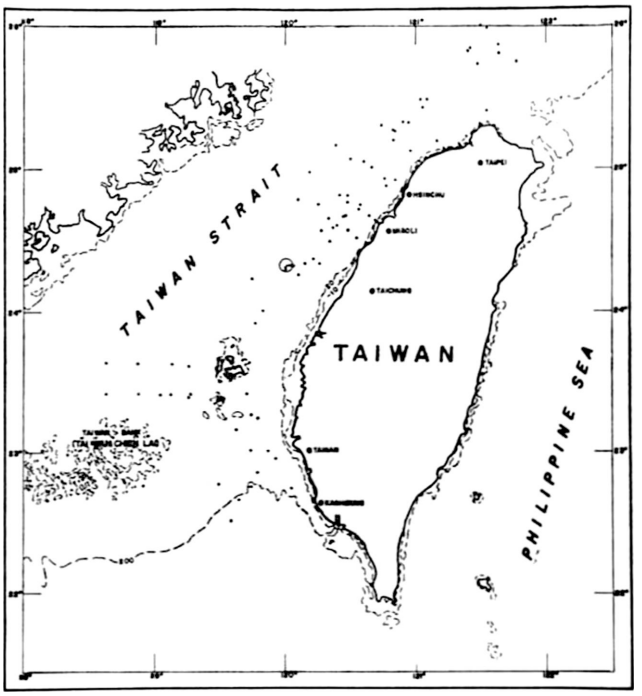

Figure III-13. Geographic distribution of *Hastigerina pelagica* and its percentage of the total planktonic foraminiferal fauna at stations in Taiwan Strait.

near the Taichung Bank. Its absence in the other samples may be due to the great fragility of its test.

Family GLOBOROTALIIDAE Cushman, 1927

Genus *Globorotalia* Cushman, 1927

Globorotalia crassaformis crassaformis (Galloway and Wissler) = *Globigerina crassaformis* Galloway and Wissler, 1927, Jour. Paleont., vol. 1, p. 41, pl. 7, fig. 12.

This species is rare in the surface sediments, and a small number of specimens was found at only nine stations in the strait (Fig. III-14); they are young and small-sized, and the character of the periphery varies from somewhat lobulate and angled (or even keeled) to non-lobulate and rounded. Both forms have been found together in the same samples. The maximum diameter of the tests is about 0.35 mm.

Globorotalia crassaformis ronda Blow, 1969, 1st Intern. Conf. Planktonic Microfossils, vol. 1, p. 348; 388-390, pl. 4, figs. 4-6; pl. 37, figs. 6-9.

Some poor specimens of this species were found at stations 7b, 17, and 33 (Fig. III-15). This species is commonly found in the Pliocene and Pleistocene sediments of western Taiwan. According to Blow (1969), it ranges from within the early part of Zone N. 17 to Zone N. 22 or the early part of Zone N. 23, but not up to Recent time. Con-

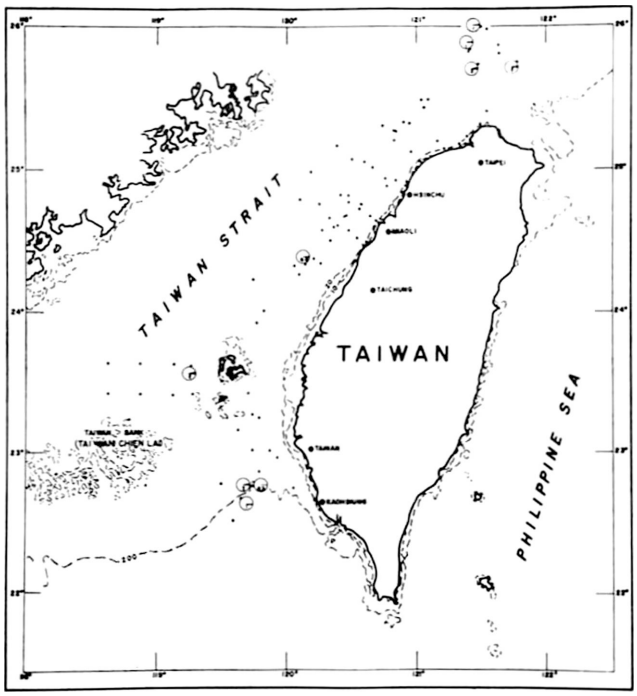

Figure III-14. Geographic distribution of *Globorotalia crassaformis* and its percentage of the total planktonic foraminiferal fauna at stations in Taiwan Strait.

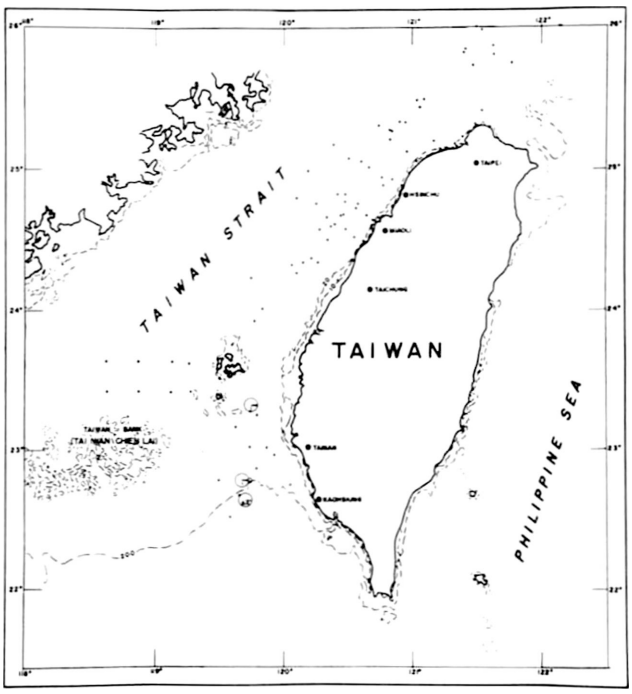

Figure III-15. Geographic distribution of *Globorotalia crassaformis ronda* and its percentage of the total planktonic foraminiferal fauna at stations in Taiwan Strait.

sidering the known range and the state of preservation, the specimens may be re-worked fossils.

Globorotalia cultrata menardii (Parker, Jones, and Brady) = *Rotalia menardii* Parker, Jones, and Brady, 1865; see Banner and Blow, 1860, Contrib. Cushman Found. Foram. Res., vol. XI, pt. 1, p. 31, pl. 6, figs. 2a-c.

(Plate III-3, figs. 31-35)

This species usually constitutes less than ten per cent of the planktonic assemblages and it is fairly widespread in the southern half of the strait and on the north side of the Chilung Channel (Fig. III-16). The specimens are all of the same form as *Rotalia menardii* Parker, Jones, and Brady, as described and illustrated by the lectotype selected by Banner and Blow (1960), but no forma *tumida* was found in the present samples. The specimens do not have a very strong development of the peripheral keel, the umbilical side is flattened, the umbilicus is open, and the wall is thin and smooth. The maximum diameter of the specimens is 1.05 mm and they have 5 or 6 chambers in the final whorl. Orr (1967) has given 120 m as the depth below which secondary thickening takes place in living specimens of *G. cultrata* (d'Orbigny). The specimens of this species from the strait do not have the accretion of a secondary crust of calcite over the surface of the test because most of the strait area is less than 150 m in depth. The coiling direction is dominantly sinistral in all samples.

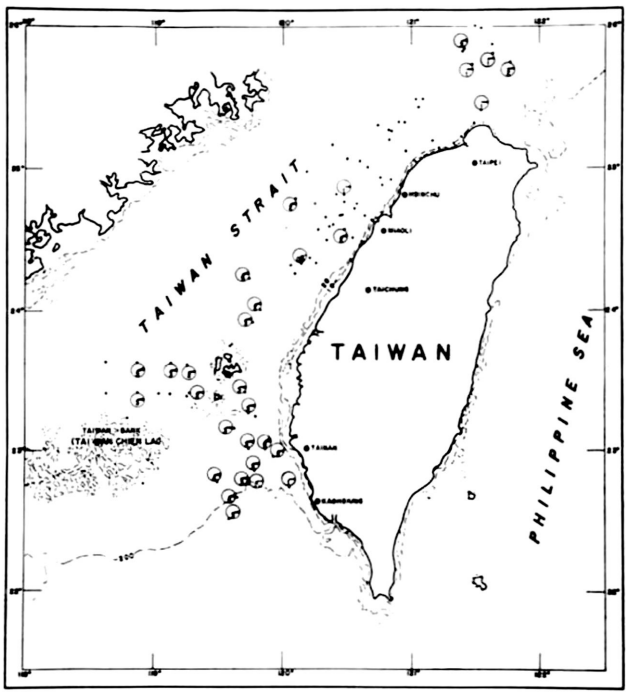

Figure III-16. Geographic distribution of *Globorotalia cultrata menardii* and its percentage of the total planktonic foraminiferal fauna at stations in Taiwan Strait.

Globorotalia scitula (Brady) = *Pulvinulina scitula* Brady, 1882; see Banner and Blow, 1960, Contrib. Cushman Found. Foram. Res., vol. XI, pt. 1, p. 27-28, pl. 5, figs. 5a-c (lectotype).

Very few specimens of this species (less than 1 per cent) were found only at four stations (9, 15, 25, and 34) in two areas, northeast of the Taichung Bank and south of the Penghu Channel (Fig. III-17). The specimens found are mostly young, thin walled, and small-sized but a few typical specimens were found. The final whorl always has five chambers and all the specimens are sinistrally coiled.

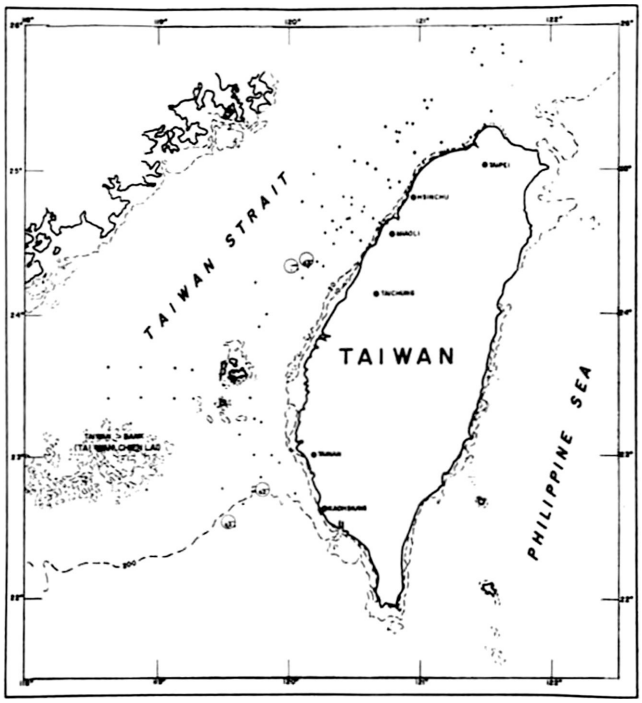

Figure III-17. Geographic distribution of *Globorotalia scitula* and its percentage of the total planktonic foraminiferal fauna at stations in Taiwan Strait.

Globorotalia truncatulinoides (d'Orbigny) = *Rotalia truncatulinoides* d'Orbigny, 1839; see Blow, 1969, Ist Intern. Conf. Planktonic Microfossils, vol. 1, p. 370, 405-408, pl. 5, figs. 13-15; pl. 48, figs. 1-5.

(Plate III-3, figs. 29, 30)

This species constitutes less than one per cent of the planktonic forms in the fraction larger than 0.075 mm and is found only at five stations: 8, 9, 13, 18, and 34 (Fig. III-18). The specimens are all of small size, thin-shelled, sharply angled and rather compressed, similar to the forms in cold-water areas (Kennett, 1968a). The ratio of width to height, as measured, is more than 1.5 and the coiling is predominantly dextral although the

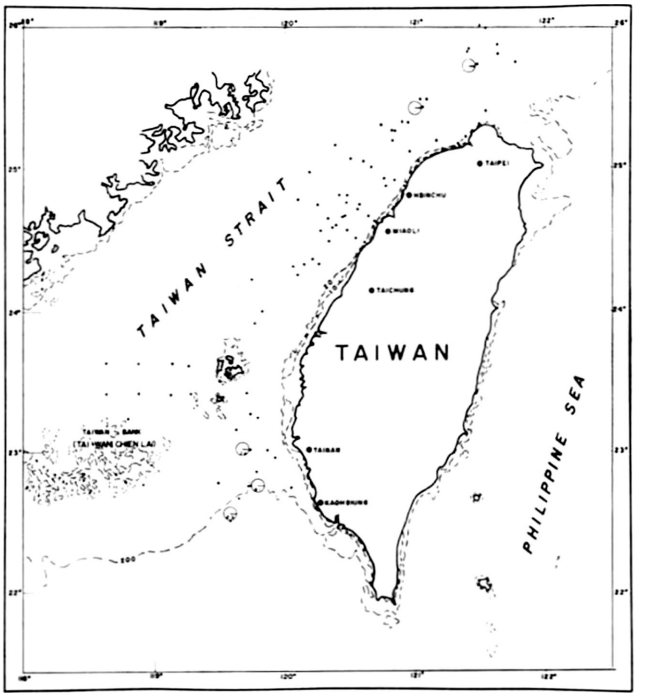

Figure III-18. Geographic distribution of *Globorotalia truncatulinoides* and its percentage of the total planktonic foraminiferal fauna at stations in Taiwan Strait.

number of specimens is not sufficient to determine the coiling ratio. The maximum diameter of the tests is 0.35 mm.

Family GLOBIGERINIDAE Carpenter, Parker, and Jones, 1862

Genus *Globigerina* d'Orbigny, 1826

Globigerina borealis Brady (= *Globigerina bulloides* d'Orbigny var. *borealis* Brady, 1881); see Banner and Blow, 1960, Contrib. Cushman Found. Foram. Res., vol. XI, pt. 1, p. 4, pl. 3, figs. 4a-c (lectotype).

(Plate III-3, figs. 5-7, 20, 28)

This was the only species typical of high latitudes observed in the sediments of Taiwan Strait. The appropriate synonymies are given in a paper by Kennett (1968b). Although *G. borealis* is generally considered to be characteristic of high-latitudes, the studies of Ericson (1959), Bandy (1960) and others on the coiling characteristics of this species have made it possible to divide the Recent populations of *G. borealis* into two categories: the sinistrally-coiled cool-water type and the dextrally-coiled warm-water type; the former is confined to high latitudes and the latter is abundant in temperate waters of the middle latitudes but it sometimes extends to low latitudes. In the samples from Taiwan Strait, all the specimens of *G. borealis* are dextrally coiled and, in this respect, fit the latter category.

G. incompta Cifelli has been regarded as a synonym of *G. borealis*. According to

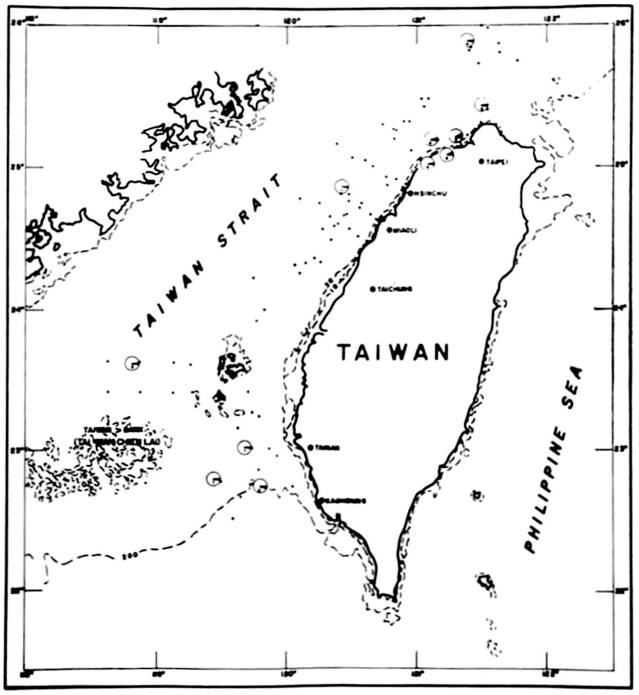

Figure III-19. Geographic distribution of *Globigerina borealis* and its percentage of the total planktonic foraminiferal fauna at stations in Taiwan Strait.

Parker's observation (1962), *G. incompta* is the lower latitude form of *G. borealis*. The specimens in Taiwan Strait are not the typical form of *G. borealis* and they partly resemble Kennett's *G. pachyderma* (1968) and Cifelli's *G. incompta* (1961). The specimens show considerable variation and the final whorl may contain 4 or 5 chambers; all of them, however, are typical in that they have a thinner test and lack the characteristic coarse crystalline wall structure typical of cold-water specimens of the species. This species is very rare in the strait and was found only at twelve stations (Fig. III-19). The diameter of the test ranges from 0.22 mm to a maximum of 0.33 mm.

Globigerina bulloides d'Orbigny, 1826; see Banner and Blow, 1960, Contrib. Cushman Found. Foram. Res., vol. XI, pt. 1, p. 3-4, pl. 1, figs. 1a-c.
(Plate III-3, figs. 8, 22, 23)

This species is fairly widespread and abundant in the collection, but rare in the southern half of the strait (Fig. III-20); it constitutes from 5 to 15 per cent of the planktonic foraminiferal fauna in the southern half of the strait and reaches its maximum in abundance (60 to 70 per cent fraction larger than 0.075 mm) in the northern half. The specimens show considerable variation in shape of the test and the coiling of the test is at random; the maximum diameter of the tests varies from 0.25 mm to 0.35 mm.

The surface water temperatures of the strait range between 24° and 26°C; these are unusually high temperatures for *G. bulloides* and *G. borealis* and the highest temper-

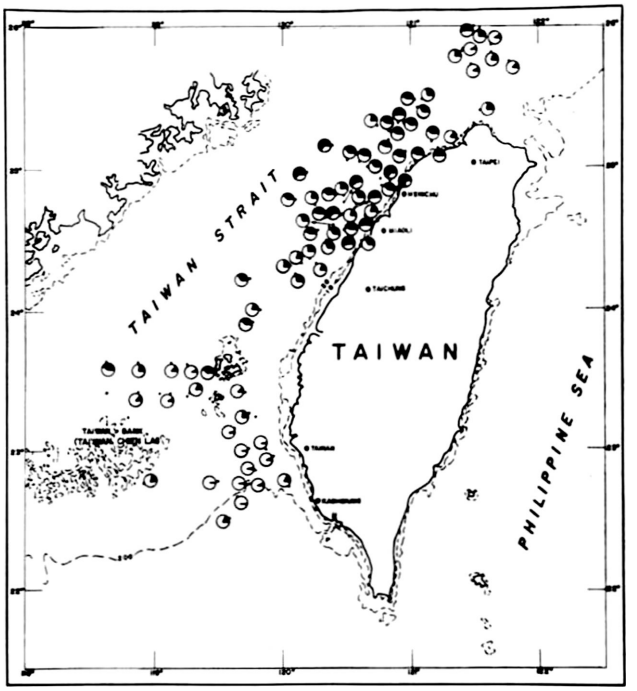

Figure III-20. Geographic distribution of *Globigerina bulloides* and its percentage of the total planktonic foraminiferal fauna at stations in Taiwan Strait.

atures in which they have been found previously (Boltovskoy, 1968) were between 21° and 22°C in the South Atlantic. Undoubtedly the specimens found commonly in the sediment samples from Taiwan Strait were brought there from higher latitudes by the China Coastal Stream, which is stronger in winter.

Globigerina conglomerata Schwager, 1866; see Banner and Blow, 1960, Contrib. Cushman Found. Foram. Res., vol. XI, pt. 1, p. 7-8, pl. 2, figs. 3a-c (reotype).

A few specimens of this species are found only at stations 25 and 53 (Fig. III-21) and all are poorly preserved.

Globigerina quinqueloba Natland, 1938, Univ. Calif., Scripps Inst. Oceanography, Bull., Tech. Ser., vol. 4, no. 5, p. 149, pl. 6, fig. 7.

(Plate III-3, figs. 17, 18)

When present, this species constitutes less than one per cent of the total sample except at stations 9 and I-6; it increases in frequency in the middle portion of the strait (Fig. III-22). In the South Pacific, *G. quinqueloba* is the dominant species at middle latitudes (Parker, 1962; Kennett, 1969) and it is observed north of 19°S latitude (Parker, 1962).

Specimens from the strait are smaller than usual and the modified smaller final chamber, which forms a flap over the umbilicus, is less developed. According to Parker

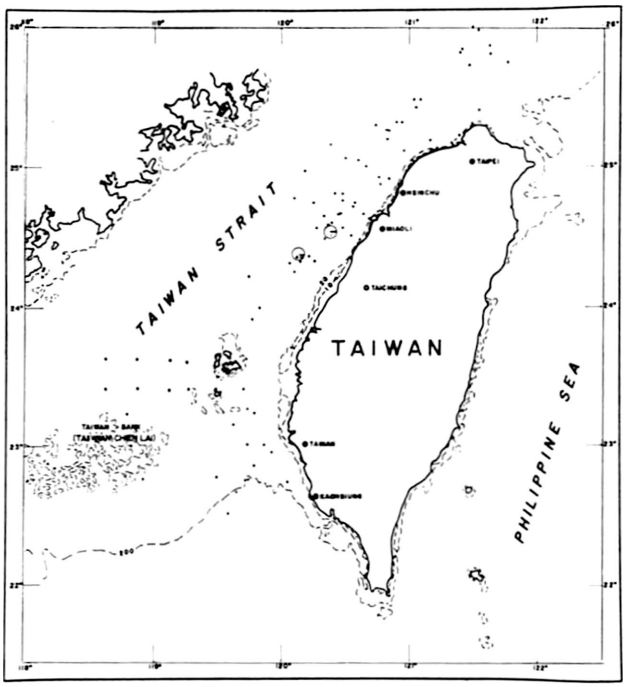

Figure III-21. Geographic distribution of *Globigerina conglomerata* and its percentage of the total planktonic foraminiferal fauna at stations in Taiwan Strait.

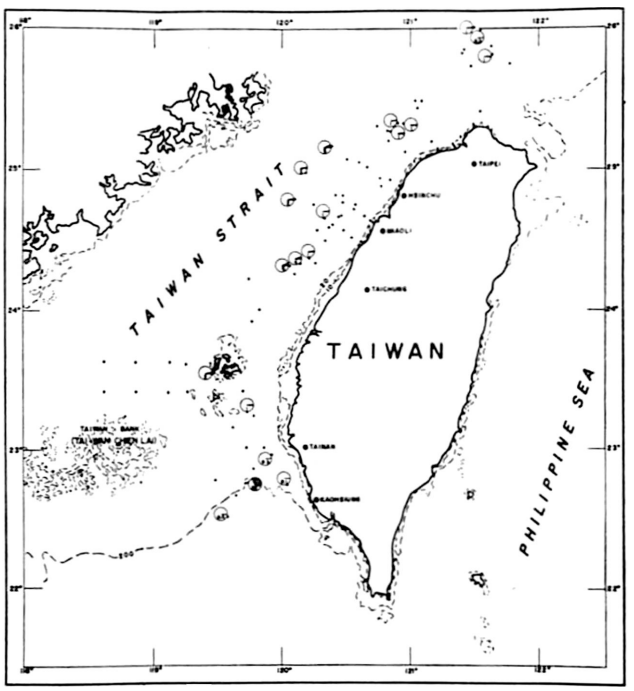

Figure III-22. Geographic distribution of *Globigerina quinqueloba* and its percentage of the total planktonic foraminiferal fauna at stations in Taiwan Strait.

(1962), specimens of this species from warmer areas are smaller than those from colder areas. The coiling ratios of *G. quinqueloba* are variable throughout the area but in most

Globigerina rubescens Hofker, 1956, Copenhagen Univ., Zool. Mus., Spolia, vol. 15, samples dextral and sinistral forms are found in approximately equal proportions. The diameter of the tests varies from 0.20 mm to 0.25 mm.

Globigerina rubescens Hofker, 1956, Copenhagen Univ., Zool. Mus., Spolia, vol. 15, p. 234, pl. 35, figs. 18-21.

(Plate III-3, figs. 9-14)

This small species is fairly widespread and is frequently found in the sediments of Taiwan Strait (Fig. III-23); it is found rarely in the eastern part of the tropical Atlantic (Boltovskoy, 1968) and Parker (1962) has recorded it in sediment samples from the Atlantic. The tests have a maximum diameter of about 0.80 mm; the coiling ratios are variable throughout the area, but most samples contain dextral and sinistral forms in about equal proportions.

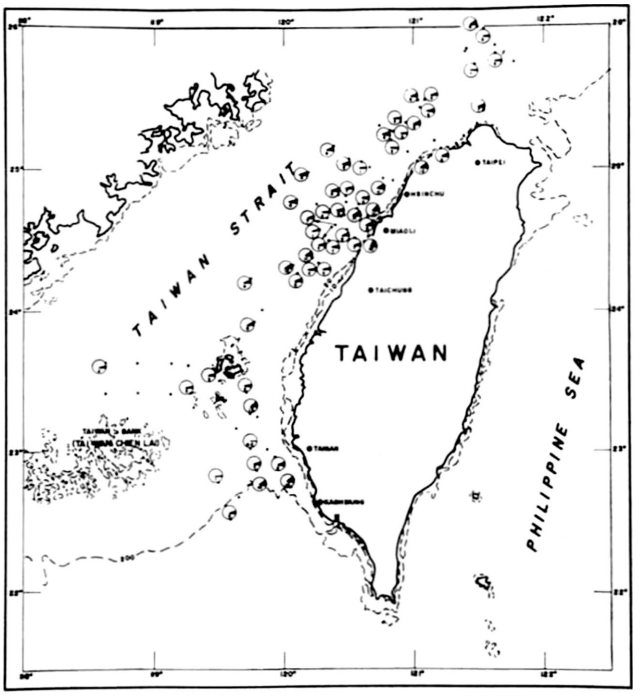

Figure III-23. Geographic distribution of *Globigerina rubescens* and its percentage of the total planktonic foraminiferal fauna at stations in Taiwan Strait.

Genus *Globigerinoides* Cushman, 1927

Globigerinoides conglobatus (Brady) = *Globigerina conglobata* Brady, 1879, Quart. Journ. Micr. Sci., n. s., vol. 19, p. 286; see Banner and Blow, 1960, Contrib. Cushman Found. Foram. Res., vol. XI, pt. 1, p. 6, pl. 4, figs. 4a-c (lectotype).

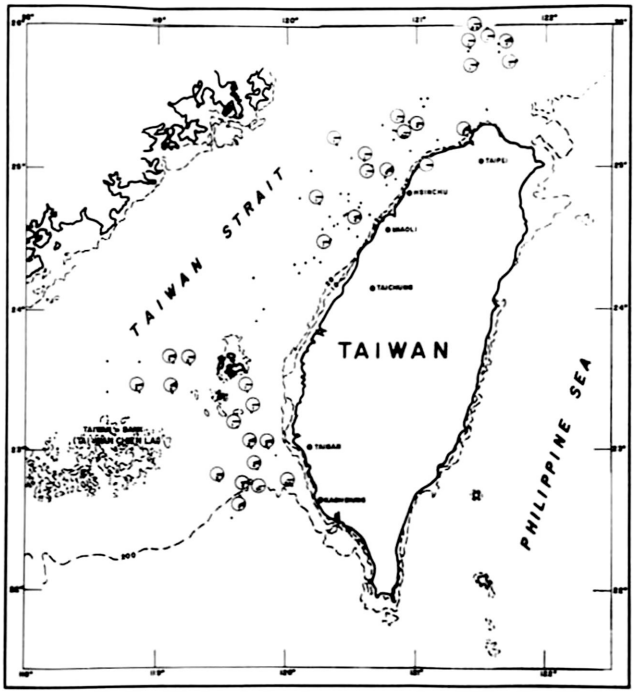

Figure III-24. Geographic distribution of *Globigerinoides conglobatus* and its percentage of the total planktonic foraminiferal fauna at stations in Taiwan Strait.

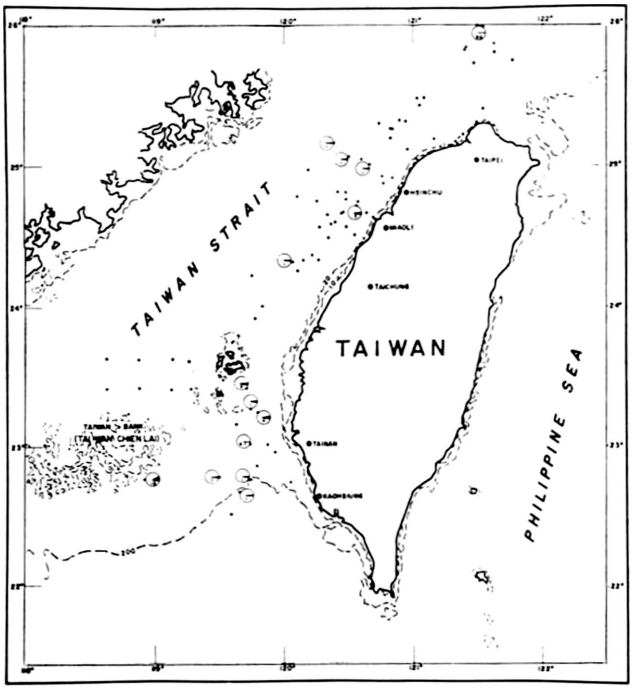

Figure III-25. Geographic distribution of *Globigerinoides elongatus* and its percentage of the total planktonic foraminiferal fauna at stations in Taiwan Strait.

(Plate III-2, fig. 24; plate III-3, fig. 21)

This species is widespread; it is rare in the near-shore area of western Taiwan and on the Taiwan Bank, but is found more frequently in the middle part of the strait (Fig. III-24). The specimens are mostly small, probably juvenile, and they lack the small bulla-like chambers; the maximum diameter of the tests is about 0.35 mm.

Globigerinoides elongatus (d'Orbigny) = *Globigerina elongata* d'Orbigny, 1826; see Banner and Blow, 1960, Contrib. Cushman Found. Foram. Res., vol. XI, pt. 1, p. 12-13, pl. 3, figs. 10a-c.

(Plate III-2, figs. 22, 23)

This species is found rarely at seventeen stations (Fig. III-25). Although it closely resembles *G. ruber*, this form, characterized by a high spire, is considered to be a separate species. The maximum diameter of the tests is about 0.40 mm.

Globigerinoides quadrilobatus sacculifer (Brady) = *Globigerina sacculifera* Brady, 1877; see Banner and Blow, 1960, Contrib. Cushman Found. Foram. Res., vol. XI, pt. 1, p. 21, pl. 4, figs. 1a-b.

(Plate III-2, figs. 26-29)

This species is among the most abundant found in the samples from Taiwan Strait (Fig. III-26). Tests both with and without the final sac-like chambers are found to-

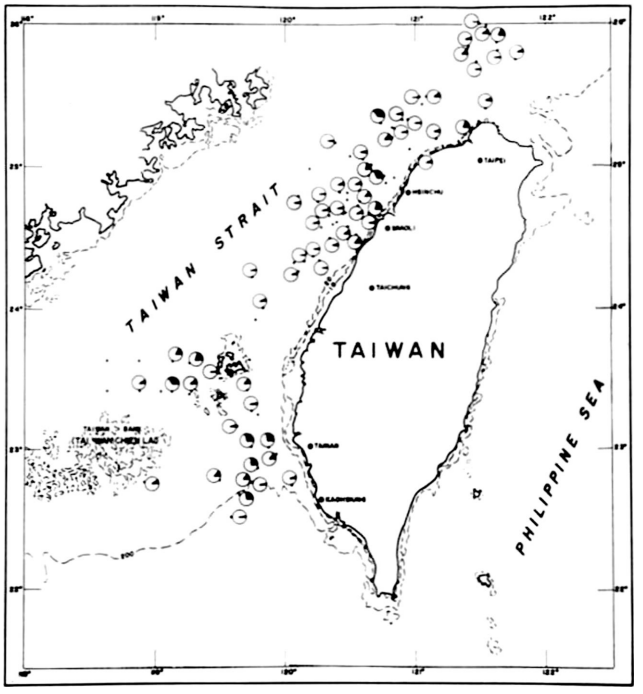

Figure III-26. Geographic distribution of *Globigerinoides quadrilobatus sacculifer* and its percentage of the total planktonic foraminiferal fauna at stations in Taiwan Strait.

gether in the samples; most of the specimens have no sac-like chamber as figured by Parker (1962, pl. 3, fig. 10), but a few have the final sac-like chambers as figured by Banner and Blow (1960, pl. 4, figs. 1 and 2). This form is easily distinguished from *G. quadrilobatus trilobus* by its larger aperture and secondary apertures.

Globigerinoides quadrilobatus trilobus (Reuss) = *Globigerina triloba* Reuss, Denkschr. Akad. Wiss. Wien. Math-Nat. Classe, vol. 1, p. 374, pl. 47, figs. 11a–d, 1850; see Bolli, 1957, Bull. U.S. Nat. Mus., 215, p. 112, pl. 25, figs. 2a–c.

(Plate III-2, figs. 18-21)

This species is common in the strait (Fig. III-27), but its distribution is rather irregular. Only specimens of the typical form originally described by Reuss are included in this species. The maximum diameter of the tests is about 0.35 mm.

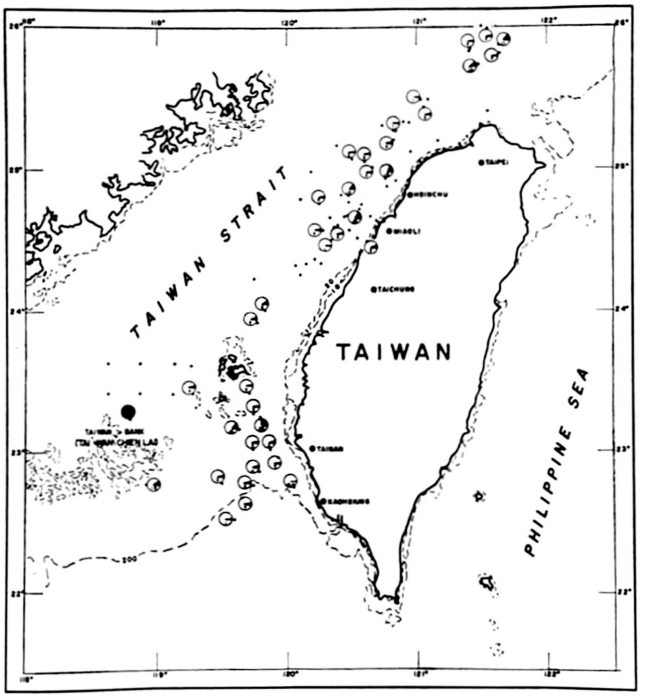

Figure III-27. Geographic distribution of *Globigerinoides quadrilobatus* and its percentage of the total planktonic foraminiferal fauna at stations in Taiwan Strait.

Globigerinoides ruber (d'Orbigny) = *Globigerina ruber* d'Orbigny, 1839, *in* de la Sagra, Hist. Phys. Pol. Nat. Cuba, "Foraminiferes", p. 82; vol. 8, pl. 4, figs. 12–14; see Banner and Blow, 1960, Contrib. Cushman Found. Foram. Res., vol. XI, pt. 1, p. 19-20, pl. 3, figs. 8a-b (lectotype).

(Plate III-2, figs. 4-6, 12, 13, 15-17)

This species is found commonly all over the strait (Fig. III-28) and it constitutes about 10 to 30 per cent of the fraction larger than 0.075 mm.

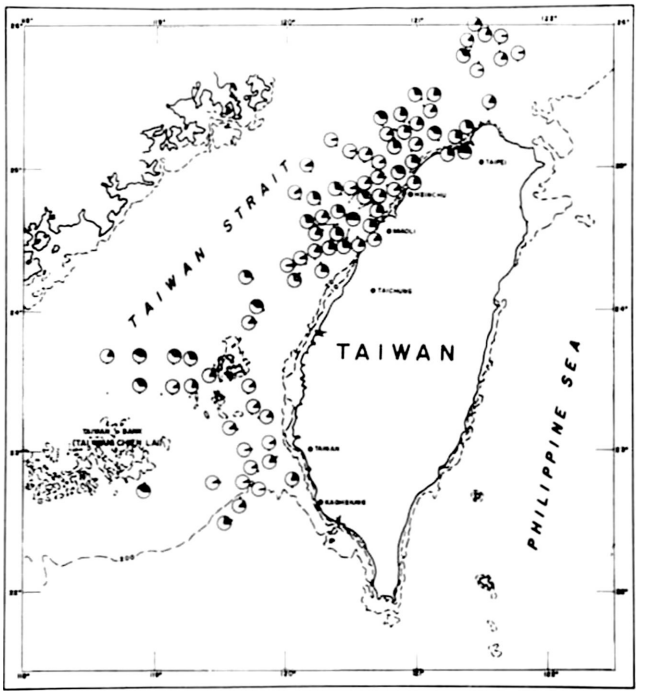

Figure III-28. Geographic distribution of *Globigerinoides ruber* and its percentage of the total planktonic foraminiferal fauna at stations in Taiwan Strait.

At almost all the stations, *G. ruber* is dominant in the sediments and most of the tests are of the smaller size. According to Boltovskoy's investigation (1968), the smaller sized tests of this species are usually found in areas of low salinity. According to Berger (1967), the number of forms with diminutive chambers is less in shallow water, and the reproduction of *Globigerina bulloides*, *G. quinqueloba*, *Globoquadrina eggeri* and *Globigerinoides ruber*, seems to take place mainly in the upper one hundred metres.

Two different formae can be distinguished in this species on the basis of morphology and aperture form: (a) one of these (Pl. III-2, figs. 14, 16) is characterized by having a large arched aperture, somewhat less conspicuous secondary apertures, less inflation and growth of the chambers, and a rather quadrangular equatorial outline of the test; this form is correlated to the lectotype of this species described and illustrated by Banner and Blow (1960) under the name of *Globigerina rubra* d'Orbigny; (b) the other form (Pl. III-2, figs. 5, 6) resembles *Globigerina cyclostoma* Galloway and Wissler, 1927 (= *Globigerinoides gomitulus* (Seguenza), 1880, according to Blow, 1969). The outline of the test closely resembles that of the other form but it has a more compact test with less globular chambers, less distinct secondary apertures, and a smaller, circular aperture. Whether these forms represent subspecies or phenotypic variants is open to question, and no subspecific designations are given here.

No particular trends could be distinguished in the distribution of these two forms

in the strait. In this paper, *Globigerinoides elongatus* is treated as being separate from this species.

Globigerinoides tenellus Parker, 1958, Repts. Swedish Deep-Sea Exped., 1947–48, vol. 8, no. 4, p. 280, pl. 6, figs. 7-11.

(Plate III-2, fig. 25)

This small species of *Globigerinoides* was found only rarely in each sample and it is most abundant (5 per cent) in those from the south side of the Matsu Basin (Fig. III-29). The form found in the strait is identical with that from the South Pacific described by Parker (1962, pl. 4, figs. 12a–c). This species is easily distinguished from *Globigerina rubescens* Hofker by its high arched aperture and secondary sutural apertures; it has a maximum diameter of 0.30 mm and up to 17 chambers.

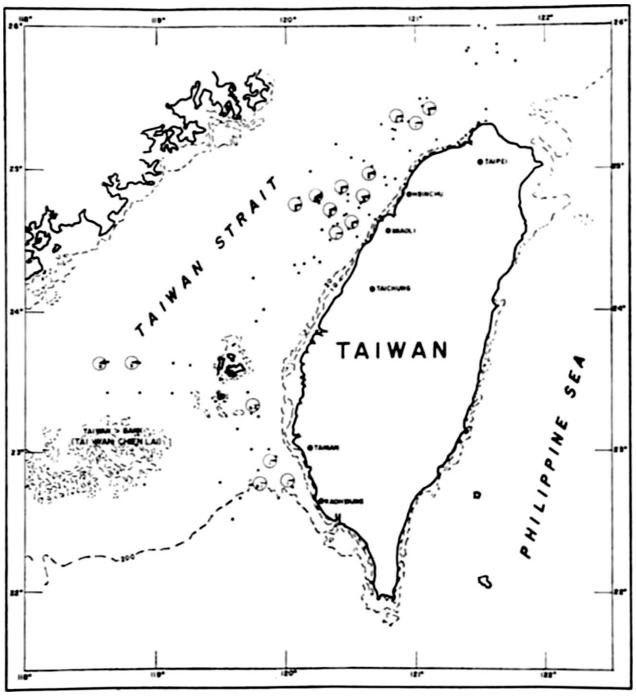

Figure III-29. Geographic distribution of *Globigerinoides tenellus* and its percentage of the total planktonic foraminiferal fauna at stations in Taiwan Strait.

Genus *Neogloboquadrina* Bandy, Frerichs and Vincent, 1967

Neogloboquadrina dutertrei humerosa (Takayanagi and Saito) = *Globorotalia humerosa* Takayanagi and Saito, 1962, Tohoku Univ., Sci. Rept., 2nd Ser. (Geol.), spec. vol., no. 5, p. 78, figs. 1a–2b.

(Plate III-1, figs. 1-21)

This species is common in the surface sediments of the strait (Fig. III-30) and it

appears to occur frequently in the Indo-Pacific region (Blow, 1969; Zobel, 1968). The writer agrees with Parker (1962) that *Globigerina dutertrei* d'Orbigny is the same as *Globigerina eggeri* Rhumbler and *Globigerina subcretacea* Lemnicki. *Globorotalia humerosa* is a significant addition to this group; these "species" and "subspecies" may be phenotypic variants and further study of their taxonomy is needed.

The specimens from Taiwan Strait correspond with *Globoquadrina dutertrei* (d'-Orbigny) var. 3 of Parker (1962, pl. 7, figs. 10–13) and are referable to *G. humerosa* which has from 5 to 7 chambers in the final whorl and a deep, clearly marked and open umbilicus; the test is in the form of a lower spire with a strongly lobate peripheral margin, an interio-marginal aperture, and with the umbilical-extraumbilical aperture bordered with a developed lip which forms flaps that extend across the umbilical depression. The test has a maximum diameter of about 0.52 mm. Based on these features of the test, the specimens from Taiwan Strait are regarded here as belonging to *G. dutertrei humerosa*, although this form has probably been included with *G. dutertrei* or *Globoquadrina dutertrei* in other studies of Recent planktonic foraminifers.

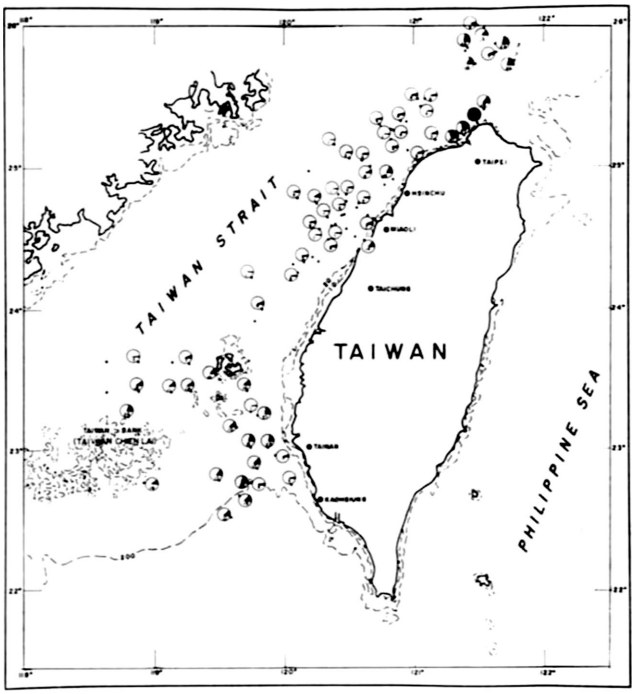

Figure III-30. Geographic distribution of *Neogloboquadrina dutertrei humerosa* and its percentage of the total planktonic foraminiferal fauna at stations in Taiwan Strait.

Genus *Globorotaloides* Bolli, 1957

Globorotaloides hexagona (Natland) = *Globigerina hexagona* Natland, 1938, Calif. Univ., Scripps Inst. Oceanography, Bull., Tech. Ser., vol. 4, no. 5, p. 149, pl. 7, fig. 1.

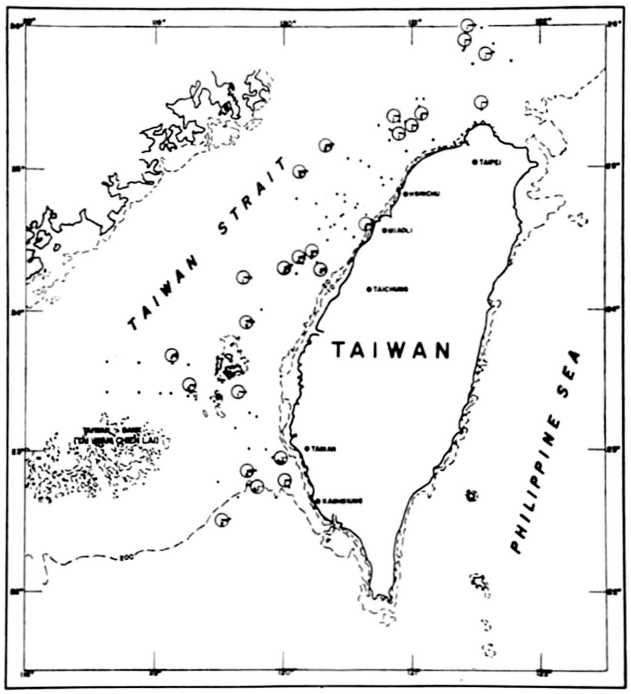

Figure III-31. Geographic distribution of *Globorotaloides hexagona* and its percentage of the total planktonic foraminiferal fauna at stations in Taiwan Strait.

This species was found rarely (less than 2 per cent) at twenty-five stations in the strait (Fig. III-31). Most of the tests are young, with the umbilical teeth not observed.

Genus *Pulleniatina* Cushman, 1927

Pulleniatina obliquiloculata (Parker and Jones) = *Pullenia obliquiloculata* Parker and Jones, 1862; see Banner and Blow, 1960, Contrib. Cushman Found. Foram. Res., vol. XI, pt. 1, p. 25, pl. 7, figs. 4a-c.

(Plate III-2, figs. 1-3; plate III-3, fig. 19)

This species is fairly widespread, comprising about 70 per cent of the whole population, but it is rare (less than 5 per cent) in the Taichung Bank area (Fig. III-32). The tests are mostly small juvenile forms without smooth tests; they are all coiled dextrally and their maximum diameter is about 0.50 mm.

Genus *Subbotina* Brotzen and Pozaryska, 1961

Subbotina falconensis (Blow) = *Globigerina falconensis* Blow, 1959, Bull. Amer. Pal., vol. 39, no. 178, p. 177, pl. 9, figs. 40-41.

(Plate III-3, figs. 1-4)

This species is frequently found in the strait but it does not comprise more than 5 per cent of the assemblage in each sample and it is absent from the near-shore sediments (Fig. III-33). This species has a more lobulate periphery than *G. bulloides* and a low-

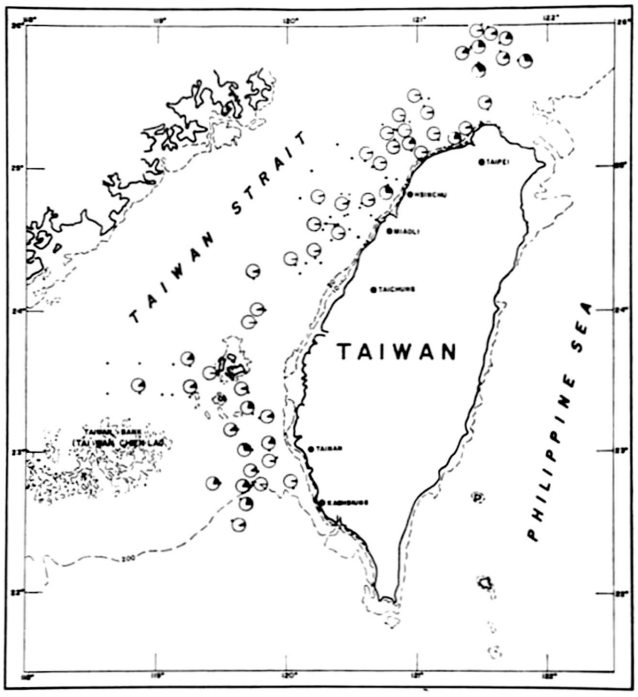

Figure III-32. Geographic distribution of *Pulleniatina obliquiloculata* and its percentage of the total planktonic foraminiferal fauna at stations in Taiwan Strait.

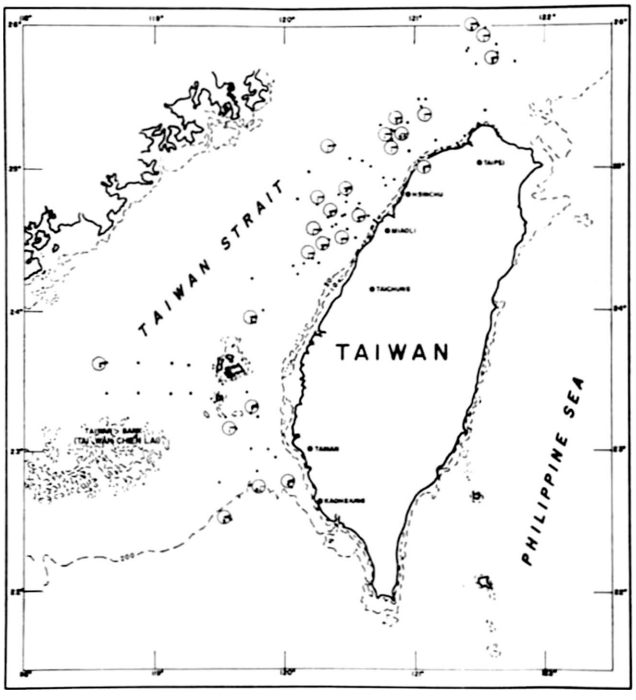

Figure III-33. Geographic distribution of *Subbotina falconensis* and its percentage of the total planktonic foraminiferal fauna at stations in Taiwan Strait.

arched aperture with a broad lip, while the final chamber is usually smaller than the penultimate one. The writer therefore separates this form from *G. bulloides*, with which it has been included by some authors in studies of Recent planktonic foraminifers.

Genus *Sphaeroidinella* Cushman, 1927

Sphaeroidinella dehiscens (Parker and Jones) = *Sphaeroidina bulloides* d'Orbigny var. *dehiscens* Parker and Jones, 1865; see Banner and Blow, 1960, Contrib. Cushman Found. Foram. Res., vol. XI, pt. 1, p. 35, pl. 7, fig. 3 (lectotype).

(Plate III-2, fig.11)

This species comprises less than 1 per cent of the assemblage in the two samples in which it was found (Fig. III-34); its distribution in the strait about the same as that of *Orbulina universa*. Hecht and Savin (1970) concluded that this species is not a late stage encrusted phenotype of *G. sacculifer* (Be, 1960), but that the two are distinct species. The typical form of *S. dehiscens excavata* was not found in the samples examined.

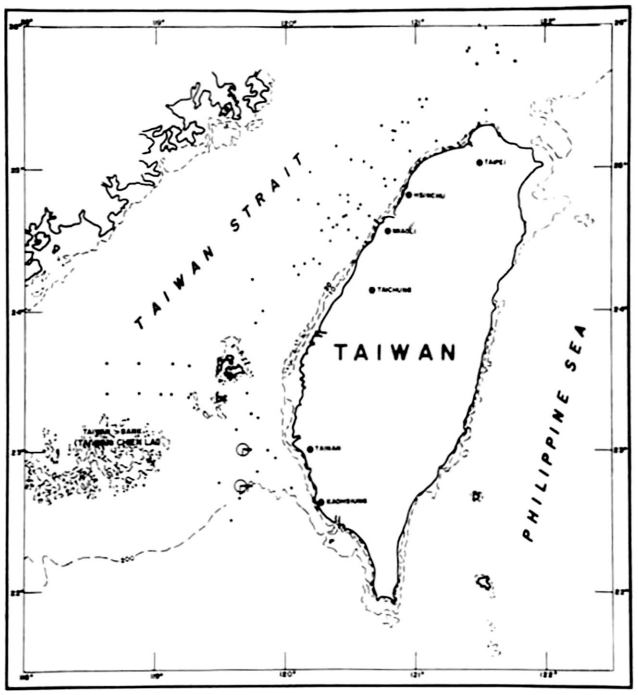

Figure III-34. Geographic distribution of *Sphaeroidinella dehiscens* and its percentage of the total planktonic foraminiferal fauna at stations in Taiwan Strait.

Genus *Orbulina* d'Orbigny, 1839

Orbulina universa d'Orbigny, 1839, *in* de la Sagra, Hist. Phys. Pol. Nat. Cuba, "Foraminiferes", p. 3, vol. 8, pl. 1, fig. 1.

(Plate III-3, fig. 36)

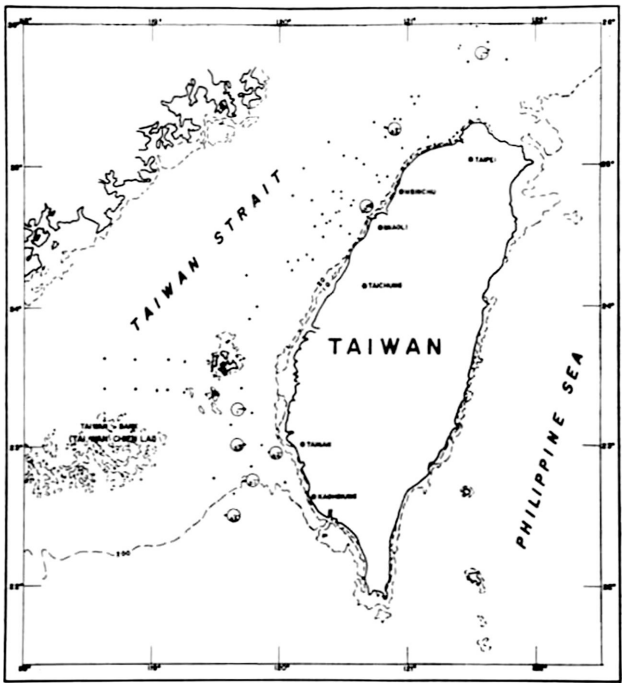

Figure III-35. Geographic distribution of *Orbulina universa* and its percentage of the total planktonic foraminiferal fauna at stations in Taiwan Strait.

This species was found very rarely at only eight stations (Fig. III-35). All the tests are large, with a maximum diameter of about 1.00 mm, and they have the typical perforations of this species, consisting of numerous small pores and fewer larger ones.

Genus *Globigerinita* Bronniman, 1951

Globigerinita glutinata (Egger) = *Globigerina glutinata* Egger, 1893, Abhandl. K. Bayer. Akad. Wiss. Munchen, CLII, vol. 18, p. 371, pl. 13, figs. 19-21.

(Plate III-3, figs. 26, 27)

The specimens from the strait have a finely hispid wall but none have a bullate last-formed chamber. It is found more frequently in the upwelling area off the west coast of Taiwan and in the area northeast of the Taichung Bank (Fig. III-36).

Globigerinita humilis (Brady) = *Truncatulina humilis* Brady, 1884; see Banner and Blow, 1960, Contrib. Cushman Found. Foram. Res., vol. XI, pt. 1, p. 36, pl. 8, figs. 1a–c (lectotype).

This small species is found very rarely in the fraction larger than 0.075 mm; it is widely distributed in the South Pacific (Parker, 1962) but is rarely seen in the samples from Taiwan Strait (Fig. III-37).

Globigerinita iota Parker, 1962, Micropaleont., vol. 8, no. 2, pl. 10, figs. 26–30, 250–252.

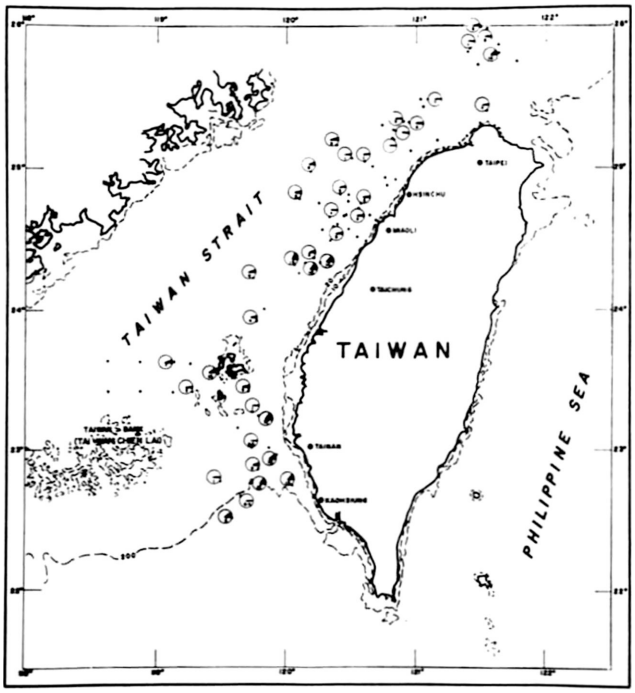

Figure III-36. Geographic distribution of *Globigerinita glutinata* and its percentage of the total planktonic foraminiferal fauna at stations in Taiwan Strait.

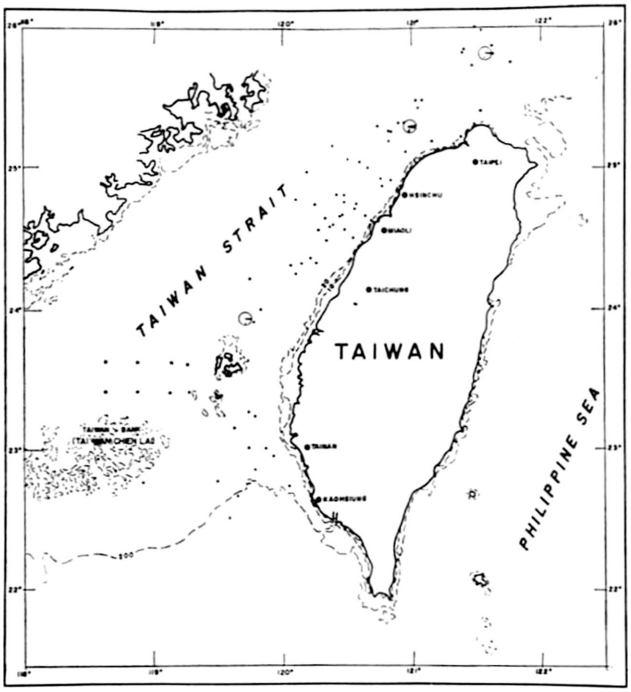

Figure III-37. Geographic distribution of *Globigerinita humilis* and its percentage of the total planktonic foraminiferal fauna at stations in Taiwan Strait.

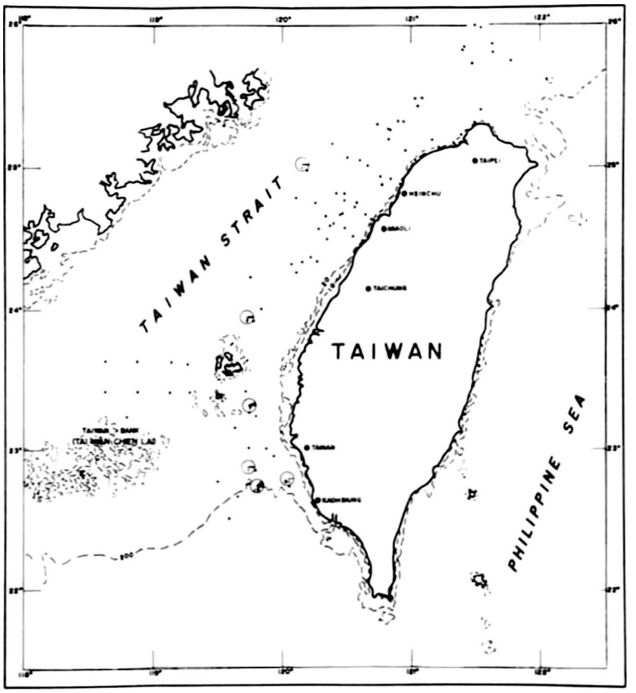

Figure III-38. Geographic distribution of *Globigerinita iota* and its percentage of the total planktonic foraminiferal fauna at stations in Taiwan Strait.

This species was described from sediments of the South Pacific region by Parker (1962). It is distinguished from *G. humilis* by its smoother wall, fewer chambers in a whorl, and its less compressed test. A modified non-lobate last-formed chamber, as found in *G. humilis*, is not developed in the specimens from the strait. This small species comprised less than 10 per cent of the fraction larger than 0.075 mm and was found at only six stations (Fig. III-38).

Globigerinita uvula (Ehrenberg) = *Pyloxdexia uvula* Ehrenberg, 1861; see Parker, 1962, Micropaleont., vol. 8, no. 2, p. 252–253, pl. 8, figs. 14–26.

This very small species was found only in two samples, from stations 9 and 15, and it comprised less than 1 per cent of the assemblages in them (Fig. III-39). The specimens are elongate and do not have an umbilical bulla.

SUMMARY OF CONCLUSIONS

The variation of surface temperature across Taiwan Strait is quite large in the winter months, ranging in February from 12°C near Amoy on the mainland to 23°C near the southern tip of Taiwan. In summer (August), however, the surface temperature

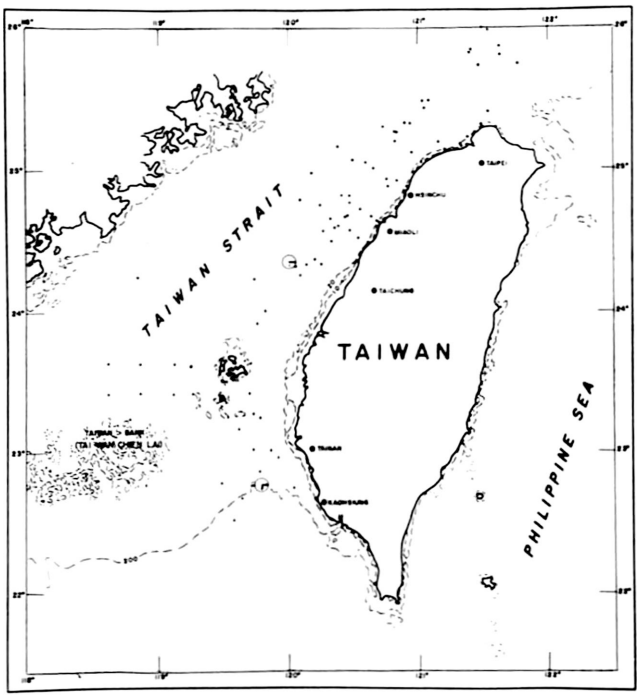

Figure III-39. Geographic distribution of *Globigerinita uvula* and its percentage of the total planktonic foraminiferal fauna at stations in Taiwan Strait.

throughout the strait is nearly uniform and ranges less than 1 °C above or below 28 °C. The salinity in the strait is generally about 34,000 ppm but, along the coast of the mainland, it sometimes becomes lower than 33,000 ppm. The runoff from the rivers on Taiwan greatly dilutes the sea water along the western coast of Taiwan and flow measurements of the fifteen major rivers entering the strait from Taiwan amount to a total of $36.54 \times 10^9 m^3$ annually.

Three major currents influence the waters of Taiwan Strait: the warm Kuroshio Current, the cold China Coastal Stream, and the warm monsoonal drift from the South China Sea; they undoubtedly have a great influence on the composition of the planktonic foraminiferal assemblages in the bottom sediments. The quantitative distribution patterns of the total zooplankton correspond in general approximately to those of the planktonic foraminifers in the sediments.

Twenty-seven planktonic species and subspecies have been found in the sediment samples studied. Planktonic foraminifers are common in the sediments of the strait and are dominantly tropical in character. Only two species (*Globigerina borealis* and *G. bulloides*) are typical of cool water and two others (*Globigerinita glutinata* and *Orbulina universa*) are found normally in both cool and warm water areas. They are abundant in the deeper portions of the strait but are less common over banks and in the shallower areas near the shores. The diversity of the assemblages is greatest in the deeper portions of the strait.

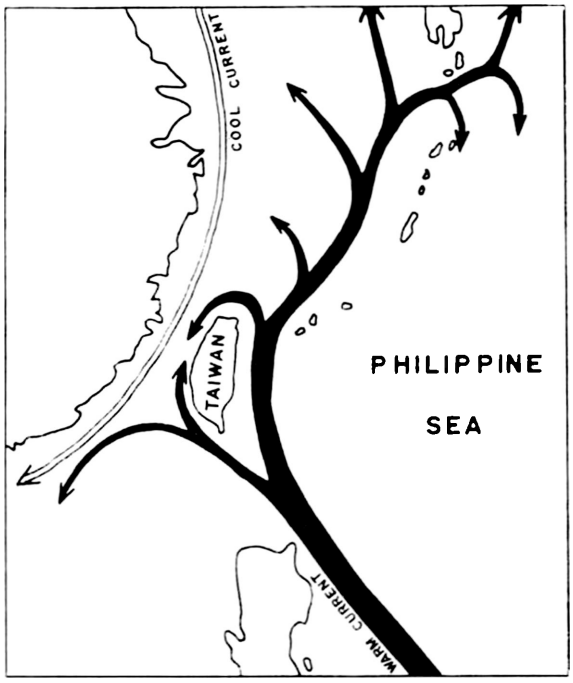

Figure III-40. The pattern of the currents affecting Taiwan Strait reflected by the analysis of the distribution of planktonic foraminifers in the surface sediments.

The patterns of geographic distribution of the individual species of planktonic foraminifers correspond closely to the current movements in the strait, which affect particularly the water temperatures; consequently, the distribution patterns of the warm and cool faunal assemblages on the floor of the strait are similar to those of the currents in the area. Evidence of the influence of the cold China Coastal Stream is given by the presence of *Globigerina borealis* and the common occurrence of *G. bulloides*, both cold-water forms, in the bottom sediments of the strait.

The distribution of planktonic foraminifers in the sediments of Taiwan Strait is significantly modified by all the variations of physical, chemical and biological factors that may effect the productivity of the foraminifers.

ACKNOWLEDGMENTS

This investigation was supported by the National Council on Science Development with appropriated research funds. Ship operations were supported by a contract between the Taiwan Fisheries Research Institute and the Chinese National Committee for the Scientific Committee on Oceanic Research. The writer thanks the officers, crew, and scientific staff for their co-operation, as well as all the technical assistants of the Paleontology Laboratory of the Chinese Petroleum Corporation (CPC) who assisted

with the laboratory work. Many thanks are due to Professor Veichow C. Juan, President, Chinese National Committee for SCOR, CSK, and Professor Tsuyou Chu, Director, Institute of Oceanography, National Taiwan University, for their encouragement; and to Mr. Tei-Mei Wu, Vice President of CPC, and Dr. C. Y. Meng, Chief Geologist of CPC, for their generous support of this research.

REFERENCES

Asano, K., 1957, The foraminifera from the adjacent seas of Japan, collected by the S.S. Soyo-maru, 1922–1930; pt. 3, planktonic species: *Tohoku Univ., Sci. Rept., 2nd ser. (Geol.)*, vol. 28, p. 1–26, fig. 1, pls. 1–2.

Bandy, O. L., 1960, Geologic significance of coiling ratio in the foraminifer *Globigerina pachyderma: Journ. Paleont.*, vol. 34, no. 4, p. 671–681.

———, and Arnal, R. E., 1960, Concepts of foraminiferal paleoecology: *Bull. Amer. Assoc. Petroleum Geologists*, vol. 44, p. 1921–1932.

Banner, F. T., and Blow, W. H., 1960, Some primary types of species belonging to the superfamily Globigerinaceae: *Contrib. Cushman Found. Foram. Res.*, vol. XI, pt. 1, p. 1–41.

Be, A.W.H., 1960, Ecology of Recent planktonic foraminifera: Part 2–Bathymetric and seasonal distributions in the Sargasso Sea off Bermuda: *Micropaleont.*, vol. 6, no. 4, p. 373–392.

Berger, W. H., and Parker, F. L., 1970, Diversity of planktonic foraminifera in deep-sea sediments: *Science*, vol. 168, p. 1345–1347.

Blow, W. H., 1969, Late Middle Eocene to Recent planktonic foraminiferal biostratigraphy: *1st Internat. Conf. Plank. Microfossils, (1967), Proc.*, vol. 1, p. 199–421, 43 figs., pls. 1–54.

Boltovskoy, E., 1959, Foraminifera as biological indicators in the study of ocean currents: *Micropaleont.*, vol. 5, no. 4, p. 473–481.

———, 1968, Living planktonic foraminifera of the eastern part of the tropical Atlantic: *Rev. Micropaleont.*, vol. 11, no. 2, p. 85–98.

Bradshaw, J. S., 1959, Ecology of living planktonic foraminifera in the north and equatorial Pacific Ocean: *Contrib. Cushman Found. Foram. Res.*, vol. X, pt. 2, p. 25–64.

Cheng, T., and Cheng, S., 1964, The planktonic foraminifera of the northern South China Sea: *Oceanol. Limnol. Sinica*, vol. 6, no. 1, p. 38–77, text-figs. 1–10, pls. 1–6.

Chu, T. Y., 1971, Environmental study of the surrounding water of Taiwan: *Sino-American Science Cooperation Colloquium on Ocean Resources*, 28 April–7 May, Taipei, vol. II, p. 1–38.

Cifelli, R., 1961, *Globigerina incompta*, a new species of pelagic foraminifera from the North Atlantic: *Contrib. Cushman Found. Foram. Res.*, vol. 12, pt. 3, p. 83–86, pl. 4.

Emery, K. O., *et al.*, 1969, Geological structure and some water characteristics of the East China Sea and the Yellow Sea: United Nations ECAFE, *CCOP Tech. Bull.*, vol. 2, p. 3–43.

Ericson, D. B., 1959, Coiling direction of *G. pachyderma* as a climatic index: *Science*, vol. 130, p. 219–220.

Galloway, J. J., and Wissler, S. G., 1927, Pleistocene foraminifera from the Lomita Quarry, Palos Verde Hills, California: *Journ. Paleont.*, vol. 1, no. 1, p. 35–87, pls. 1–12.

Hecht, A. D., and Savin, S. M., 1971, Oxygen-18 studies of Recent planktonic foraminifera: *Science*, vol. 173, p. 167–169.

Huang, Tunyow, 1971, Foraminiferal trends in the surface sediments of Taiwan Strait: United Nations ECAFE, *CCOP Tech. Bull.*, vol. 4, p. 23–61.

Kennett, J. P., 1968a, *Globorotalia truncatulinoides* as a paleooceanographic index: *Science*, vol. 159, p. 1461–1463.

———, 1968b, Latitudinal variation in *Globigerina pachyderma* (Ehrenberg) in surface sediments of the southwest Pacific Ocean: *Micropaleont.*, vol. 14, no. 3, p. 305–318, pl. 1.

———, 1969, Distribution of planktonic foraminifera in surface sediments southeast of New Zealand: *1st Internat. Conf. Plank. Microfossils, (1967), Proc.*, vol. 2, p. 307–322.

Lipps, J. H., and Valentine, J. W., 1970, The role of foraminifera in the trophic structure of marine communities: *Lethia*, vol. 3, no. 3, p. 279–286, text-fig. 1 (diagram).

Orr, W. N., 1967, Secondary calcification in the foraminiferal genus *Globorotalia: Science*, vol. 157, p. 1554–1555.

Parker, F. L., 1962, Planktonic foraminiferal species in Pacific sediments: *Micropaleont.*, vol. 8, no. 2, p. 219–254.

Saito, T., 1963, Miocene planktonic foraminifera from Honshu, Japan: *Tohoku Univ., Sci. Rept. 2nd Ser. (Geol.)*, vol. 35, no. 2, p. 123–209, pls. 53–56.

Tan, T. H., 1971, On distribution of biomass and abundance of zooplankton in waters surrounding Taiwan, with attention of upwelling at region near station 14: *Sino-American Science Cooperation Colloquium on Ocean Resources*, vol. II, p. 307–323.

Tseng, W. Y., 1971, Plankton community in the upwelling regions of Taiwan: *Ibid.*, vol. II, p. 325–345.

Waller, H. O., and Polski, W., 1959, Planktonic foraminifera of the Asiatic shelf: *Contrib. Cushman Found. Foram. Res.*, vol. X, pt. 4, p. 123–126.

EXPLANATION OF PLATE III-1

Figures

1–21 *Neogloboquadrina dutertrei humerosa* (Takayanagi and Saito). 1, 2, 3, 4–5, 6–7, 8–9, 15–17, and 18 from sample No. 31, × 75; 10–11, 12–14, and 19–21 from sample No. 28, × 75.

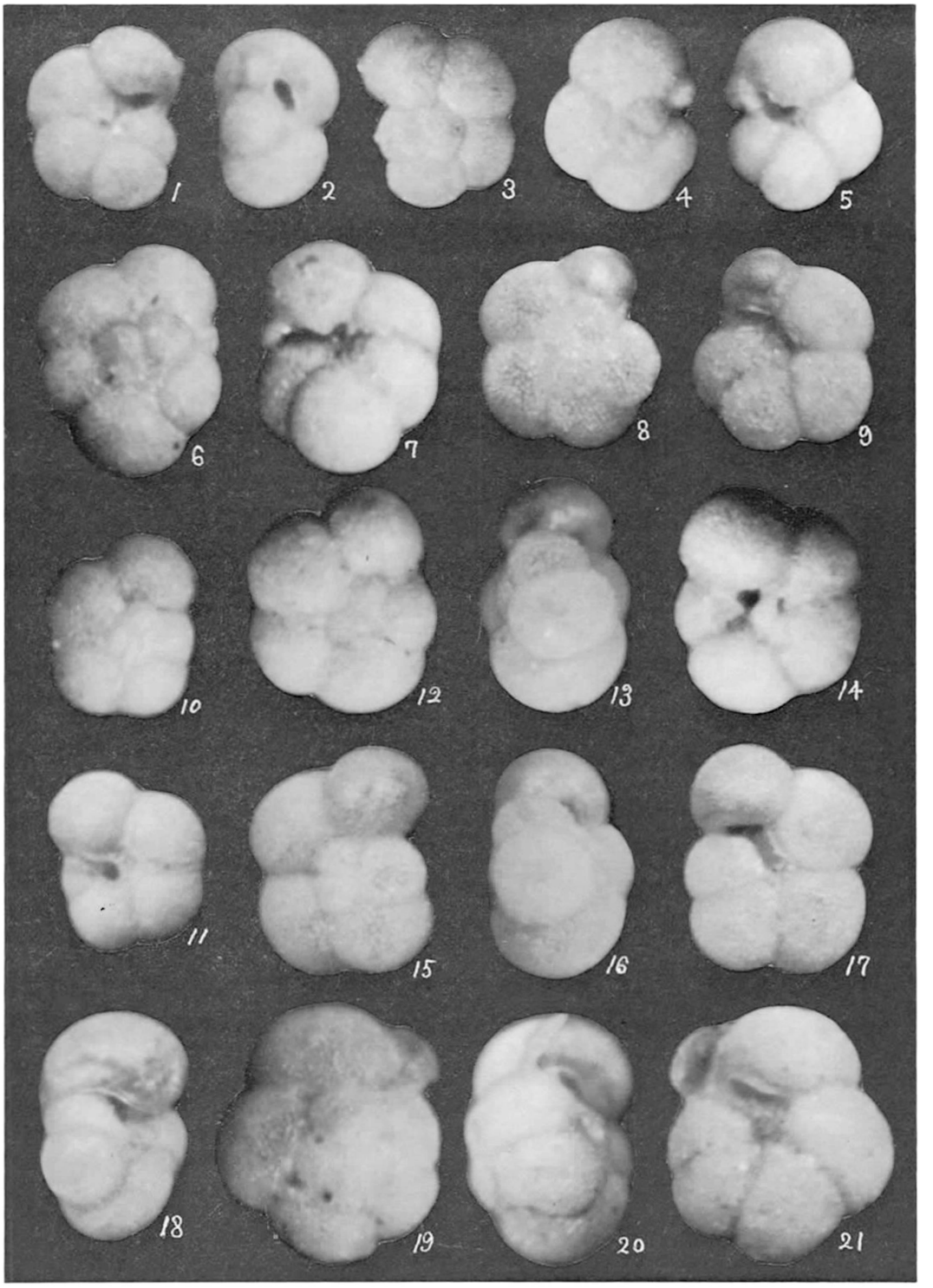

T. Huang: Planktonic Foraminifers from Taiwan Strait

EXPLANATION OF PLATE III–2

Figures

1, 2, 3 *Pulleniatina obliquiloculata* (Parker and Jones). From sample No. 42, ×45.

4, 5, 6, 12–17 *Globigerinoides ruber* (d'Orbigny). 4 from sample No. 34, ×66; 5 from sample No. 49, ×63; 6 from sample No. 49, ×80; 12 from sample No. 49, ×72; 13–15 from No. 49, ×74; 16–17 from sample No. 49, ×68.

7–10 *Hastigerina siphonifera* (d'Orbigny). 7 and 8 from sample No. 41, ×105; 9 from sample No. 42, ×80; 10 from sample No. 42, ×80.

11 *Sphaeroidinella dehiscens* (Parker and Jones). From sample No. 8, ×58.

18–21 *Globigerinoides quadrilobatus trilobus* (Reuss). From sample No. 42, ×66.

22, 23 *Globigerinoides elongatus* (d'Orbigny). Both from sample No. 8; 22, ×72; 23, ×83.

24 *Globigerinoides conglobatus* (Brady). From sample No. 43, ×62.

25 *Globigerinoides tenellus* Parker. From sample No. 49, ×110.

26–29 *Globigerinoides quadrilobatus sacculifer* (Brady). 26 and 27 from sample No. 28, ×60; 28 and 29 from sample No. 43, ×45.

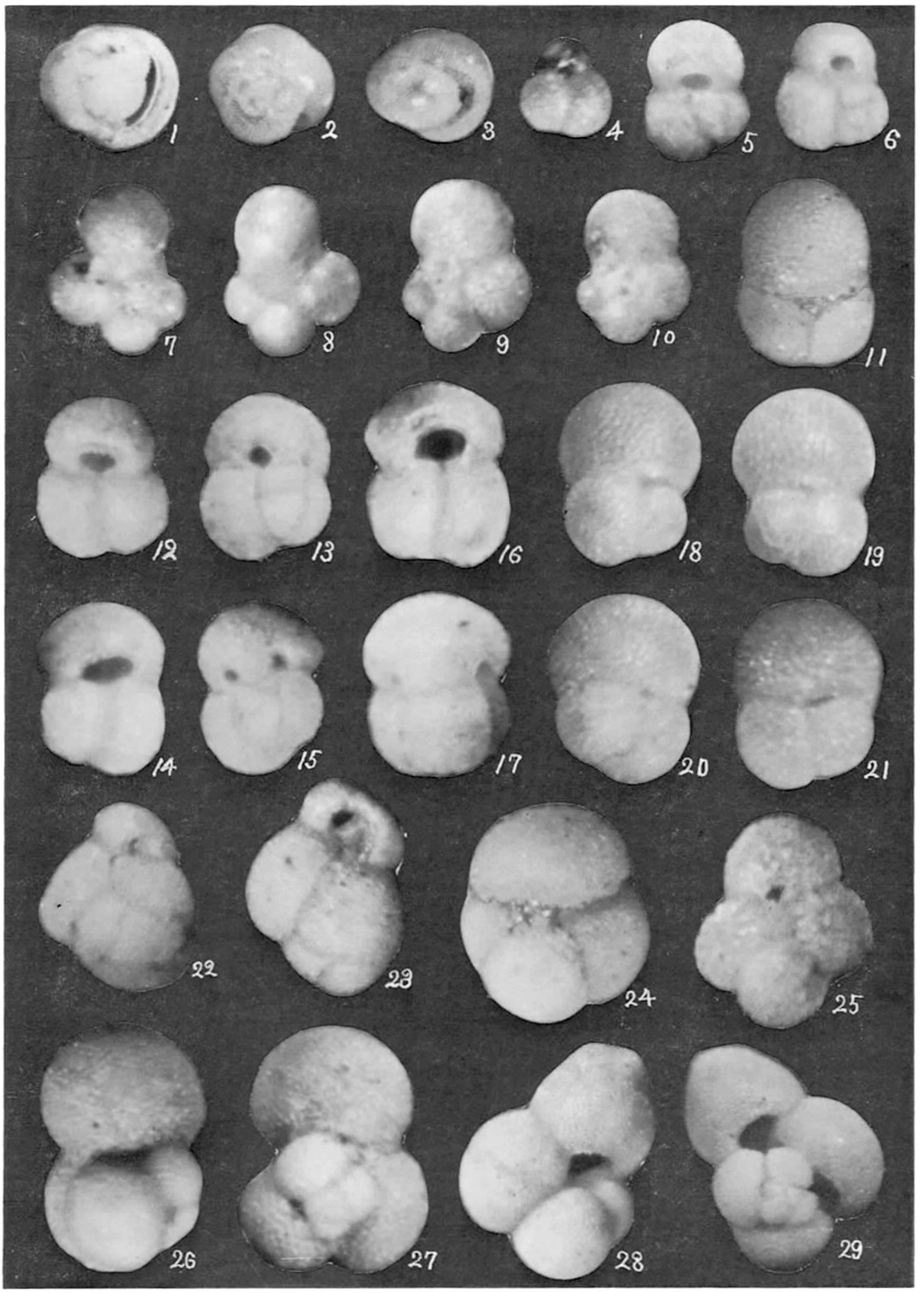

T. Huang: Planktonic Foraminifers from Taiwan Strait

EXPLANATION OF PLATE III–3

Figures

1–4 *Subbotina falconensis* (Blow). 1 from sample No. 28, ×62; 2 and 3 from sample No. 44, ×62; 4 from sample No. 42, ×62.

5–7, 20, 28 *Globigerina borealis* Brady. 5 from sample No. 9, ×52; 6 from sample No. 9, ×65; 7 from sample No. 9, ×70; 20 from sample No. 9, ×65; 28 from sample No. 9, ×92.

8, 22, 23 *Globigerina bulloides* d'Orbigny. 8 from sample No. 50, ×65; 22 and 23 from sample No. 34, ×66.

9–14 *Globigerina rubescens* Hofker. 9 from sample No. III–6, ×102; 10, 11, 12 from sample No. 50, ×65; 13 from sample No. III–6, ×60; 14 from sample No. 50, ×100.

15, 16 *Hastigerina pelagica* (d'Orbigny). From sample No. 15, ×90.

17, 18 *Globigerina quinqueloba* Natland. From sample No. 44, ×66.

19 *Pulleniatina obliquiloculata* (Parker and Jones). From sample No. 42, ×65.

21 *Globigerinoides conglobatus* (Brady). From sample No. 45, ×68.

24, 25 *Hastigerina siphonifera* (d'Orbigny). From sample No. 42, ×43.

26, 27 *Globigerinita glutinata* (Egger). From sample No. 44, ×90.

29, 30 *Globorotalia truncatulinoides* (d'Orbigny). From sample No. 9, ×85.

31–35 *Globorotalia cultrata menardii* (Parker, Jones, and Brady). 31, 32 from sample No. 42, ×36; 33–35 from sample No. 42, ×43.

36 *Orbulina universa* d'Orbigny. From sample No. 42, ×43.

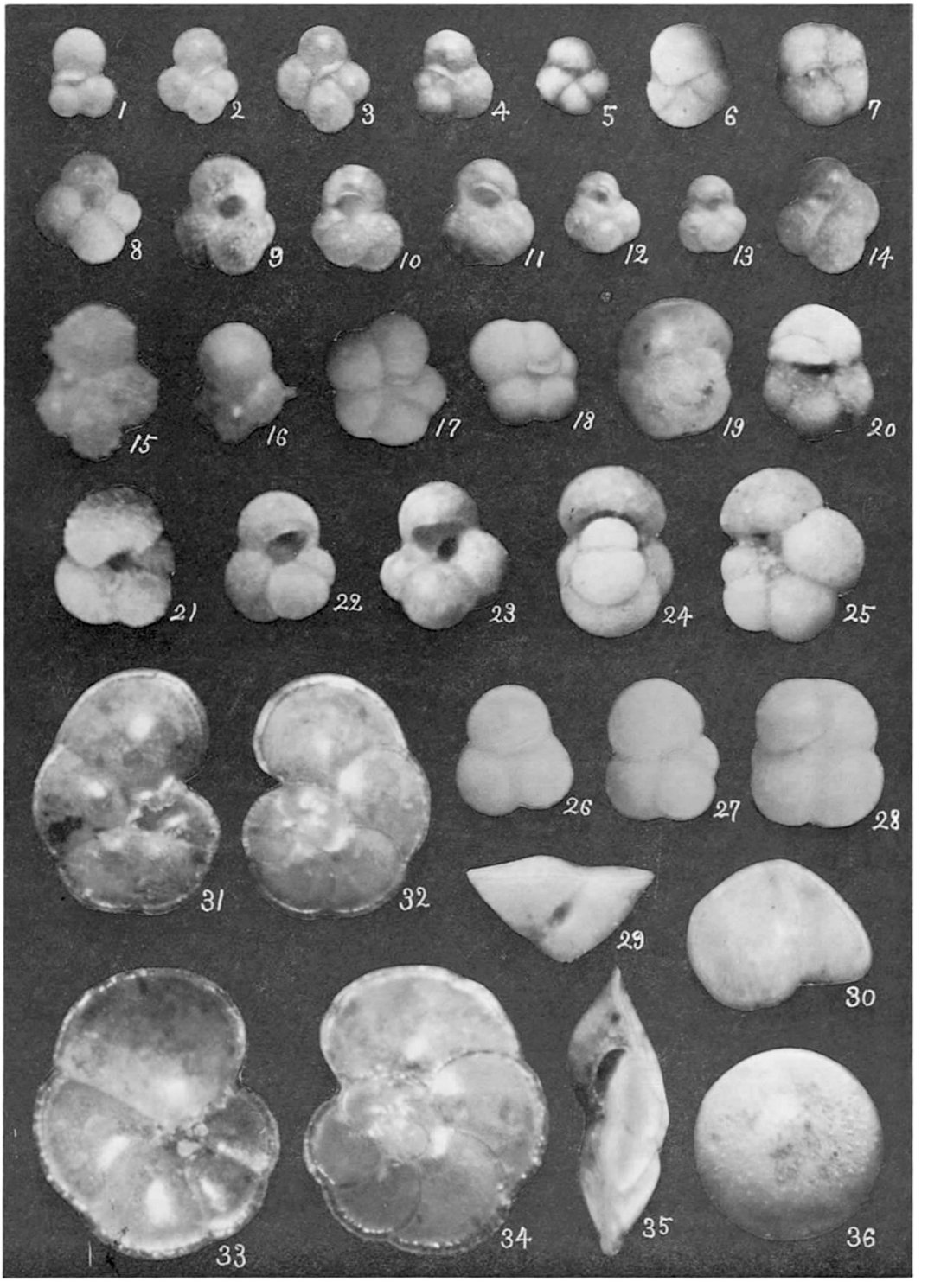

T. Huang: Planktonic Foraminifers from Taiwan Strait

Blank page

Page blanche

Volume 6 United Nations ECAFE, CCOP TECHNICAL BULLETIN July 1972

IV. SEDIMENTS OF TAIWAN STRAIT AND THE SOUTHERN PART OF THE TAIWAN BASIN

(Project CCOP-1/ROC. 3)

By

J. T. Chou

Chinese Petroleum Corporation,
Miaoli, Taiwan, China

(with figures IV–1 to IV–10; and tables IV–1 to IV–4)

ABSTRACT

General descriptions of the total sediments and organic fraction, the grain size analysis of the terrigenous fraction, and a mineralogical study of the light, heavy, and clay fractions, have been made on 67 samples of sea floor sediments from Taiwan Strait and the southern part of the Taiwan Basin, together with seven samples of beach sands from northern Taiwan.

The sandy sediments in the northeastern part of Taiwan Strait contain small amounts of the calcareous remains of molluscs, foraminifers, corals and other organisms, and they become finer to the west, towards the mainland coast of China. In the southern part of the Taiwan Basin, the sea bottom sediments are mainly sandy and are characterized by a high content of the calcareous remains of molluscs together with small amounts of foraminifers, corals, algae and other organisms, and the sediments gradually become more silty towards the northeast. The beach sediments from northern Taiwan are mostly sandy and are characterized by their abundant content of heavy minerals and small amounts of foraminifers and molluscan fragments. As for the calcareous organic remains in general, fragments of molluscs are dominant in the sandy sediments and foraminiferal tests are dominant in the silty sediments.

The beach sediments in northern Taiwan are the coarsest among all the samples examined and the sea bottom sediments in the southern part of the Taiwan Basin are slightly coarser than those in Taiwan Strait. The coarser sea bottom sediments in Taiwan Strait and the southern part of the Taiwan Basin are mainly very well to moderately well sorted and negatively skewed or lower in *phi* skewness values; in these respects, they are quite similar to the beach sands of northern Taiwan and some other districts. Based on their textural parameters, these coarser sediments might have been deposited mainly in a littoral environment, whereas the less coarse sediments might have been deposited mainly in fluvial, eolian, and neritic environments during a Pleistocene glacial epoch of lowered sea level, all of which may therefore be relict sediments preserved after the rise of sea level following that glacial interval.

The sea bottom sediments are composed mainly of grains of quartz, feldspars, rock fragments, large amounts of the remains of molluscs and small amounts of the remains of other calcareous organisms, together with clay and heavy minerals. The non-calcareous part of the

sea bottom sediments is mainly arkosic and it can be variously classed as arkose sand, subarkose sand, graywacke sand, sandy silt, silt and clay.

The contents of heavy minerals in the sea bottom sediments from the southern part of the Taiwan Basin are higher than in those from Taiwan Strait and the shallow part of the South China Sea. The heavy minerals from the southern part of the Taiwan Basin are mainly hornblende and alterite with small amounts of magnetite, epidote, garnet, and tourmaline; those in the northern part of Taiwan Strait are characterized by hornblende and alterite and in the southern part, by zircon, tourmaline, garnet, and epidote.

Minerals of the clay fraction of the sea bottom sediments from the southern part of the Taiwan Basin are illite, chlorite, kaolinite, quartz, feldspars (albite-oligoclase and K-feldspar), calcite, gypsum, and a small amount of smectite.

INTRODUCTION

After the third session of the Committee for Co-ordination of Joint Prospecting for Mineral Resources in Asian Offshore Areas (CCOP), at Seoul, Korea, in June-July 1967, the Chinese Petroleum Corporation (CPC) decided to undertake a sea bottom sampling project off the shores of Taiwan. The main purposes of this project are: (a) to make various physical oceanographic measurements; (b) to take samples of bottom sediments and bedrock with a piston-corer and a gravity-corer, as well as by dredging; (c) to make analyses of the samples at the Sedimentation Laboratory of CPC and paleontologic studies of the organic remains in the sediments and bedrock at the Paleontology Laboratory of CPC.

The research vessel HAIHSIEN, with a full displacement of 91 tons and all the necessary facilities, was lent to CPC by the Taiwan Fisheries Research Institute for the bottom sampling project. Part of the field work was carried out from 12 to 18 September 1968 but it was suspended due to trouble with the ship's engines. Only 36 samples of sea bottom sediments were taken by dredging and physical oceanographic measurements could be made only at a few points during this voyage. The area surveyed extends seaward for about 60 km from the shore of western Taiwan and includes the area between the Taiwan Bank and the Penghu (Pescadores) Islands.

Another 31 samples of sea bottom sediments were taken by dredging from the southern part of the Taiwan Basin by the R/V CHIULIEN, the research vessel of the Institute of Oceanography of the National Taiwan University, during the period from December 1969 to June 1970. The area referred to as the "Taiwan Basin" in this report (see Fig. IV-1) is the broad area of continental shelf to the northeast of the northern end of Taiwan in which substantial thicknesses of sediments of probably Neogene to Recent age have been shown to exist (Emery, *et al.*, 1969; Wageman, *et al.*, 1970). In addition, seven samples of sediment from the beaches of northern Taiwan were collected by staff of CPC in November 1970.

A general study was made of the total sediments of the 67 sea bottom samples from Taiwan Strait and the southern part of the Taiwan Basin, as well as the seven sand samples from the beaches of northern Taiwan; hydrochloric acid treatment, grain size analysis and a mineralogical study of the light and heavy fractions in them was made

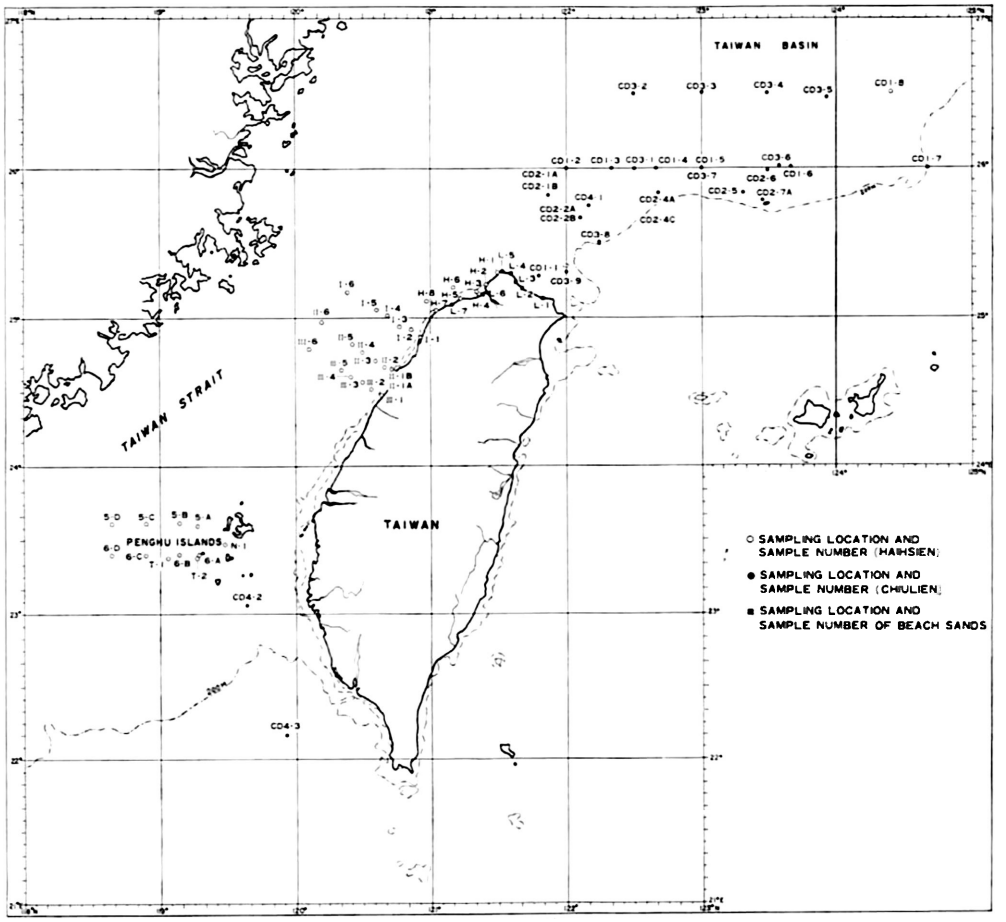

Figure IV-1. Locations of samples of sea bottom sediments collected in the vicinity of Taiwan and samples of beach sediments from northern Taiwan.

at the Sedimentation Laboratory of CPC from December 1970 to November 1971.

The minerals in the clay fractions (particles less than 5 microns) of 22 of the sea bottom samples from the Taiwan Basin were identified by Professor Y. Wang (1971) at the Institute of Geology of the National Taiwan University. The area studied covers part of the continental shelf in the vicinity of Taiwan, including the eastern half of Taiwan Strait and the southern part of the Taiwan Basin between latitudes 23°N and 27°N and longitudes 118°E and 125°E. The sample numbers and sampling locations are shown in Table IV-1 and Figure IV-1.

PREVIOUS STUDIES

About 300 samples dredged from the shallow parts of the East China Sea and the

South China Sea were made available for foraminiferal studies for the master's theses of W. Polski and H. O. Waller at the University of Southern California. The results were published by Polski (1959) for the East China Sea and by Waller (1960) for the shallow part of the South China Sea. C. S. Wang (1960) studied the sand fraction of the shelf sediments off the mainland coast of China. Nearly 1,000 bottom samples dredged from the shallow parts of the East China Sea and South China Sea were studied and compared with the oceanographic conditions and source areas by Niino and Emery (1961). Emery *et al.* (1969) reported on the geologic structure and some water characteristics of the East China Sea and the Yellow Sea and these results were also published elsewhere by Wageman, Hilde, and Emery (1970). Chou (1971) studied the planktonic foraminifers and heavy minerals in Recent sediments from the shallow part of the South China Sea. J. C. Chen and Chin Chen (1971) studied the mineralogy, geochemistry, and paleontology of shelf sediments of the South China Sea and Taiwan Strait. Chou and Wu (1971) studied the grain size and light minerals of the sea bottom sediments from the southern part of the Taiwan Basin and Huang (1971) reported on the foraminiferal trends in the surface sediments of Taiwan Strait.

TOTAL SEDIMENTS

A dried part of each sample was examined under the binocular microscope and a general description was made before acid treatment, grain size analysis, and the mineralogical study of each sample was undertaken. Table IV-1 shows the sample numbers, sampling dates, locations and depths, together with a general description of the total sediments in the samples dredged from Taiwan Strait and the southern part of the Taiwan Basin, and of the beach sediments taken from northern Taiwan.

In the area between the Taiwan Bank and the Penghu Islands, sandy sediments are present on both the west and east sides. In the northeastern part of Taiwan Strait, a narrow belt near the northwestern coast of Taiwan is characterized by sandy sediments, but they become finer eastward to the coast of Taiwan and westward off the coast of the mainland of China. These sandy and silty sediments in Taiwan Strait contain small amounts of the remains of molluscs, foraminifers, corals and other calcareous organisms.

In the southern part of the Taiwan Basin, the sea bottom sediments are mainly sandy and are characterized by a high content of the remains of molluscs and small amounts of foraminifers, corals, algae and other calcareous organisms. The sediments gradually become silty towards the northeast.

The beach sediments from northern Taiwan are mostly sandy and are characterized by a high content of heavy minerals and small amounts of foraminifers and molluscan fragments.

ORGANIC FRACTION

The fraction of organic origin in the sea bottom sediments from Taiwan Strait and the southern part of the Taiwan Basin, and of the beach sediments from northern Taiwan,

Table IV–1. Data on samples and general description of sea bottom sediments from the vicinity of Taiwan and beach sediments from northern Taiwan.

Locality	Sample no.	Sampling data	Location latitude	Location Longitude	Depth (m)	General description of total sediments
Southern part of the Taiwan Basin	CD1–1	25 Dec 1969	25°17′N	121°47.5′E	90	Mollusca (>50%), granules, and pebbles with small amounts of sand, clay, corals, and Foraminifera.
	CD1–2	〃	26°00′N	121°59.9′E	110	Mollusca (60%) and f.g. sand with small amounts of corals and Foraminifera.
	CD1–3	〃	〃	122°20′E	〃	Mollusca (>50%) and f.g. sand with small amounts of Foraminifera.
	CD1–4	〃	〃	122°40′E	〃	Mollusca (>50%) and f.g. sand.
	CD1–5	〃	〃	123°00′E	〃	Mollusca (>50%) and f.g. sand with small amounts of Foraminifera and Centipedes.
	CD1–6	26 Dec. 1969	26°00.8′N	123°39.5′E	140	F.g. sand and Mollusca with small amounts of Foraminifera.
	CD1–7	〃	26°00′N	124°40′E	200	F.g. sand with Mollusca and Foraminifera.
	CD1–8	〃	26°30′N	124°24′E	145	〃
	CD2–1a	6 May 1970	25°49′N	121°51.4′E	135	Mollusca and m.g.- f.g. sand with small amounts of granules and Foraminifera.
	CD2–1b	〃	〃	〃	〃	Mollusca and muddy sand with small amounts of granules, pebbles, and Foraminifera.
	CD2–2a	〃	25°40.6′N	122°05.6′E	120	Mollusca (70%) and f.g. sand with small amounts of granules, pebbles, and Foraminifera.
	CD2–2b	〃	〃	〃	〃	Mollusca (60–70%) and m.g.- f.g. sand with small amounts of corals and Foraminifera.
	CD2–4a	7 May 1970	25°50′N	122°40.8′E	110	Mollusca (70%) and f.g. sand with corals, algae, echinoides, and Foraminifera.
	CD2–4b	〃	〃	〃	〃	Mollusca (>90%) and f.g. sand with small amounts of Foraminifera and corals.
	CD2–4c	〃	〃	〃	〃	〃
	CD2–5	〃	〃	123°18′E	120	Mollusca (>50%) and, f.g. sand with Foraminifera and algae.
	CD2–6	〃	25°58.8′N	123°29′E	125	Mollusca (>50%) and f.g. sand with Foraminifera, algae, and corals.
	CD2–7a	〃	25°47′N	123°27′E	120	Mollusca (>60%) and f.g. sand with corals, Foram., algae, and crustaceous.
	CD4–1	9 May 1970	25°45′N	122°09′E	165	Gy. silt with a small amount of fossils.
	CD3–1	11 June 1970	26°00′N	122°30′E	〃	Mollusca (>90%), f.g. sand, corals, and Foraminifera with small amounts of pebbles.
	CD3–2	〃	26°30′N	〃	〃	Brn. gy. f.g. sand with small amounts of Mollusca (10%), Foraminifera (5%) and other fossils.
	CD3–3	〃	〃	123°00′E	140	Yl. gy. f.g. sand with Mollusca (15%), Foraminifera (15%, mainly planktonic), and other fossils.
	CD3–4	〃	〃	123°29′E	150	Gy. v.f.g. sand Mollusca (10%), Foraminifera (35%, mainly planktonic), and other fossils.
	CD3–5	〃	26°28′10″N	123°55′30″E	140	Muddy v.f.g. sand with Foraminifera and Mollusca.
	CD3–6	12 June 1970	26°01′N	123°34.5′E	160	Mollusca (>60%) and f.g. sand with Foraminifera and algae.
	CD3–7	〃	26°00′N	123°00′E	150	Fine-grained sand with Foraminifera, Mollusca, and corals.
	CD3–8	〃	25°30.8′N	122°14′E	〃	Corals, Mollusca, and Foraminifera with c.g. sand and granules.
	CD3–9	〃	25°18.6′N	121°59.5′E	160	F.g. sand with granules, pebbles, Mollusca, Foraminifera, and corals.
Taiwan Strait	H–1	12 Sep. 1968	25°17.5′N	121°29.5′E	30	Coaly matters and Mollusca.
	H–2	〃	25°13.2′N	121°24.2′E	20	Fossiliferous gy. silty f.g. sand.
	H–3	〃	25°10′N	121°20′E	17	Dk. gy. f.g. sand with Foraminifera.
	H–4	〃	25°09.6′N	121°21′E	5	Dk. gy. v.f.g.- f.g. sand.
	H–5	13 Sep. 1968	25°08′N	121°13′E	4	Dk. gy. silty v.f.g. sand.
	H–6	〃	25°12′N	121°10′E	34	Dk. gy. f.g. sand.
	H–7	〃	25°03′N	121°02′E	10.5	Gy. silty v.f.g.-f.g. sand.
	H–8	〃	25°07′N	120°58.2′E	45	Gy. m.g. sand.
	I–1	〃	24°52′N	120°55′E	9	Dk. gy. v.f.g.-f.g. sand.

Table IV–1. (*Cont.*)

Locality	Sample no.	Sampling data	Location		Depth (m)	General description of total sediments
			Latitude	Longitude		
Taiwan Strait	I–2	13. Sep. 1968	24°55′N	120°51′E	34	Gy. f.g.-m.g. sand with pebbles and molluscan fragments.
	I–3	〃	24°56′N	120°46′E	38	Gy. f.g.-m.g. sand with Mollusca.
	I–4	〃	25°01′N	120°40′E	46	Dk. gy. f.g. sand with Mollusca fragments.
	I–5	〃	25°03′N	120°36′E	43	Gy. silty sand with abundant Mollusca.
	I–6	〃	25°10′N	120°23′E	34	Gy. silt.
	II–6	14 Sep. 1968	24°58′N	120°11′E	32	〃
	II–5	〃	24°49′N	120°25′E	37	Gy. silty f.g. sand with molluscan fragments.
	II–4	〃	24°46′N	120°29′E	33	Gy. silty m.g.-f.g. sand with molluscan fragments.
	II–3	〃	24°43′N	120°34′E	30.2	Gy. silty f.g. sand with molluscan fragments.
	II–2	〃	24°40′N	120°39′E	27.8	Gy. silty sand with molluscan fragments.
	II–1a	〃	24°39′N	120°42′E	3	Gy. v.f.g.-m.g. sand.
	II–1b	〃	24°39′N	120°42′E	18	Gy. sandy silt.
	III–1	〃	24°29′N	120°37′E	9	Gy. silty v.f.g. sand.
	III–2	〃	24°31′N	120°33′E	27	Gy. silty f.g.-m.g. sand with molluscan fragments.
	III–3	〃	24°34′N	120°29′E	31	Gy. sandy silt with molluscan fragments.
	III–4	〃	24°36′N	120°24′E	—	〃
	III–5	〃	24°39′N	120°20′E	36	〃
	III–6	〃	24°47′N	120°06′E	31	〃
	5–A	15 Sep. 1968	23°36′N	119°16′E	34	Yl. wh. f.g.-c.g. sand with Mollusca (45%), corals (5%), and Foraminifera (5%).
	5–B	〃	23°37′N	119°08′E	33.5	Lt. yl. gy. pebbly m.g.-c.g. sand with Mollusca (35%).
	5–C	〃	〃	118°53′E	30	Dk. gy. f.g. sand with small amounts of Mollusca (10%) and Foraminifera (2%).
	5–D	〃	〃	118°38′E	28.5	Yl. gy. f.g. sand with molluscan fragments (5%).
	6–D	〃	23°24′N	〃	21.8	Yl. wh. c.g.-v.c.g. sand with molluscan fragments (5%) and corals (2%).
	6–C	〃	〃	118°53′E	25.5	Yl. gy. pebbly f.g.-m.g. sand with molluscan fragments (15%), Foraminifera (3%), corals (2%), and other fossils.
	6–A	17 Sep. 1968	〃	119°17′E	25.2	Corals (40%), Mollusca (37%), Foraminifera (3%) and yl. gy. f.g. sand (20%).
	6–B	〃	〃	119°08′E	25	Yl. wh. pebbly f.g.-m.g. sand with molluscan fragments (15%), Foraminifera (3%), corals (2%), and other fossils.
	N–1	18 Sep. 1968	23°28.3′N	119°28′E	7	Gy. silty v.f.g.-f.g. sand with Foraminifera (10%).
	CD4–2	29 May 1970	23°03.9′N	119°37.2′E	80	Gy. silty v.f.g.-f.g. sand with Mollusca (15%) and Foraminifera (2%).
	CD4–3	〃	22°10′N	119°56′E	130	Mollusca (60%), corals (20%) and other fossils with yl. gy. f.g. sand.
	CD4–4	〃	20°40′N	120°06′E	140	Yl. gy. v.f.g.-f.g. sand with a small amount of Foraminifera (5%).
Beach in northern Taiwan	L–1	4 Nov. 1970	Juipin Beach		—	Gy. m.g. sand with Mollusca and Foraminifera (20–30%).
	L–2	〃	Wanli Beach		—	Lt. gy. m.g. sand with heavy minerals (magnetite, hornblends, augite, rock fragments etc.).
	L–3	〃	Chinshan Beach		—	Brn. blk. m.g. heavy sand (80%) (magnetite, hornblende, and augite).
	L–4	〃	Shihmen		—	Lt. gy. v.c.g. sand with granules, f.g. blk. hornblende, augite, Mollusca (60%), corals, Foraminifera, and andesite fragments.
	L–5	〃	Paishawan Beach		—	Brn. gy. m.g. sand (65%) with molluscan fragments, and heavy minerals.
	L–6	〃	Pali Beach		—	Brn. blk. f.g.-m.g. sand with heavy minerals.
	L–7	〃	Hsutsokang		—	

f.g.: fine-grained, v.f.g.: very fine-grained, m.g.: medium-grained, c.g.: coarse-grained, v.c.g.: very coarse-grained, gy.: gray, brn.: brown, yl.: yellow, wh.: white, blk.: black, dk.: dark, and lt.: light.

comprises calcium carbonate, silica, and organic carbon. The portion of the fraction that is soluble in dilute hydrochloric acid is classed for convenience as calcium carbonate, although it contains some magnesium carbonate. Figure IV-2 shows that the total carbonate is most abundant, more than 50 per cent, in the sediments from the area between the coast of northern Taiwan and the Tiaoyutai Islands (Senkaku Islands).

The three possible sources of the calcium carbonate are from biogenic debris, reworked limestone, and chemical precipitation. Most of the calcium carbonate is of direct biogenic origin, chiefly in the form of molluscan shells and fragments of them, followed in order by foraminiferal tests, corals and other calcareous organisms, either complete or fragmentary. Molluscan remains are usually dominant in the sandy sediments, and foraminiferal tests are dominant in the silty sediments.

The sea bottom sediments in the area between the coast of northern Taiwan and the Tiaoyutai Islands (Senkaku Islands) are characterized by abundant remains of molluscs, whereas those in the shallower areas of Taiwan Strait and the southwestern part of the Taiwan Basin have more benthonic foraminiferal tests with fewer planktonic foraminiferal tests, and the percentage of planktonic forms in the foraminiferal assemblages increases with depth below sea level.

TERRIGENOUS FRACTION

Size analysis

After the acid-soluble part of 64 of the sediment samples had been removed by treatment with dilute hydrochloric acid, the insoluble residue was washed and wet-sieved through a wire screen with openings of 0.062 mm. As a basis for discussion of the grain size distribution, screen analyses of all the samples were made to determine the percentage of the fine fraction, the main grain sizes, the *phi* median, the *phi* mean, the *phi* deviation, and the skewness of the sediments from each locality, in order to deduce the horizontal variation.

The results of these analyses are shown in Table IV-2, together with the *phi* statistical measures, which were calculated in the way used by Inman (1952, p. 130). The main grain sizes are underlined in this table. All particles smaller than 1/16 mm are placed in one class, namely, silt plus clay. Because of the lack of data that would have permitted further subdivision to be made, it is impossible to state whether the grain size distribution is actually, or only apparently, unimodal in all the sediments analyzed. However, most of the sediments are actually unimodal and only a few are clearly bimodal.

Fine fraction

The percentages of fine fraction (finer than 0.062 mm) are shown in Table IV-2 and Figure IV-3. They are lower in the area between the Taiwan Bank and the Penghu Islands, and become higher towards the northwest and the east. They are also lower in the area west of Hsinchu, and become higher eastward to the coast of Taiwan and westward to the coast of the mainland of China. The percentages of the fine fraction are lower in the broad area of the southern part of the Taiwan Basin, northeast of northern Taiwan.

Table IV-2. Main physical characteristics of sea bottom sediments from the vicinity of Taiwan and beach sediments form northern Taiwan.

Locality	Sample no.	Carbonate (%)	Fine fraction <0.0625 mm	Heavy minerals (%)	Light minerals (%)	Grain size distribution of noncalcareous sediments % (weight percentage) >4 mm Pebble	2-4 mm Granule	1-2 mm V.c.g.	1/2-1 mm C.g.	1/4-1/2 mm M.g.	1/8-1/4 mm F.g.	1/16-1/8 mm V.f.g.	<1/16 mm Silt + Clay	*Phi* median Mdφ	*Phi* mean Mφ	*Phi* deviation σφ	*Phi* skewness αφ
Southern part of the Taiwan Basin	CD1-7	50.3	4.3	2.6	42.8					1.1	78.5	9.5	10.9	2.4	2.75	0.55	0.64
	CD3-5	28.2	19.2	0.1	52.5					0.3	8.4	64.6	26.7	3.7	3.85	0.55	0.27
	CD1-6	39.8	4.2	2.2	53.8					1.8	78.1	13.1	7.0	2.6	2.8	0.4	0.5
	CD3-6	85.5	2.7	0.5	11.3				1.4	19.3	53.1	7.6	18.6	2.2	3.15	1.25	0.76
	CD2-6	74.8	2.6	0.9	21.7					21.8	53.6	14.3	10.3	2.5	2.7	0.8	0.25
	CD3-4	25.4	1.6	1.8	71.2					0.9	5.4	91.6	2.1	3.4	3.35	0.05	−1.00
	CD2-7a	67.9	8.3	0.9	22.9					11.8	54.8	7.5	25.9	2.3	3.85	1.85	0.83
	CD2-5	63.9	1.8	1.8	32.8				0.6	19.6	64.8	10.0	5.0	2.2	2.4	0.5	0.4
	CD3-3	24.1	0.3	1.9	73.7					1.4	49.7	48.5	0.4	3.0	2.8	0.3	−0.06
	CD1-5	57.4	1.0	1.0	40.6					9.9	85.0	2.8	2.3	2.6	2.55	0.25	−0.2
	CD3-7	32.5	1.1	0.2	66.2				0.1	19.6	76.8	1.9	1.6	2.1	2.1	0.2	0
	CD2-4a	72.7	0.6	1.8	24.9				0.4	16.5	74.3	6.6	2.2	2.1	2.25	0.25	0.6
	CD2-4b	92.9	0.4	0.5	6.2				1.4	8.5	70.4	14.1	5.6	2.6	2.7	0.5	0.2
	CD2-4c	91.7	1.6	0.6	6.1					3.6	59.0	18.1	19.3	2.8	3.2	1.1	0.36
	CD3-2	15.4	0.2	1.6	82.8					1.5	84.1	14.2	0.2	2.5	2.6	0.3	0.33
	CD1-3	56.0	1.2	1.1	41.7				0.7	17.7	76.4	2.5	2.7	2.4	2.3	0.4	−0.25
	CD1-2	60.7	1.5	1.2	36.6				0.2	24.4	68.3	3.3	3.8	2.3	2.25	0.45	−0.11
	CD2-1a	47.2	14.4	1.6	36.8	0.9	1.7	0.6	0.4	31.4	35.2	2.5	27.3	2.3	4.0	2.2	0.77
	CD2-1b	48.9	19.7	2.0	29.4	2.7	2.7	1.4	0.4	26.5	25.2	2.5	38.6	2.4	4.05	2.25	0.51
	CD4-1	25.5	30.2	0.01	44.0					6.4	6.7	46.3	40.6	4.0	3.8	0.5	−0.4
	CD2-2a	75.7	6.9	1.0	16.4	2.1	1.2	1.2	1.6	24.7	29.7	11.1	28.4	2.5	3.6	2.0	0.55
	CD2-2b	74.2	7.5	1.0	17.3			0.4		29.1	26.4	13.4	29.1	2.7	3.65	1.95	0.49
	CD1-1	73.3	4.5	2.7	19.5	38.2	2.6	2.6		5.2	23.3	9.0	16.9	1.8	0.65	3.45	−0.33
Taiwan Strait	H-2	25.0	29.8	1.9	43.3			0.3	1.7	11.7	41.7	5.0	39.6	2.7	4.4	2.4	0.71
	H-4	8.0	8.7	0.2	83.1					0.4	38.5	51.7	9.4	3.1	3.1	0.5	0
	H-3	15.2	3.1	2.3	79.4			0.3	0.4	7.8	81.6	6.3	3.6	2.5	2.45	0.25	−0.2
	H-5	7.7	24.0	0.2	68.1					0.4	10.1	63.5	26.0	3.8	3.75	0.45	−0.11
	H-6	14.8	12.2	1.5	71.5				0.2	0.6	66.1	18.8	14.3	2.8	3.25	0.55	0.82
	H-7	12.7	27.7	0.6	59.0				0.1	1.3	39.6	27.3	31.7	3.3	3.75	1.05	0.43
	H-8	19.2	2.0	0.5	78.2		0.3	1.9	8.0	70.3	15.2	1.9	2.4	1.6	1.65	0.45	0.11
	I-1	8.0	12.0	0.3	79.7					0.7	38.6	47.7	13.0	3.1	3.25	0.55	0.27
	I-2	23.0	3.9	0.6	72.5	4.2	0.6	1.0	7.9	41.0	37.5	2.7	5.1	1.9	1.75	0.55	−0.27
	I-3	15.6	2.6	0.3	81.5			0.2	6.9	46.2	41.0	2.7	3.0	2.0	1.9	0.3	−0.33
	I-4	29.0	6.2	0.3	64.5				0.6	10.1	74.1	6.5	8.7	2.2	2.4	0.4	0.5
	I-5	53.9	18.0	0.1	28.0				0.5	1.9	32.6	26.0	39.0	3.4	4.3	1.5	0.6
	I-6	12.0	80.67	0.02	7.31						0.4	7.9	91.7	5.5	5.7	1.1	0.18
	II-1B	10.8	76.4	0.03	12.77						1.8	12.6	85.6	5.1	5.1	0.9	0
	II-2	20.0	31.8	0.2	48.0			0.4	5.8	27.0	25.4	1.7	39.7	2.7	3.95	2.25	0.56
	II-3	14.0	22.7	0.4	62.9			0.4	5.8	19.4	44.9	3.1	26.4	2.2	3.9	2.2	0.77
	II-4	31.2	30.7	0.1	38.0			0.4	5.2	27.8	20.6	2.7	43.3	2.7	4.15	2.45	0.59
	II-5	19.0	35.6	0.1	45.3				1.4	12.9	33.6	8.1	44.0	3.1	4.25	2.05	0.56
	II-6	13.0	82.0	0.04	4.95						0.3	5.4	94.3	5.8	5.65	0.75	−0.2
	III-1	8.0	36.0	0.2	55.8					0.3	5.1	55.5	39.1	3.8	4.1	0.8	0.33
	III-2	13.3	34.3	0.2	52.2			0.4	3.8	24.6	25.4	6.2	39.6	2.6	4.05	2.35	0.62
	III-3	15.0	56.0	0.1	28.9				0.8	9.0	19.2	5.1	65.9	5.7	4.4	2.3	−0.57
	III-4	29.4	48.8	0.03	21.77				0.7	12.1	14.2	2.8	70.2	6.3	4.5	3.4	−0.56
	III-5	16.67	55.67	0.03	26.63				0.8	8.0	16.0	7.2	68.0	5.7	4.7	2.1	−0.48
	III-6	11.33	67.67	0.03	20.97					0.4	0.4	22.9	76.3	4.5	4.65	0.75	0.2
	5-A	31.6	0.2	0.1	68.0		0.6	6.4	24.9	36.6	28.9	2.3	0.3	1.5	1.45	0.95	−0.05
	5-B	24.5	—	0.08	75.0		1.3	18.5	36.5	31.1	11.9	0.7		0.8	0.9	1.1	0.09
	5-C	13.5	—	0.33	85.9			3.8	7.5	3.8	77.2	7.7		2.7	2.55	0.45	−0.33
	5-D	6.1	17.1	0.77	74.4		0.8	5.3	15.9	18.5	30.6	10.4	18.5	2.2	2.5	1.8	0.17
	6-B	28.5	0.5	0.05	70.7		2.8	12.6	18.5	58.8	6.3	0.3	0.7	1.4	1.0	0.9	−0.44
	6-C	29.7	12.5	0.31	68.5	3.2	10.7	8.9	8.2	23.5	40.5	3.2	1.8	1.8	1.75	0.75	−0.07
	6-D	2.9	—	0.03	95.7			8.8	44.1	44.1	3.0			1.0	0.95	0.65	−0.08
	N-1	17.7	30.6	0.2	51.3					0.4	33.6	28.7	37.3	3.5	3.8	1.3	0.23
	CD4-2	27.9	19.9	0.1	52.1		1.8	6.8	9.7	28.2	19.1	6.8	27.6	2.1	2.8	2.0	0.35

Table IV–2. (*Cont.*)

	Locality	Sample no.	Carbonate (%)	Fine fraction < 0.0625 mm	Heavy minerals (%)	Light minerals (%)	Grain size distribution of noncalcareous sediments % (weight percentage) >4 mm Pebble	2–4 mm Granule	1–2 mm V.c.g.	1/2–1 mm C.g.	1/4–1/2 mm M.g.	1/8–1/4 mm F.g.	1/16–1/8 mm V.f.g.	<1/16 mm Silt + Clay	*Phi* median Mdϕ	*Phi* mean Mϕ	*Phi* deviation $\sigma\phi$	*Phi* skewne $\alpha\phi$
Beach in northern Taiwan	Juipin	L–1	53.2	Tr.	4.45	42.38		0.2	0.2	4.5	73.3	20.1	1.3	0.4	1.9	1.85	0.25	−0.2
	Wanli	L–2	5.2	〃	7.95	86.85		0.3	1.3	18.7	72.6	6.6	0.4	0.1	1.1	1.15	0.25	0.2
	Chinshan	L–3	3.7	〃	79.59	16.73			0.1	2.9	76.4	20.3	0.3		1.6	1.75	0.35	0.29
	Shihmen	L–4	61.4	〃	9.73	28.9		6.2	45.6	18.9	20.2	6.7	1.6	0.8	−0.1	0.4	1.2	0.41
	Paishawan	L–5	28.2	〃	7.32	64.48				1.9	82.2	14.2	1.1	0.6	1.5	1.55	0.35	0.14
	Pali	L–6	8.1	〃	0.95	90.97				0.5	52.5	44.8	1.5	0.7	2.0	1.95	0.35	−0.14
	Hsutsokang	L–7	8.0	〃	0.58	91.44				0.8	42.0	52.1	5.1		2.1	2.0	0.7	−0.14

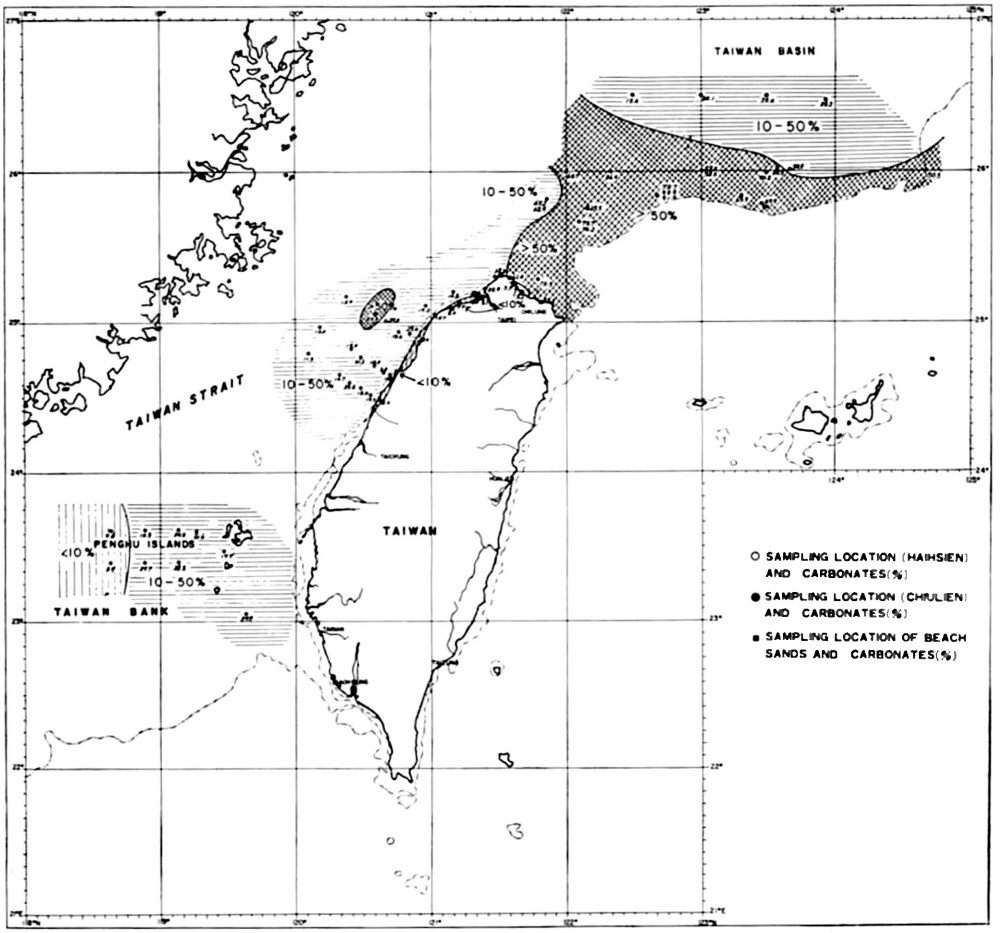

Figure IV-2. Percentages of carbonates (mainly calcium carbonate) in sea bottom sediments in the vicinity of Taiwan and in beach sediments of northern Taiwan.

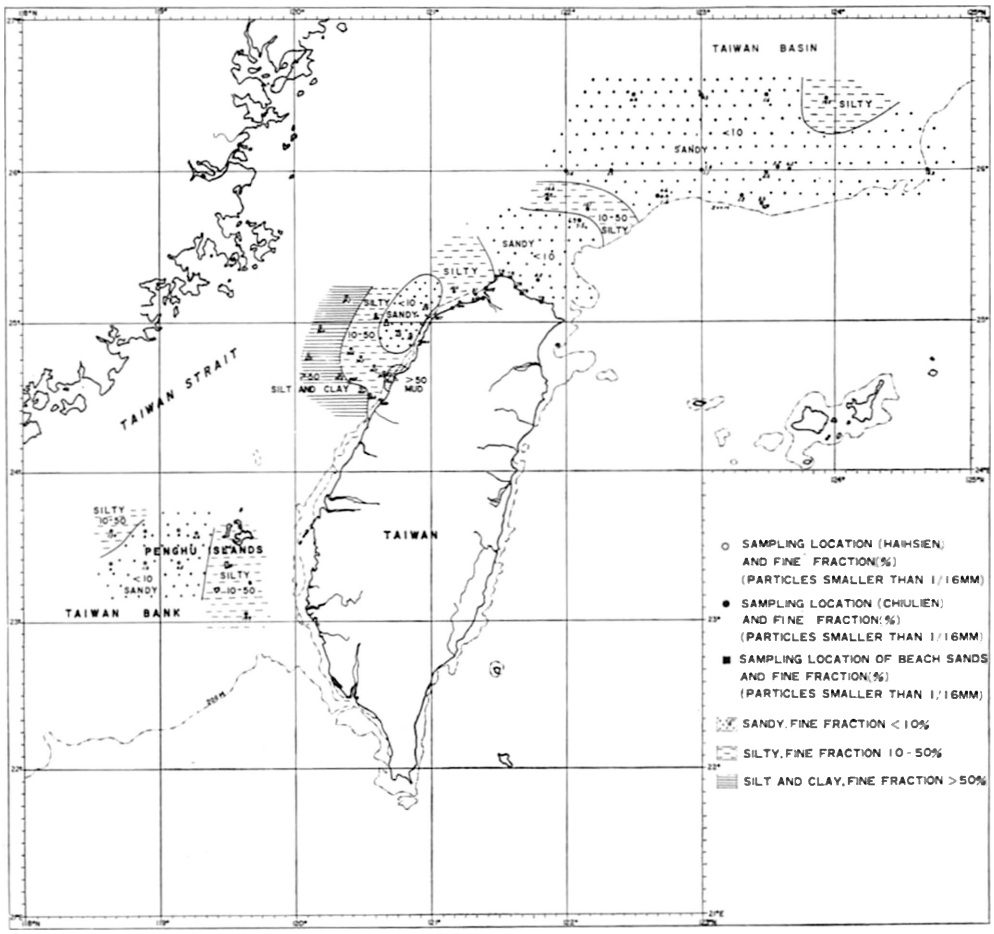

Figure IV-3. Percentages of the fine fraction (particles less than 1/16 mm) in sea bottom sediments in the vicinity of Taiwan and in beach sediments of northern Taiwan.

Main grain size

The main grain sizes of the sea bottom and beach sediments are shown in Table IV-2 and Figure IV-4. The sea bottom sediments are the coarsest in the area north of Chilung, where they consist of pebbly sand, and they become gradually finer towards the northeast. Medium- to fine-grained sand is present in a narrow belt off Hsinchu, and it becomes gradually finer eastward to the west coast of Taiwan and westward to the coast of the mainland of China. Medium-grained sand is found in the area between the Taiwan Bank and the Penghu Islands, and it becomes finer towards the west and the northeast.

Phi mean

The *phi* means of the grain size of the sea bottom and beach sediments are shown

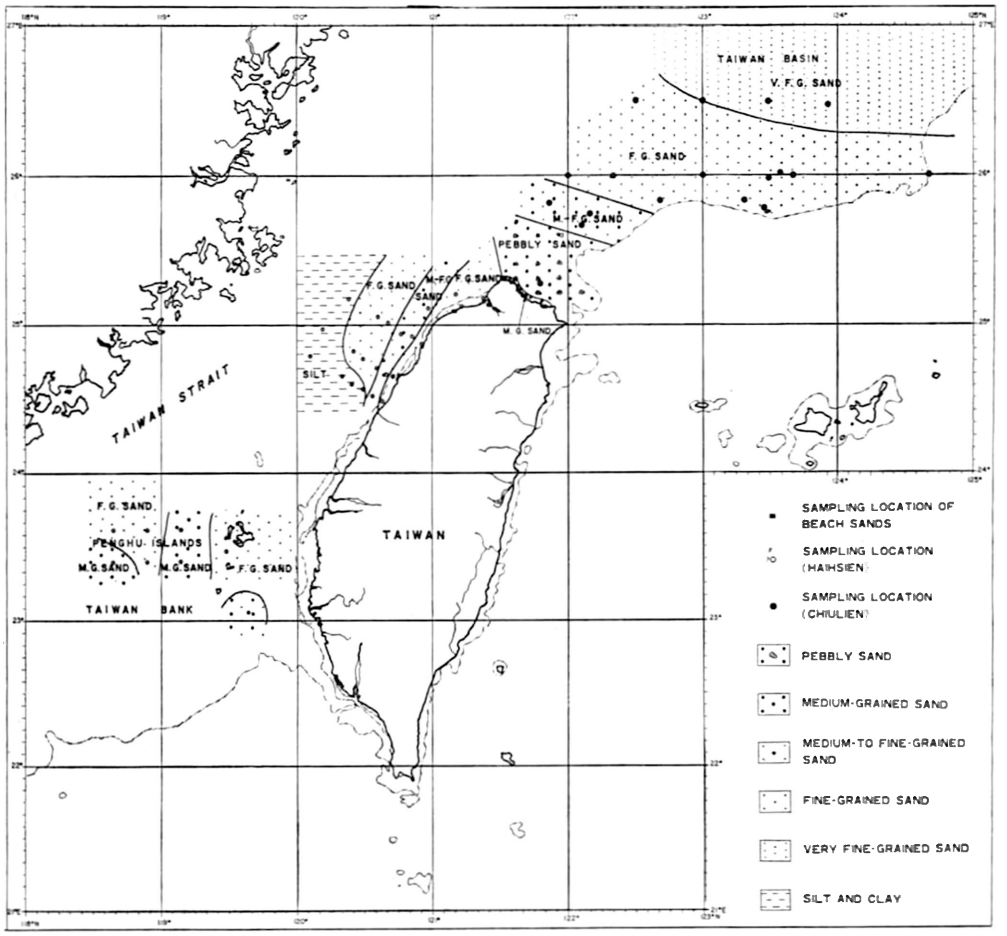

Figure IV-4. Main grain size of sea bottom sediments in the vicinity of Taiwan and beach sediments in northern Taiwan.

in Table IV-2 and Figure IV-5. These values range from 0.65 to 4.05 in the southern part of the Taiwan Basin, from 0.9 to 5.65 in Taiwan Strait, and from 0.4 to 2.0 on the beaches of northern Taiwan. The beach sediments in northern Taiwan are therefore the coarsest, and the sea bottom sediments are coarser in the southern part of the Taiwan Basin than in Taiwan Strait and the shallow part of the South China Sea. Some *phi* means of the grain size of the sea bottom sediments are nearly equivalent to the *phi* means of the beach sediments in northern Taiwan; this suggests that these sea bottom sediments may have been deposited in a littoral environment during a Pleistocene glacial epoch of lowered sea level and they may therefore be relict sediments preserved after the rise of sea level following that glacial interval.

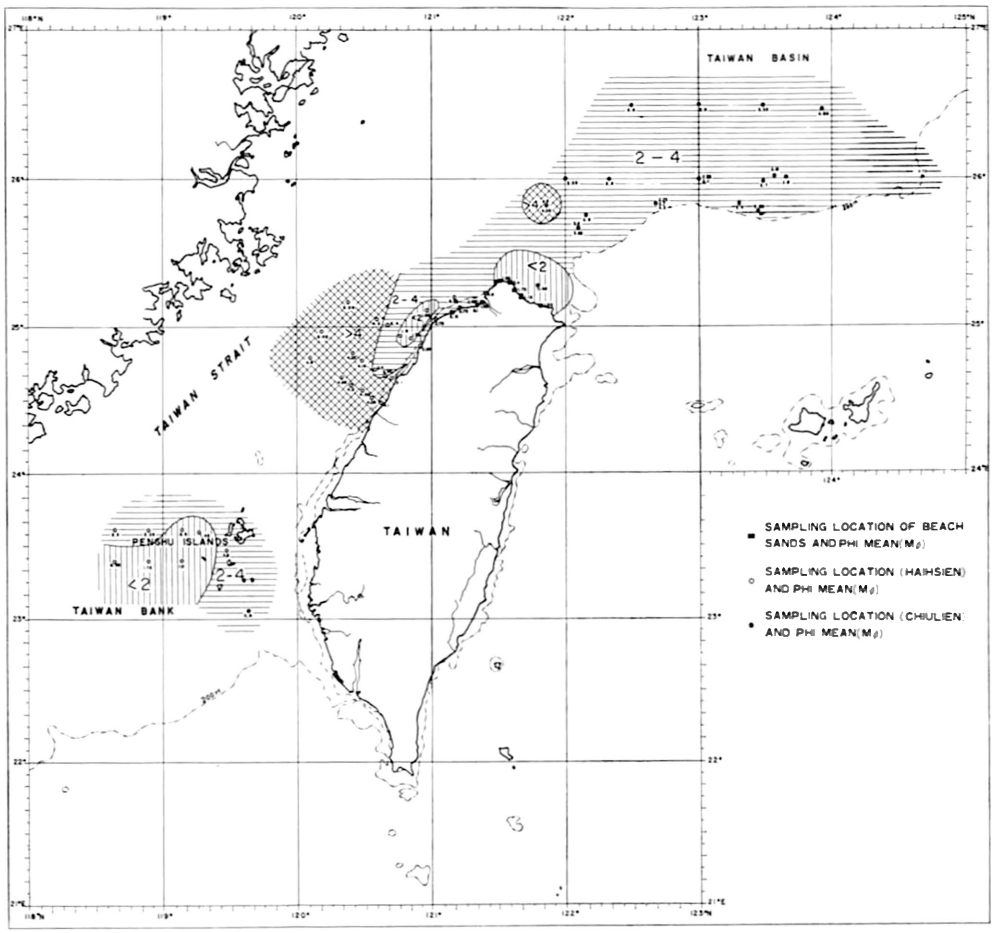

Figure IV-5. *Phi* mean values of grain size of sea bottom sediments in the vicinity of Taiwan and beach sediments in northern Taiwan.

Phi deviation

The sorting designations (*phi* deviations) of the sea bottom and beach sediments are indicated in Table IV-2 and Figure IV-6. These values range from 0.05 to 3.45 in the southern part of the Taiwan Basin (very well to very poorly sorted); from 0.25 to 3.4 in Taiwan Strait (also very well to very poorly sorted); and from 0.25 to 1.2 (very well to moderately sorted) in the beaches of northern Taiwan. The beach sediments in northern Taiwan are therefore the best sorted, and the sea bottom sediments in the southern part of the Taiwan Basin are slightly better sorted than those in Taiwan Strait. Inman and Chamberlain (1955), Friedman (1962), and Shepard and Young (1961 and 1965) reported that most beach and dune (eolian) sands are very well to well sorted (*phi* deviation 0.25–0.46), whereas most sands of rivers and on the continental shelf are moderately well sorted (*phi* deviation 0.46–0.73). Many river sands as well as many con-

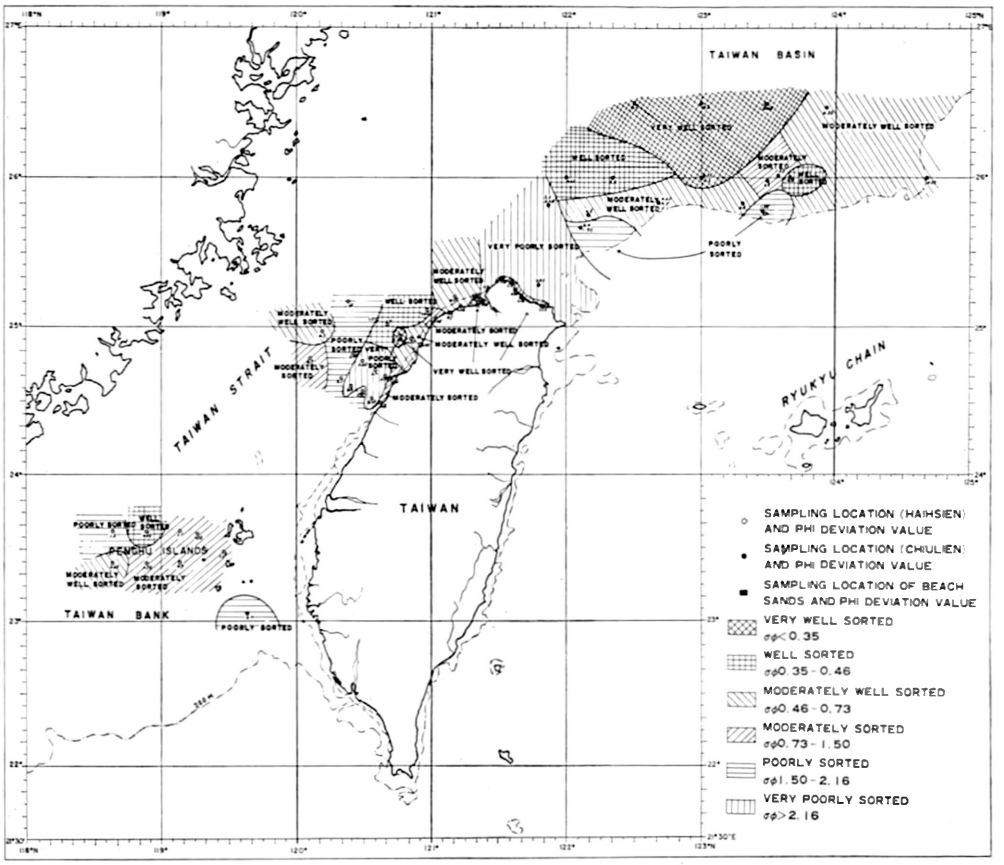

Figure IV-6. Sorting designations (*phi* deviation values) of sea bottom sediments in the vicinity of Taiwan and beach sediments in northern Taiwan.

tinental shelf sands below wave base were found by Friedman (1962) to be moderately sorted (*phi* deviation 0.73–1.50). Much of the sea bottom sediments in Taiwan Strait and the southern part of the Taiwan Basin are very well to moderately well sorted (*phi* deviation 0.05–0.65) and, in this respect, are quite similar to the beach sands of northern Taiwan and the beach and dune sands of some other districts. It is probable, therefore, that the sandy sea bottom sediments in Taiwan Strait and the southern part of the Taiwan Basin were deposited mainly in littoral and/or eolian environments and partly in an alluvial or neritic environment during a period of glacially lowered sea level in Pleistocene times.

Phi skewness

The *phi* skewnesses of the sea bottom and beach sediments are shown in Table IV-2 and Figure IV-7. These values range from –1.00 to 0.83 in the southern part of the Taiwan Basin, from –0.57 to 0.82 in Taiwan Strait, and from –0.2 to 0.41 on the beaches

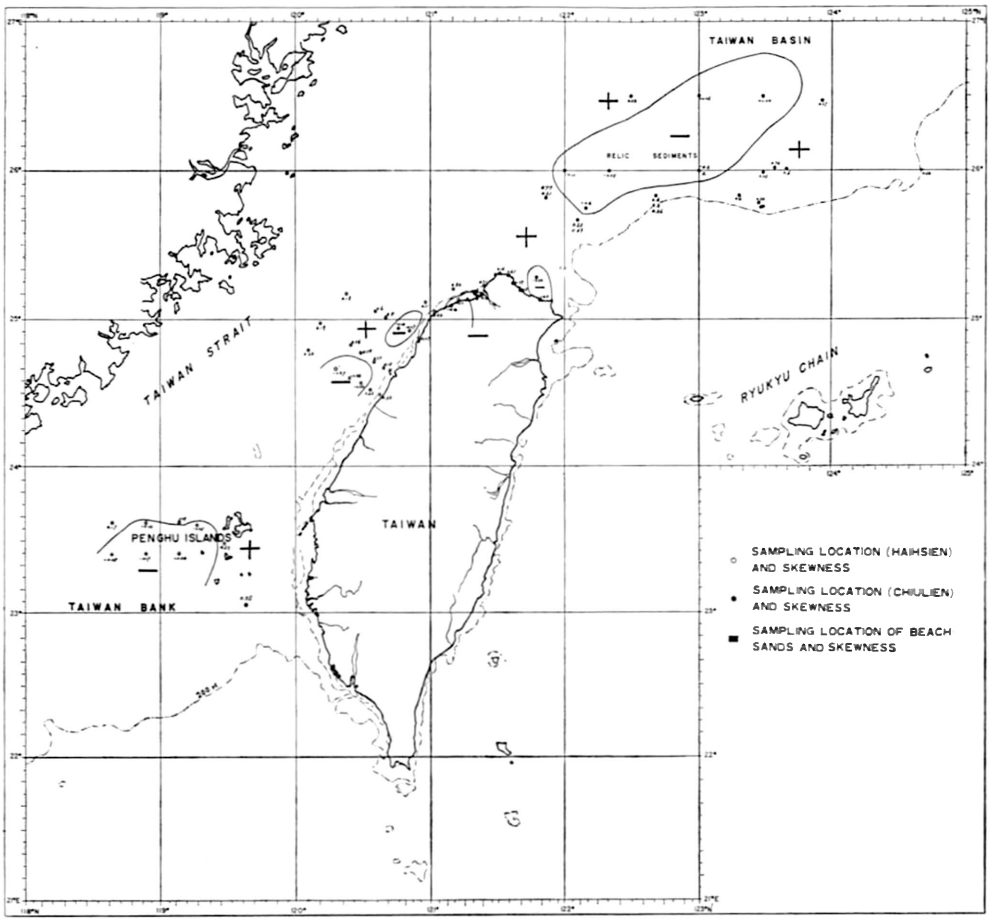

Figure IV-7. *Phi* skewnesses of sea bottom sediments in the vicinity of Taiwan and beach sediments in northern Taiwan.

of northern Taiwan. Dune and river sands are usually positively skewed whereas beach sands are mainly negatively skewed. Thus, river sands are distinguished from dune sands on the basis of their higher *phi* deviation, and beach sands are distinguishable by negative skewness from the other two, which are positively skewed (Friedman, 1961). Much of the coarse sea bottom sediments in Taiwan Strait and the southern part of the Taiwan Basin are distinguishable from dune and river sands by their negative skewness, which indicates that they were deposited in a littoral environment.

Based on the textural parameters, therefore, the coarse sea bottom sediments distributed in Taiwan Strait and the southern part of the Taiwan Basin might have been deposited mainly in a littoral environment, whereas the less coarse sediments may have been deposited mainly in alluvial, eolian, and neritic environments during a Pleistocene glacial epoch of lowered sea level.

MINERALOGY

The insoluble residue remaining after treatment with hydrochloric acid is composed mainly of the detrital mineral fraction and only negligible amounts of insoluble grains of authigenic, volcanic or organic origin are present. A separation of the sand-size insoluble residue into light and heavy fractions was made by floating or sinking with the heavy liquid bromoform ($CHBr_3$). The light minerals were identified by standard staining techniques and the heavy minerals by their optical characteristics.

Light fractions

The staining method used consisted of subjecting the dry material to hydrochloric acid fumes and then staining it with sodium cobaltinitrite solution (Russel, 1935). After treatment, the potash feldspar grains are intensely yellow, the quartz transparent, and the plagioclase white and opaque. The grains of the treated samples were identified and counted under the binocular microscope and the results of identification of the light minerals are shown in Table IV-3.

Table IV-3. Composition of the light mineral constituents in sea bottom sediments from the vicinity of Taiwan and in beach sediments from northern Taiwan.

Locality	Sample no.	Color	Roundness* (Pettijohn, 1957)	Light mineralogical composition (%)					Maturity Quartz /Feldspars +rock fragments	Source rock index Feldspars/ Rock fragments	Classification (Pettijohn, 1957)
				Quartz	K feldspar	Plagioclase	Rock fragments	others			
Southern part of the Taiwan Basin	CD1-7	Pale olive gray	SA-SR	59.2	0.5	16.7	23.6	—	1.45	0.72	Arkosic graywacke sand
	CD3-5	〃	〃	62.1	7.1	12.4	18.1	0.3	1.65	1.07	Silty arkose sand
	CD1-6	〃	〃	58.7	5.1	25.0	11.2	—	1.42	2.68	Arkose sand
	CD3-6	Pale red gray	SA-R	61.8	12.2	14.4	11.2	0.4	1.63	2.37	〃
	CD2-6	Pale olive gray	〃	57.8	2.9	16.4	22.8	0.1	1.37	0.84	Arkosic graywacke sand
	CD3-4	Light gray	SA-SR	68.9	1.2	13.7	14.3	1.9	4.62	1.04	Arkose sand
	CD2-7a	〃	SA-R	66.4	5.2	14.6	13.8	—	1.97	1.43	Silty arkose sand
	CD2-5	Pale yellowish brown	〃	53.1	13.5	17.2	16.2	—	1.13	1.89	Arkose sand
	CD3-3	Light gray	A-SA	51.0	12.5	12.6	19.3	4.4	1.15	1.30	Arkosic graywacke sand
	CD1-5	Pale olive gray	SA-SR	61.0	5.1	17.4	16.5	—	1.56	1.36	Arkose sand
	CD3-7	Pale red gray	SA-R	61.6	12.7	17.0	8.7	—	1.6	3.41	〃
	CD2-4a	Pale olive gray	〃	68.9	1.6	13.7	15.8	—	2.21	0.96	Arkosic graywacke sand
	CD2-4b	〃	〃	64.2	4.9	10.3	20.6	—	1.79	0.73	〃
	CD2-4c	〃	〃	62.1	8.6	13.7	15.6	—	1.63	1.42	Arkose sand
	CD3-2	Light gray	A-SA	46.3	12.1	16.0	21.9	3.7	0.92	1.28	〃
	CD1-3	Pale olive gray	SA-R	58.2	1.6	22.2	18.0	—	1.39	1.32	〃
	CD1-2	〃	SA-SR	56.1	5.5	21.0	16.4	1.0	1.3	1.61	〃
	CD2-1a	〃	SA-R	54.0	9.2	20.3	16.5	—	1.17	1.78	Pebbly arkose sand
	CD2-1b	〃	SA-SR	53.5	9.7	17.3	19.5	—	1.15	1.38	〃
	CD2-2a	〃	SA-R	52.8	3.8	14.9	28.5	—	1.11	0.65	Pebbly arkosic graywacke sand
	CD2-2b	〃	〃	61.7	2.1	11.1	25.1	—	1.61	0.52	〃
	CD1-1	〃	SA-SR	65.3	9.5	11.3	13.6	0.3	1.89	1.52	Pebbly arkose sand

Table IV–3. (*Cont.*)

Locality	Sample no.	Color	Roundness* (Pettijohn, 1957)	Light mineralogical composition (%)					Maturity Quartz /Feldspars +rock fragments	Source rock index Feldspars/ Rock fragments	Classification (Pettijohn, 1957)
				Quartz	K feldspar	Plagioclase	Rock fragments	others			
Taiwan Strait	H–2	Reddish gray–brownish gray	SA-R	67.5	4.0	14.8	13.7	—	2.07	1.37	Silty arkose sand
	H–4	Gray ~ dark gray	SA-SR	57.5	1.2	13.1	28.1	—	1.35	0.51	Arkosic graywacke sand
	H–3	Reddish gray ~ brownish gray	〃	56.6	18.4	8.2	16.8	—	1.3	1.58	Arkose sand
	H–5	Light gray ~ dark gray	〃	66.4	—	10.9	22.7	—	1.97	0.48	Silty graywacke sand
	H–6	Pale brownish gray	〃	45.2	21.8	18.0	14.3	—	0.83	2.78	Arkose sand
	H–7	〃	〃	63.0	4.9	10.3	21.8	—	1.7	0.69	Silty arkosic graywacke sand
	H–8	Pale gray ~ pale brownish gray	SA-R	74.7	3.8	13.0	8.5	—	2.95	1.97	Pebbly arkose sand
	I–1	Light gray	SA-SR	78.7	2.1	9.3	9.9	—	2.69	1.15	Subarkose sand
	I–2	〃	〃	68.8	5.1	11.5	14.5	—	1.21	1.14	Pebble arkose sand
	I–3	Very light gray	〃	63.2	9.7	15.3	11.8	—	0.71	2.11	Arkose sand
	I–4	〃	〃	66.0	11.9	11.2	10.9	—	1.94	2.11	〃
	I–5	Very light gray ~ light gray	〃	59.8	—	14.8	25.3	—	1.49	0.58	Silty arkosic graywacke sand
	I–6	〃	SA	45.9	—	10.7	43.4	—	0.84	0.24	Silt and clay
	II–1B	〃	SA-SR	70.3	—	11.6	18.1	—	2.36	0.64	〃
	II–2	Light gray	〃	73.9	7.4	15.3	3.4	—	1.83	6.67	Silty arkose sand
	II–3	Very light gray ~ light gray	〃	67.0	9.9	16.1	7.0	—	2.03	3.71	〃
	II–4	〃	SA-R	70.4	9.9	11.9	7.8	—	2.37	2.79	〃
	II–5	〃	〃	75.2	7.1	13.6	4.1	—	3.03	5.04	〃
	II–6	Gray ~ dark gray	SA	53.7	—	7.0	39.3	—	1.15	0.17	Silt and clay
	III–1	Light gray ~ dark gray	SA-SR	72.7	11.7	15.6	—	—	2.66	∞	Silty arkose sand
	III–2	Light gray	〃	74.8	9.5	8.4	7.3	—	2.96	2.45	〃
	III–3	Light gray ~ dark gray	〃	68.3	4.4	15.4	11.8	—	2.16	1.67	Sandy silt
	III–4	Gray ~ dark gray	〃	63.1	3.9	16.9	16.1	—	1.71	1.29	〃
	III–5	〃	〃	64.7	4.8	9.8	20.7	—	1.83	0.71	〃
	III–6	〃	SA	61.8	—	14.4	23.8	—	1.61	0.61	〃
	5–A	White	SR	77.4	5.4	5.4	11.8	—	2.42	0.91	Pebbly subarkose sand
	5–C	Very light gray	SR-R	64.3	7.3	10.8	15.4	2.2	1.92	1.17	Arkose sand
	5–D	White	〃	67.3	11.1	10.0	8.1	3.5	2.30	2.59	Pebbly arkose sand
	6–B	〃	〃	78.0	17.8	2.8	1.4	—	3.55	14.71	〃
	6–C	Very light gray	〃	62.9	15.4	9.3	12.4	—	1.67	2.79	〃
	6–D	White	〃	89.6	5.3	3.2	1.9	—	8.53	4.52	Subarkose sand
	N–1	Medium gray	SR	56.0	2.4	13.1	26.5	2.0	3.61	0.58	Silty arkosic graywacke sand
	CD4–2	〃	SR-R	42.1	5.8	7.8	43.3	1.0	0.73	0.31	Pebbly arkosic graywacke sand
	CD4–3	Light gray	SR	37.6	5.5	14.1	41.1	1.7	0.62	0.48	〃
	CD4–4	Light olive gray	SA-SR	65.3	5.6	11.8	14.7	2.6	2.03	1.18	Arkose sand
Beach in northern Taiwan: Juipin	L–1	Brownish gray	SA-R	56.5	7.0	5.1	31.4	—	1.29	0.38	Arkosic graywacke sand
Wanli	L–2	Light gray	SA-SR	88.3	3.5	7.0	1.2	—	7.54	8.75	Subarkose sand
Chinshan	L–3	Brownish black	SA-WR	61.1	6.1	17.7	15.1	—	1.57	1.57	Arkose sand
Shihmen	L–4	Light gray	SA	37.4	3.6	19.9	39.1	—	0.59	0.6	Arkosic graywacke sand
Paishawan	L–5	Brownish gray	SA-WR	64.6	7.4	9.5	18.5	—	1.82	0.91	〃
Pali	L–6	Brownish black	SA-R	53.5	2.6	3.5	40.4	—	1.15	0.15	Silty graywacke sand
Hsutsokang	L–7	〃	〃	51.3	3.2	5.9	39.6	—	1.05	0.22	〃

* Roundness: WR = well rounded, R = rounded, SR = subrounded, SA = subangular, A = angular

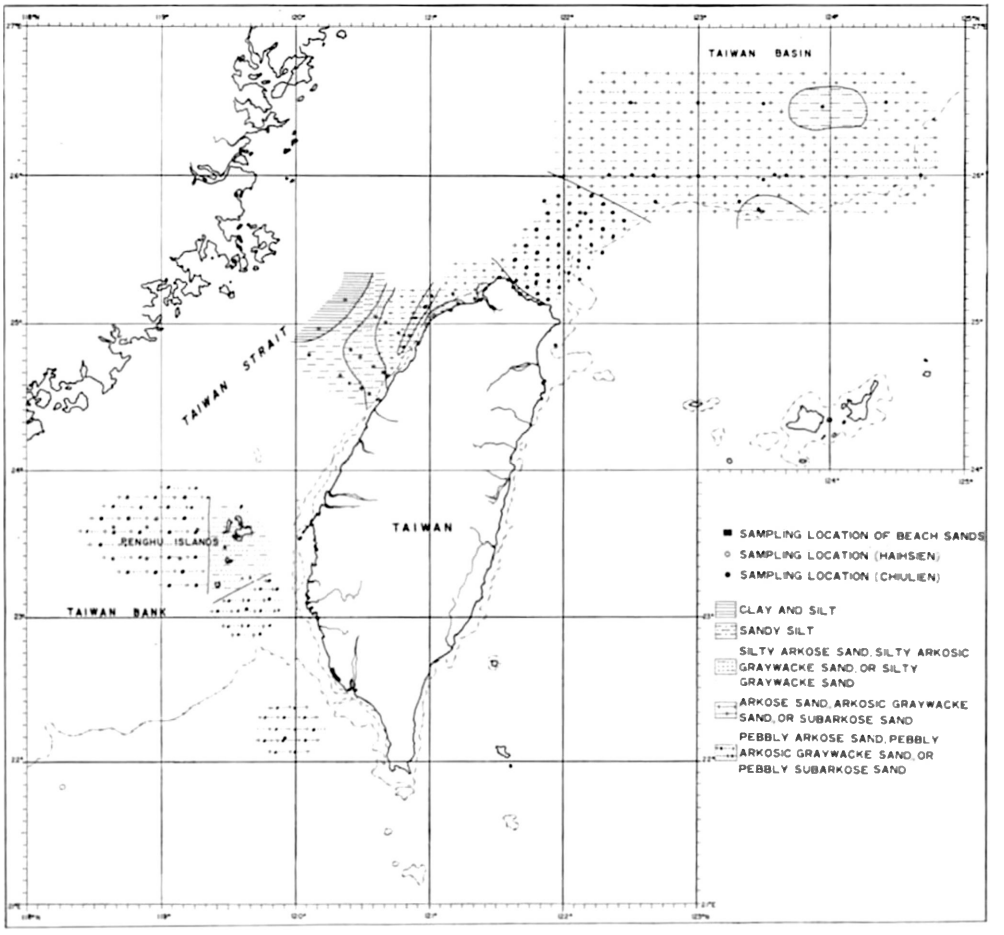

Figure IV-8. Lithofacies of sea bottom sediments in the vicinity of Taiwan.

The light fractions of the sediments are characterized by abundant quartz, rock fragments, plagioclase, and potash feldspar. Except in the area southeast of the Penghu Islands and the northwestern part of Taiwan Strait, most of the sea bottom and beach sediments are arkosic, containing abundant feldspars. The non-calcareous part of the sea bottom sediments may be classified as arkose sand, subarkose sand, graywacke sand, sandy silt, and silt and clay (Table IV-3). The lithofacies of the sediments are shown in Figure IV-8.

The maturity, ratio of quartz to feldspars plus rock fragments, is relatively low, being from 0.59 to 8.53 (Table IV-3), and the sediments can be regarded as not well matured. The source rock index, ratio of feldspars to rock fragments, is relatively high in the coarse sediments; they might therefore have been derived from plutonic source rocks, whereas the fine sediments with a low source rock index might have been derived from supracrustal rocks (Figure IV-9).

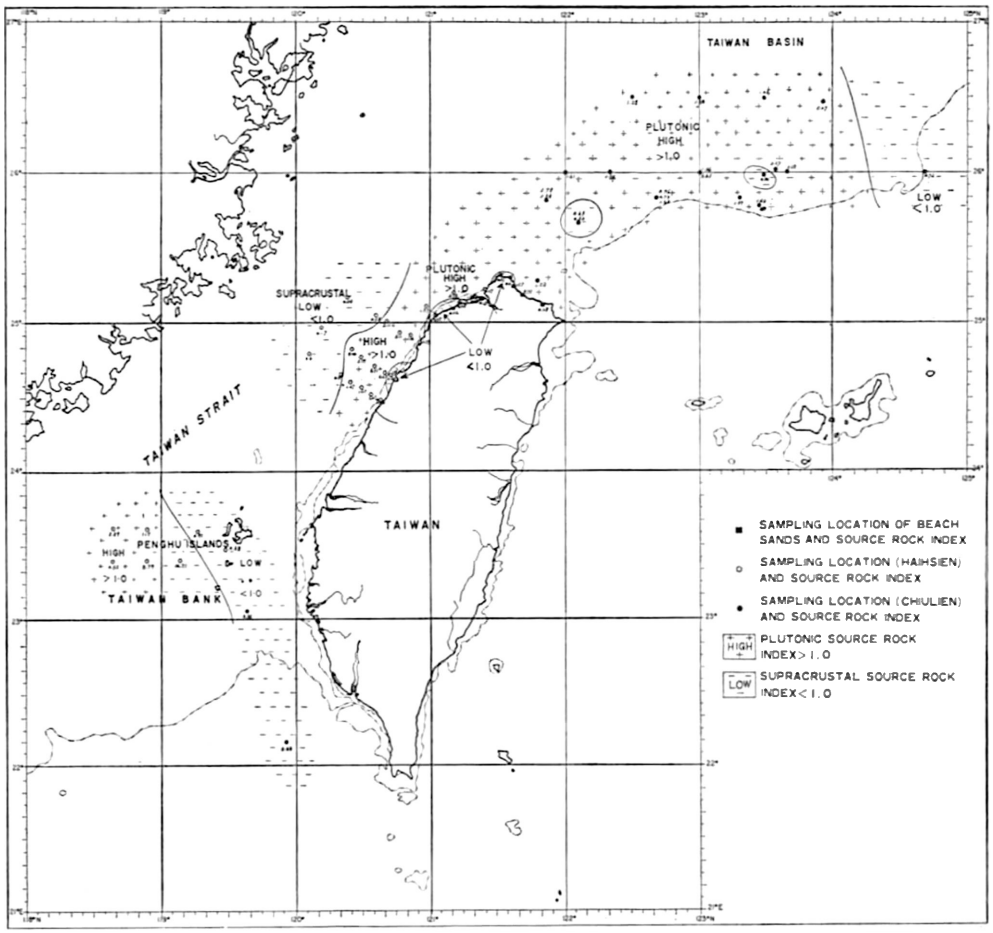

Figure IV-9. Source rock index, ratio of feldspar (plutonic) to rock fragments (supracrustal), of sea bottom sediments in the vicinity of Taiwan and beach sediments in northern Taiwan.

Heavy fractions

The heavy mineral contents in the total sediments are shown in Table IV-2 and Figure IV-10. The heavy mineral contents of the sediments from the southern part of the Taiwan Basin, ranging from 0.1 to 2.7 per cent by weight, are higher than those of sediments from Taiwan Strait and the shallow part of the South China Sea.

The heavy minerals from the southern part of the Taiwan Basin are characterized by hornblende and alterite with small amounts of magnetite, epidote, garnet, and tourmaline; they might have been derived partly from Pleistocene andesite and partly from the Tertiary sediments of northern Taiwan.

The heavy minerals of the sediments in the northern part of Taiwan Strait are characterized by hornblende and alterite with small amounts of zircon, tourmaline, and garnet; towards the south, however, there is a gradual decrease in content of horn-

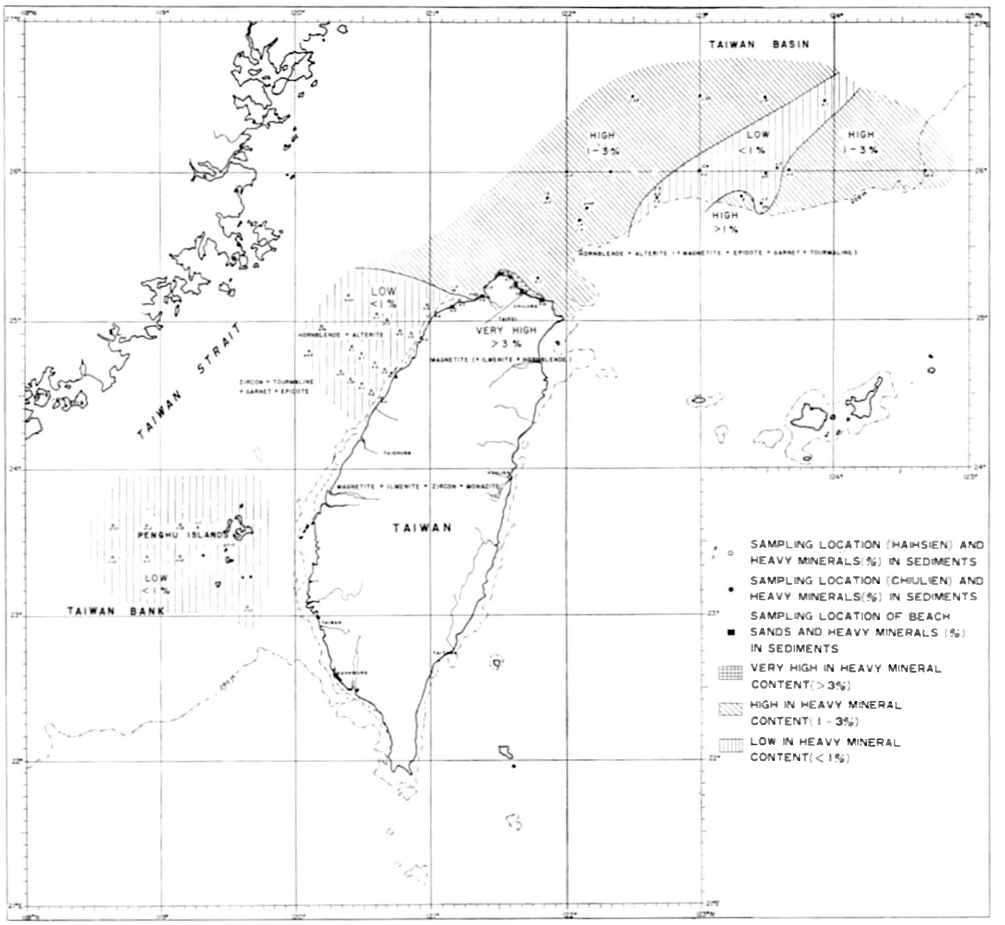

Figure IV-10. Contents of heavy minerals in sea bottom sediments in the vicinity of Taiwan and in beach sediments in northern Taiwan.

blende, and a steady increase in the contents of zircon, tourmaline, garnet, and epidote. The heavy minerals in the sea bottom sediments of Taiwan Strait might have been derived mainly from the Tertiary metamorphic and sedimentary rocks exposed in western Taiwan.

The content of heavy minerals in the beach sediments from northern Taiwan is relatively very high as compared with that of the sea bottom in the total samples and it ranges from 0.58 to 79.59 per cent by weight. The heavy mineral assemblage of the beach sands is characterized by abundant magnetite with small amounts of ilmenite and hornblende, which are derived mainly from the Pleistocene andesite of the Tatun volcanos in northern Taiwan; towards the south along the west coast, however, the content of magnetite in the beach sands gradually decreases and the contents of ilmenite, zircon and monazite increase. The heavy minerals from the latter area are derived mainly from the Tertiary metamorphic and sedimentary rocks exposed in western

Taiwan, but a small part of them may come from the sea bottom sediments in Taiwan Strait or the Taiwan Basin in the East China Sea.

Clay fractions

Most of the 22 sea bottom samples from the southern part of the Taiwan Basin can be disaggregated and dispersed without great difficulty by immersing in water for several days, and few of them need further treatment in an agate mortar (Y. Wang, 1971). The clay fractions (diameter less than 5 microns) are obtained by the usual precipitation method in compliance with Stokes' law, assisted further by centrifuging. Two oriented clay slides of each sample were prepared for study by the X-ray diffraction method, for which a Norelco type X-ray diffractometer with a wide-angle goniometer was used (Y. Wang, 1971).

The minerals of the clay fractions in the 22 sea bottom samples identified by the X-ray diffraction method are illite, chlorite, kaolinite, quartz, feldspars (albite-oligoclase and K-feldspar), calcite, gypsum, and a small amount of smectite; their contents are given in Table IV-4 (Y. Wang, 1971). Illite, the most common of them, may be identified by its (002) reflection at 10 Å and subsequent (001) reflections; its strongest peak (006) is superposed on the strongest peak of quartz at $2\theta = 26.6°$. Chlorite can be easily identified by the presence of a 14 Å peak and its subsequent reflections. From the intensity ratio of its even- and odd-numbered peak reflections, the chlorite in these samples is a very iron-rich type. Identification of kaolinite needs treatment of the clay fraction in hot HCl solution. The 7 Å peak of kaolinite is superposed by the (002) reflection of chlorite; however, after treatment with HCl all the clay slides show a vanishing of the 14 Å peak but the 7 Å one peak remains, proving that kaolinite is

Table IV-4. Mineral composition of the clay fraction (particles less than 5 microns) of sea bottom sediments from the southern part of the Taiwan Basin (after Y. Wang, 1971).

Sample no.	Illite	Chlorite	Kaolinite	Quartz	Feldspars	Calcite	Gypsum	Smectite
CD1-1	v v v	v v	v	v v	v	v v	—	—
CD1-2	v v v	v v	v	v	v	v	—	v
CD1-3	v v v	v	v	v	v	—	—	—
CD1-4	v v	v	v	v v	v	v	—	—
CD1-5	v v v	v	v	v	v	v	—	v
CD1-6	v v v	v	v	v	v	v	—	v
CD1-7	v v v	v	v	v	v	v	—	—
CD1-8	v		v	v v v	v v	v v	—	—
CD2-1a	v v v	v	v	v	v	v	v	v
CD2-1b	v v v	v v	v	v v	v	v	v	v
CD2-2a	v v v	v v	v	v v	v	v	v	v
CD2-2b	v v v	v v	v	v	v	v	v	v
CD2-4a	v v v	v	v	v	v	v	v	—
CD2-4b	v v v	v v	v	v v	v	v	v v	v
CD2-4c	v v v	v v	v	v v	v	v	v	v
CD2-5	v v v	v	v	v	v	v	v	v
CD2-6	v v v v	v v	v	v	v	v	—	v
CD2-7a	v v v	v	v	v	v	v	—	—
CD3-5	v v v	v v	v	v	v	v	—	—
CD3-6	v v v v	v	v	v	v	v	—	—
CD3-7	v v v	v	v	v v	v	v	v	v
CD3-8	v v v	v v	v	v	v	v v	v v	—

v = rare, v v = present, v v v = common, v v v v = abundant.

present in every sample although the amount is not great. Identification of quartz, feldspar, calcite, and gypsum usually presents no problems. Smectite may be identified by the presence of the 14 Å peak and also shifting of the peak to about 17 Å after glycolation. In the samples studied, this effect was not very distinctive, indicating that only traces of smectite were present in certain of the samples.

CONCLUSIONS

The sandy sediments in the northeastern part of Taiwan Strait contain small amounts of the remains of molluscs, foraminifers, corals and other calcareous organisms and they become finer westward to the coast of the mainland of China. In the southern part of the Taiwan Basin, the sea bottom sediments are mostly sandy and characterized by a high content of the remains of molluscs and small amounts of foraminifers, corals, algae and other calcareous organisms and they gradually become silty towards the northeast. The beach sediments of northern Taiwan are almost entirely sandy and are characterized by the presence of abundant heavy minerals and small amounts of foraminifers and molluscan fragments. In general, the remains of molluscs are dominant in the sandy sediments, and foraminiferal tests are dominant in the silty sediments.

The beach sediments in northern Taiwan are the coarsest, while the sea bottom sediments in the southern part of the Taiwan Basin are slightly coarser than those in Taiwan Strait and the shallow part of the South China Sea. The coarser sea bottom sediments in Taiwan Strait and the southern part of the Taiwan Basin are mainly very well to moderately well sorted and negatively skewed or lower in *phi* skewness values, and are quite similar in this respect to the beach sands of northern Taiwan and some other districts. Based on their textural parameters, these coarser sediments might have been deposited mainly in a littoral environment, while the less coarse sediments might have been deposited mainly in fluvial, eolian and neritic environments during a Pleistocene glacial epoch of lowered sea level, and now preserved as relict sediments by the rise of sea level after that glacial period.

The sea bottom sediments are composed mainly of quartz, feldspars, rock fragments, large amounts of molluscan and other calcareous remains and small amounts of clay and heavy minerals. Except in the area southeast of the Penghu Islands and in the northwestern part of Taiwan Strait, most of the sea bottom and beach sediments contain abundant feldspars and are arkosic and not very mature. The non-calcareous part of the sea bottom sediments may be classified as arkose sand, subarkose sand, graywacke sand, sandy silt, silt and clay.

The heavy mineral contents of the sediments from the southern part of the Taiwan Basin, ranging from 0.1 to 2.7 per cent by weight, are higher than those of the sediments in Taiwan Strait and the shallow part of the South China Sea. The heavy minerals from the southern part of the Taiwan Basin are characterized by the presence of hornblende and alterite with small amounts of magnetite, epidote, garnet, and tourmaline; they might have been derived partly from the Pleistocene andesite and Tertiary sediments of northern Taiwan. The heavy minerals from Taiwan Strait are characterized by hornblende and alterite in the northern part and by zircon, tourmaline, garnet, and

epidote in the southern part; they might have been derived mainly from the Tertiary metamorphic and sedimentary rocks exposed in western Taiwan.

The heavy mineral contents of the beach sediments from northern Taiwan form a relatively very high proportion of the total sediments; the assemblage is characterized by abundant magnetite with small amounts of ilmenite and hornblende, derived mainly from the Pleistocene andesite of the Tatun volcanos in northern Taiwan. Southward along the west coast the content of magnetite in the beach sediments gradually decreases and the contents of ilmenite, zircon, and monazite steadily increase; they are derived mainly from the Tertiary metamorphic and sedimentary rocks in western Taiwan, and more rarely from the sea bottom sediments in Taiwan Strait.

The minerals in the clay fraction of the sea bottom sediments from the southern part of the Taiwan Basin are illite, chlorite, kaolinite, quartz, feldspars (albite-oligoclase and K-feldspar), calcite, gypsum, and a small amount of smectite.

ACKNOWLEDGMENTS

The writer is greatly obliged to Dr. V. C. Juan, President, Chinese National Committee for the Scientific Committee on Oceanic Research, and Professor Tsu-you Chu, Director, Institute of Oceanography of the National Taiwan University, for their encouragement and for their generosity in providing the dredged samples of sea bottom sediments from the southern part of the Taiwan Basin.

This study was supported by the Chinese Petroleum Corporation (CPC). Acknowledgments are due to Mr. T. M. Wu, Vice President of CPC, Dr. C. Y. Meng, Chief Geologist of CPC, and to Mr. Stanley S. L. Chang, Chief Geologist of the Taiwan Petroleum Exploration Division of CPC, for their invaluable guidance and generous support of this study.

Thanks are due to Mr. F. T. Wu, Mr. Y. K. Lim, and the assistants of the Sedimentation Laboratory of CPC for their help with the laboratory work.

REFERENCES

Chen, Ju-chin, and Chin Chen, 1971, Mineralogy, geochemistry and paleontology of shelf sediments of the South China Sea and Taiwan Strait: *Sino-American Science Co-operation Colloquium on Ocean Resources*, vol. I, Marine Geology and Geophysics, p. 147–187.

Chinese Petroleum Corporation, 1970, Note on sea bottom sampling in the offshore area of Taiwan, China: United Nations ECAFE, *CCOP Tech. Bull.*, vol. 3, p. 35–36.

Chou, J. T., 1971, Recent sediments in the shallow part of the South China Sea: *Proc. Geol. Soc. China*, no. 14, p. 99–117.

———, and Wu, Fu-Tai, 1971, Sediments of the Taiwan Basin (Part 1): *Pet. Geol. Taiwan*, no. 9 (Chinese with English abstract).

Emery, K. O., 1968, Relict sediments on continental shelves of the world: *Bull. Amer. Assoc. Petrol. Geol.*, vol. 52, p. 445–464.

Emery, K. O., Hayashi, Y., Hilde, T.W.C., Kobayashi, K., Koo, J. H., Meng, C. Y., Niino, H., Osterhagen, J. H., Reynolds, L. M., Wageman, J. M., Wang, C. S., and Yang, S. J., 1969,

Geological structure and some water characteristics of the East China Sea and the Yellow Sea: United Nations ECAFE, *CCOP Tech. Bull.*, vol. 2, p. 4–43, figs. 1–17.

Friedman, G. M., 1961, Distinction between dune, beach, and river sands from their textural characteristics: *Jour. Sed. Petrology*, vol. 31, p. 514–529.

————, 1962, On sorting, sorting coefficients, and the log normality of the grain-size distribution of sandstones: *Jour. Geol.*, vol. 70, p. 737–753.

Huang, Tunyow, 1971, Foraminiferal trends in the surface sediments of Taiwan Strait: United Nations ECAFE, *CCOP Tech. Bull.*, vol. 4, p. 23–61.

Inman, D. L., 1952, Measures for describing the size distribution of sediments: *Jour. Sed. Petrology*, vol. 22, p. 125–145.

Meng, Chao-yi, and Li, William Y. L., 1970, Geologic map of the Republic of China: Chinese Petroleum Corporation.

Niino, H., and Emery, K. O., 1961, Sediments of shallow portions of East China Sea and South China Sea: *Bull. Geol. Soc. Amer.*, vol. 72, p. 731–762.

Pettijohn, F. J., 1957, Sedimentary rocks: 2nd ed., Harper and Brothers, New York, 718 p.

Polski, W., 1959, Foraminiferal biofacies off the North Asiatic Coast: *Jour. Paleont.*, vol. 33, no. 4, p. 569–587.

Russel, R. D., 1935, Frequency percentage determinations of detrital quartz and feldspar: *Jour. Sed. Petrology*, vol. 5.

Shepard, F. P. and Young, Ruth, 1961, Distinguishing between beach and dune sands: *Jour. Sed. Petrology*, vol. 31, p. 196–214.

Wageman, J. M., Hilde, T.W.C., and Emery, K. O., 1970, Structural framework of East China Sea and Yellow Sea: *Bull. Amer. Assoc. Petrol. Geol.*, vol. 54, no. 9, p. 1611–1643, figs. 1–22.

Waller, H. O., 1960, Foraminiferal biofacies off the South China coast: *Jour. Paleont.*, vol. 34, p. 1164–1182.

Wang, C. S., 1960, Sand fraction study of the shelf sediments off the China coast: *Proc. Geol. Soc. China*, no. 4, p. 33–49.

Wang, Y., 1971, Note on the clay mineral identification of Taiwan Basin: Unpublished report, Institute of Geology, National Taiwan University, CPC files.

Yen, T. P., 1971, Geology of Taiwan–A review, especially on stratigraphy: *Sino-American Science Co-operation Colloquium on Ocean Resources*, vol. I, Marine Geology and Geophysics, p. 1–24.

Blank page

Page blanche

V. MINERALOGY AND GEOCHEMISTRY OF SHELF SEDIMENTS OF THE SOUTH CHINA SEA AND TAIWAN STRAIT

(Project CCOP-1/ROC. 3)

By

Ju-chin Chen

Institute of Oceanography, National Taiwan University
Taipei, Taiwan, China

(with figures V–1 to V–12; and tables V–1 to V–3)

ABSTRACT

The mineralogy and geochemistry of shelf sediments from the South China Sea and Taiwan Strait have been studied to gain some knowledge of their provenance and depositional environments. Two distinct types of neritic sediments were recognized based on mineralogical and chemical data; they are: (1) the near-shore sediments in Taiwan Strait, and (2) the continental shelf sediments of the South China Sea. The former are characterized by a relatively higher percentage of terrigenous sediments, higher quartz/K-feldspar ratio, lower CaO and Sr and higher contents of MgO, total Fe as Fe_2O_3, K_2O, Rb and Li as compared with the latter. The mineralogical data suggest that the near-shore sediments in Taiwan Strait are derived mainly from Taiwan Island while the shelf sediments in the South China Sea are derived mainly from southern China where granites of Mesozoic age, rich in potash feldspar, are widely distributed. The decrease of quartz/calcite ratio in relation to distance off the China coast strongly indicates that the depositional environment becomes more biogenic towards the edge of the shelf. The effects of environment and provenance are the most important factors controlling the mineralogical and chemical variations of the sediments studied.

INTRODUCTION

The research vessel "CHIU LIEN," of the Institute of Oceanography, National Taiwan University, a former American tug, started multiple-purpose oceanographic work in October 1969. Bottom sediment sampling in the shallow portion of the China Sea and adjacent areas is one of the major programmes. About one hundred samples have been collected with a modified pipe dredge and a gravity corer in Taiwan Strait, the Gulf of Thailand and over the continental shelves of the South China Sea and the East China Sea.

The results from the study of thirty-six samples of bottom sediments from two sources are reported in this paper. Seventeen dredged samples were collected by the R/V CHIU LIEN from the area north of Taiwan and in Taiwan Strait and nineteen snapper samples taken around Hainan were obtained through arrangements made by Drs. K. O. Emery and Chin Chen. The locations of these samples are shown in Table V-1 and Figure V-1. Brief lithologic descriptions of the samples are given in Table V-1.

The area studied covers the continental shelf between latitudes 16°N and 30°N and longitudes 108°E to 126°E. Hainan Island is located at the southwest corner and Taiwan at the northeast corner of this area. The continental shelf of the China Sea is

Table V-1. Locations of samples of sea bottom sediments studied, from the vicinity of Taiwan 4—: samples provided by K.O. Emery and Chin Chen.

SAMPLE NUMBER	CRUISE AND STATION	LOCATION		DEPTH OF WATER (M)
1	C.L. 19-5	26°28.2′N	123°55.5′E	140
2	C.L. 19-6	26°01.0′N	123°34.5′E	160
3	C.L. 19-7	26°00.0′N	123°00.0′E	150
4	C.L. 19-8	25°30.8′N	122°14.0′E	150
5	C.L. 19-9	25°18.6′N	121°59.5′E	160
6	4-5	29°21′N	123°52′E	77
7	4-21	29°59′N	126°20′E	82
8	4-28	23°40′N	118°31′E	48
9	4-33	21°29′N	115°47′E	116
10	4-38	20°56′N	114°32′E	84
11	4-40	20°53′N	114°55′E	100
12	4-41	20°15′N	114°33′E	130
13	4-42	20°15′N	113°54′E	117
14	4-44	20°47′N	113°30′E	78
15	4-45	20°30′N	113°10′E	88
16	4-50	19°00′N	111°56′E	170
17	4-53	20°13′N	111°56′E	85
18	4-56	19°31′N	111°27′E	100
19	4-59	18°52′N	111°31′E	140
20	4-64	19°02′N	111°02′E	115
21	4-65	18°01′N	110°06′E	97
22	4-66	17°02′N	109°10′E	113
23	4-68	16°21′N	108°24′E	84
24	4-71	21°01′N	111°59′E	46
25	C.L. 20-0	22°59′N	119°15′E	35
26	C.L. 20-1	22°13.5′N	118°28.5′E	75
27	C.L. 20-2	20°52′N	117°00′E	305
29	C.L. 23-2	25°10.4′N	121°09.2′E	40
30	C.L. 23-3	24°55′N	120°32′E	67
31	C.L. 23-4	24°24′N	120°25.8′E	48
33	C.L. 23-6	23°23.8′N	119°55.1′E	65
35	C.L. 23-8	22°50′N	120°05.6′E	45
36	C.L. 23-9	22°39.5′N	119°55′E	380
37	C.L. 23-10	22°28′N	120°12.5′E	80
38	C.L. 23-14	22°18′N	120°19.4′E	180
39	C.L. 23-15	22°05.3′N	120°36.7′E	355

one of the widest shelves in the world and one of the least known. Wang (1960), Niino and Emery (1961), Emery and Niino (1963), Emery *et al.* (1969), Wageman, Hilde and Emery (1970) and Chou (1970) have studied the marine geology, tectonic structure and sediments in the China Sea. Studies on foraminifers from Recent sediments along the northern Asiatic coast were published by Polski (1959), and by Waller (1960) on those from the southern China coast.

Niino and Emery (1961) made a general distribution map of sediments on the continental shelf of the South China Sea and Taiwan Strait (Fig. V-2). Sands are predominantly distributed in the central portion of Taiwan Strait, and muds are present

and Hainan Islands and the South China Sea; C.L.: samples collected from R/V CHIU LIEN;

BRIEF LITHOLOGIC DESCRIPTIONS
light gray sand with relatively abundant mollusks and foraminiferas
light yellow coarse-grained sand with extremely abundant mollusks & foraminiferas
light yellow coarse-grained sand with abundant foraminiferas
light yellowish brown sand with abundant foraminiferas but rare mollusks
light yellowish brown sand with relatively abundant mollusks & foraminiferas
light gray muddy sand with relatively abundant foraminiferas
light gray muddy sand with relatively abundant foraminiferas & few mollusk fragments
light yellow, coarse-grained sand with abundant quartz and some organic debris
light gray muddy sand with abundant foraminiferas and few mollusks
light yellow, coarse-grained quartz sand with relatively abundant foraminiferas and some mollusks
light gray muddy sand with relatively abundant foraminiferas and few mollusks
light yellow coarse-grained quartz sand with relatively abundant foraminiferas and mollusks
light gray muddy sand with abundant foraminiferas and some mollusks
light yellow coarse-grained quartz sand with few rock fragments, abundant foraminiferas and some mollusks
light gray muddy sand with relatively abundant foraminiferas and some mollusks
light gray coarse-grained sand with extremely abundant foraminiferas and some mollusks
light gray sand with relatively abundant foraminiferas and mollusks
light yellowish gray muddy sand with relatively abundant foraminiferas and few mollusks
light gray sand with relatively abundant foraminiferas and mollusks
light yellowish gray sand with relatively abundant foraminiferas and few mollusks
light yellowish gray muddy sand with relatively abundant foraminiferas and some mollusks
light gray muddy sand with relatively abundant foraminiferas and some mollusks
light yellowish gray muddy sand with relatively abundant foraminiferas and rare mollusks
light yellowish gray sand with relatively abundant foraminiferas and few mollusks
light yellow coarse-grained quartz sand with abundant organic debris
light gray sand with abundant foraminiferas and mollusks
light yellow sand consisting almost entirely of foraminiferas and mollusks
light gray sand with some foraminiferas and mollusks
light yellowish gray sand with few foraminiferas and mollusks
light gray sand with rare foraminiferas and mollusks
light gray sand with rare foraminiferas and mollusks
light gray sand with rare foraminiferas but no mollusks
light gray sand with few foraminiferas and rare mollusks
light yellowish gray sand with few foraminiferas and rare mollusks
light gray sand with few foraminiferas and rare mollusks
light yellowish gray sand with few foraminiferas and mollusks

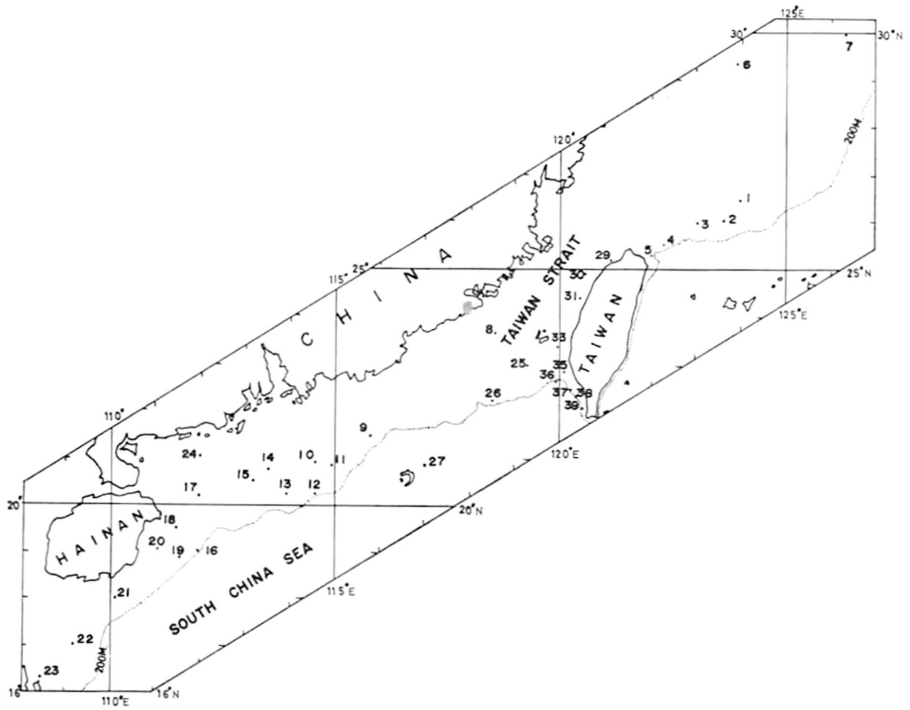

Figure V-1. Locations of samples of sea bottom sediments studied, in the vicinity of Taiwan and Hainan islands and in the South China Sea (see also Table V-1).

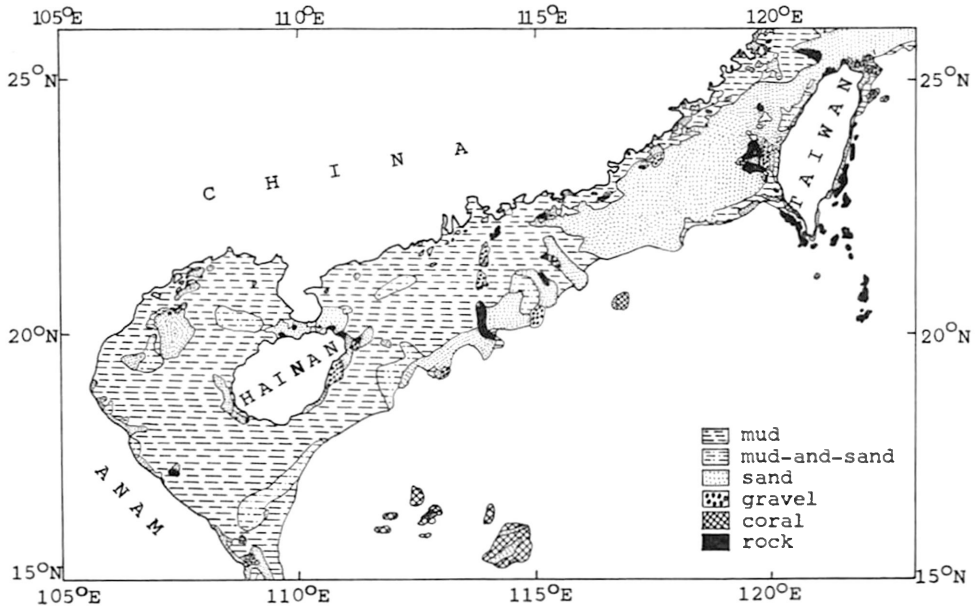

Figure V-2. General distribution of sea floor sediments on the continental shelf between Taiwan and Hainan islands (after Niino and Emery 1961).

along the Taiwan and mainland coasts. In the South China Sea, fine sediments occur on the inner shelf, coarse sands are present on the outer half of the shelf and these grade into finer sediments in deeper water beyond the edge of the shelf. In general, the sorting of sands from the central portion of Taiwan Strait and the outer shelf of the South China Sea is better than that of the muds from the inner shelf of the South China Sea and along the Taiwan coast.

To complement the previous studies of shelf sediments in the China Sea, the present author concentrated on obtaining additional quantitative and qualitative data by the following means: (1) determination of mineral composition of the shelf sediments by X-ray diffraction; (2) chemical analysis of the sediments by atomic absorption spectrophotometry; (3) study of the depositional environments of the sediments; and (4) study of the source areas of the sediments.

MINERALOGY OF THE SEDIMENTS

The mineralogy of each bulk sample was analyzed on a Philips Norelco X-ray diffractometer with Cu-radiation according to the standard powder method. The minerals identified were defined by their X-ray characters based on comparison with ASTM powder files. Representative fractions of bulk sediments were ground into powders (grain size less than about 100 mesh) in an agate mortar for X-ray analysis. With 1° of divergence, an 0.001-inch receiving slit and 1° per minute scanning rate, each powdered sample was investigated by X-ray through the angular range of 4° to 40°.

Quartz, calcite, aragonite, plagioclase, potash feldspar, hydromica, kaolin, chlorite and amphibole were found in the samples analyzed by X-ray. The detailed mineralogy of each sample studied is listed in Table V-2.

Quartz, calcite and feldspar are the most common constituents of the sediments. Hydromica and aragonite are also commonly found in the samples and the former appears to be more abundant in the sediments from Taiwan Strait (samples 29, 30, 31, 33, 35, 37, 38 and 39). Microscopic observation suggests that the quartz, plagioclase and potash feldspar are of terrigenous origin; however, the calcite and aragonite in the sediments are almost exclusively of biogenic origin (shells, foraminifers, etc.). The amounts of kaolin and chlorite are relatively low in the sediments and it is difficult to confirm their presence in many cases; generally, however, the sediments off the Taiwan coast (samples 31, 33, 35, 37, 38 and 39) are relatively richer in chlorite than those from the South China Sea. The presence of amphibole has been confirmed only in sample 29.

The quartz/calcite, quartz/plagioclase and quartz/K-feldspar ratios of the sediments have been studied and these are listed in Table V-2. The ratios were determined by dividing the height of the quartz 3.34 Å peak by the heights of the calcite 3.03 Å, plagioclase 3.20Å and potash-feldspar 3.24Å peaks, respectively. As the operations were standardized throughout the investigation, the heights of these major peaks are approximately proportional to the abundances of the minerals under consideration.

The geographic variations of quartz/calcite, quartz/plagioclase and quartz/K-feldspar ratios are shown in Figs. V-3, 4 and 5, respectively. It is of interest to note

Table V–2. Mineral constituents of Recent sediments from the South China Sea and Taiwan Strait.
Qtz. quartz; Pc. plagioclase; Kf. potash-feldspar; Cal. calcite; H-Mi. hydro-mica; Kao. kaolin; Chl. chlorite; Arag. aragonite; Anhy. anhydrite; Amph. amphibole. × presence; ? doubtful occurrence; ... absence. Numbers indicate peak heights and peak height ratios.

	Qtz.	Pc.	Kf.	Cal.	H-Mi.	Kao.	Chl.	Arag.	Anhy.	Amph.	Qtz/Cal	Qtz/Pc	Qtz/Kf
1	113	18	6	19	×	×	?	×	—	—	6.0	6.3	18.8
2	41	—	?	26	—	—	—	×	—	—	1.6	∞	→∞
3	146	29	42	14	×	?	?	×	—	—	10.4	5.0	3.5
4	10	—	—	30	—	—	—	×	—	—	0.3	∞	∞
5	88	15	20	5	×	—	—	×	—	—	17.6	5.9	4.4
6	135	33.5	18.5	11.5	×	?	?	×	—	—	11.7	4.0	7.3
7	154	18	11	11	×	?	?	—	—	?	14.0	8.6	14.0
8	>230	?	12	4	—	—	—	—	—	—	>57.5	→∞	>19.2
9	120	25	10.5	38.5	×	?	?	—	?	—	3.1	4.8	11.4
10	>230	3.5	42.5	8	—	—	—	—	—	—	>28.8	>65.7	>5.4
11	179	15	41	20	—	—	—	?	—	—	9.0	11.9	4.4
12	>229	—	29	11	—	—	—	—	—	—	>20.8	∞	>7.9
13	129	7.5	7.5	31.5	×	?	?	×	—	—	4.1	17.2	17.2
14	165	4	18	23.5	—	—	—	×	—	—	7.0	41.3	9.2
15	200	6	13.5	19	—	—	—	×	—	?	10.5	33.3	14.8
16	33.5	—	—	44	—	—	—	×	—	—	0.8	∞	∞
17	112	10	15	21	×	?	×	—	—	—	5.3	11.2	7.5
18	195	5	17	15.5	—	—	—	×	?	—	12.6	39.0	11.5
19	102	10	6	34.5	×	?	?	?	—	—	3.0	10.2	17.0
20	107	8	4	13	×	?	×	—	—	—	8.2	13.4	26.8
21	152	10	17	10.5	×	—	—	×	—	—	14.5	15.2	8.9
22	136.5	8	19	24	×	?	?	—	—	—	5.7	17.1	7.2
23	130	5.5	4	15.5	×	—	—	—	—	—	8.4	23.6	32.5
24	172	13	37.5	10.5	×	?	?	—	—	—	16.4	13.2	4.6
25	211	4	8	28	—	—	—	×	—	—	7.5	52.8	26.4
26	118	?	18	12	×	?	?	×	—	—	9.8	→∞	6.6
27	—	—	—	23	—	—	—	×	—	—	0.0	—	—
29	123	8	7	—	×	×	?	—	—	×	∞	15.4	17.6
30	109	18	7	7	×	×	?	×	—	—	15.6	6.1	15.6
31	115	16	5	—	×	×	×	—	—	—	∞	7.2	23.0
33	124	24	7	4	×	×	×	—	—	—	31.0	5.2	17.7
35	149	11	9	—	×	×	×	—	—	—	∞	13.5	16.6
36	134	7	—	5	×	×	?	—	—	—	26.8	19.1	∞
37	106	13	7	6	×	×	×	—	—	—	17.7	8.2	15.1
38	117	20	—	—	×	×	×	—	—	—	∞	5.9	∞
39	111	10	—	?	×	×	×	—	—	—	→∞	11.1	—

that the quartz/calcite ratios in the sediments generally decrease with the distance off the coast, which suggests that biogenic contributions become increasingly more important away from the shoreline. In addition, it seems that the sediments from the South China Sea have a relatively lower quartz/calcite ratio than those from Taiwan Strait; this indicates that terrigenous contributions from the island play an important role in determining the constituents of the sediments just off the Taiwan coast. It should be mentioned that total bulk of organisms in the sediments of Taiwan Strait is less than in those of the South China Sea (C. Chen, personal communication).

Both the quartz/plagioclase and quartz/K-feldspar ratios tend to increase with

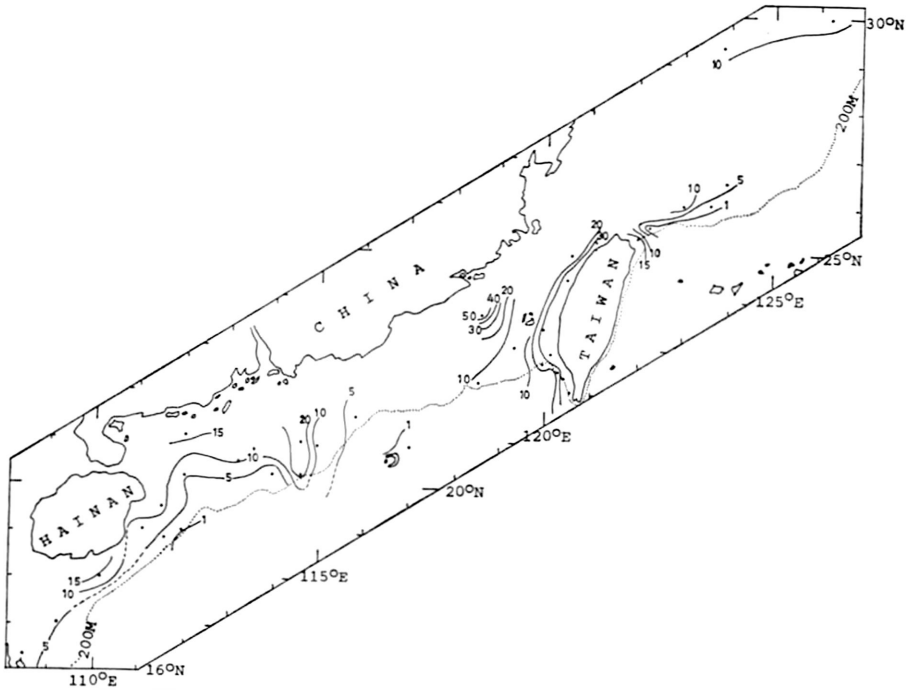

Figure V-3. Quartz/calcite ratios of Recent sediments on the continental shelf between Taiwan and Hainan islands.

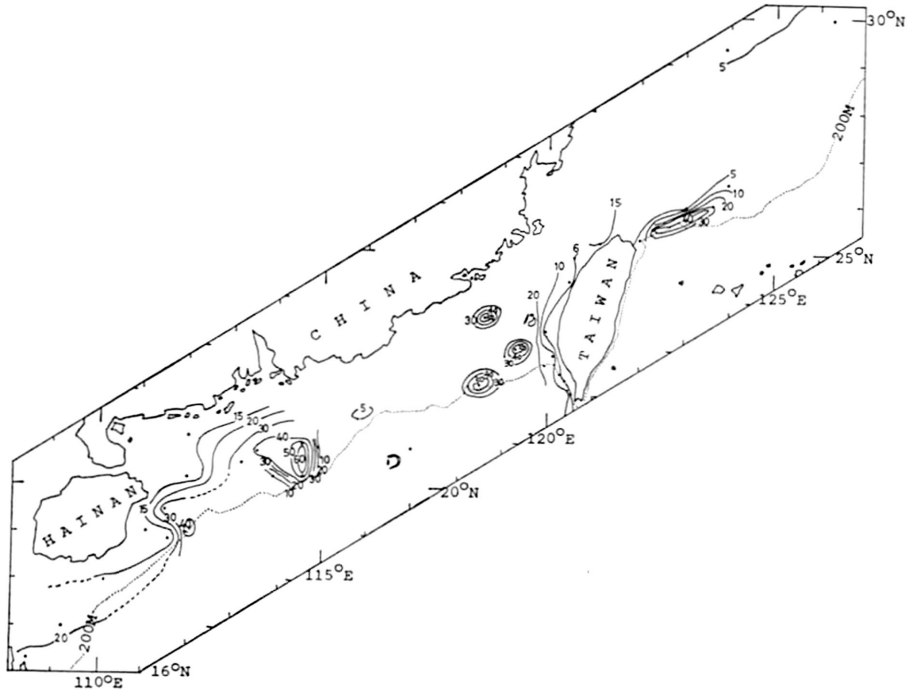

Figure V-4. Quartz/plagioclase ratios of Recent sediments on the continental shelf between Taiwan and Hainan islands.

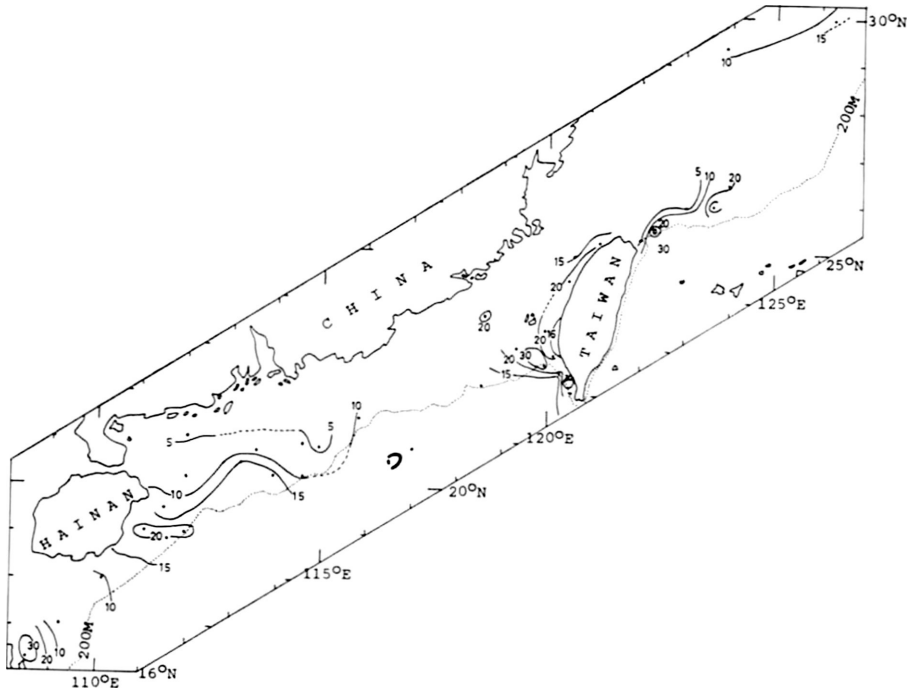

Figure V-5. Quartz/K-feldspar ratios of Recent sediments on the continental shelf between Taiwan and Hainan islands.

distance off the coast (Figs. V-4 and 5). This might be due to increasing alteration and/or decomposition of feldspars in relation to distance of transportation. It should be noted that, in general, the sediments from the South China Sea are lower in quartz/K-feldspar ratio than those from Taiwan Strait; this is discussed in more detail later in this report.

CHEMISTRY OF THE SEDIMENTS

The sediments were prepared for chemical analysis by washing three times with distilled water and then drying them under heat lamps; the dried sediments were then ground into powders (grain size generally between 100 and 150-mesh) in an agate mortar.

One gram of each of the sample powders was dissolved in a mixture of 5cc HF and 10cc HNO_3 in teflon beakers and the chemical analyses were carried out with a Perkin-Elmer Model 303 atomic absorption spectrophotometer using solutions of various dilutions. The instrumental settings used were those listed in Perkin-Elmer, Analytical Methods for Atomic Absorption Spectrophotometry.

Ten artificial standards containing Al, Ti, Fe, Mn, Mg, Ca, Na, K, Cu, Li, Rb and Sr were carefully prepared from Johnson and Matthey spectrographically pure chemicals and these were used to construct the working curves. U.S. Geological Survey rock

Table V–3. Chemical data of Recent sediments from the South China Sea and Taiwan Strait.

Sample No.	% Na_2O	% K_2O	% CaO	% MgO	% total Fe as Fe_2O_3	ppm Mn	ppm Rb	ppm Cu	ppm Sr	ppm Li	Na_2O/K_2O
1	2.39	1.17	24.00	2.15	3.27	475	73.4	5.5	380	30.5	1.398
3	1.58	1.46	33.63	1.17	2.43	510	56.0	5.5	835	14.5	1.082
5	1.25	1.61	28.50	1.15	4.83	1235	63.8	6.2	683	17.0	0.776
7	1.98	2.33	12.25	1.35	3.10	400	83.0	8.0	235	29.0	0.850
9	1.15	1.64	27.75	1.62	3.90	250	71.0	8.0	423	29.5	0.701
11	0.72	1.58	19.25	0.79	1.33	60	84.5	6.2	315	21.5	0.456
13	1.08	1.40	32.88	1.30	2.23	475	70.0	8.0	530	29.3	0.771
15	0.52	1.42	17.25	0.90	2.72	190	71.0	9.0	260	23.5	0.366
17	1.83	2.02	18.83	1.90	3.44	535	86.6	9.5	298	51.6	0.906
19	2.03	1.73	26.75	1.72	2.95	150	74.0	11.0	480	43.0	1.173
21	0.79	1.52	15.50	1.33	3.05	535	70.0	6.2	290	33.0	0.520
23	1.55	2.00	15.50	1.78	3.35	1060	85.0	22.8	210	50.3	0.775
25	0.62	0.34	30.68	0.57	0.59	80	15.0	2.7	905	6.7	1.824
29	1.53	1.80	13.50	1.82	5.13	1525	83.0	10.0	238	50.0	0.850
31	1.98	2.73	0.76	1.93	5.13	550	128.0	9.0	27	66.7	0.725
33	2.23	2.64	0.35	1.78	4.93	565	122.0	15.0	12	72.5	0.845
35	2.15	2.30	0.62	1.53	4.04	440	99.0	9.5	20	53.8	0.935
37	1.62	2.68	0.76	1.83	5.13	675	125.0	14.3	30	70.0	0.604

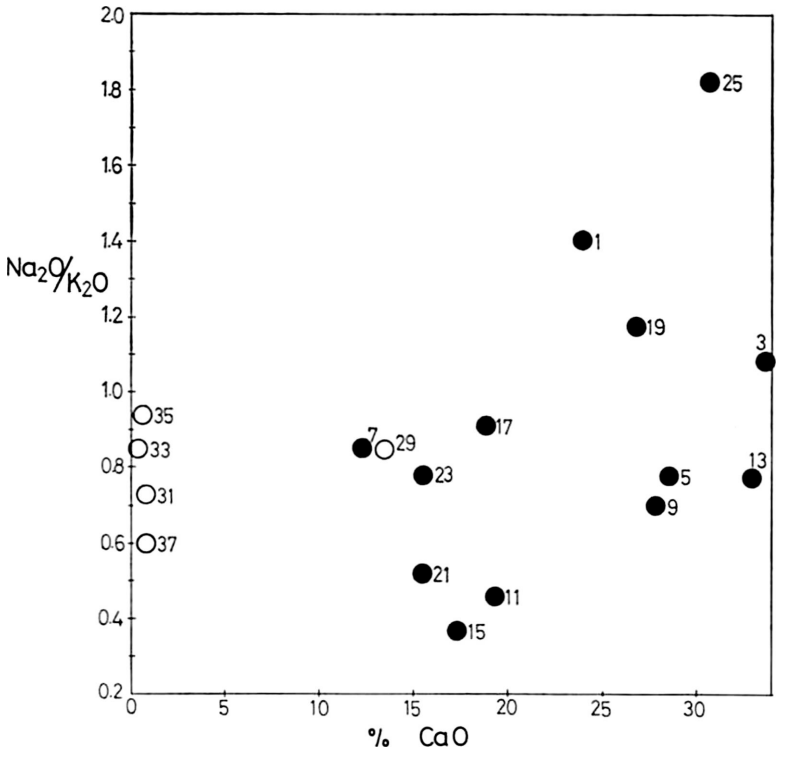

Figure V-6. Na_2O/K_2O ratios in relation to CaO in Recent sediments from the South China Sea and Taiwan Strait; circles indicate near-shore sediments off the coast of Taiwan.

standards G-2, GS P-1, AGV-1 and W-1 were used as references. Duplicate analyses on ten samples indicate the following precisions: Na, ±2%; K, ±1%; Ca, ±2%; Mg, ±2%; Mn, ±1%; Fe, ±3%; Rb, ±2%; Cu, ±4%; Sr, ±4%; and Li, ±4% of the amounts present.

The results of the analyses are listed in Table V-3. The range and average of the analyses are: Na_2O, 0.62–2.39%, avg. 1.50%; K_2O, 0.34–2.73%, avg. 1.83%; CaO, 0.35–33.63%, avg. 17.71%; MgO, 0.57–2.15%, avg. 1.48%; total Fe as Fe_2O_3, 0.59–5.13%, avg. 3.42%; Mn, 60–1525 ppm, avg. 539 ppm; Rb, 15.0–128.0 ppm, avg. 81.1 ppm; Cu, 2.7–22.8 ppm, avg. 9.2 ppm; Sr, 12–905 ppm, avg. 343 ppm; and Li, 6.7–72.5 ppm, avg. 38.5 ppm.

In general, the contents of alkali in the sediments are similar to those found in the near-shore sands from the Gulf of Paria as reported by Hirst (1962a). Most of the samples studied have Na_2O/K_2O ratios of less than one (Table V-3) and the ratios show no regular variation in relation to the contents of CaO in the sediments (Fig. V-6). This is contrary to the case in the sediments of the Gulf of Mexico which show a negative correlation between the K/Na ratios and the CaO contents of the sediments (Chester, 1965). Although both sodium and potassium may become located in clays by being taken into the clay minerals by cation exchange and by incorporation into structural positions, potash-feldspar, sodic plagioclase and hydromica are still probably the most important alkali-carrying minerals in the sediments.

The sediments off the coast of Taiwan (samples 29, 31, 33, 35 and 37) generally

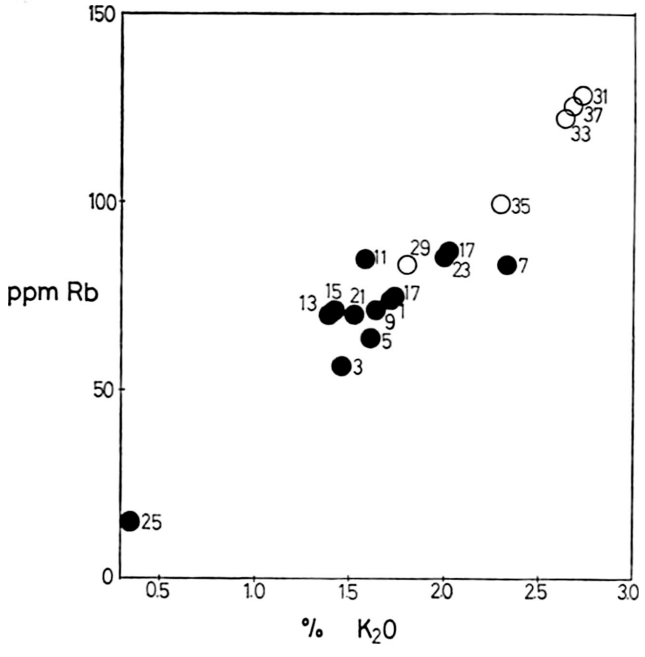

Figure V-7. Content of Rb in relation to K_2O in Recent sediments from the South China Sea and Taiwan Strait; circles indicate near-shore sediments off the coast of Taiwan.

have a higher content of K_2O than those from the South China Sea (samples 9, 11, 13, 15, 17, 19, 21 and 23), although the former have relatively higher quartz/K-feldspar ratios; this suggests that potassium-bearing minerals other than K-feldspar (i.e., hydromica) are relatively more abundant in the sediments off the coast of Taiwan and this is supported by the X-ray diffraction data.

Horstman (1957) concluded that rubidium follows potassium in the weathering cycle. The positive correlation between Rb and K_2O in the samples studied (Fig. V-7) supports his conclusion. Potassium-feldspar and hydromica are probably the major rubidium-carrying minerals in the sediments. In general, the sediments from Taiwan Strait (samples 31, 33, 35 and 37) have higher contents of Rb than those of the South China Sea (samples 9, 11, 13, 15, 17, 19, 21, 23 and 25) and this is probably related to the relatively higher contents of potassium in the sediments off the coast of Taiwan.

A review of Table V-3 indicates that the contents of calcium in the sediments off the coast of Taiwan (samples 29, 31, 33, 35 and 37) are relatively lower than those found in the sediments of the South China Sea (samples 9, 11, 13, 15, 17, 19, 21 and 23). This is apparently due to the impoverishment of biogenic calcium carbonate in the sediments

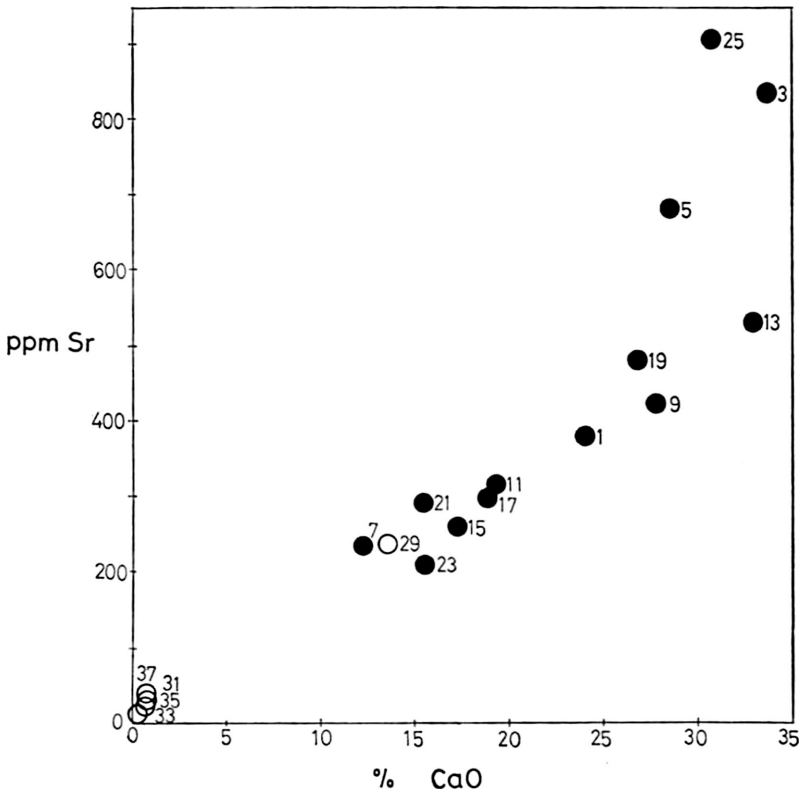

Figure V-8. Content of Sr in relation to CaO in Recent sediments from the South China Sea and Taiwan Strait; circles indicate near-shore sediments off the coast of Taiwan.

off the coast of Taiwan, as suggested by the optical and X-ray analyses. The low content of CaO in the sediments off the coast of Taiwan suggests that contributions of terrigenous material from the island play the most important role in determining the composition of the sediments in that area.

As the contribution of calcium from minerals other than calcite and aragonite (i.e., plagioclase) appears to be small according to the X-ray data, it is possible, therefore, to estimate the average calcium carbonate content in the sediments, indirectly, from the average CaO content (17.71 %); on this basis, the average calcium carbonate content in the sediments is about 30 per cent by weight.

The positive correlation between the content of Sr and CaO in the sediments studied (Fig. V-8) suggests that the Sr is included mainly in the calcium carbonate of biogenic origin, although some strontium may be associated with clay minerals either by ion exchange or by incorporation in the clay mineral lattices. The average content of Sr in the sediments (343 ppm) is comparable to the average Sr content (296 ppm) of near-shore sediments reported by Young (1954) but it is lower than that (1,110 ppm) of pelagic sediments from all the major oceans as compiled by Chester (1965).

The variation of MgO in the samples analyzed is relatively smaller (from 0.57 to 2.15 per cent) in comparison with the variation of CaO. The weak positive correlation between MgO and total Fe as Fe_2O_3 (Fig. V-9) and the lack of covariance of MgO with CaO (Fig. V-10) in the samples lead to the inference that most of the MgO is of ter-

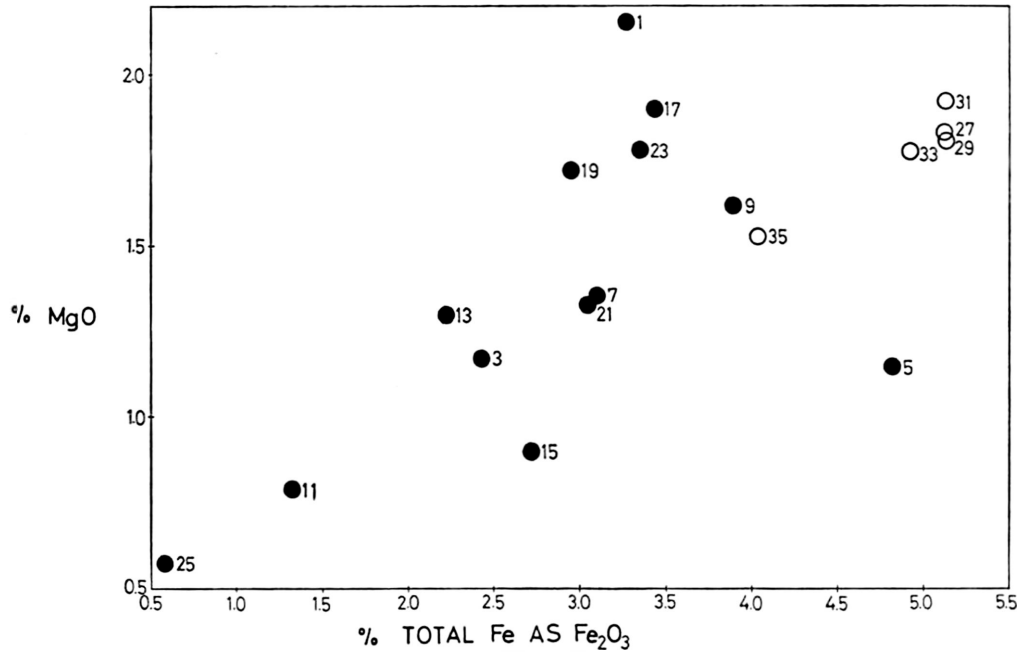

Figure V-9. Content of MgO in relation to total Fe as Fe_2O_3 in Recent sediments from the South China Sea and Taiwan Strait; circles indicate near-shore sediments off the coast of Taiwan.

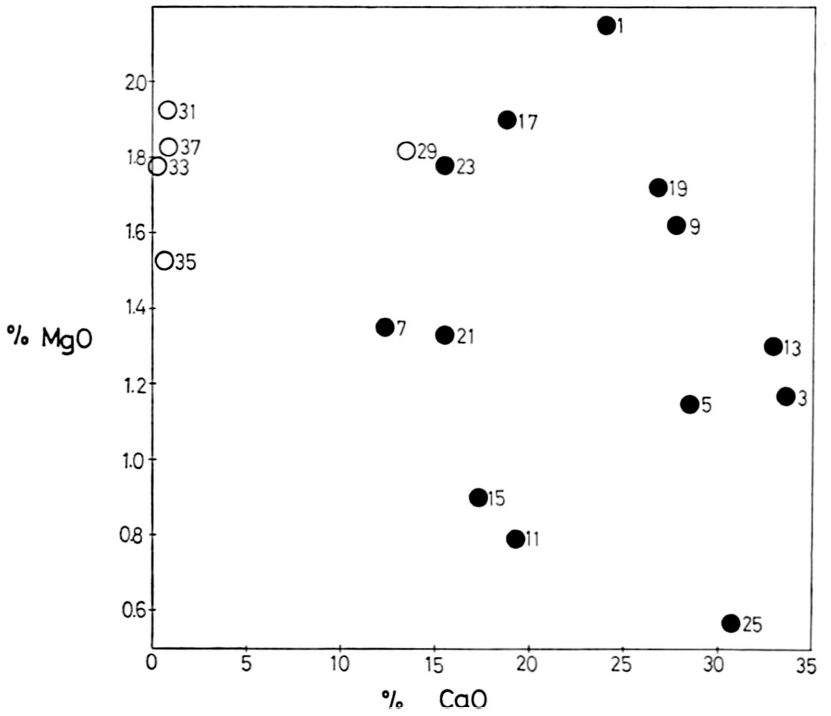

Figure V-10. Content of MgO in relation to CaO in Recent sediments from the South China Sea and Taiwan Strait; circles indicate near-shore sediments off the coast of Taiwan.

rigenous rather than biogenic (carbonate) origin. The most important magnesium-bearing mineral in the sediments is probably chlorite. The relatively higher content of MgO found in sediments off the coast of Taiwan (samples 29, 31, 33 and 37) might be related to the relatively higher chlorite contents in the sediments as suggested by X-ray diffraction.

The content of lithium in the sediments studied is similar to that found in igneous rocks. The positive correlation between Li and MgO in the sediments (Fig. V-11) suggests that lithium replaces magnesium in the chlorite structure due to its small ionic radius. In general, the sediments off the coast of Taiwan (samples 31, 33, 35 and 37) have a higher content of lithium than those from the South China Sea (samples 9, 11, 13, 15, 17, 19, 21 and 23); this may be attributed to the relatively higher content of magnesium in the sediments off the coast of Taiwan.

The author suggests that the iron content of the sediments may be related to the abundance of chlorite which contains significant amounts of FeO and Fe_2O_3; heavy minerals such as magnetite may also contribute significant amounts of iron. Although the occurrence of magnetite and other iron-bearing heavy minerals has not been confirmed by X-ray diffraction, due to their rarity, their presence in the sediments has been noted by microscopic observation.

It is of interest to note that the content of manganese varies considerably in the sediments analyzed, from 60 to 1,525 ppm. The average content of Mn in the sediments

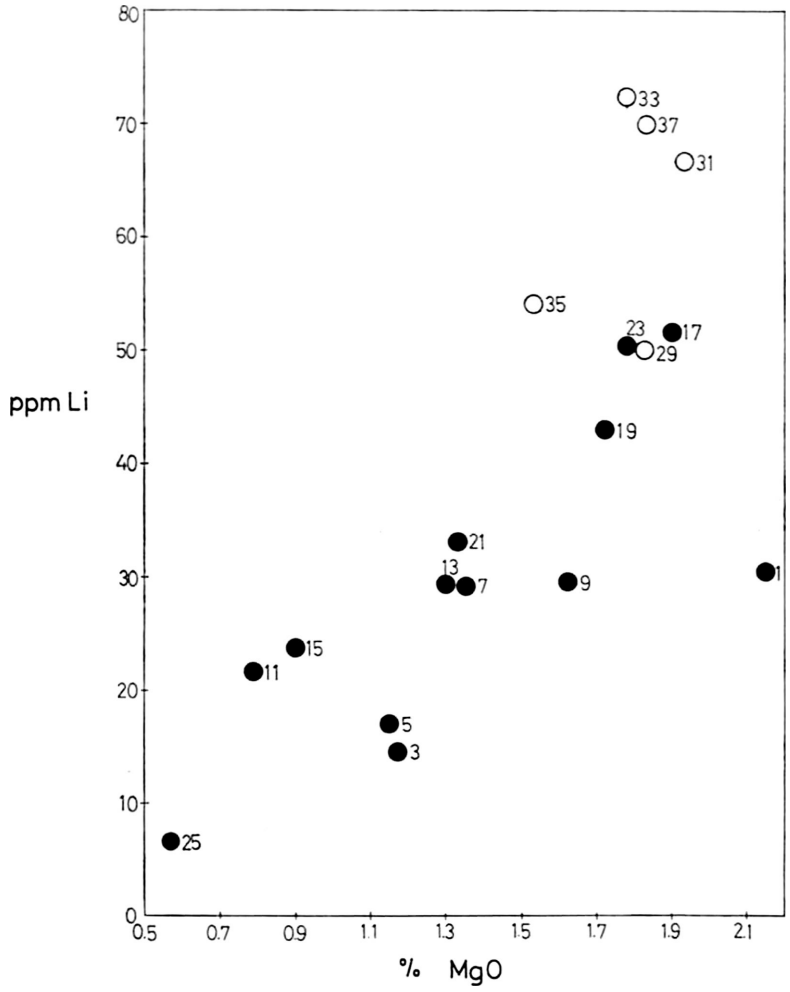

Figure V-11. Content of Li in relation to MgO in Recent sediments from the South China Sea and Taiwan Strait; circles indicate near-shore sediments off the coast of Taiwan.

is comparable to that found in near-shore sands in the Gulf of Paria, as reported by Hirst (1962a). There is a weak covariance of Mn in relation to total Fe as Fe_2O_3 (Fig. V-12) and it seems reasonable to suggest that the manganese in the sediments is probably present in iron-rich minerals such as magnetite and chlorite.

The content of copper in the sediments investigated is similar to that found in near-shore sands of the Gulf of Paria (Hirst, 1962b). Goldberg and Arrhenius (1958) have noted that copper in the sediments came mainly from igneous ferro-magnesian minerals such as pyroxene and also from the fine-grained fractions of the sediments which consist essentially of clay minerals; some of the copper in the sediments may also have been adsorbed from the overlying sea waters through the surfaces of clay minerals.

In conclusion, it is evident that the chemistry of the sediments is closely related to

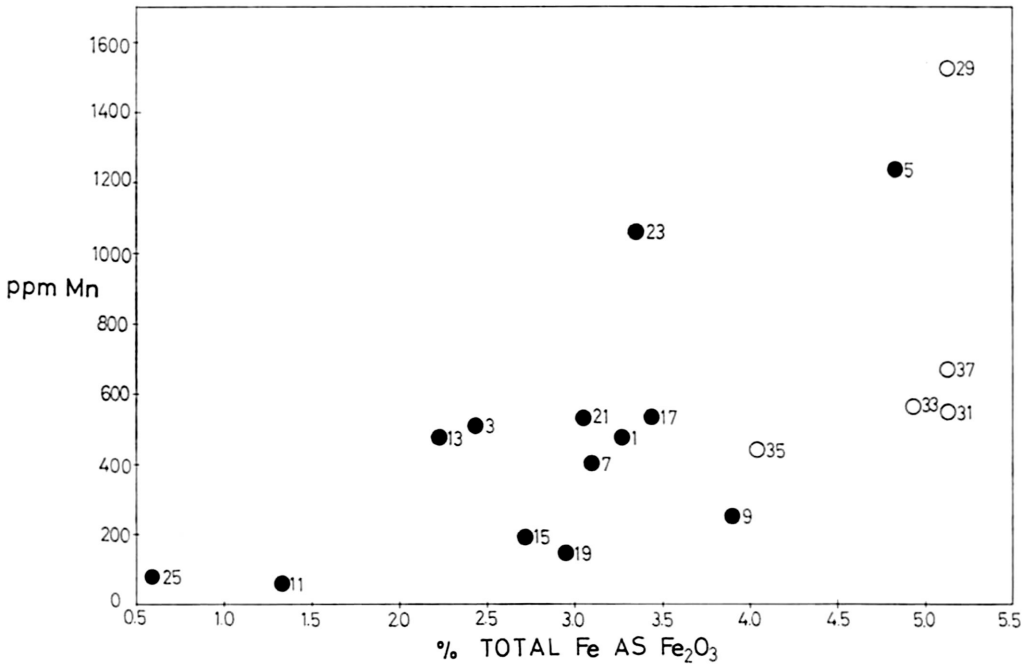

Figure V-12. Content of Mn in relation to total Fe as Fe_2O_3 in Recent sediments from the South China Sea and Taiwan Strait; circles indicate near-shore sediments off the coast of Taiwan.

their mineralogical composition. The sediments off the coast of Taiwan are generally characterized by higher contents of MgO, total Fe as Fe_2O_3, K_2O, Rb and Li, and lower CaO and Sr, as compared with those of the South China Sea; this can be interpreted as being due to the relatively higher content of hydromica and chlorite, and lower content of calcite in the sediments off the coast of Taiwan.

DISCUSSION

Based on the mineralogical and chemical data, two distinct types of neritic sediments can be recognized.

Near-shore sediments in Taiwan Strait

Mineralogical data indicate that the near-shore sediments in Taiwan Strait have a higher percentage of terrigenous material than those from the South China Sea; this is evidently due to the relatively high rate of erosion on the island of Taiwan. Furthermore, the near-shore sediments in Taiwan Strait are characterized by a lower number of total organisms, a higher quartz/K-feldspar ratio and probably higher contents of chlorite and hydromica than the sediments on the shelf in the South China Sea. The lower CaO content in the near-shore sediments is due to the lesser number of organisms than in the sediments farther offshore (Table V-3).

The high quartz/K-feldspar ratio suggests that the near-shore sediments off the coast of Taiwan were derived mainly from the island, which consists mainly of Neogene sandstones and shales with some intercalated basalts and limestones as well as younger andesites, Paleogene argillaceous sediments, and crystalline schists of late Paleozoic to Cretaceous age; there are, however, no intrusive granites on the island. The relative abundance of chlorite in the near-shore sediments of Taiwan Strait is probably due to weathering in temperate environments of the source rocks from which the chlorite was derived. It is evident from this study that environment and provenance were the most important factors controlling the mineralogical and chemical variations of the sediments.

Sediments of the continental shelf in the South China Sea

The sediments of the continental shelf in the South China Sea are characterized by the high number of total organisms in them, a low quartz/K-feldspar ratio, a high content of CaO and Sr, and low contents of MgO, total Fe as Fe_2O_3, K_2O, Rb and Li. The low quartz/K-feldspar ratio suggests that the shelf sediments of the South China Sea were derived mostly from southern China (Kwangtung province) where Mesozoic granites rich in potash-feldspar, and granodiorite, are widespread.

The decrease of the quartz/calcite ratio in relation to distance from the coast, together with other evidence previously mentioned, indicate that the depositional environment of the shelf sediments becomes more biogenic towards the edge of the shelf. It should be mentioned that Wang (1960) and Emery *et al.* (1969) concluded that sediments of the continental shelf of the China Sea and the Yellow Sea exhibit a simple pattern of silt and clay on the inner half and sand on the outer half of the shelf. This distribution pattern may be interpreted as due to the changes in sea level during and after the Pleistocene glacial ages. Niino and Emery (1961) regarded the sediments of the shelf of the China Sea as being relict sediments that have remained unburied on the continental shelves since Pleistocene times of glacially lowered sea levels.

ACKNOWLEDGMENTS

I am grateful to Captain Y. K. Jen of the Chinese Navy, Mr. S. Chang of our Institute and all crew members of R/V CHIU LIEN for their co-operation and assistance during sample collecting. I am deeply indebted to Dr. K. O. Emery and Dr. Chin Chen who provided some of the samples for this study; and to Drs. D. Ericson, P. Biscaye, V. C. Juan, T. Y. Chu, Chin Chen and P. Y. Chen for helpful discussions and criticism. I would like to thank Messrs. W. L. Jeng, T. C. Huang, C. Y. Kuo, Y. C. Liu and Y. H. Liao for their assistance with the laboratory work. This study was supported by the National Science Council.

REFERENCES

Chester, R., 1965, Elemental geochemistry of marine sediments: in Riley, J. P. and Skirrow, G., ed., Chemical Oceanography, vol. 2, p. 23–80, Academic Press, N. Y.

Chou, J. T., 1970, A study of the Recent sediments in the shallow portions of the South China Sea and Taiwan Strait: Ocean World, Tokyo.

Emery, K. O. and Niino, H., 1963, Sediments of the Gulf of Thailand and adjacent continental shelf: *Bull. Geol. Soc. Am.*, vol. 74, p. 541–554.

Emery, K. O.; Hayashi, Y.; Hilde, T.W.C.; Kobayashi, K.; Koo, J. H.; Meng, C. Y.; Niino, H.; Osterhagen, J. H.; Reynolds, L. M.; Wageman, J. M.; Wang, C. S.; and S. J. Yang; 1969; Geological structure and some water characteristics of the East China Sea and the Yellow Sea: United Nations ECAFE, *CCOP Tech. Bull.*, vol. 2, p. 3–43, figs. 1–17.

Goldberg, E. D. and Arrhenius, G.O.S., 1958, Chemistry of Pacific pelagic sediments: *Geochim. Cosmochim. Acta*, vol. 13, p. 153–212.

Hirst, D. M., 1962a, The geochemistry of modern sediments from the Gulf of Paria–I. The relationship between the mineralogy and the distribution of major elements: *Geochim. Cosmochim. Acta*, vol. 26, p. 309–334.

Hirst, D. M., 1962b, The geochemistry of modern sediments from the Gulf of Paria–II. The location and distribution of trace elements: *Geochim. Cosmochim. Acta*, vol. 26, p. 1147–1187.

Horstman, E. L., 1957, The distribution of lithium, rubidium and cesium in igneous and sedimentary rocks: *Geochim. Cosmochim. Acta*, vol. 12, p. 1–28.

Niino, H. and Emery, K. O., 1961, Sediments of shallow portions of East China Sea and South China Sea: *Bull. Geol. Soc. Am.*, vol. 72, p. 731–762.

Polski, W., 1959, Foraminiferal biofacies off the North Asiatic Coast: *Jour. Paleont.*, vol. 33, p. 569–587.

Wageman, J. M.; Hilde, T.W.C.; and Emery, K. O.; 1970; Structural framework of East China Sea and Yellow Sea: *Bull. Amer. Assoc. Petrol. Geol.*, vol. 54, no. 9, p. 1611–1643, figs. 1–22.

Waller, H. O., 1960, Foraminiferal biofacies off the South China coast: *Jour. Paleont.*, vol. 34, p. 1164–1182.

Wang, C. S., 1960, Sand fraction study of the shelf sediments off the China coast: *Proc. Geol. Soc. China*, no. 4, p. 33–49.

Young, E. J., 1954, Trace elements in recent marine sediments (abstract): *Bull. Geol. Soc. Am.*, vol. 65, p. 1329.

Blank page

Page blanche

VI. STRUCTURE AND STRATIGRAPHY OF THE CHINA BASIN[1]

By

K. O. Emery and Zvi Ben-Avraham[2]

(with figures VI-1 to VI-17)

ABSTRACT

Continuous seismic reflection profiles accompanied by total-field magnetic measurements were made in the China Basin by civilian survey ships on contract to the U.S. Naval Oceanographic Office between 1967 and 1969. The results show the presence of stratigraphic units similar to those previously found in the adjacent East China Sea and South China Sea: 1. acoustic basement in the southern part of the basin that may be a continuation of the igneous and metamorphic rocks beneath the adjacent shelf that were peneplained during Late Cretaceous—Early Cenozoic time, and much more irregular basement in the northern part of the basin that may be oceanic basement (Layer 2). 2. pre-deformational sediment conformable with the surface of much of the acoustic basement (probably Paleogene), and 3. post-deformational sediment largely turbidites deposited in deeper areas (probably Neogene to present) after the main episode of deformation. During the deformation a series of northeasterly-trending ridges was folded along the floor of the China Basin. Similar ridges underlie the basin side slopes, and these served as dams to trap sediments brought to the ocean by streams from the adjacent land areas. Another ridge separates the Manila Trench and the West Luzon Trough, and it extends northeastward as the Central Range of Taiwan. Oil potential appears to be greatest beneath the shelf between Taiwan and Hainan off mainland China, but the basin ridges that are surmounted by banks and islands also warrant further investigation.

1: Reprinted from Bulletin American Association of Petroleum Geologists, 1972, volume 56 by kind permission of that organization.

2: Woods Hole Oceanographic Institution, Woods Hole, Massachusetts 02543 U.S.A., Contribution No. 2218.

Appreciation is due the U.S. Naval Oceanographic Office through the interest of M. L. Parke, Jr., and L. M. Reynolds for providing the microfilms and other field records needed for this study. Copies of the seismic data are now available at the National Geophysical Data Center and copies of the magnetic data are in the Magnetics Library, U.S. Naval Oceanographic Office. We also thank J. D. Phillips of Woods Hole Oceanographic Institution for his kind assistance with the reduction of the geomagnetic data. Financial support was provided by the National Science Foundation (Grant GA-27449) and the Office of Naval Research (Contract N00014-66-C0241). This is one of a series of geophysical studies conducted off eastern Asia in support of the United Nations Economic Commission for Asia and the Far East, and particularly of its Committee for Co-ordination of Offshore Prospecting (CCOP).

INTRODUCTION

Since 1960 there has been a general increase of geological interest in the continental margin along eastern Asia. Studies of sediments, stratigraphy, and structure have bordered or included parts of the China Basin (Fig. VI-1), a large depression bordered clockwise by Taiwan, Philippine Islands, Borneo, Vietnam, Hainan, and mainland China (Fig. VI-2). Sediments of the shelf north of the China Basin were described by Niino and Emery (1961), and of the shelf southwest of it by Emery and Niino (1963). In both areas the sediments were considered as chiefly relict from glacially lowered sea level and typical of the outer parts of most continental shelves of the world. An advance in the knowledge of the structure of the region came from broad reconnaissance seismic and magnetic surveys, first in the East China Sea (Emery *et al.*, 1969; Wageman, Hilde, and Emery, 1970) and then in the South China Sea (Parke *et al.*, 1971) and in the Java Sea (Emery *et al.*, 1972). Each of these geophysical studies showed the presence of tectonic ridges that served as submerged dams to trap sediments derived from adjacent lands. Only after several million cubic km of Cenozoic sediments had accumulated in basins behind the dams were sediments able to escape in quantity over the dams and build thick sequences on the floor of the deep ocean of the China Basin.

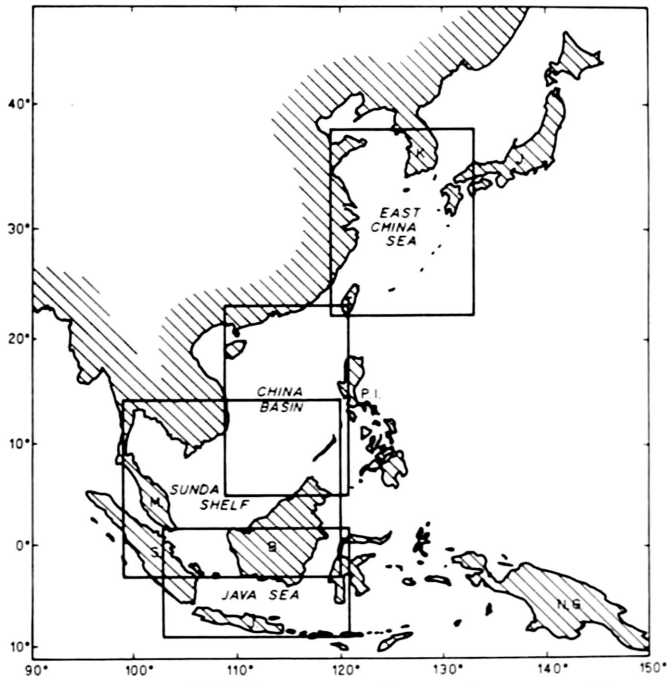

Figure VI-1. Outlines of areas investigated in previous studies and in this one (China Basin). Letters on land areas from north to south are: K—Korea, J—Japan, T—Taiwan, P. I.—Philippine Islands, M—Malay Peninsula, S—Sumatra, B—Borneo, N. G.—New Guinea, and J—Java.

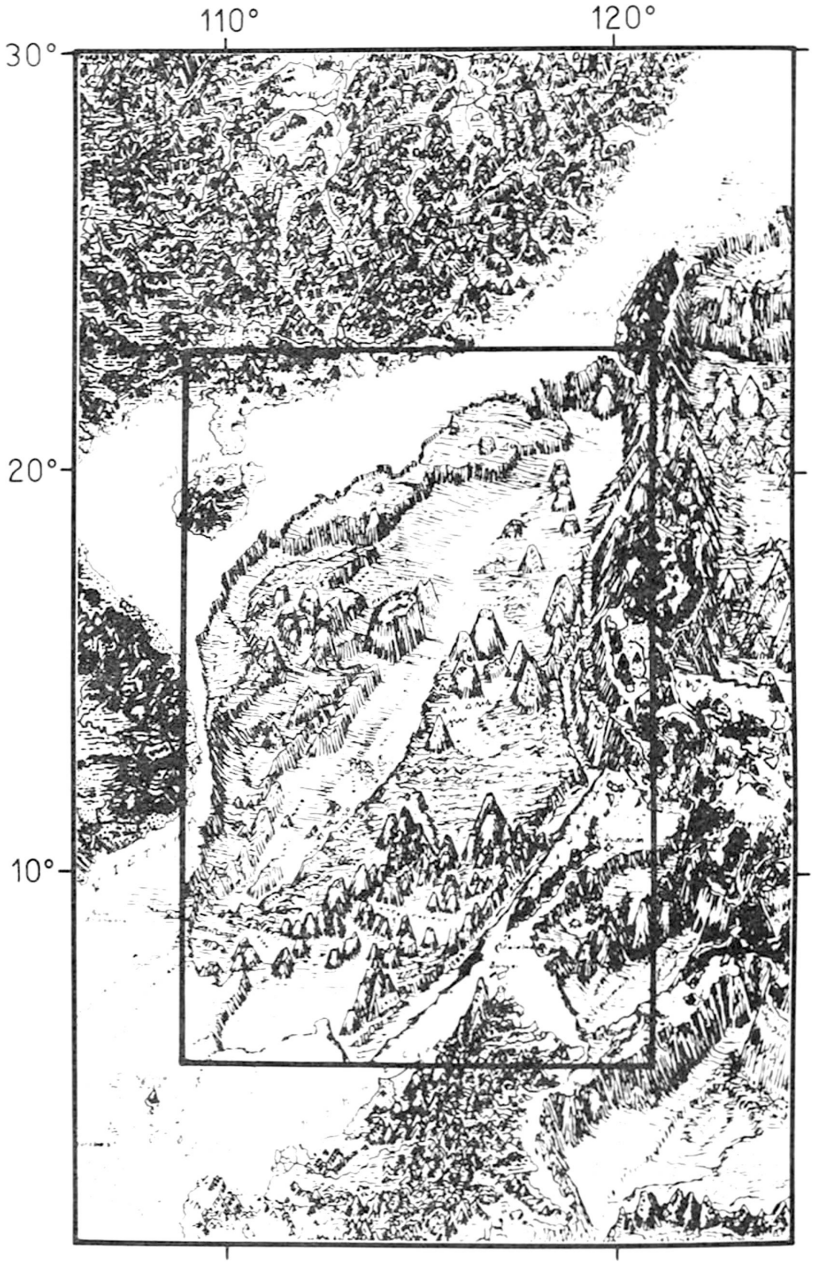

Figure VI-2. Diagrammatic map of the China Basin and vicinity. Wide lines frame the area that is portrayed in subsequent charts. From Heezen and Tharp (1971).

At the eastern side of the China Basin, the bottom topography of the Manila Trench and the West Luzon Trough drawn by Irving (1951) and Dietz (1954) was updated by Ludwig, Hayes, and Ewing (1967) and by Chase and Menard (1969). Seismic profiles made chiefly by geophysical ships of the Lamont-Doherty Geological Observatory arriving and departing Manila used mainly half-pound charges of TNT as the sound source. These profiles of Ludwig, Hayes, and Ewing showed sediments about 1.5 km thick in the West Luzon Trough, of variable thickness in the Manila Trench, and 0 to 1.5 km thick on the floor of the eastern China Basin where the nearly horizontal layers tended to smooth irregular bottom that was identified as oceanic basement (or Layer 2). Hayes and Ludwig (1967) found that the trench and trough have negative free-air gravity anomalies, and magnetic anomalies that could not be traced over appreciable distances. Seismic velocity measured at 13 refraction stations in the eastern China Basin by Ludwig (1970), yielded 2.1 to 2.6 km/sec for sediments, and 4.4 km/sec for basement. Earthquakes are rare in the China Basin except near the Philippine Islands (Gutenberg and Richter, 1949, pp. 58–61; Hayes and Ludwig, 1967) and east of Taiwan (Katsumata and Sykes, 1969). Most are shallow (less than 100 km) and exhibit little relationship to known faults (Allen, 1962), but they do lie along a westward-dipping focal plane.

Between 3 June and 26 August 1969 a general geophysical study of the South China Sea was made aboard R/V F. V. HUNT on contract to the U. S. Naval Oceanographic Office from the Marine Acoustical Services of Miami, Florida. Transit to and from Chilung, Taiwan, plus traverses previously reported by Parke *et al.* (1971) in the southern end of the China Basin total about 8,900 line km. All of these traverses included seismic profiles using a 30,000-joule sparker with analog recording, and magnetic measurements using a proton-precession detector. Unknown to us at that time were additional seismic profiles with a 20,000-joule sparker plus magnetometer measurements made between 15 September 1967 and 27 February 1968 aboard RUTH ANN and SANTA MARIA, two ships of Alpine Geophysical Corporation of Norwood, New Jersey, on contract to the U. S. Naval Oceanographic Office (May *et al.*, 1969). About 9,400 km of fair to good seismic profiles are from traverses of RUTH ANN, which combined with the seismic profiles of HUNT total 18,300 line km. An additional 10,100 km of seismic profiles mainly from SANTA MARIA are poor in quality but they yield somewhat more information than would simple bathymetric recordings. Geomagnetic records from all three ships plus four traverses from Project MAGNET total about 26,500 line km.

TOPOGRAPHY

Bathymetric contours of the China Basin and vicinity (Fig. VI-3) were taken from the compilation by Chase and Menard (1969) through interpolation at 1-km depth intervals from their 200-fathom contours. The chart also includes the 150-m contour to show the approximate position of the shelf-break. The widely-spaced contours of Figure VI-3 fail to reveal many of the topographic details of Figure 2, but the two figures supplement each other. In contrast to the flat shelves, most side slopes of the China

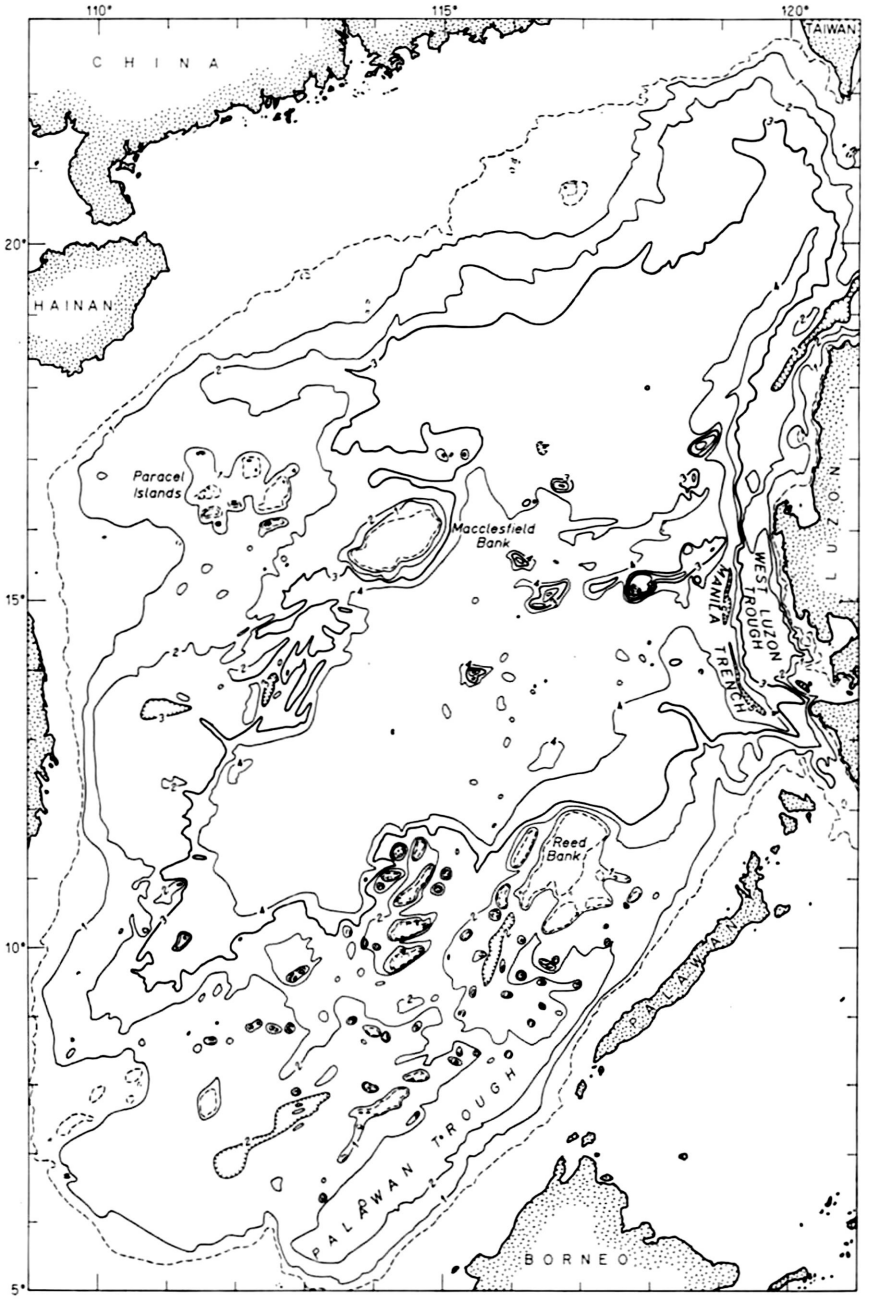

Figure VI-3. Topography of China Basin and adjacent shelves. Contours are at 1-km intervals, with the 150-m contour added as a dashed line. Interpolated and redrawn from Chase and Menard (1969).

Basin are very irregular owing to the presence of fault blocks, volcanoes, and calcareous reef structures. Fault blocks or slumps also are present low on the slope bordering the northwestern (mainland China) side of the basin where they interrupt the surface of a basin rise. Smooth side slopes occur only at the southwestern end of the China Basin, where Parke *et al.* (1971) showed the presence of sediment prograding northeastward from the adjacent northern Sunda Shelf.

On the floor of the basin are broad hilly areas—again fault blocks, volcanoes, and calcareous reefs. The hilly area at the southwest includes Reed Bank and many smaller banks and reefs, many of which have been names for ships that were wrecked upon them—giving rise to the general name for this region as the Dangerous Ground. Another large area of hilly basin floor borders the western and northwestern side of the basin; it includes Macclesfield Bank, the Paracel Islands, and many smaller reefs. The Paracel Islands have a small village with a tower and meteorological station. This group and the other islets containing only temporary habitations and inadequate navigational aids are poorly mapped (U. S. Naval Oceanographic Office, 1967, p. 71–88) and have uncertain sovereignty.

The smooth prograded side slopes at the southwestern and to a lesser extent at the northeastern end of the China Basin continue basinward as gently-sloping aprons or basin rises that gradually flatten into abyssal plains. The largest abyssal plain occupies the central area of the basin, where the bottom is exceedingly flat at about 4,350 m. A much smaller abyssal plain floors the Palawan Trough near Borneo at about 2,850 m. Additional bottom contours that show the prograded sediments, their lower slopes, and their abyssal plains have been included on the geological map of the China Basin (Fig. VI-15) as interpreted from the seismic profiles that are available.

Sediments at the eastern side of the China Basin slope downward from the nearly flat basin floor into the steep-sided Manila Trench; the southeastern end of the trench also has a smooth slope toward the 5,000-m deepest point of the trench just west of Luzon. East of the trench, the West Luzon Trogch has a flat floor at about 2,600 m that may be blocked off from the deeper (about 3,200-m) floor of the northern extension of the steep-sided trough which has been termed the North Luzon Trough (Ludwig, 1970).

The entire area of Figure VI-3 is 2.7 million square km, and the area of the China Basin beyond the shelf-break is 1.8 million square km—nearly one-quarter the area of the conterminous United States.

GEOMAGNETICS

Magnetometer data from R/V F. V. HUNT, RUTH ANN, SANTA MARIA, and Project MAGNET were digitized and the regional gradient was removed by a computer program at Woods Hole Oceanographic Institution. The resulting lines of magnetic anomalies were plotted along the various traverses (Fig. VI-4). Anomalies in the southern, western, and northeastern parts of the basin are subdued, presumably because of the great depth that magnetic basement has been buried beneath sediments. Anomalies west of Luzon are larger, probably reflecting the presence of volcanic moun-

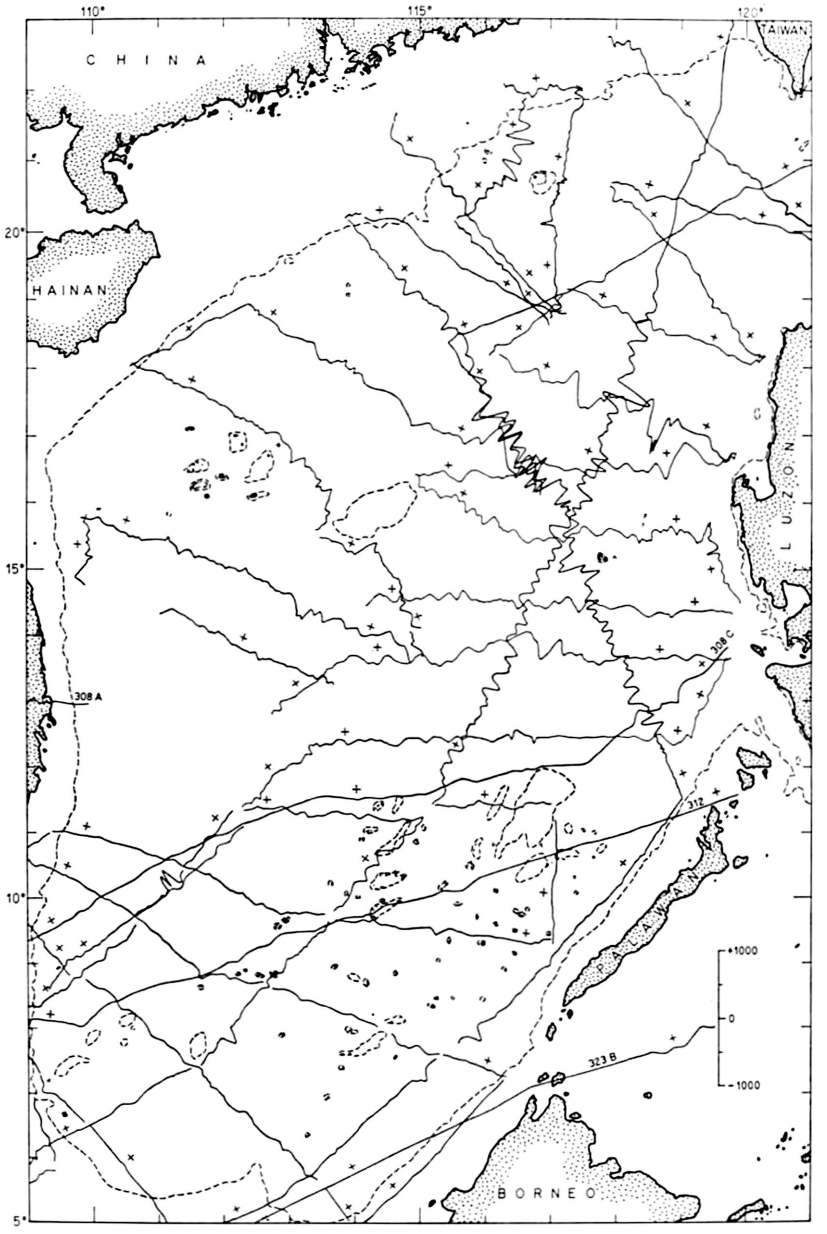

Figure VI-4. Lines of magnetic anomalies from ship and airplane measurements across the China Basin. The four airplane lines (Project MAGNET) are identified by 3-digit numbers.

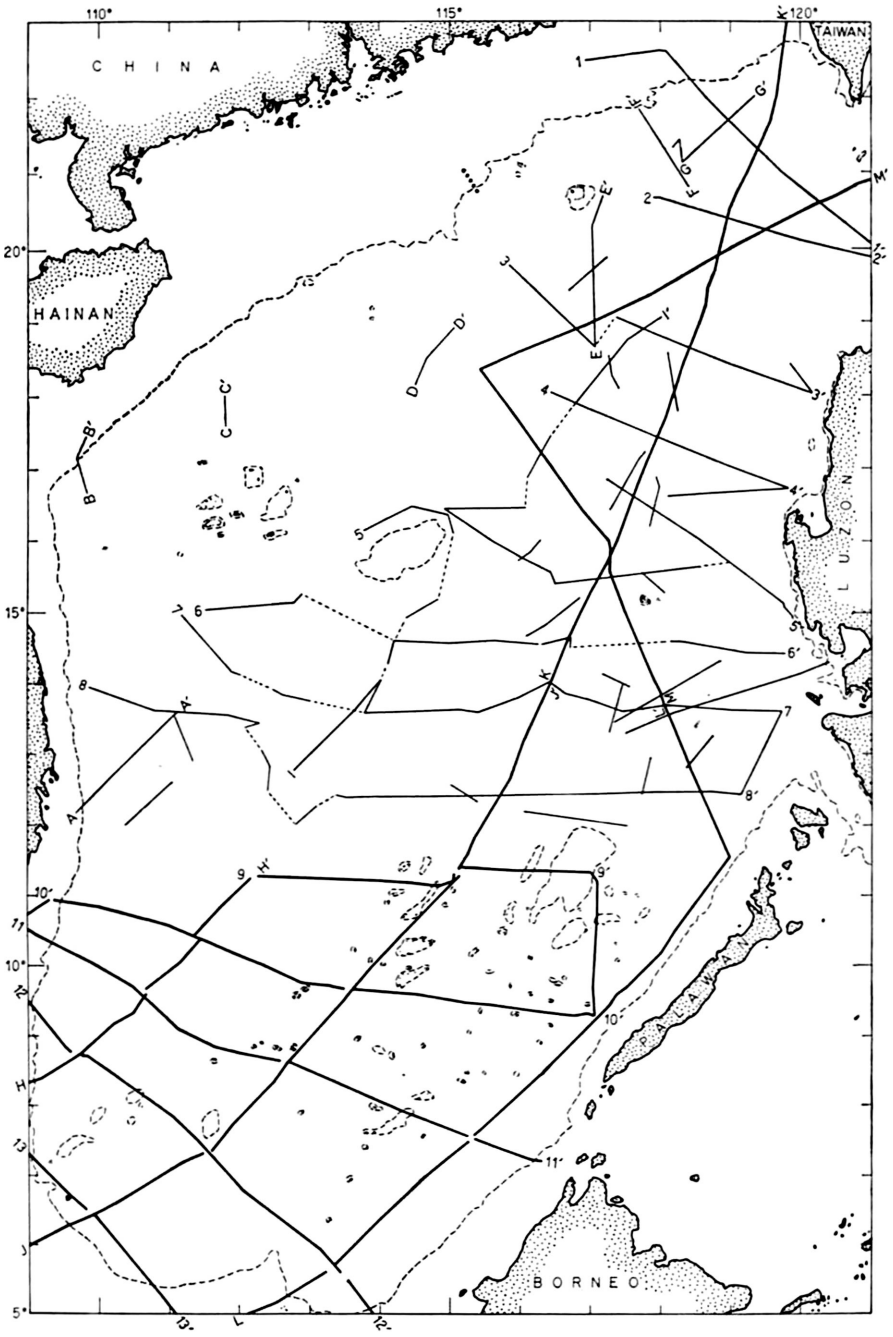

Figure VI-5. Positions of the best seismic profiles—from R/V F. V. HUNT (wide lines) and RUTH ANN (narrow lines). The dotted line across the outer shelf at Lat. 21° N., Long. 115° E. is from United Geophysical Corporation (Fig. VI-13). Interpretive drawings are shown on Figures VI-6 to VI-11.

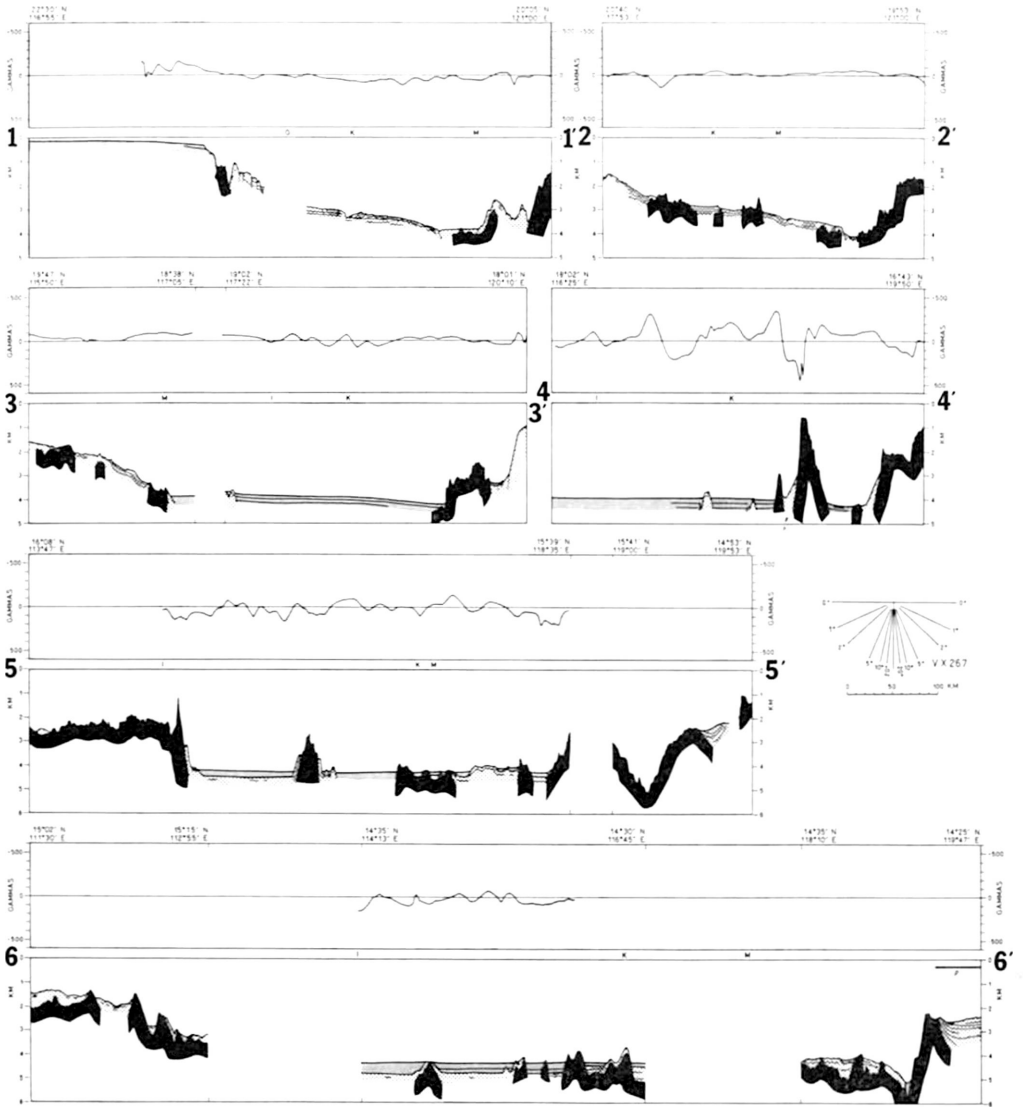

Figure VI-6. Interpretative seismic and magnetic profiles along traverses 1–1′, 2–2′, 3–3′, 4–4′, 5–5′, and 6–6′ (Fig. VI-5), assuming an acoustic velocity of 1.5 km/sec in the water and 2.0 km/sec in the sediments:

Top: Total intensity magnetic anomalies.

Bottom: Line drawing interpretation of continuous seismic reflection profiles at a vertical exaggeration of 26.7 times. Black indicates acoustic basement, coarse dots—pre-deformation sediments, and fine dots—post-deformation sediments. Where present, the small horizontal bar and *p* designate a portion of the recording that is illustrated by a photograph.

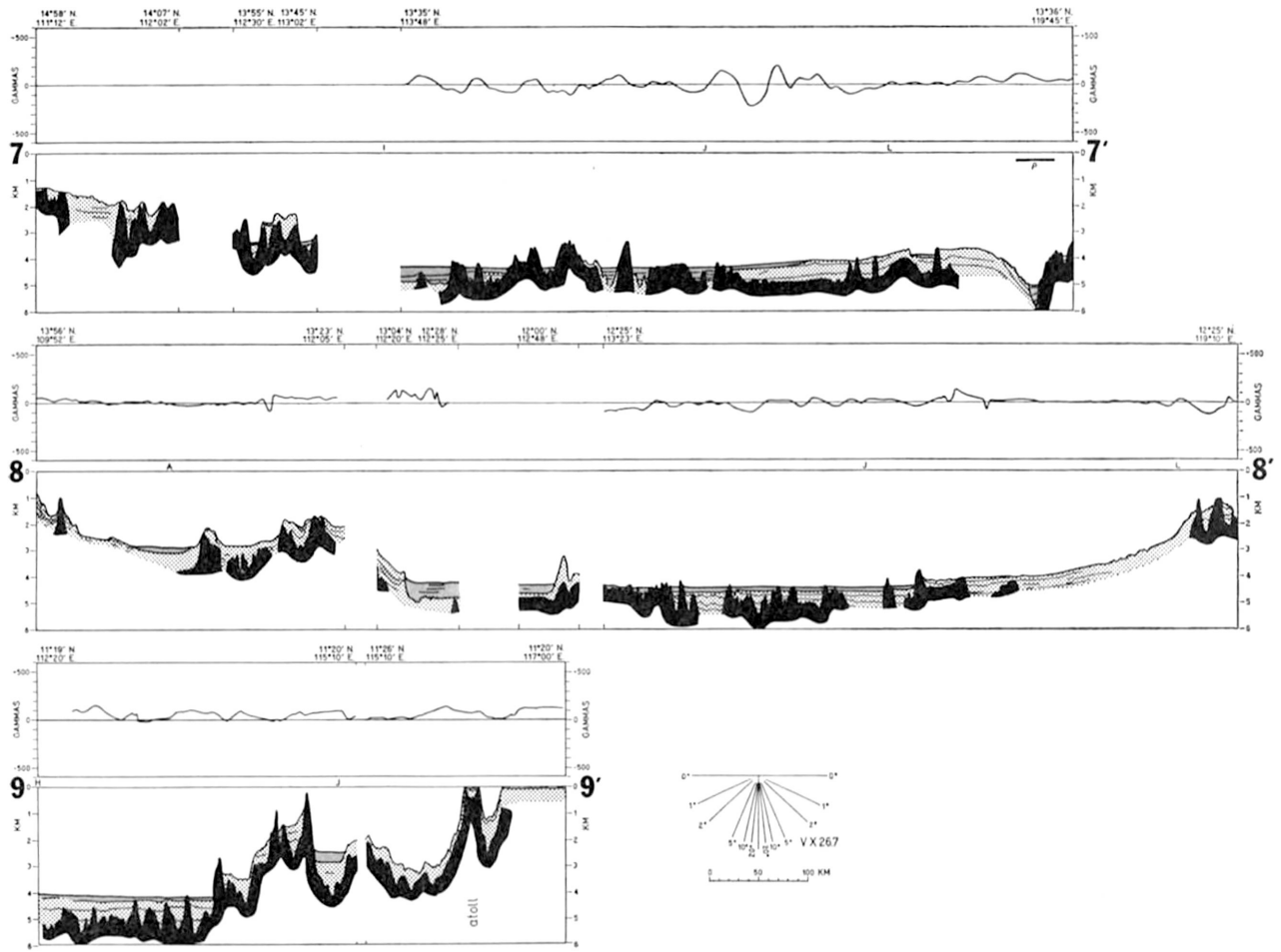

Figure VI-7. Traverses 7–7′, 8–8′ ,and 9–9′. Symbols are the same as for Figure VI-6.

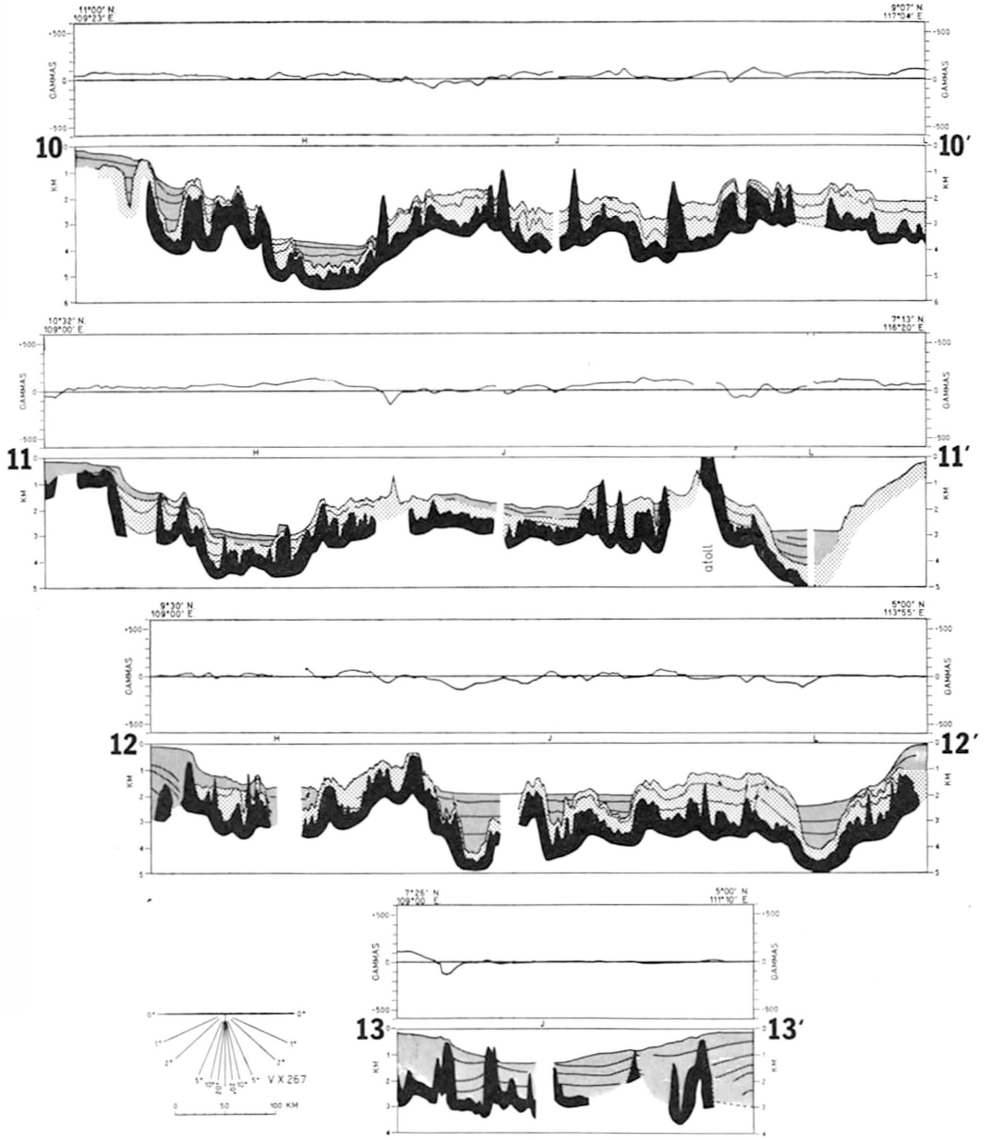

Figure VI-8. Traverses for 10–10′, 11–11′, 12–12′, and 13–13′. Symbols are the same as for Figure VI-6.

tains that rise high above their surroundings. The degree of correspondence of magnetic anomalies with topography and structure is best shown on the geophysical profiles of the subsequent Figures VI-6 to 11.

SEISMIC PROFILES

The paper recordings of the continuous seismic profiles had been microfilmed and only flow-camera prints of the films were available to us. On these prints we marked in colored pencil the various kinds of reflecting surfaces. Only previous experience with the high-quality records from HUNT permitted identifications on many of the seismic records from RUTH ANN because of the generally lower power, poor microfilms, and short discontinuous traverses of the latter (Fig. VI-5). However, the final product from all three ships provides good coverage of the entire China Basin in the form of structural sections.

The records revealed three main kinds of acoustic units, as already discussed by Parke *et al.* (1971) for the southern part of the basin. Deepest is acoustic basement, the deepest reflector for the available energy, and the one which is believed to consist largely of igneous rock—the oceanic basement, or Layer 2. Locally, volcanic peaks, massive coral reefs, and older folded sediments have similar reflective properties and must be included with acoustic basement. In the southern part of the China Basin

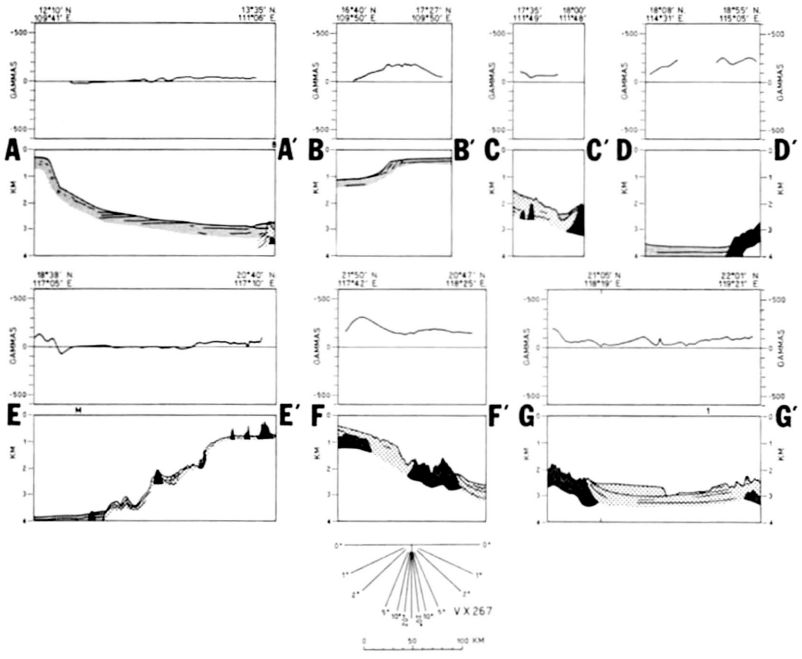

Figure VI-9. Traverses A-A′, B-B′, C-C′, D-D′, E-E′, F-F′, and G-G′. Symbols are the same as for Figure VI-6.

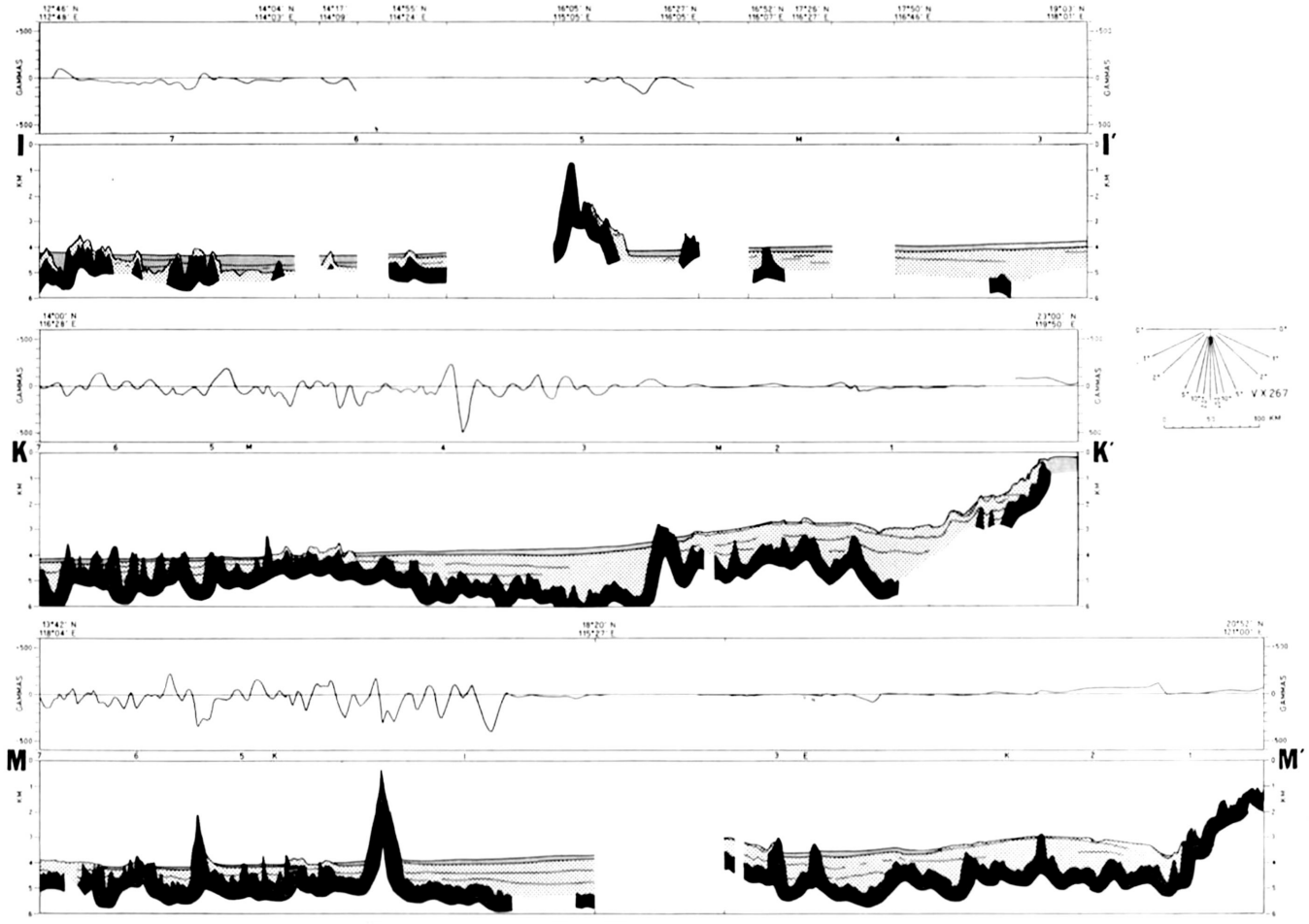

Figure VI-10. Traverses I-I′, K-K′, and M-M′. Symbols are the same as for Figure VI-6.

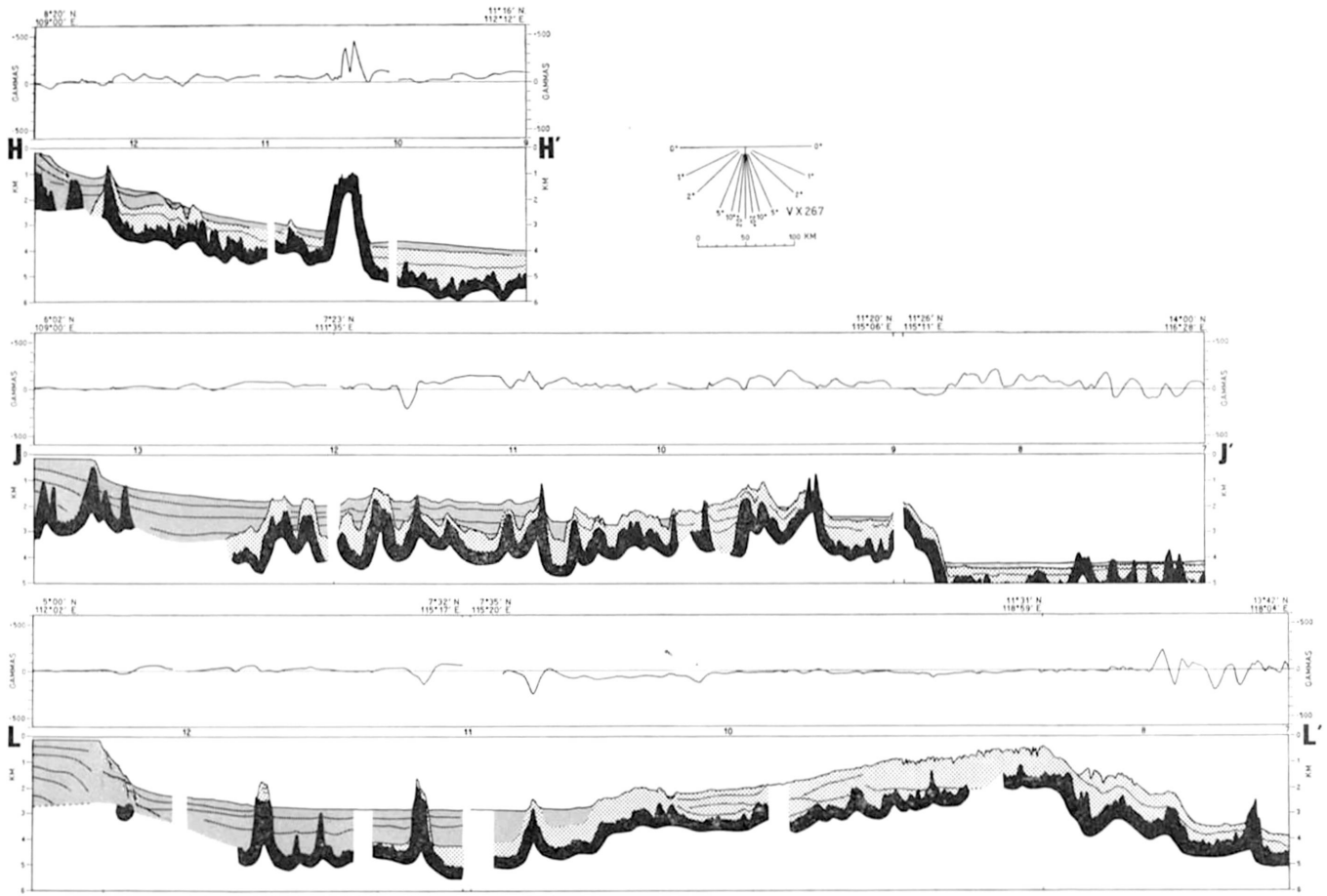

Figure VI-11. Traverses H-H′, J-J′, and L-L′. Symbols are the same as for Figure VI-6.

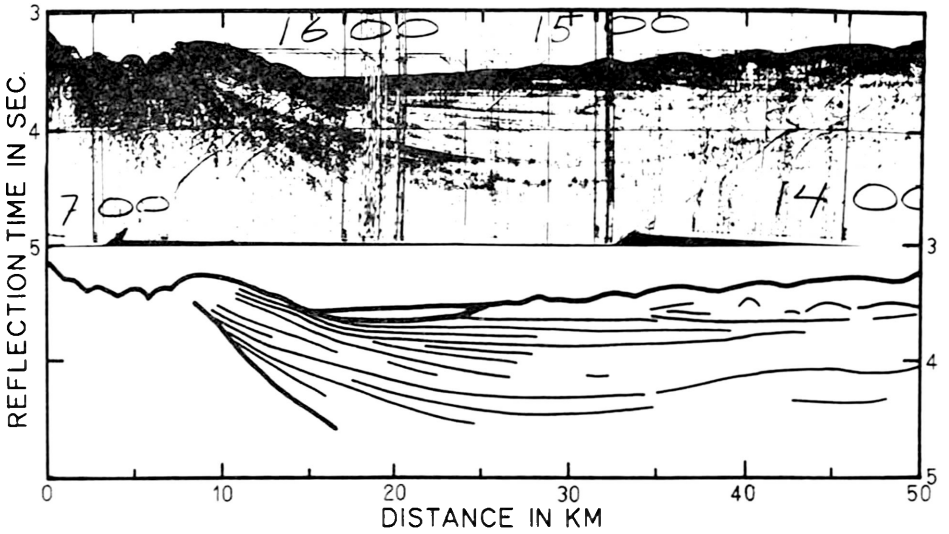

Figure VI-12. Section of seismic recording and of its interpretation showing repeated westward thinning of sediments in the West Luzon Trough (Profile 6–6′ of Figure 6 at Lat. 14°25′; Long. 119°35′) caused by repeated uplift of the bordering ridge.

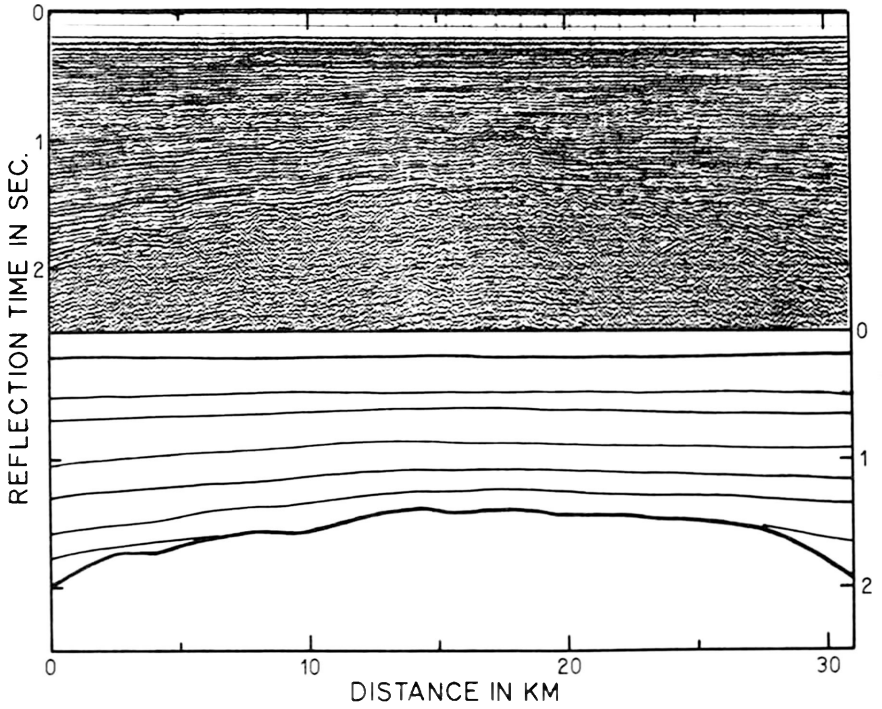

Figure VI-13. Section of seismic recording across the outer part of the continental shelf southeast of Hong Kong (Fig. VI-5) showing a barrier ridge beneath the outer shelf backed by thicker sediments that have been trapped by the ridge. This seismic section was kindly provided by United Geophysical Corporation and it was electronically enhanced by GEOCOM Corporation.

basement was peneplained before being buried under sediments and then folded (Parke *et al.*, 1971, figs. 21, 22, 23); this may be a northward continuation of pre-Cenozoic igneous and metamorphic rocks beneath the Sunda Shelf. Acoustic basement generally is buried beneath sediments, but locally it protrudes upward as isolated peaks or areas having very irregular topography.

Above the acoustic basement is a sedimentary blanket that follows many of the undulations of the basement. Elsewhere, it is folded and faulted and abuts the steeper slopes of basement topography. The most intense folding is associated with basement projections and it occurs in a series of ridges that trend northeast-southwest. These ridges are crossed by the profiles of Figures VI-6, VI-7, and VI-8 and are paralleled by those of Figures VI-9, VI-10, VI-11. Where the unit crops out, the topography is gently rolling and smoother than that for outcrops of acoustic basement (Fig. VI-12). Following the usage in Parke *et al.* (1971), the sequence is termed pre-deformational sediment. This is somewhat simplified terminology because at least two periods of deformation can be discerned locally through the presence of unconformities, but they cannot be traced for more than a few km nor correlated from place to place.

The third and shallowest consistent sequence occupies the troughs beneath the continental shelves (Fig. VI-13) and the areas of lowest topography within the China

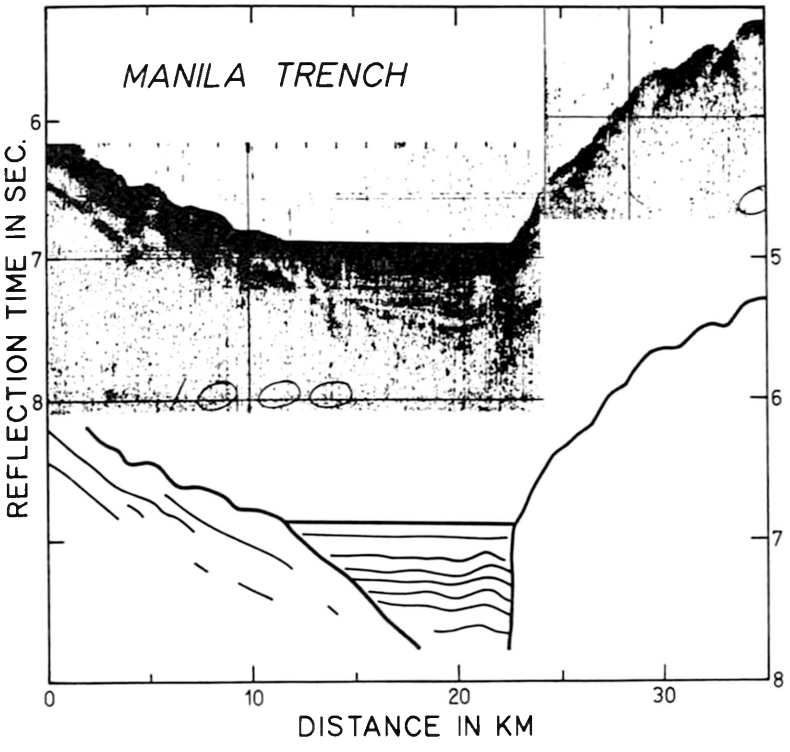

Figure VI-14. Section of seismic recording and of its interpretation showing slight folding of post-depositional sediments in the Manila Trench (Profile 7–7′ of Figure VI-7 at Lat. 13°24′; Long. 119°38′) due to underthrusting.

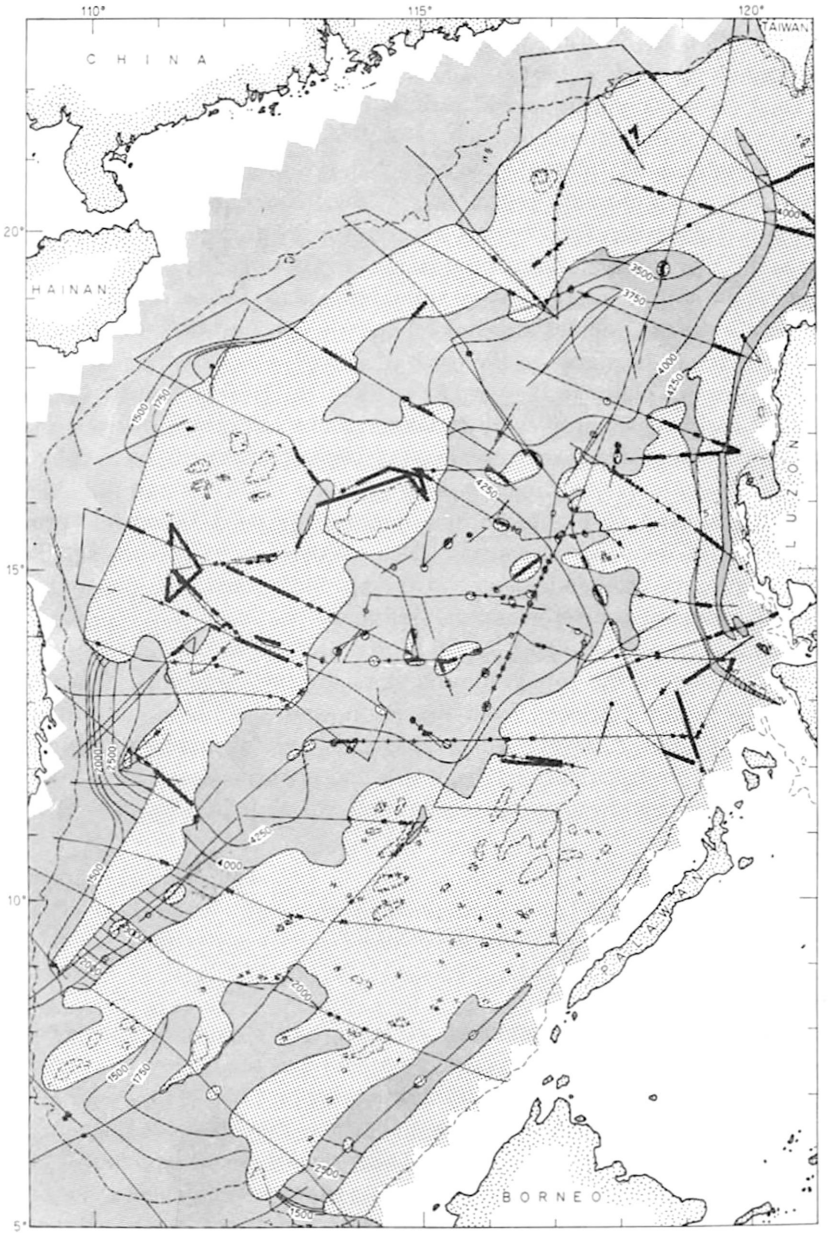

Figure VI-15. Geological map that shows the areas of post-deformational sediments (fine dots) with topographic contours at 250-m depth intervals. Exposed pre-deformational sediment is denoted by the coarse dots; it occurs in areas of positive relief. Outcrops of acoustic basement shown by the seismic profiles are so discontinuous that they are drawn only as wide parts of the lines that denote the positions of traverses. Note that many more traverses are shown as control for the geological map than were useful as structural sections (Fig. VI-5).

Basin. Quite clearly, it is a sedimentary fill dating from the cessation of most diastrophic activity. This fill is termed the post-deformational sediment, again in accordance with the terminology used in Parke *et al.* (1971), and in spite of the fact that some slight deformation is evident in several profiles across this unit due to slumping or to underthrusting along the Manila Trench (Fig. VI-14). The post-deformational sediments contain many good internal reflectors that are interpreted as sandy turbidites. In contrast, continuous discrete reflectors are less frequent in the pre-deformational sediment, which locally can even be termed acoustically transparent. The interpretation of the post-deformational sediment as being largely turbidite in origin accords with its distribution as a progradation from the continental shelves down the basin side slopes. Where sediment sources appear to be great, the post-deformational unit continues smoothly down the slopes in the form of narrow aprons whose slopes gradually merge into flat abyssal plains in the deepest parts of the basins (Fig. VI-15). Detailed examination of bathymetric profiles by J. Mammerickx of Scripps Institute of Oceanography (personal communication) revealed the longest apron to be cut by deep-sea channels with natural levees, particularly near Latitude 12°N., Longitude 113°E.

The geological map of Figure 15 also denotes the parts of seismic profiles that indicate outcrops of acoustic basement. Because these outcrops are small and discontinuous no attempt was made to group them. Note, however, that most of them occur within the areas of pre-deformational sediment.

A generalized impression of the distribution pattern of the three stratigraphic units and their relationship to the topography is given by the three-dimensional model of Figure 16. This model is viewed from the south, and it contains parts of profiles 9–9′, 10–10′, 11–11′, 12–12′, H–H′, J–J′, and L–L′. Careful inspection reveals several ridges composed of pre-deformational sediment and acoustic basement trending northeasterly and separated by low areas having flat bottoms underlain by post-deformational sediment.

DISCUSSION

Geological Dates

The major events recorded in the stratigraphy and structure of the China Basin appear to be the peneplanation of acoustic basement and the folding that separates the pre-deformational and the post-deformational sediments.

The basement rocks of the Indochina Peninsula, the Malay Peninsula, Sumatra, and Borneo continue beneath the shallow Sunda Sea, and they consist mainly of Paleozoic and Mesozoic metamorphic and igneous rocks. A review of evidence for the Late Cretaceous age of the peneplain on acoustic basement south of the China Basin is provided by Parke *et al.* (1971) and Todd and Pulunggono (1971). Magnetic (Bosum *et al.*, 1970) and gravity (Pan, 1967, Hsieh and Ho, 1971) surveys and drill-hole samples from the Penghu Islands west of Taiwan (Huang, 1967; Chou, 1969) indicate that Mesozoic strata are far denser than Cenozoic ones, in agreement with the concept that the top of acoustic basement there could be the Late Cretaceous peneplain. In the Philippines a major unconformity also occurs between the Cretaceous and Tertiary

periods (Gervasio, 1966, 1968). No more specific evidence for the age of the acoustic basement rock or its peneplain is known from the China Basin.

The large Northwest Borneo Geosyncline contains thick highly folded and faulted Paleogene sediments. Only sediments younger than Middle Miocene have gentle dips. In this region the Paleogene sediments appear to have been deposited in deep water, and the late Neogene ones in shallow water, presumably the reverse of the depth sequence in the China Basin (Parke *et al.*, 1971). In Taiwan, the Cenozoic sediments older than Pliocene are folded and faulted, and they form much of the Central Range (Juan and Wang, 1971). Lapping against them are thick "muddy sediments" of Late Pleistocene age. The Miocene sediments are largely bedded sandstones with ripple marks, and the Pleistocene "muddy sediments" are massive mudstones possibly of deep-water origin. In the Philippine Islands as on Taiwan there was a major tectonic episode during Late Miocene time followed by post-orogenic sedimentation interrupted by volcanism and other tectonic activity (Gervasio, 1968). Uplifts and subsidence during the entire Cenozoic are well documented on the islands of Palawan, Mindoro, and Luzon; these movements resulted in cycles of arkosic marine sediments alternating with limestones. Folding and uplift has continued to the present along the eastern edge of the China Basin, as indicated by raised Holocene calcareous reefs near the south end of Taiwan (Hashimoto *et al.*, 1970), by a 25-km left-lateral movement of the East Taiwan Rift since Late Pleistocene time (Biq, 1967), by the presently active 1,200-km long left-lateral movement of the Philippine Fault (Allen, 1962), and by the folding of "post-deformational" sediment in the Manila Trench (Fig. VI-14).

Until drill data are available from the floor of the China Basin, we believe that the best estimate for the unconformity at the top of the acoustic basement is Late Cretaceous. The main time of subsequent folding is probably early Neogene, with activity continuing to the present along the eastern side of the China Basin.

Structural Implications

The distribution of the ridges beneath the outer edges of the continental shelves and across the floor of the China Basin (Figs. VI-6 to 11, and VI-16) is presented in simplified form in Figure VI-17. Ridges surround the basin where they served as submerged dams to trap large quantities of detrital sediments brought to the ocean by rivers. One of the ridges bordering the shelf off Borneo continues northeasterly as the elongate Palawan Island. These barriers appear to be close parallels to the ones previously observed in the East China Sea and the South China Sea. The ridge at the edge of the continental shelf off mainland China is known from only a few traverses, best of which is one by United Geophysical Corporation across the outer part of the shelf directly southeast of Hong Kong (Figs. VI-5, and 13). In this area the ridge is buried beneath about 1.4 km of sediments that are much thicker on either side of the ridge (Fig. VI-13).

Other ridges on the floor of the basin are best known where post-deformational sediments are absent or thin, and they trend northeasterly except along the easternmost edge of the basin where the trend is northerly. As shown by the structural sections, the ridges are complexly folded and faulted, and some appear to be penetrated by volcanic peaks. At the northeastern and southwestern ends of the China Basin the

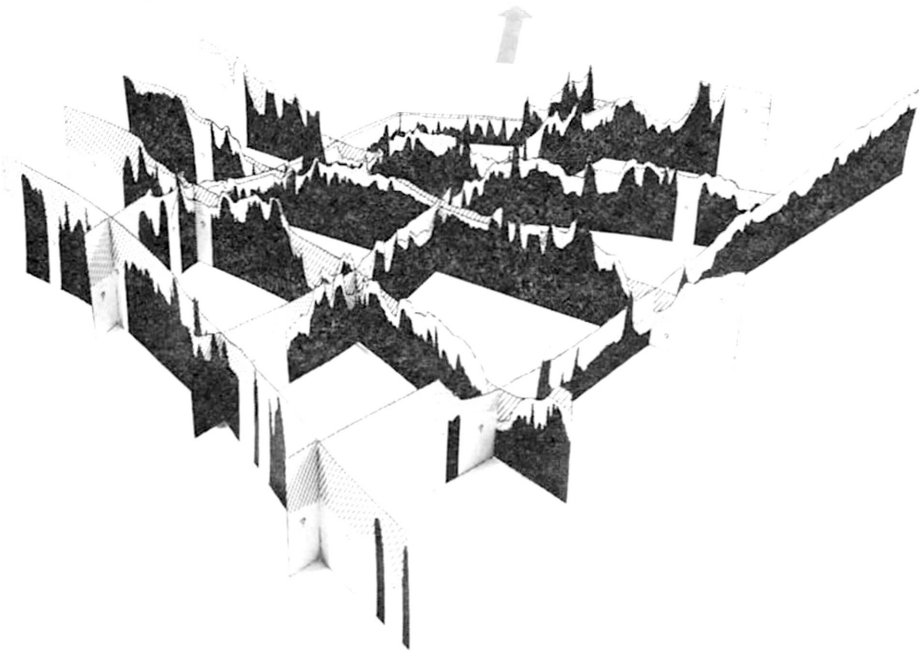

Figure VI-16. Photograph of a three-dimensional cardboard model depicting acoustic basement in black, pre-deformational sediment—dotted, and post-deformational sediment—diagonally hatched. The broad arrow at the top indicates north. Parts of profiles 9–9′, 10–10′, 11–11′, 12–12′, H-H′, J-J′, and L-L′.

northeasterly-trending ridges are truncated by other ridges or are buried beneath later sediments that have prograded basinward. The small acoustic power source and the restriction to analog recording (that could not remove bottom multiples) prevent their clear recognition beneath the thick sediments of the shelves. However, one very long and nearly continuous ridge appears to extend northeasterly beneath Formosa Strait (between Taiwan and the mainland). It may underlie and be the origin of the Penghu Islands (Lat. 23°35′N.; Long. 119°35′E.), in which a drill hole shows the presence of hydrothermally altered Mesozoic and Paleogene sedimentary rocks and of Pliocene-Pleistocene tuffs and basalts (Huang, 1967). This significance, however, may be reduced by the frequency of igneous rocks of many ages on Taiwan (Yen, 1971).

The Central Range of Taiwan appears to be a northerly continuation of a ridge that farther south separates the Manila Trench and the West Luzon Trough and may continue southeastward through the central Philippine island of Mindoro (Geological Survey Division, 1963) (Fig. VI-17). This interpretation differs from that of Bosum *et al.* (1970) and Juan and Wang (1971) who believed that the structures of Taiwan are separated from those of the Philippines by a fracture zone, and that of Meng and Chang (1971) who lacked submarine data and suggested that the structures on land in both Taiwan and the Philippines are directly connected. The relationship of the large strike-slip fault of the Philippines (Allen, 1962) to that of Taiwan (Biq, 1967) is unknown.

The pattern of sub-parallel folded ridges along the length of the China Basin is

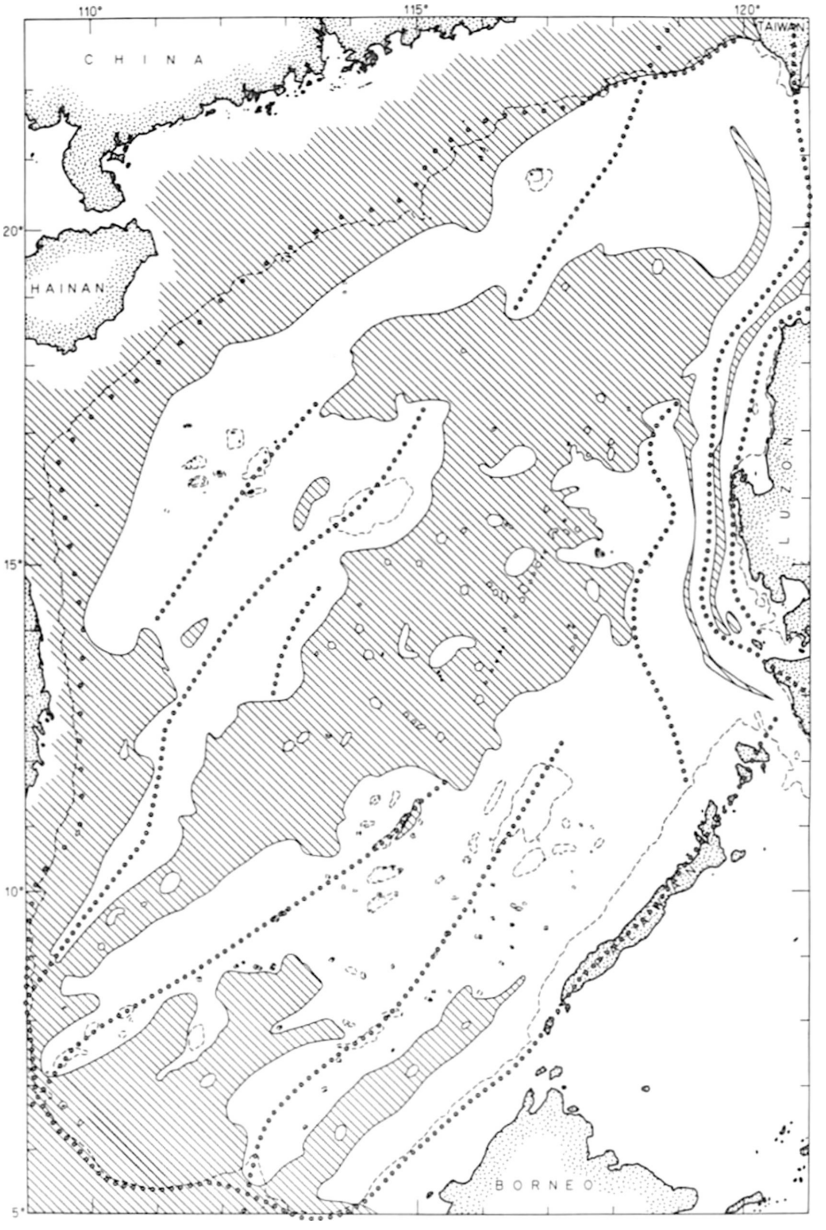

Figure VI-17. Pattern of ridges (dotted lines) peripheral to the China Basin and passing diagonally through it. The hatching depicts the areas of post-deformational sediments that are shown in more detail on Figure VI-15.

strongly suggestive that the last major deformation was compression along a southeast-northwest axis through the China Basin, not the tension that was earlier suggested by van Bemmelen (1949) and Rodolfo (1969). The compression is easiest to visualize in

terms of sea-floor spreading, whereby the Philippine plate beneath the Pacific Ocean is underthrusting continental plates of southeastern Asia in the manner suggested by Isacks, Oliver, and Sykes (1968), Le Pichon (1968), Morgan (1968), and Oliver (1970). Underthrusting south of Latitude 14°N. appears to occur in the Philippine Trench, which extends along the southern part of the eastern side of the Philippine Islands. Farther north, the underthrusting is in the Manila Trench west of the northern part of the Philippines, indicating that a small segment of the Philippine Plate is pushing westward into the China Basin (Dewey and Bird, 1970). The two trenches on opposite sides of the islands must be separated by a fault, as suggested by Fitch (1970). Active underthrusting accounts for the repeated uplift of the ridge bordering the West Luzon Trough (Fig. VI-12), the slight folding of sediments in the Manila Trench (Fig. VI-14), and the westward overthrusting on Taiwan described by Meng and Chang (1971). West of Luzon are three ridges that trend northerly and parallel to the Manila Trench. The similarity of trend suggests that these three ridges are presently active and thus are younger than the northeasterly-trending ridges located farther west in the China Basin.

Oil Potential

Oil exploration activity during 1969 and 1970 was confined to the marginal areas of Figure 17 and to a few seismic lines on Reed Bank; several holes were drilled off northwestern Borneo and off northwestern Palawan in the Philippine Islands (Humphrey, 1970, 1971). Activity in mainland China is confined to land areas (Meyerhoff, 1970) with no geological interest exhibited so far in the offshore region bordering the China Basin.

The results of this geophysical study suggest that the thickest Neogene sediments (the age of the producing horizons in Taiwan) are likely to be present in the filled marginal trough that underlies the continental shelf between Taiwan and Hainan, mostly off the southern coast of mainland China. The oil potential of the linear ridges that underlie the outer edges of the continental shelves and cross the floor of the China Basin is of even more speculative interest. The islands and banks that cap many of the ridges could serve as drilling platforms, but nothing is known of the organic content and reservoir characteristics of the folded and faulted probable Paleogene strata that cap the acoustic basement and form the ridges themselves.

Clearly, more closely-spaced geophysical traverses are needed across the shelf and the ridges before further speculation is warranted about oil potential of the region.

REFERENCES

Allen, C. R., 1962 Circum-Pacific faulting in the Philippines-Taiwan region: *Jour. Geophys. Research*, vol. 67, p. 4795–4812.

Biq, Ching Chang, 1967, The east Taiwan rift: *Petroleum Geol. of Taiwan*, vol. 4, p. 93–106.

Bosum, W., G. D. Burton, S. H. Hsieh, E. G. Kind, A. Schreiber, and C. H. Tang, 1970, Aeromagnetic survey of offshore Taiwan: United Nations ECAFE, *CCOP Tech. Bull.*, vol. 3, p. 1–34.

Chase, T. E. and H. W. Menard, 1969, Bathymetric Atlas of the Northwestern Pacific Ocean: U.S. Naval Oceanographic Office, Washington, D. C., 50 sheets.

Chou, J. T., 1969, A petrographic study of the Mesozoic and Cenozoic rock formations in the Tungliang well TL-1 of the Penghu Islands, Taiwan, China: United Nations ECAFE, *CCOP Tech. Bull.*, vol. 2, p. 97–115.

Dewey, J. F., and J. M. Bird, 1970, Mountain belts and the new global tectonics: *Jour. Geophys. Research*, vol. 75, p. 2625–2647.

Dietz, R. S., 1954, Marine geology of northwestern Pacific: Description of Japanese bathymetric chart 6901: *Geol. Soc. America Bull.*, vol. 65, p. 1199–1224.

Emery, K. O., Y. Hayashi, T.W.C. Hilde, K. Kobayashi, J. H. Koo, C. Y. Meng, H. Niino, J. H. Osterhagen, L. M. Reynolds, J. M. Wageman, C. S. Wang, and S. J. Yang, 1969, Geological structure and some water characteristics of the East China Sea and the Yellow Sea: United Nations ECAFE, *CCOP Tech. Bull.*, vol. 2, p. 3–43.

———, and Hiroshi Niino, 1963, Sediments of the Gulf of Thailand and adjacent continental shelf: *Geol. Soc. America Bull.*, vol. 74, p. 541–554.

———, Elazar Uchupi, John Sunderland, H. L. Uktolseja, and E. M. Young, 1972, Geological structure and some water characteristics of the Java Sea and adjacent continental shelf: United Nations ECAFE, *CCOP Tech. Bull.*, vol. 6.

Fitch, T. J., 1970, Earthquake mechanisms and island arc tectonics in the Indonesian-Philippine region: *Seismol. Soc. America Bull.*, vol. 60, p. 565–591.

Geological Survey Division, 1963, Geological Map of the Philippines: Bureau of Mines, Manila, scale 1:1,000,000, 8 sheets.

Gervasio, F. C., 1966, A study of the tectonics of the Philippine Archipelago: *The Philippine Geologist*, vol. 20, no. 2, p. 51–75.

———, 1968, Age and nature of orogenesis of the Philippines: United Nations ECAFE *CCOP Tech. Bull.*, vol. 1, p. 113–128.

Gutenberg, B., and C. F. Richter, 1949, Seismicity of the Earth and Associated Phenomena: Princeton Univ. Press, Princeton, N. J., 310 pp.

Hashimoto, Wataru, Kazuhiro Taira, Kenji Kurihara, Toyoji Imai, and Yasuhiko Makino, 1970, Studies on the younger Cenozoic deposits in Taiwan (Formosa): Part I. The younger Cenozoic deposits of the middle part of west Taiwan: *Geol. and Palaeontology of Southeast Asia*, vol. 8, p. 237–252.

Hayes, D. E., and W. J. Ludwig, 1967, The Manila Trench and West Luzon Trough—II. Gravity and magnetics measurements: *Deep-Sea Research*, vol. 14, p. 545–560.

Heezen, B. C., and Marie Tharp, 1971, Physiographic Diagram of the Western Pacific Ocean: Geol. Soc. America.

Hsieh, S. H., and C. C. Hu, 1971, Gravimetric and magnetic studies of Taiwan: *Sino-American Science Cooperation Colloquium on Ocean Resources*, vol. 1, Marine geology and geophysics, Taipei, Taiwan, p. 87–145.

Huang, Tunyow, 1967, Foraminiferal study of the Tungliang well TL-1 of the Penghu Islands: *Petroleum Geol. of Taiwan*, vol. 5, p. 131–149.

Humphrey, Wilson, 1970, Petroleum developments in Far East in 1969: *Am. Assoc. Petroleum Geologists Bull.*, vol. 54, p. 1551–1566.

———, 1971, Petroleum developments in Far East in 1971: *Am. Assoc. Petroleum Geologists Bull.*, vol. 55.

Irving, E. M., 1951, Submarine morphology of the Philippine archipelago and its geologic significance: *Philipp. Jour. Science*, vol. 80, p. 55–88.

Isacks, Bryan, Jack Oliver, and L. R. Sykes, 1968, Seismology and the new global tectonics: *Jour. Geophys. Research*, vol. 73, p. 5855–5899.

Juan, V. C., and Y. Wang, 1971, Taiwan in relation with the tectonic framework of the western Pacific: *Sino-American Science Cooperation Colloquium on Ocean Resources*, vol. 1, Marine geology and geophysics, Taipei, Taiwan, p. 241–263.

Katsumata, M., and L. R. Sykes, 1969, Seismicity and tectonics of the Western Pacific: Izu—Mariana—Caroline and Ryukyu—Taiwan regions: *Jour. Geophys. Research*, vol. 74, p. 5923–5948.

Le Pichon, Xavier, 1968, Sea-floor spreading and continental drift: *Jour. Geophys. Research*, vol. 73, p. 3661–3697.

Ludwig, W. J., 1970, The Manila Trench and West Luzon Trough—III. Seismic-refraction measurements: *Deep-Sea Research*, vol. 17, p. 553–571.

————, D. E. Hayes, and J. I. Ewing, 1967, The Manila Trench and West Luzon Trough—I. Bathymetry and sediment distribution: *Deep-Sea Research*, vol. 14, p. 533–544.

May, M., R. A. Wehnau, K. Griffiths, and A. Most, 1969, Marine geological survey program 65–67, Western North Pacific Ocean and South China Sea; Area 15, vol. 7—Ship operations, measurements at sea and data analysis procedures: Alpine Geophys. Assoc., Inc., Norwood, N. J., 98 p. (multilithed).

Meng, Chao-Yi, and S.S.L. Chang, 1971, The geologic structure of Taiwan: *Sino-American Science Cooperation Colloquium on Ocean Resources*, vol. 1, Marine Geology and geophysics, Taipei, Taiwan, p. 189–239.

Meyerhoff, A. A., 1970, Developments in Mainland China, 1949–1968: *Am. Assoc. Petroleum Geologists Bull.*, vol. 54, p. 1567–1580.

Morgan, W. J., 1968, Rises, trenches, great faults, and crustal blocks: *Jour. Geophys. Research*, vol. 73, p. 1959–1982.

Niino, Hiroshi, and K. O. Emery, 1961, Sediments of shallow portions of East China Sea and South China Sea: *Geol. Soc. America Bull.*, vol. 72, p. 731–762.

Oliver, Jack, 1970, Structure and evolution of the mobile seismic belts: *Phys. Earth Planet Interiors*, vol. 2, p. 350–362.

Pan, Y. S., 1967, The regional gravity of the Penghu Islands, Taiwan, China: *Petroleum Geol. of Taiwan*, vol. 5, p. 117–129.

Parke, M. L., Jr., K. O. Emery, Raymond Szymankiewicz, and L. M. Reynolds, 1971, Structural framework of continental margin in South China Sea: *Am. Assoc. Petroleum Geologists Bull.*, vol. 55, p. 723–751.

Rodolfo, K. S., 1969, Bathymetry and marine geology of the Andaman Basin, and tectonic implications for Southeast Asia: *Geol. Soc. America Bull.*, vol. 80, p. 1203–1230.

Todd, D. F., and A. Pulunggono, 1971, Wildcatters score in Indonesia: *Oil and Gas Jour.*, vol. 69, no. 24, p. 105–110.

U.S. Naval Oceanographic Office, 1967, Sailing Directions for the Western Shores of South China Sea—Singapore Strait to Hong Kong, revised edition: H. O. Pub. 93, U.S. Govt. Printing Office, Washington, D. C.

van Bemmelen, R. W., 1949, The Geology of Indonesia: The Hague, Martinus Nijhoff, 2. v.

Wageman, J. M., T.W.C. Hilde, and K. O. Emery, 1970, Structural framework of East China Sea and Yellow Sea: *Am. Assoc. Petroleum Geologists Bull.*, vol. 54, p. 1611–1643.

Yen, T. P., 1971, Geology of Taiwan—A review especially on stratigraphy: *Sino-American Science Cooperation Colloquium on Ocean Resources*, vol. 1, Marine geology and geophysics, Taipei, Taiwan, p. 1–24.

VII. AEROMAGNETIC SURVEY OF THE PALAWAN-SULU OFFSHORE AREA OF THE PHILIPPINES

(Project CCOP-1/PH. 1)

By

W. Bosum[1], J. C. Fernandez[2], E. G. Kind[1] and C. F. Teodoro[2]

(with figures VII-1 to VII-9)[3]

ABSTRACT

An aeromagnetic survey of the Palawan-Sulu offshore areas in the southwestern part of the Philippine archipelago was conducted in the period 7 June to 3 July 1969 through the medium of Project MAGNET of the U.S. Naval Oceanographic Office as a contribution to the survey projects of the work programme of CCOP. A meta-stable helium magnetometer mounted in a C-54 aircraft was used and about 21,000 line-km of traverses were flown at an altitude of about 1,000 feet and at a spacing of about 8 km, covering an area of about 136,000 sq km. Compilation and processing of the data was done at the Geomagnetics Division of the U.S. Naval Oceanographic Office and total magnetic intensity contour charts of the area were prepared there.

The geologic interpretation of the total magnetic intensity charts was made at the Bundesanstalt für Bodenforschung, Hannover, Federal Republic of Germany, from December 1970 to May 1971 by geophysicists of that organization with the assistance of two geophysicists from the Philippine Bureau of Mines.

Two quantitative methods of mathematical analysis of the magnetic anomalies were used. For anomalies where the sources could be considered as due to isolated bodies located near the surface, the two-dimensional method of mathematical analysis was applied, whereas for the areas of smooth magnetic field, the sources of which could be considered as being a magnetized layer, the method of harmonic analysis based on two-dimensional finite Fourier series was used to calculate the relief of the magnetic basement.

In the offshore area of northern Palawan there are two magnetic horizons, the shallower one ranging in depth from 1 to 3 km, possibly plunging towards the northeast, and the deeper horizon at an average depth of 9 km. In the offshore area of southern Palawan the magnetic basement ranges in depth from 5 to 11 km, the deepest portion being in the southeastern part of the area surveyed.

1: Bundesanstalt für Bodenforschung, 3 Hannover-Buchholz, Federal Republic of Germany.
2: Bureau of Mines, Manila, Philippines.
3: Figure VII-3. in envelop on back cover.

INTRODUCTION

The need to locate and exploit local resources of petroleum in the Philippines to reduce expenditures on imports has encouraged the government and both local and foreign private companies to intensify efforts to locate geologically favourable areas. The marine shelves of the Palawan-Sulu region, in the southwestern part of the Philippine archipelago, is considered to be one of the most promising areas partly because of its proximity to the oil producing regions of Brunei and northern Borneo. It was therefore one of the areas selected for aeromagnetic survey to determine the thickness of sedimentary rocks over the magnetic basement and to obtain data regarding the geologic structure of the region relevant to the occurrence of petroleum.

The area covered by the aeromagnetic survey is situated between latitudes 6°30′N and 12°30′N and longitudes 116°00′E and 122°00′E. It is bounded on the west side by the South China Sea and to the east by the Sulu Sea, and it extends from northern Borneo in the south to Mindoro Island in the north (Fig. VII-1).

The field operations were conducted in mid-1969 as a contribution of the United States Government, through the medium of the "Project MAGNET" programme of the U.S. Naval Oceanographic Office, towards assisting the member countries of CCOP in the exploration of their offshore mineral resources. The survey was included as project CCOP-1/PH. 1 in the work programme of CCOP and scientists from the Philippine Bureau of Mines participated in all phases of the work during the survey operations.

The data compilation and reduction was done at the U. S. Naval Oceanographic Office, Washington, D. C., from which a total magnetic intensity map of the area was produced. The mathematical analysis and interpretation of the magnetic anomalies shown on the total magnetic intensity map were carried out with the use of modern computer techniques by the German Geological Survey (Bundesanstalt für Bodenforschung) at Hannover, Federal Republic of Germany, in co-operation with scientists of the Philippine Bureau of Mines; this co-operation was made possible through fellowships provided by the Government of the Federal Republic of Germany under the sponsorship of the Federal Minister of Economic Co-operation.

GENERAL GEOLOGY

The Palawan-Sulu Island Group covered by the aeromagnetic survey is tectonically a possible extension from northern Borneo of Molengraaf's "Sundaland" (Corby, 1951). The islands follow a SW–NE trend from the Balabac Islands and extend for about 630 kilometres northeastward to the Busuanga Islands. Palawan Island is the largest of these, with a length of 425 km and an average width of 30 km. The bathymetric contours follow almost the same trend as the main island, particularly on the western side (Fig. VII-1).

The geomorphology of Palawan reflects the varied and complex character of the underlying rocks; most of the mountain ranges are relatively narrow and sharp-crested

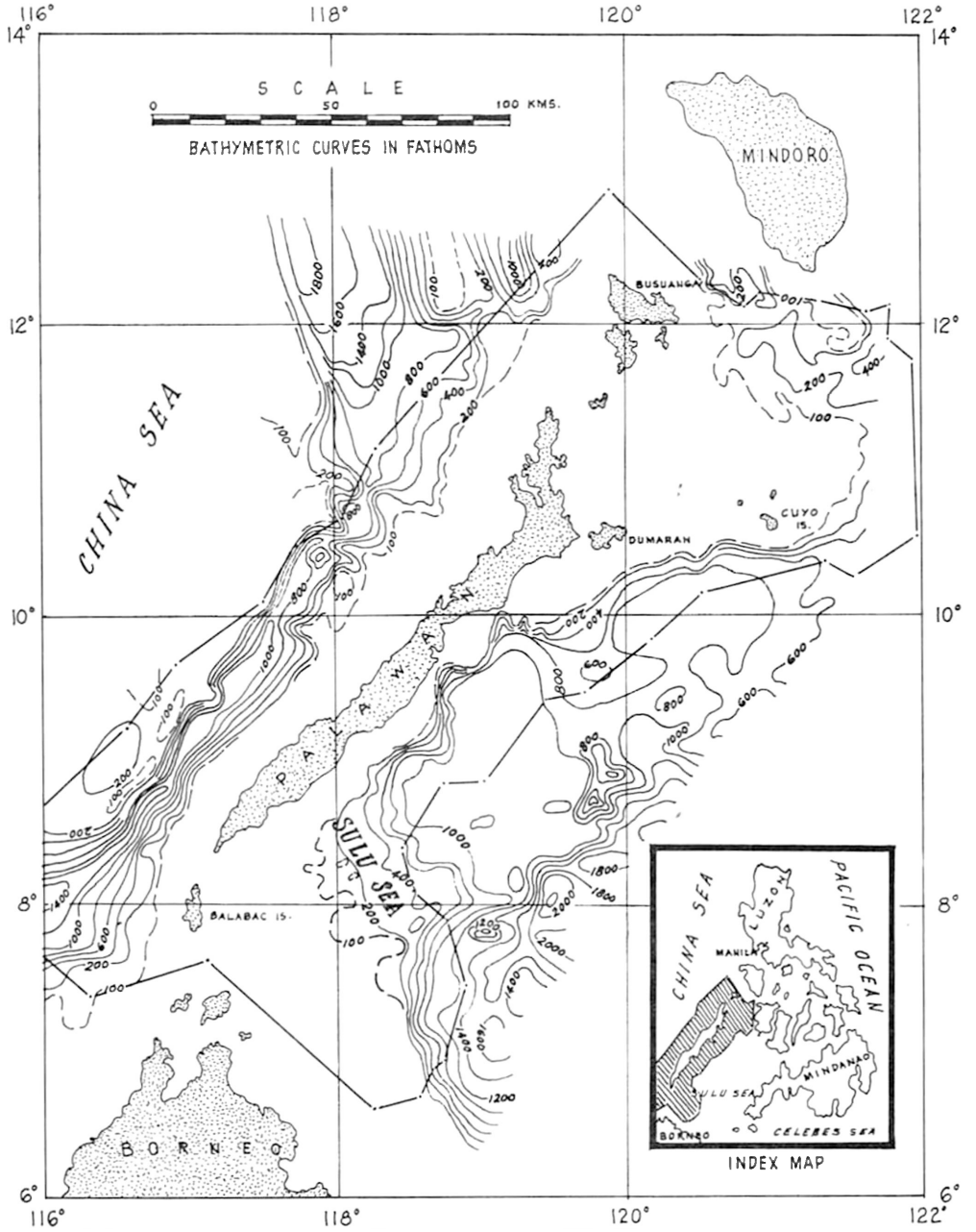

Figure VII-1. Map of Palawan-Sulu offshore region of the Philippines showing the area covered by aeromagnetic survey.

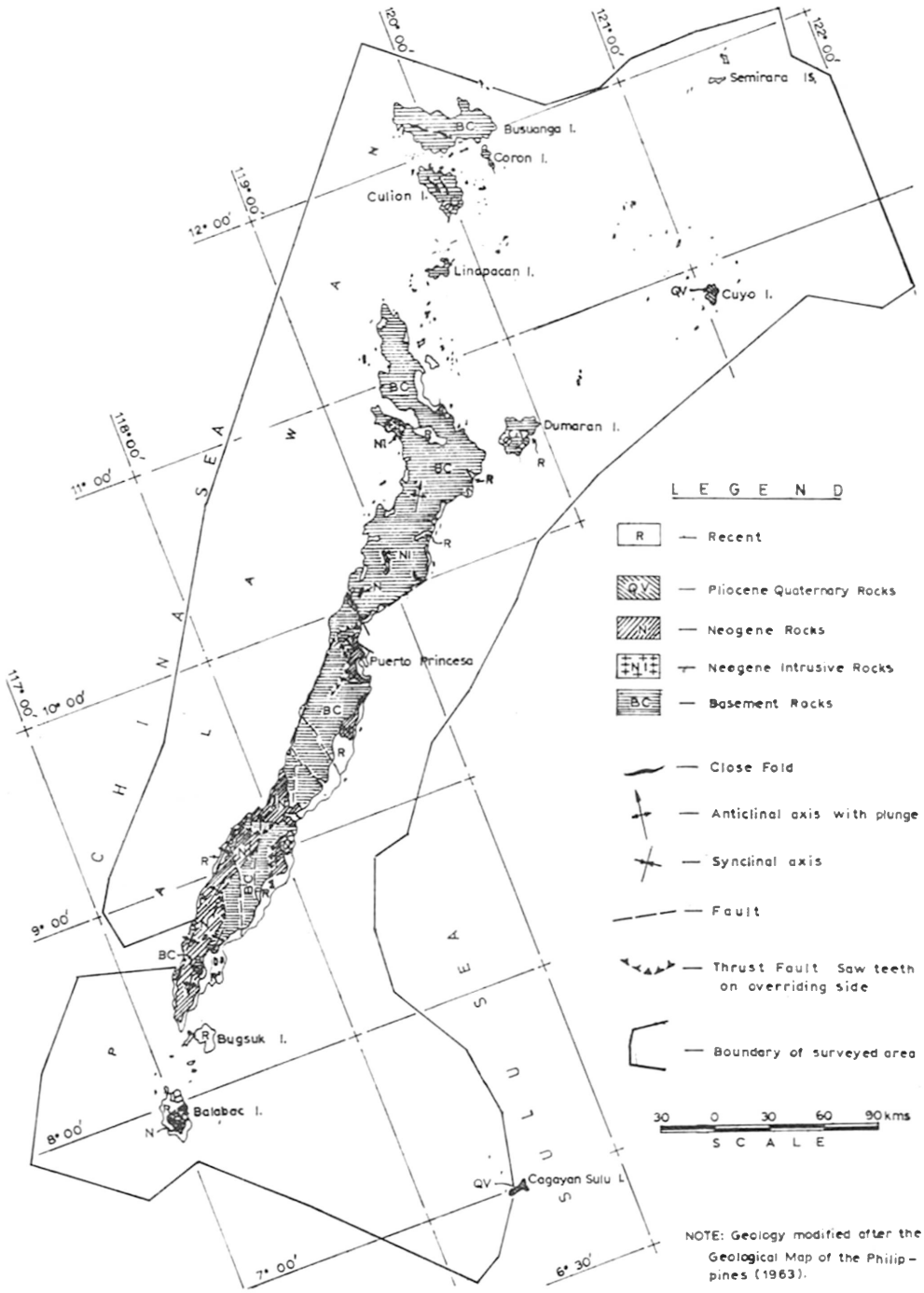

Figure VII-2. Geologic map of Palawan Island, Philippines.

and sometimes show serrate features. Cleopatra's Needle is the highest landmark in the area, reaching to an elevation of 1,593 metres above sea level. Narrow stretches of alluvial plains are present only along parts of the shorelines and in some river valleys. The presence of several hundreds of islands in the northern and southern parts of the region suggests that submergence of the shelf probably took place recently.

The area has a geological setting different from that of other parts of the Philippines (Fig. VII-2). Irving (1950) considered this southwestern region as being the outer portion of the pre-Tertiary and early Tertiary Sundaland, where most of the lithologic units exposed (Fitch, 1963) have greater affinities to those of western Borneo than to other parts of the Philippines.

The oldest rocks in the region, referred to as "basement", are tentatively dated as pre-Jurassic; they consist mainly of slate, green schist, piedmontite schist, schistose quartzite and phyllites in the southern half (Belandres, 1964), and undifferentiated amphibolite, quartzo-feldspathic and mica schist in the area north of Puerto Princesa. Farther north, including the Busuanga Islands, the predominant rocks are of early geosynclinal type, consisting of arkosic sandstone, slate, graywacke, ferruginous shale and a chert-basalt sequence, ranging in age from Jurassic to Cretaceous; these rock assemblages, mostly unmetamorphosed, were deposited unconformably over the metamorphic complex comprising the basement in a sinking trough during late Mesozoic times. Spilitic basalts with associated chert are exposed fairly extensively in southern Palawan and Balabac Island (John, 1963) while other basic volcanic flows are intercalated with the greywackes. The tectonism that followed deposition produced fractures which served as channels for the emplacement of the igneous rock complex; these rocks, consisting of pyroxene peridotites, gabbros, diabases and diorites, generally occur along the basement belts.

The southern half of Palawan, particularly the southwestern coastal areas, are mostly blanketed by Tertiary mio-geosynclinal sedimentary rocks unconformably deposited over the older rocks. The sedimentary rocks consist largely of transgressive, mixed marine shelf deposits of wackes, shale and reef limestone, with some conglomerates and agglomerates. However, these types of sediments are notably absent northwards from Puerto Princesa.

The northeastern part of the area covered by the survey consists of a broad shelf with a number of scattered islands consisting essentially of pyroxene andesites with associated olivine basalts. The volcanic outflows in this area, specifically in the vicinity of the Cuyo Islands, took place at the end of the main orogeny in the miogeosynclinal regions, possibly during Quaternary times. Recent alluvial deposits and elevated coral reefs are widespread along the beaches and islets, respectively, while extensive coral reefs are developed on the shelf area of the Sulu Sea.

This area as a whole appears to be a portion of the Philippine stable region (Gervasio, 1966) and the grain of the structures of the Mesozoic and Tertiary rocks appears to be similar to those of northern Borneo (Fitch, 1961). The northwest Borneo geosyncline (Liechti, 1950) appears to have a possible extension in the Palawan-Sulu area (Gervasio, 1966). Generally, however, thrust faults define the boundaries between the early and mio-geosynclinal sediments and the basement rocks. On the other hand, high-angle normal faults trending between north-south and NE–SW, and probably with

some horizontal displacement, are common along the shorelines and across the island of Palawan. Close folding and overturned beds are common in both the Tertiary sediments in the south and in some of the Jurassic rocks in the north; the intensity of folding, however, is usually greater in the Tertiary sediments.

SURVEY OPERATIONS AND DATA REDUCTION

The survey operations in the Palawan-Sulu offshore areas were carried out from 7 June to 3 July 1969 with the C-54 aircraft "KIWI", assigned to Project MAGNET of the U.S. Naval Oceanographic Office. The survey covered an area of about 136,000 sq km and about 21,000 line-km of magnetic data were obtained along traverses flown NW to SE at an altitude of 1,000 feet above sea level and at a spacing not exceeding 8 km.

Measurements of the total magnetic intensity were obtained from a metastable helium magnetometer with the magnetometer sensor towed about 200 feet below the aircraft. A Vector Magnetometer (fluxgate type) installed within the aircraft served as a back-up unit. All measurements were recorded in analogue charts and digital tapes.

The measured geomagnetic elements at the Muntinlupa Observatory of the Philippine Coast and Geodetic Survey during the survey period were used in the determination of the temporal variations in the total magnetic intensity. It was also used in the determination of the mean value of the total magnetic field for the ground station. The Muntinlupa Observatory is located about 250 km north of the northern boundary of the area surveyed. Any deviations of the calculated total magnetic intensity at Muntinlupa from the established mean value were removed from the track data to reduce all survey values to a common datum level. From these data, total magnetic intensity charts were prepared, with contours at intervals of 20 gammas (Fig. VII-3).

INTERPRETATION METHODS

The interpretation method selected for the mathematical analysis of the magnetic intensity contour charts depended upon the size, shape and characteristics of the magnetic anomalies.

Isolated magnetic anomalies chiefly caused by sources near the surface were interpreted by assuming two-dimensional and three-dimensional model bodies. In the two-dimensional analysis method, the causative body is assumed to extend infinitely along the strike direction. Initially, the magnetic values are taken from profiles normal to the strike of the anomalies; consequently, appropriate two-dimensional model bodies (such as circular cylinder, infinite and finite thin plates, broad dike and steps) are assumed and their theoretical magnetic values were computed and compared with the measured anomaly. The process is repeated until the observed and computed theoretical values of the magnetic profile show the best fit. The form of the model body is varied after each comparison (Bosum, 1965).

To facilitate the iteration method described above, a computer programme was

prepared based on the method of least squares (Bosum, 1968). If further details such as plunge, displacement of the body, etc., are required or if the two-dimensional interpretation based on the shape of the magnetic anomaly is not satisfactory, a three-dimensional body is constructed, its field computed and thereafter it is approximated to the measured anomaly. A computer programme was prepared for a body of arbitrary magnetization bordered by planes (Kind, 1964).

In areas of smooth magnetic field the harmonic analysis method based on two-dimensional finite Fourier series was used to calculate the relief of the magnetized layer (Hahn, 1965). The only parameters which entered into the calculation are the mean depth and the contrast of magnetization at the relief plane which, in general, is equal to the magnetization of the lower layer, and the resulting relief represents a model of the pre-given field completely. With this method the product of relief amplitude and magnetization contrast is practically constant; for example, if the magnetization contrast is 200 γ a relief amplitude of 3 km is calculated, whereas a magnetization contrast of 100 γ would involve a relief amplitude of 6 km.

RESULTS OF INTERPRETATION

Fig. VII-6 shows two-dimensional model bodies of anomalies in Central Palawan. Fig. VII-5 shows the relief of magnetic basement in the southern Palawan offshore region and Figs. VII-7 and 8 the relief of the deeper and shallower magnetic horizons, respectively, in the northern Palawan offshore area, while Fig. VII-9 shows the structural features of the whole area as interpreted from the magnetic data.

A homogeneous magnetization has been assumed, parallel to the earth's magnetic field (inclination I = 5°), for an analysis of the iso-anomalies above different model bodies to obtain a first qualitative interpretation, and several theoretical curves have been represented above the two-dimensional model bodies, as shown in Fig. VII-4.

Fig. VII-4A shows the ΔT-anomalies above a dike at different angles of dip (0°, 45° N, 90°, 45° S). The model with a dip of 0° actually represents a step of a magnetic sheet which, in one case, is situated south of the body and, in the other case, to the north of it. The relation between the maximum and minimum values of the magnetic anomaly is altered as the angle of dip of the dike changes; a south-maximum indicates a north-dipping body and a north-maximum a south-dipping body. Generally, the minimum value is stronger than the maximum.

Fig. VII-4B, the anomaly of a circular cylinder, shows a strong minimum above the cylinder accompanied by a weak maximum in the south. Geologically, this mathematical model implies a body of which its extensions are small compared to its depth; it could, for instance, be a dike-like body of small extension as indicated in the figure by hatchings.

In the case of strong positive anomalies, an anomalous magnetization direction must be expected. Furthermore, it should be kept in mind that because of the wide flight spacing the anomalies of shallow bodies are not fully represented, and the calculated depth values for them are not very significant.

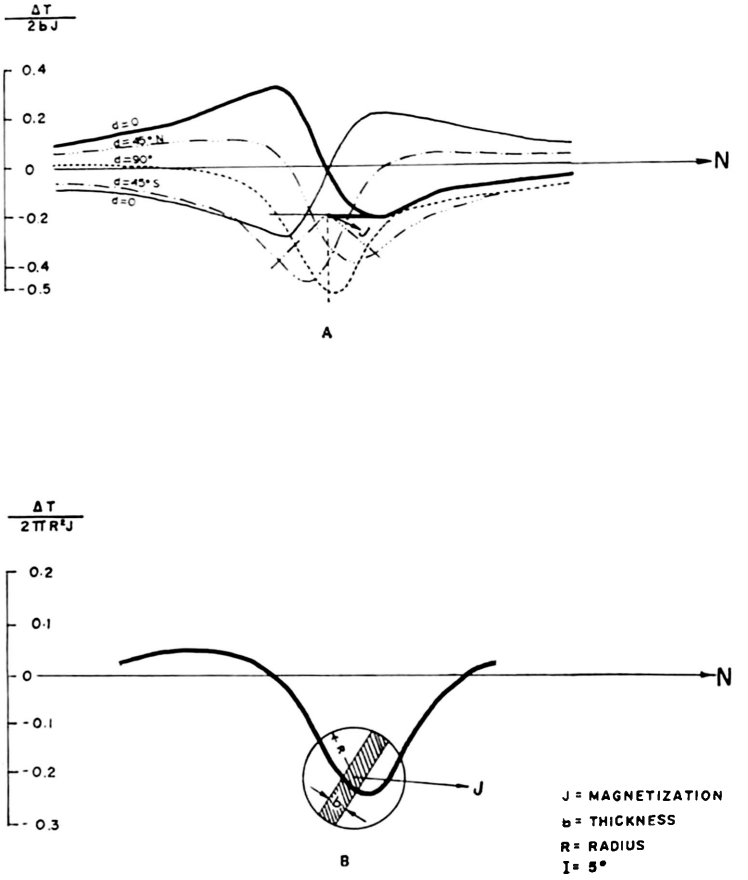

Figure VII-4. Theoretical magnetic profiles for ΔT-anomalies above (A) two-dimensional thin dike-like bodies of different dip, and (B) a circular cylinder.

DISCUSSION OF RESULTS AND INTERPRETATION

An analysis of the iso-anomaly map (Fig. VII-3) suggests that the area surveyed can be divided into four regions: (1) the southern offshore region of the Palawan-Sulu area; (2) the central Palawan offshore region; (3) the northern Palawan offshore region; and (4) the Cuyo Island region.

The southern offshore region of the Palawan-Sulu area

This area comprises the entire region south of Line 1 (Fig. VII-3). The area in the vicinity of Line 1 follows a magnetic lineament indicated by a pronounced magnetic anomaly trending nearly east-west.

The area is characterized generally by broad, smooth anomalies except in two localities where strong, narrow anomalies are evident. One of these localities, rectan-

gular in shape, is situated east of Balabac Island. The northwest and the southeast boundaries of the anomalies are indicated by straight patterns of the isogamma lines, possibly indicating faults; the southwest and northeast boundaries are more pronounced and they can be traced over longer distances. The structure in the northwestern part extends north to San Antonio Bay and its extension can be observed on land.

The anomalies are caused by relatively shallow bodies and, by two-dimensional interpretation, a maximum depth of about 3 km below sea level was obtained. It is probable that the bodies causing these anomalies are volcanic and ultrabasic rocks similar to those exposed on Balabac and the Cagayan-Sulu islands.

The other anomalous area is over San Antonio Bay, but the extension of the anomalies inland was not measured. However, it is assumed that these anomalies indicate the extension of the volcanic and ultrabasic rocks exposed on the island towards the sea at a relatively shallow depth. Some narrow elongated anomalies confirm the presence of faults which controlled the intrusion of the igneous rocks.

A calculation of the relief of the magnetic basement, using an assumed magnetization of 250γ, is presented in Fig. VII-5. In the magnetically disturbed areas of Balabac Island and San Antonio Bay, filtering was applied to remove the surface effects of shallow bodies. As a result of the influence of the magnetically disturbed field over these areas, there is a gap and it is not possible to connect the relief of the southeastern and the western part.

Southeast of the area, the existence of a sequence of parallel swells and troughs of the magnetic horizon is indicated, which have a general NW–SE trend. These structures can be traced over long distances, sometimes more than 100 km, and the depths of the swells range from 8 to 10 km, while those of the troughs extend to 11 km. About 40 km northwest of Cagayan-Sulu Island they are apparently displaced by a lineament trending NE–SW (Fig. VII-9). The position of Cagayan-Sulu Island may be related to the long swell with a doubly plunging central section present on the northwest portion of the island. The anomaly in the southeastern end of the area surveyed is possibly due to the presence of basaltic rocks underlying the island.

The Fourier analysis shows that the magnetic horizon becomes shallower towards the northwestern part of the region; the higher parts are at a depth of about 5 km, while the bottoms of the troughs lie between 7 and 9 km below sea level. Although a gap exists between the southeastern and the northwestern sectors, it appears that the structures continue farther to northwest. In the southern part, these structures can be followed nearly continuously from southeast to northwest (Fig. VII-9), but most of the NW–SE structures immediately to the north either abut or terminate on the two strong parallel lineaments trending NE–SW; these lineaments, about 60 km apart, form the west and east boundaries of the magnetically disturbed Balabac Island area. Apparently, the lineament on the northwest is an extension of the faults of the same trend observed in southern Palawan and Balabac Islands and, locally, it coincides with a magnetic basement trough.

The northern part of region 1 is notably different from the southern part in that the relief of the magnetic horizon is smooth. The shallowest section given by Fourier analysis amounts to 5 km, while the deepest part is about 7 km. The structural elements trend predominantly N–S and are apparently the extensions of faults known on land;

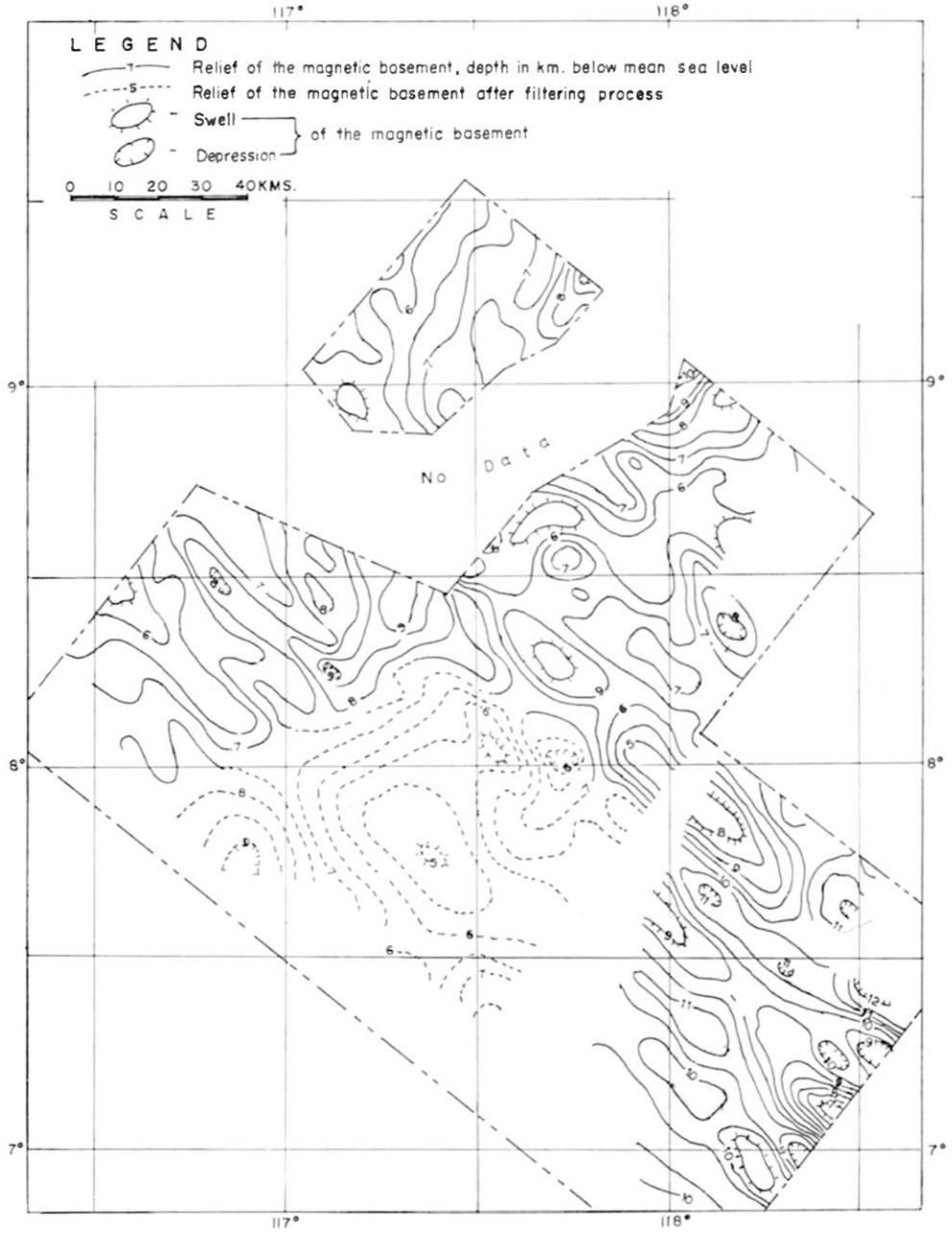

Figure VII-5. The relief of the magnetic basement (J = 250w) in the offshore area around the southern part of Palawan Island, Philippines.

however, there is no striking relation of these structural elements to those in the south. This suggests that a fault zone or geanticlinal ridge separates the north and south areas in the southern tip of Palawan Island.

The central Palawan offshore region

This area lies between Lines 1 and 2 (Fig. VII-3) and, except in its northwestern part, it is intensely magnetically disturbed. The boundaries between the areas of the rugged and smooth magnetic fields are straight lines which probably represent faults (Fig. VII-9).

In the immediate vicinity of the shoreline, the anomalies are narrow, closely spaced, with relatively high peak values, and they trend generally NE–SW. In some cases, however, as verified by other surveys with closer flight spacings, a few of the anomalies trend almost east-west. Generally, the character of these anomalies is a positive indication of shallow sources of highly magnetic rocks; taking into account the geology of the adjoining land, where most of the lithologic units exposed are ultrabasic and volcanic rocks, it is evident that the magnetic anomalies indicate seaward extensions of these magnetic rocks. The depth of the magnetic sources ranges between 0.7 and 2.2 km below sea level for dike-like bodies (Fig. VII-6).

The magnetic contours have a pronounced linear pattern and, although minor east-west lineaments are indicated in a few places in this particular area, the prevalent general trend of the lineaments varies from N–S to NNE–SSW. The structures indicated by the magnetic data are mostly discontinuous, similar to the faults mapped on land, but they are apparently all of the same trend. The extension and limits of the faults cutting the narrow section of Palawan Island at Puerto Princesa are indicated in the adjoining offshore area by the magnetic data.

In the westernmost sector of the region the magnetic data suggest conditions characteristic of deep magnetic basement and it appears to be similar in all aspects to the adjacent regions to the north and south. Because of its limited areal extent, no calculation of the magnetic basement relief could be made; however, by analogy, it is presumed that the basement depth approaches that of the adjacent areas to the north and south, and is probably in the order of 10 km.

In the eastern part of this region there are comparatively strong anomalies and the top of the magnetic body is at a depth of 4 km (Fig. VII-6). As this depth is greater than that in the west, it is inferred that this area is down-thrown in relation to the western side. The boundary is marked by the lineament trending NNE–SSW immediately east of Puerto Princesa, along which the movement may have taken place. Furthermore, the distortions of the anomalies predominantly in the N–S direction are possibly expressions of faults (Figs. VII-3 and 9).

The northern Palawan offshore region

This region covers the northern part of the area surveyed, except for a magnetically strongly disturbed area in the southwest (Fig. VII-3).

The features of the magnetic field in parts of this region show significant differences in the character of the magnetic contours. The portion south of Dumaran Island has broad, strong anomalies; the northwestern part has a smooth magnetic field and anoma-

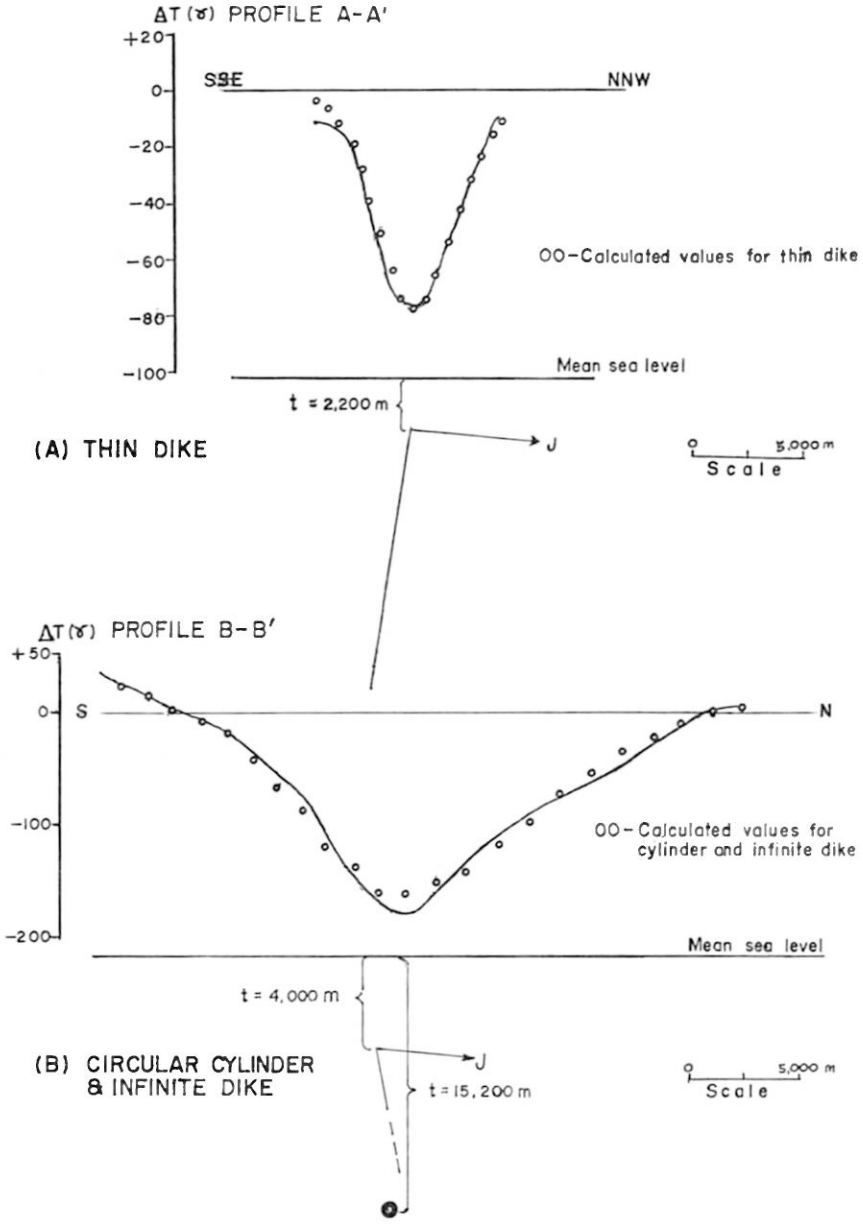

Figure VII-6. Profiles A-A' and B-B' showing two-dimensional model studies of anomalies in the offshore area around the central part of Palawan Island, Philippines.

lies of low amplitude; and the eastern part has a number of isolated narrow anomalies of higher amplitude.

Two magnetic horizons were noted in this region. The shallow layer is at a depth ranging from 1 to 3 km and it has a tendency to plunge towards the northeast; this layer is presumed to correspond to the pre-Jurassic rocks (basement complex) north of Puerto Princesa. The deeper layer is at an average depth of about 9 km; its identity is clearly shown by the magnetic field in the southern part whereas in the north, it becomes hazy and obscured by the stronger influence of the upper layer. As this layer is at the same order of depth as that interpreted in southern Palawan, it may be assumed that they can be correlated.

The relief of the magnetic horizon of the deeper layer is shown in Fig. VII-7. South of Dumaran Island, a magnetization of 250γ is assumed. A few highs, probably representing the tops of intrusive bodies, are present at a depth of about 5 km below sea level while the depths of the depressions are in the order of 9 to 12 km. The depressions in the case of intra-basement intrusions may have no geologic significance but the overlying materials are probably non-magnetic.

A comparison between the depth of the relief by Fourier analysis and by two-dimensional interpretation of the southernmost anomaly in this area shows a close agreement in the calculated depth values. The depths of 4 km and 5 km based on the two-dimensional model body and the Fourier interpretations, respectively, show fairly close agreement. The discrepancy is caused by the assumed magnetization of 250γ, which seems to be overvalued, but the depth values are within the limits of a reasonable error of interpretation.

In the northeastern part, where the magnetic character is rather different, the initial calculation of the relief using a magnetization of 250γ did not give enough details. The magnetization was therefore reduced to 125γ and this produced a relief capable of interpretation (Fig. VII-7); however, the interpretation of the relief in the northeastern sector, indicated by dashed lines, is not as reliable as that of the southwestern sector, mainly because of the influence of the relatively strong screening effect of the upper magnetic layer. In the northern part of the area the magnetic horizon is characterized by depressions and swells generally trending NW–SE, with minor trends ranging between N–S to NE–SW. The depths of the highest points in the swells are in the order of 7 to 8 km whereas those of the depressions are about 10 km below sea level.

The relief of the magnetic horizon of the upper layer is shown in Fig. VII-8 and the depth of this layer varies from 1 to 4 km. This horizon may be due to the magnetization effect of the pre-Jurassic metamorphic rocks, similar to those exposed on nearby islands. A lower magnetic horizon was also noted but its effect is not clearly separable from that of the shallower magnetic layer. The relief map does not show consistent structural trends but structures showing NW–SE and N–S trends are present in some places. The top of the magnetic body lies at 2 km below sea level in the western part (J = 125γ) whereas, in the eastern part, it ranges from 0.5 to 2 km (J = 150γ) and the depressions in the magnetic horizon are at depths between 3 and 5 km below sea level.

The numerous isolated anomalies shown in the iso-anomaly map probably indicate the presence of magnetic rocks intruded into the pre-Jurassic basement; on this assumption, the upper boundary of the geologic basement would be the interconnection of the

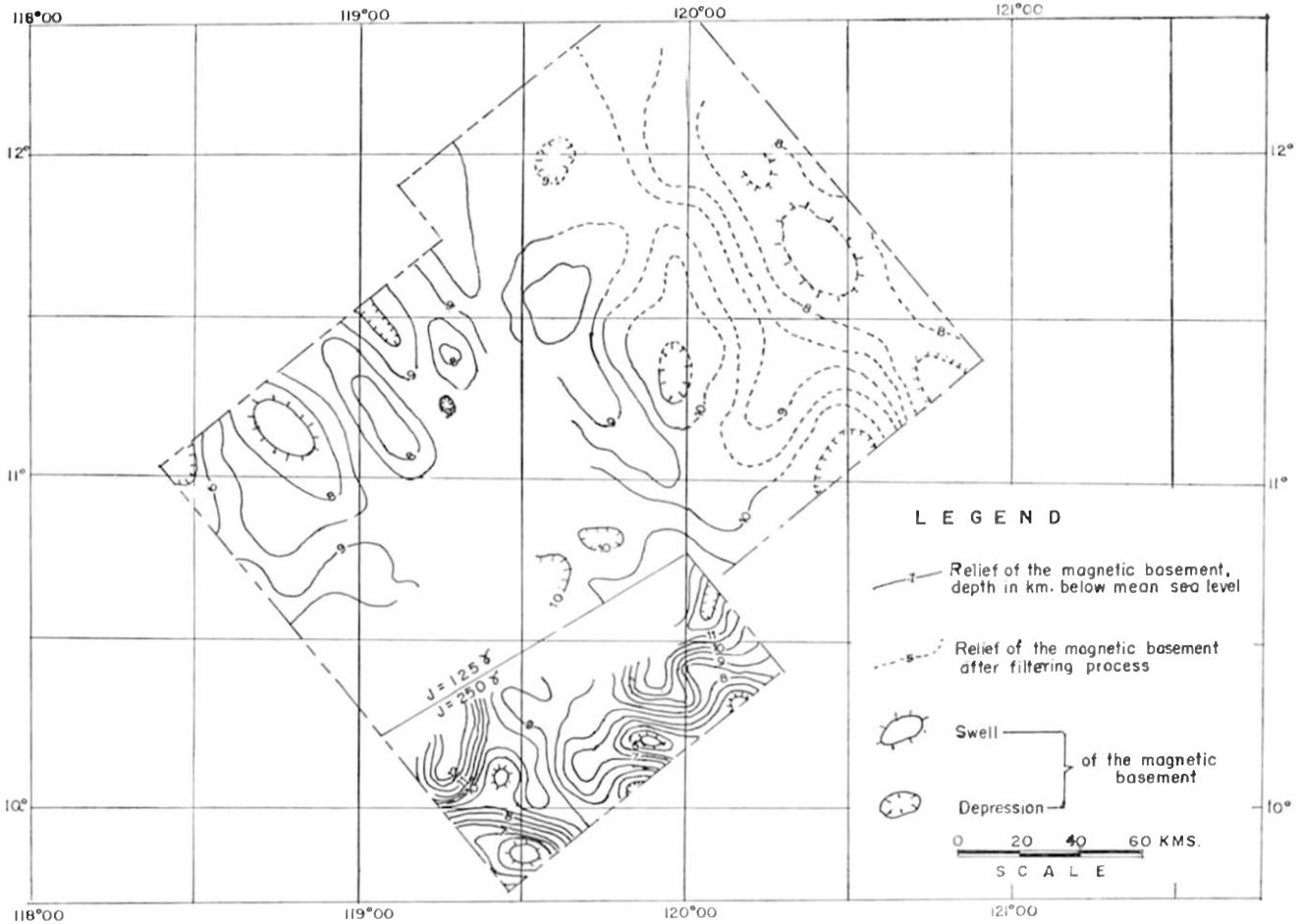

Figure VII-7. The relief of the deeper magnetic horizon in the offshore area around the northern part of Palawan Island, Philippines.

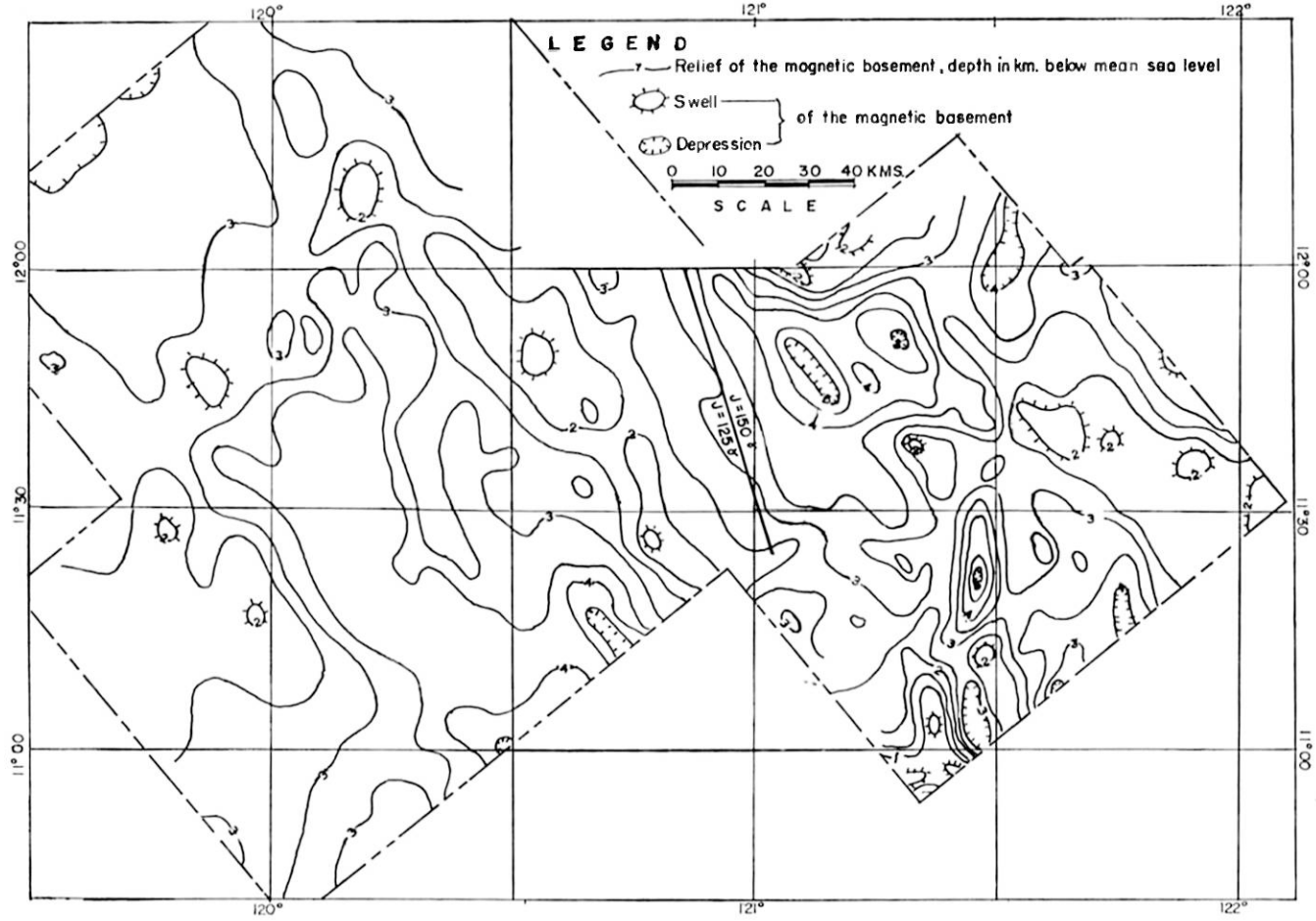

Figure VII-8. The relief of the shallower magnetic horizon in the offshore area around the northern part of Palawan Island, Philippines.

single peaks and this would result in an almost flat basement surface lying at a depth of about 2 km (Fig. VII-8) below sea level.

Based on these assumptions, it can be surmised that the upper layer corresponds with the pre-Jurassic rocks whereas the geologic identity of the lower layer is unknown.

The Cuyo Island region

This region differs magnetically from the adjoining region (3) and is characterized by its strongly disturbed field. The southwestern and northeastern limits are defined by lineaments indicated by the magnetic anomalies (Fig. VII-9) whereas the northwestern limit is an arbitrary line, approximately following the change of magnetic field (Fig. VII-3).

The magnetic contours generally show clusters of positive and negative anomalies with an apparent elongation towards the northeast. Most of the anomalies have steep gradients and high amplitudes, in the order of 200 to 500 γ. Other obvious features of the anomalies are the significant alignment of the narrow negative values and the inherent distortions of the contour lines; they can be interpreted in terms of structural elements as possibly being faults intruded by magnetic rocks. Regionally, two major trends are evident; one set strikes northeast and follows the elongated magnetic minima, whereas the other set strikes northwest and is defined by kinks in the contour lines. The structures trending northeast have longer traces, while the elements trending northwest are relatively shorter and sometimes abut on the former. The peaks of the magnetic bodies, based on two-dimensional dike-like models, are interpreted as being at depths ranging from 0.1 to 2.5 km below sea level.

The results interpreted from the magnetic data agree quite well with the geology of the Cuyo island group, where volcanic rocks (olivine basalt, pyroxene andesite, agglomerate and tuff) are exposed (Ramos and Duna, 1963). It can be concluded therefore, that the strong anomalies in this region are caused by these volcanic rocks; in addition, the iso-anomaly map indicates the existence of relatively shallow volcanic rocks over almost the entire Cuyo Island region.

CONCLUSIONS

The accuracy of the interpretation of the data from the aeromagnetic reconnaissance survey is rather limited because of the wide spacing of the flight traverses. Nevertheless, it has contributed valuable information as to the general distribution of magnetic rocks in the offshore areas of the Palawan-Sulu region and the approximate thickness of the non-magnetic rocks could be determined by mathematical interpretation methods.

The relatively smooth magnetic fields in the west and the south of the area as a whole indicate the presence of a thick section of non-magnetic rocks; calculations of the basement relief by Fourier analysis indicate that the thickness of non-magnetic rocks in these areas ranges from 8 to 11 km. The physical characteristics and composition of the magnetic and non-magnetic rocks in these parts of the area surveyed can only be conjectured; the magnetic horizon may consist mostly of basic rocks, possibly peridotites

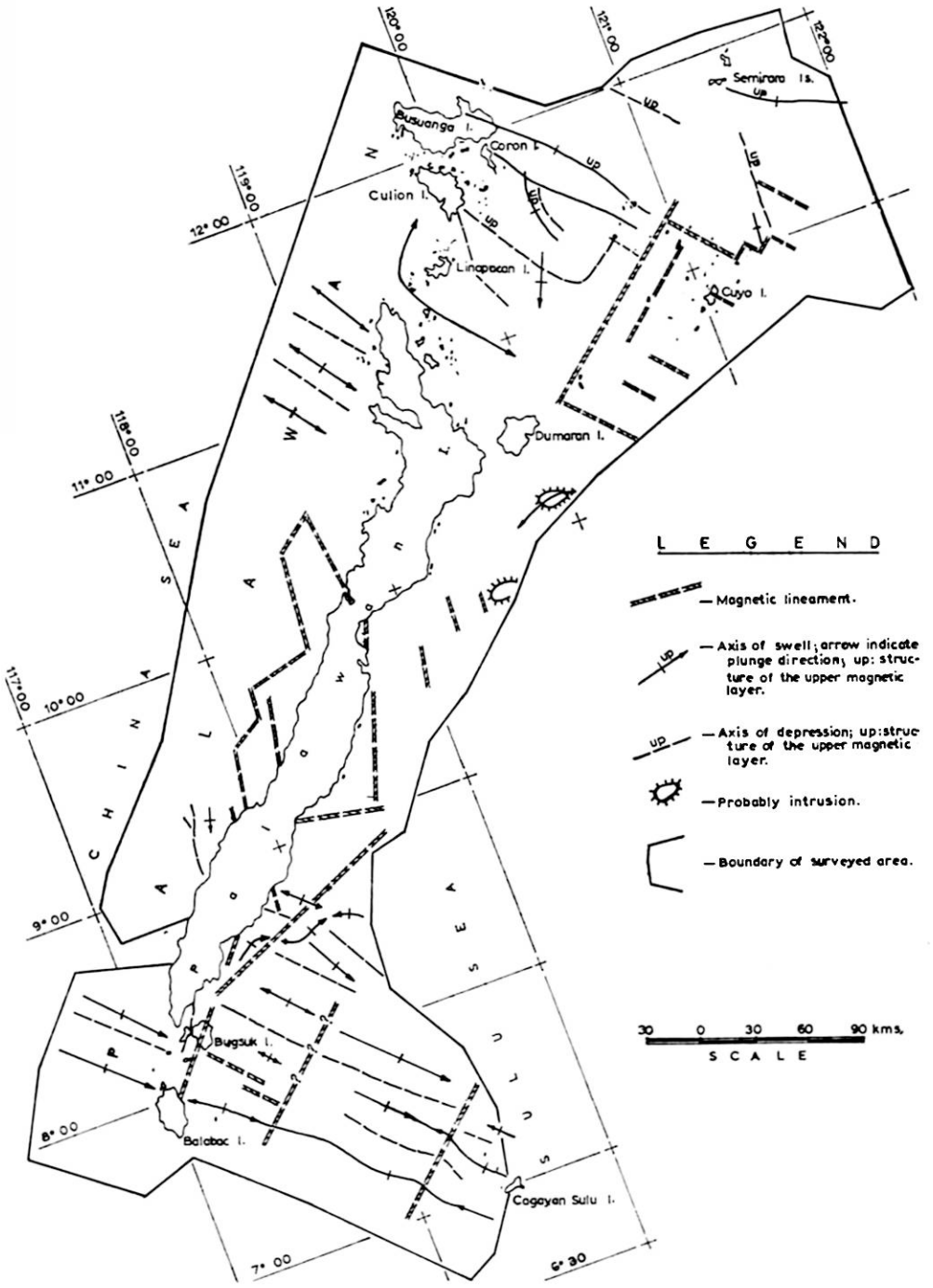

Figure VII-9. Interpretation of the geologic structure of the Palawan-Sulu offshore region of the Philippines based on aeromagnetic data.

and basalts, while the non-magnetic rocks may include lithologic units similar to those of the Jurassic and Tertiary sediments exposed on land.

In the offshore region of northern Palawan the results indicate the presence of two magnetized zones. The upper zone is at an average depth of about 3 km, while the lower horizon is at a depth of about 9 km; it is difficult, however, to detect the lower layer farther northward as it loses its identity because of the stronger shielding effect of the upper magnetic zone in that area, which may correspond to the pre-Jurassic metamorphic rocks.

The topography of the magnetic basement is characterized by asymmetric undulations in the form of swells, depressions and (or) basins. These elements generally trend NW–SE; some of them are relatively wide and can be traced over distances of hundreds of kilometres. In the part of the region where the two magnetic layers are recognized, the structural elements, in a few cases, do not appear to follow the same trend and this may be taken as an indication of the superposition of the two magnetic layers.

The areas of greatly disturbed magnetic fields, with high amplitudes and steep gradients, offshore from central Palawan, the Cuyo island group, and in some isolated places in the southern and northern parts of the area surveyed, are considered to be due to the presence of highly magnetic rocks at relatively shallow depths. From the evidence of the geology of adjoining land areas, the magnetic rocks are probably basic to intermediate igneous rocks such as pyroxene peridotites, basalts, and andesites. A quantitative interpretation of single anomalies using two-dimensional model bodies showed that the depth to the peaks of these magnetic bodies ranges from 0.1 to 2.0 km below sea level; it is possible also that many more of these bodies may be present at depths of less than 2 km, but were not detected because of the wide spacing of the flight traverses.

In the eastern part of the offshore area of central Palawan there is a zone of strong broad anomalies of apparently deep origin. The results of calculation by Fourier analysis and two-dimensional interpretation indicates that these magnetic bodies are at depths in the order of 4 to 5 km; they are interpreted as being intrusives in the basement or in the overlying non-magnetic rocks.

In addition to the structural elements interpreted from the magnetic basement relief, the iso-anomaly map exhibits distinct magnetic configurations representing major lineaments, which could be interpreted as being due to faults. There are two predominant trends, NE–SW and NW–SE, and the traces, extensions, and trends of some of the lineaments interpreted as faults correspond closely with the trends of faults observed on the adjoining land areas. The high amplitudes and great extent of the magnetic minima may be caused by magnetic rocks intruded along the faults. The structural breaks apparently delineate, in most instances, the surface boundaries of the non-magnetic and magnetic rocks.

The results of the aeromagnetic survey have served to locate particular areas which could be favourable targets for oil prospecting. The southern area, and almost the whole of the western area, are blanketed by non-magnetic materials, consisting presumably of sedimentary rocks with thicknesses of up to 11 km, and there are also indications of large and favourable structures. This, however, is only a preliminary interpretation and is subject to certain limitations as the data available at present are insufficient to

draw definite conclusions. Nevertheless, the results have delineated areas where more detailed exploration is warranted to evaluate more thoroughly the potentials for petroleum in those areas; this could take the form of more closely spaced aeromagnetic surveys over areas of interest and, of even more definitive value, the undertaking of continuous seismic profiling. Furthermore, the present survey has provided data of value for correlation with the adjoining petroleum producing areas of northern Borneo.

ACKNOWLEDGMENTS

The writers wish to thank the officers and crew of the "KIWI" and the scientists and engineers of Project MAGNET, U. S. Naval Oceanographic Office, who conducted the field operations and compiled the total magnetic intensity map. Their sincere gratitude is extended to Mr. Fernando S. Busuego, Jr., Director of the Bureau of Mines, Manila, and Mr. H. P. Stockard of the U. S. Naval Oceanographic Office, for their support and encouragement; to Prof. Dr. H. Closs of the Bundesanstalt für Bodenforschung, and the Minister of Economic Co-operation of the Federal Republic of Germany, who made possible the trip to Hannover of the Philippine scientists for collaboration in the interpretation. Special mention is due to Mr. H. Geipel who prepared the data cards for the computer work. The writers are also indebted to the Deutsches Rechenzentrum at Darmstadt and the Technische Universität, Hannover, where all calculations were carried out.

REFERENCES

Belandres, C., 1964, Notes on the geology of Palawan, south of Puerto Princesa: Unpublished report, Bureau of Mines, Manila.

Bosum, W., 1968, Ein automatisches verfahren zur interpretation der methoden der kleinsten quadrate: *Geophys. Prospecting*, vol. XVI, no. 1, p. 107–176.

Bosum, W., 1965, Diagrams for the computation of magnetic field components for their transformation into one another for their upward confirmation (two-dimensional case): *Z. Geophys., Würzburg*, vol. 32 (1966), no. 1, p. 1–75.

Bureau of Mines, 1963, Geological map of the Philippines, 1st edition: Bureau of Mines, Manila.

Corby, G. W., *et al.*, 1951, Geology and oil possibilities of the Philippines: *Dept. of Agriculture and Natural Resources, Tech. Bull.*, no. 21.

Gervasio, F. C., 1966, A study of the tectonics of the Philippine Archipelago: *Philippine Geol.*, vol. XX, no. 2, p. 51–75.

Hahn, A., 1965, Two applications of Fourier's analysis for the interpretation of geomagnetic anomalies: *Journ. Geomag. and Geoelec., Tokyo*, vol. 17, no. 3–4, p. 195–275.

Irving, E. M., 1950, Review of Philippine basement geology and its problems: *Phil. Journ. Sci.*, vol. 79, no. 3, p. 267–307.

John, T. U., 1963, Geology and mineral deposits of east-central Balabac Is., Palawan Prov., Philippines: *Philippine Geol.*, vol. XVII, p. 1–75.

Kind, E. G., 1964, Formel zur Berechung magnetischer Anomalien drei-dimensionaler Model-

lkörper und Programm für Rechenautomaten: Unpublished report, Bundesanst. Bodenforshc., Hannover.

Liechti, P., *et al.*, 1960, The geology of Sarawak, Brunei and the western part of North Borneo: *Brit. Borneo Geol. Survey Bull.*, no. 3.

Ramos, C., and Duna, B., 1963, Preliminary report on the reconnaissance geology of Cuyo-Agutaya Islands, Palawan: Unpublished report, Bureau of Mines, Manila.

VIII. PRELIMINARY REPORT ON RECONNAISSANCE OF HEAVY MINERAL SANDS IN SOUTHERN VIET-NAM[1]

(Project CCOP-1/ROV. 3)

By

L. C. Noakes

Bureau of Mineral Resources, Geology and Geophysics
Canberra, A.C.T. Australia

(with tables VIII-1 to VIII-4; figures VIII-1 to VIII-3;
and one appendix)

ABSTRACT

Earlier investigations of beach sands along the coast of Viet-Nam showed that significant quantities of detrital heavy minerals are present in some places, the dominant constituents being ilmenite, zircon, rutile and monazite. Reconnaissance by helicopter and scout car was made in May 1970 over about 60 km of coastline in the vicinity of Hue and a prospective area at Vinh My was selected for reconnaissance drilling and sampling. Analyses of the samples obtained indicate that more detailed investigation is justified and that an economically viable deposit might be proved in this area.

INTRODUCTION

Delegates of the Republic of Viet-Nam to the sixth session of the Committee for Co-ordination of Joint Prospecting for Mineral Resources in Asian Offshore Areas (Bangkok, May 1969) expressed their interest in mineral sands and arrangements were made for the writer to discuss prospects and problems with members of the Geological Survey of the Republic of Viet-Nam and to carry out a reconnaissance of promising areas following the seventh session of CCOP, held at Saigon in May 1970. This continuing project is included in the work programme of CCOP as project CCOP-1/ROV. 3.

Mineral sands in Viet-Nam include deposits of glass sand, which are currently

1: This document was issued in mimeograph form as Record 1971/42 of the Bureau of Mineral Resources, Geology and Geophysics, Department of National Development, Canberra, Australia, and submitted to the eighth session of CCOP as document CCOP/TAG(VII)/44.

exploited in the Cam Ranh area, and prospective deposits of detrital heavy minerals, principally ilmenite, zircon, rutile and monazite, at a number of localities along the beaches bordering the South China Sea. Priority was given to the investigation of heavy mineral deposits because glass sand projects had been established whereas little was known of the prospects for exploiting detrital heavy minerals.

Data recently collected by the Geological Survey provided an obvious starting point for a reconnaissance of mineral sand deposits. As a result of interest aroused by CCOP in 1968 and 1969, the Survey had collected shallow samples from a number of beaches along the eastern coast and arranged for these to be analyzed by the Geological Survey of Malaysia. The most encouraging of these samples, containing ilmenite, rutile and zircon, came from Thuan-an (also known as Eagle Beach), near Hue: although the grade of this shallow sample appeared to be marginal, the very extensive beaches of the Hue area were considered to warrant further investigation.

A field team consisting of Mr. Vu Van An, Mr. Nguyan Tan Thi and Father H. Fontaine of the Geological Survey, and the writer, spent a week in the Hue area towards the end of May 1970 and, thanks to the co-operation of Colonel Chism of CORD at Hue, who assisted greatly with transport by scout car and helicopter, it was possible in the time to carry out a reconnaissance of about 60 kilometres of coastline and to complete some reconnaissance drilling and sampling of the best prospect, found at Vinh My.

Samples taken during the reconnaissance, including those from traverse lines at Vinh My, were subsequently analyzed semiquantitatively by Australian Mineral Development Laboratories, in Adelaide, Australia, the report of which is included as appendix 1. Unfortunately, auger equipment in Saigon was not suitable for these operations, but equipment capable of recovering a sand core about two centimetres in diameter to a maximum depth of two metres was found to provide small but representative samples; however, the extension rod failed during the drilling of the deposit at Vinh My so that only a few of the holes could penetrate below a depth of one metre. This had little effect on reconnaissance beyond Vinh My, but it needs to be emphasized that reconnaissance drilling at Vinh My could only be shallow and in most holes could not explore values down to or below the water table. Moreover, no theodolite was available at the time and surveying at Vinh My was carried out by the writer using a quick-set level with a turning circle and stadia rod (marked in feet) kindly loaned by Australian Army Engineers; however, a base line and two traverse lines were established with reasonable accuracy and tied into a tomb for permanent identification so that future workers can readily re-establish these survey lines although the wooden pegs themselves are likely to disappear.

This report deals principally with reconnaissance results at the Vinh My deposit which certainly appears sufficiently attractive to warrant more detailed investigation. The results of reconnaissance sampling at other localities in the Hue area are also discussed and some data previously recorded on mineral sands elsewhere in Viet-Nam are also included.

The writer wishes to thank his colleagues in the Geological Survey of the Republic of Viet-Nam for their interest and hospitality during the investigations, Colonel Chism and Lieutenant Frederickson of CORD for their whole-hearted co-operation, and Australian Army Engineers for their assistance in providing survey equipment.

Assistance in furthering field investigations at Vinh My and associated laboratory work, already arranged by the Australian Government, should lead to establishment of techniques and equipment within the Geological Survey which can be used in due course to extend the investigations of heavy mineral sand deposits along this promising coast.

CLIMATE AND ACCESS

Southern Viet-Nam lies wholly in the tropics and is subject to the monsoonal climatic changes of Southeast Asia. The winter period, approximately October to February, is relatively dry under the influence of the southwest monsoon, but the summer period, about May to October, is the rainy season associated with the northeast monsoon. This period may include typhoons, particularly late in the summer, and the incidence of the storms will be of particular significance to beach mining.

The writer has found little information on longshore currents along the coast of Viet-Nam, but the location and configuration of sand spits in relation to river mouths and headlands observed on maps and from aerial reconnaissance strongly suggests that the principal direction of longshore current movement is from north to south; this conclusion was reached after helpful discussions with Dr. K. O. Emery. As mentioned later, concentration of heavy minerals along the coast near Hue indicates a southerly longshore movement of sand, at least in that area. On the other hand, some features of both heavy mineral concentration and of coastal morphology suggest the influence of a reversal of sand movement offshore at times; however, more data are needed to resolve these matters.

The Hue area, although the scene of the major TET offensive of 1968, was stabilized in 1970 and there appeared to be no security hazards for beach sand mining in the areas visited. Access for prospecting or mining plant and supply of ground water should present no great difficulties, but matters of possible mining tenure were not investigated during the reconnaissance. One matter likely to affect mining in some parts of this area is the occurrence of tombs and burial grounds along dunes and sandhills, some of which may prove to be economically exploitable. Little difficulty is expected at the Vinh My deposit where there are few tombs and none in the area drilled, but burial grounds could present difficulties in other areas and this matter should be kept in mind when prospecting for mineral sands.

PROSPECTS FOR HEAVY MINERAL SANDS IN THE HUE AREA

General

The mineral constitution of heavy mineral sands appears to be remarkably uniform along the whole eastern coastline of southern Viet-Nam, from Quang-tri in the north to the Mekong Delta, as shown by the data obtained from samples collected at locations shown on Fig. VIII-1. All samples contained ilmenite and zircon as the dominant valuable heavy minerals along the coast, followed by rutile and monazite in that order

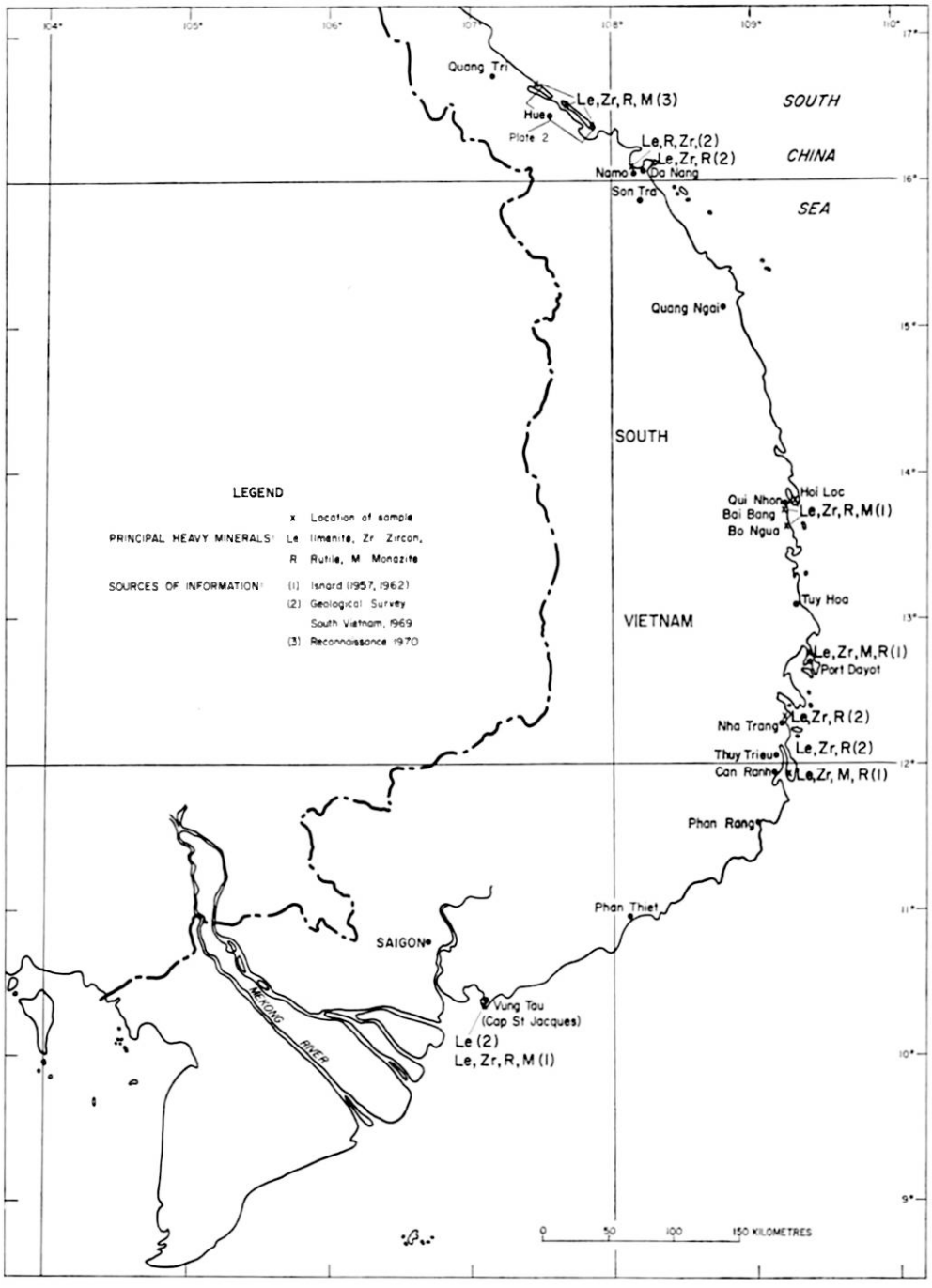

Figure VIII-1. Locations of samples of beach sands collected along the coast of southern Viet-Nam and their heavy mineral constituents.

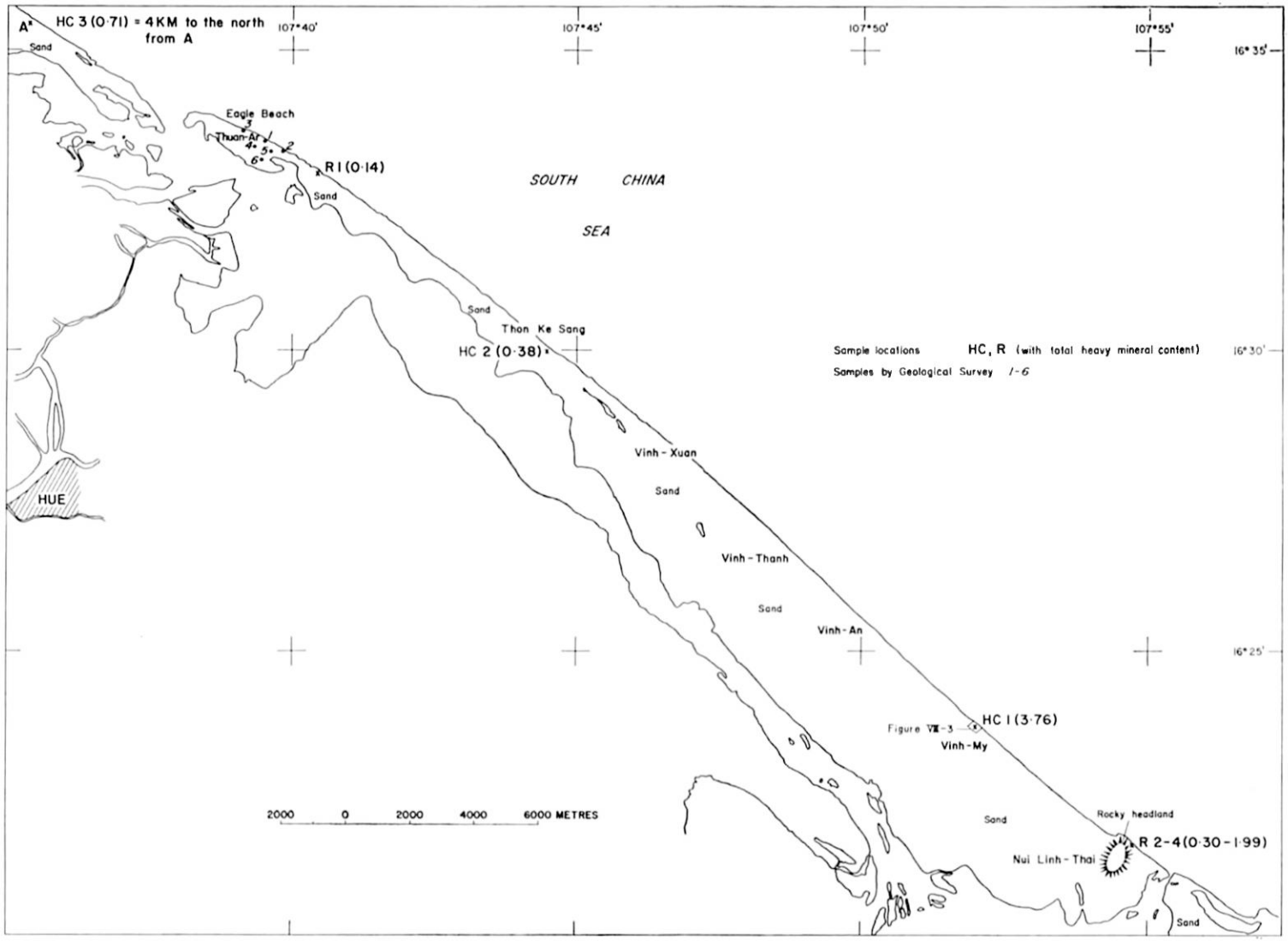

Figure VIII-2. Locations of samples of beach sands collected along the coastal area in the vicinity of Hue, Republic of Viet-Nam, with their content of heavy minerals shown as percentages by weight.

towards the northerly and southerly limits, but with monazite exceeding rutile in the central sector around Cam Ranh.

The uniformity of the heavy mineral constituents indicates a generally similar provenance for these minerals in southern Viet-Nam although no detailed work has apparently been done to determine their source. Isnard (1957, 1962) considers that they are derived from intrusive and metamorphic rocks known along the coast and immediate hinterland. Prospects for viable deposits of these heavy minerals along the coast, other than in the Hue area, will be dealt with later, but it might be noted at this stage that available data from samples collected along the coast, although establishing mineral content, do not indicate likely grades of heavy minerals in those areas.

In the Hue area, the reconnaissance by scout car and helicopter was designed to select the areas with the best concentrations of heavy minerals for more detailed investigations. The locations of the samples and their heavy mineral contents are shown on Fig. VIII-2. The procedure at each locality was to sample by auger to a depth of about one metre about ten metres above high tide level on the beach. One auger sample was bagged for analysis in Australia and another sample from an adjacent hole was panned on the spot and the results in terms of heavy minerals were noted. In most localities, samples of sand from dunes behind the beach were also panned.

This method gave a fairly clear indication of the relative amount of heavy minerals present and was confirmed later by the results of the analyses made in Australia. Aerial inspection alone provides some indication of the presence of heavy minerals but, particularly where the average heavy mineral content is relatively low (less than 10 per cent) ground sampling is required to identify worthwhile concentrations. Inspection of panned concentrates by hand lens provided no precise information, but previous analyses of samples from Thuan-an by the Malaysian Geological Survey provided a guide to the heavy mineral content and a predominance of black iron oxides with grains of zircon and rarer grains of rutile and monazite could be recognized.

Samples taken by helicopter at HC3 (see Fig. VIII-2) near Vinh My provided the best residue of heavy minerals in the pan from samples taken both from the beach and the dunes and arrangements were therefore made to reach this area by scout car to carry out reconnaissance drilling. The concentrations near Vinh My appear to be developed by a longshore current moving southwards and concentrating the heavy minerals against the subdued headland of Linh Thai Hill.

The deposit at Vinh My, for which the most detailed data are available, is described first, before dealing with occurrences elsewhere in the Hue area and in other parts of Viet-Nam.

Deposit at Vinh My

The deposit at Vinh My, where drilled, consists of a wide beach and a subdued foredune behind which is a shallow depression leading up to a dune reaching a height of about 30 metres above sea level. Behind this dune the yellow-brown beach sand containing heavy minerals gives may fairly abruptly to the fine whitish-grey sand which is characteristic of the areas behind the dunes along this section of the coast (see sections, Fig. VIII-3).

Two traverse lines were drilled from high tide mark across the beach, foredune

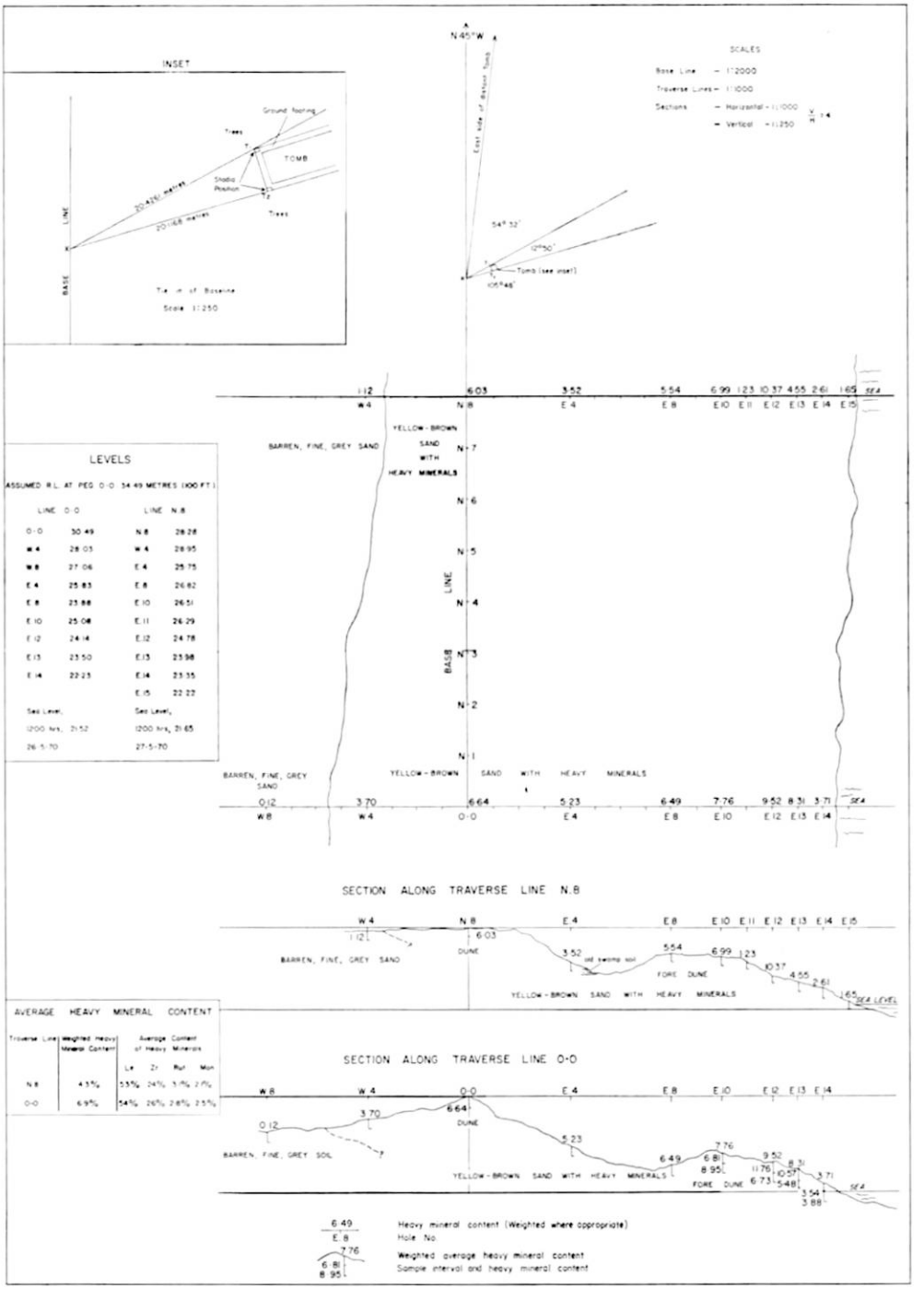

Figure VIII-3. Results of reconnaissance drilling in the coastal area at Vinh My, in the vicinity of Hue, Republic of Viet-Nam.

and dune to the sand plain; the traverse lines were 320 metres apart and the locations of both the traverse lines and drill holes were designed as part of a reconnaissance grid as indicated in the Manual on Beach Mining Practice (Macdonald, 1968). This grid can be extended and filled in during the course of more detailed investigations; details of the grid are shown in Fig. VIII-3.

The base line, traverse lines and drill holes were surveyed and all stations levelled using an assumed datum at station 0–0 on the base line. Pegs will no doubt be removed by local fishermen, but the base line, which follows the crest of the main dune, was tied into a prominent tomb (Mieu) and can readily be re-established by a surveyor. The full grid calls for traverse lines at intervals of 40 metres normal to the beach and for drill holes at intervals of 10 metres along the traverse lines; for reconnaissance purposes, only every fourth hole was drilled along the traverse lines except on the upper part of the beach itself where the interval was 10 metres to provide some detail. Auger samples were taken normally at intervals of one metre down the hole and, because the auger was of small diameter, the entire sample was bagged for analysis.

Although these procedures would normally provide satisfactory reconnaissance data, it must be emphasized that this reconnaissance at Vinh My had a number of shortcomings partly due to lack of time, but mostly due to lack of appropriate equipment. A theodolite rather than a quick-set level with turning circle would have been preferred for the surveying, but the major shortcoming was lack of augering equipment capable of sampling at depth and below the water table.

Semi-quantitative analyses of samples were carried out by Australian Mineral Development Laboratories (AMDEL) in Australia and the report is included as appendix 1. A check sample was included; sample R6 was in fact a duplicate of 0–0 and, considering the method of semi-quantitative analysis used, the check is satisfactory. Sample R5 should be deleted. The sample results should provide a good guide to grade and are adequate for the purpose, particularly as the samples taken from Vinh My are generally well above marginal grade.

The results show a very uniform mineral constitution of heavy minerals in all samples throughout the deposit. The highest grade samples in both traverse lines, showing about 10 per cent of heavy minerals, were taken from the beach well above sea level and reflect the occurrence of seams of heavy minerals 5 to 10 cm thick; however, the heavy mineral content of the dunes, at least to one metre depth, is also encouraging.

It should be noted that, although grain counts were carried out on every sample on this occasion to provide detail on the mineral assemblage, grain counting can be restricted to a composite sample per traverse line in further work at Vinh My and individual samples would need to be analyzed only for total heavy mineral content.

Weighted averages of heavy mineral content for each hole are shown on Fig. VIII-3. The weighted heavy mineral content for all samples on traverse line 0–0, excluding hole W8, is 6.9 per cent with an average mineral content (not weighted) as follows: ilmenite (both types), 53.8 per cent; zircon, 26; rutile, 2.8; and monazite, 2.5 per cent. The weighted average heavy mineral content along line N8 is lower (4.3 per cent) with a comparable average mineral content: ilmenite, 53 per cent; zircon, 24; rutile, 3.1; and monazite, 2.1 per cent.

Reconnaissance of this type cannot, of course, establish reserves but the data given

above for the two traverse lines at least gives an indication of the likely grades of the sand. Assuming prices in U.S. dollars f.o.b., which seem reasonable for production a year or so ahead, (ilmenite, $13 per ton; zircon, $40; rutile, $134; and monazite, $170) and a recovery of 85 per cent, the average grades in cents per cubic metre (assuming 1.7 tons per cubic metre) for both traverse lines would be as follows:

	Zircon	Ilmenite	Rutile	Monazite	Total
Line 0–0	103	70	37	42	252
Line N8	59	43	26	22	150

These preliminary calculations, however, assume recovery of clean concentrates all of which could be sold; in this connexion, a number of factors should be noted which require further investigation.

With reference to ilmenite, a composite sample of both types of ilmenite identified by AMDEL was analyzed by that laboratory to check on the contents of titania and trace elements; the results were as follows: TiO_2, 51.9 per cent; Cr_2O_3, 0.70; Va_2O_8, 0.20; FeO, 26.3; and Fe_2O_3, 17.5 per cent. The titania content and the iron ratio are satisfactory, the vanadium content is within acceptable limits, but the chrome content of this sample is much higher than the usual acceptable limit of 0.1 per cent. However, grains of chromite were found in most of the samples analyzed by AMDEL and it is a reasonable assumption that the content of 0.7 per cent of chromium oxide in the sample analyzed could be reduced by exclusion of chromite grains. More detailed investigation of the ilmenite and of the problems of separation in treatment will therefore need to be carried out.

There appears to be no obvious problem in the separation and sale of the rutile and monazite, but the occurrence of abundant inclusions, mainly of magnetite and ilmenite, in the zircon will need to be investigated in terms of treatment and recovery. The inclusions are not likely to affect the quality of the zircon in its main fields of use in foundry work but, by imparting some degree of magnetism, the inclusions could complicate the recovery of clean concentrates.

In general, and despite the limitations of the reconnaissance, the results of sampling at Vinh My indicate a mineral sand deposit well worthy of more detailed investigation. Panning along the beach north of Vinh My indicated that a significant heavy mineral content probably extends for at least three kilometres in that direction. No reconnaissance was carried out to the immediate south but, as the more southerly of the two traverse lines shows better values and because the main longshore current apparently moves in a southerly direction, further investigation might commence with some panning and reconnaissance southwards and the possible extension of the drilling grid in that direction.

Heavy Minerals in the vicinity of Hue

Procedures followed in sampling mineral sands in the vicinity of Hue have already been mentioned and the results in terms of heavy mineral content are shown on Fig. VIII-2. The results in terms of contents of ilmenite, rutile, zircon and monazite, shown in appendix 1, generally support a southward movement of heavy minerals along the

coast as the most northerly sampling point, HC3, contained markedly lower concentrations of these valuable heavy minerals than did all sampling points to the south; the concentration of these minerals relative to each other, however, was little changed.

The next best concentration of heavy minerals to that near Vinh My was found immediately south of the headland of Linh Thai Hill where the content of heavy minerals from samples R2–4 ranged from 0.30 to 1.99 per cent with the best values coming from a depth of 1 to 2 metres high on the beach. It is not clear whether this concentration is due to southerly migration around the headland of Linh Thai or whether it represents some concentration by northerly longshore currents against the headland, perhaps during the less effective southwestern monsoon.

In considering the results of the samples taken to date it is useful to relate heavy mineral content to approximate grade per cubic metre. Using the same prices and recovery factor as for the Vinh My deposit and assuming the same proportions of individual heavy minerals in the beach sands south of Thuan An as are found at Vinh My, one per cent of heavy minerals would be worth about 35 cents per cubic metre. Although this grade might be considered of interest where large reserves and economies of large-scale operations were possible, the writer suggests that, at this stage of investigation, a minimum grade of 60 to 70 cents would be realistic, requiring an average heavy mineral content of the order of 2 per cent.

On this basis, the results of the recent reconnaissance in the vicinity of Hue provide no encouragement immediately north of Thuan An and little encouragement north of the Vinh My area. Apart from Vinh My, concentrations found immediately south of Linh Thai Hill and possible southerly extensions of these concentrations along the beach warrant further investigation; further concentrations may have been built up against headlands south of Linh Thai Hill.

HEAVY MINERAL SANDS ELSEWHERE IN VIET-NAM

Some information on mineral sands at a number of localities along the coast of Viet-Nam has been recorded by P. Isnard (1957, 1962); details of the mineral constitution of sand samples reported by him are given in Table VIII-1 and the localities are shown on Fig. VIII-2.

From the text and from the analyses themselves it is apparent that samples referred to by Isnard were taken from heavy mineral seams occurring on or within the beaches and thus do not indicate the average grade of beach sand at those localities. Although the relative proportions of heavy minerals in Isnard's samples are different from the average content in the sands at Vinh My, the suite of valuable heavy minerals is the same, indicating a high degree of uniformity of the heavy mineral assemblage along the coast of Viet-Nam. Although samples from individual seams of heavy minerals give no indication of the average grade of beach sands, the occurrence of prominent seams is itself an indication of the presence of concentrations of heavy minerals and would suggest that further investigation of these localities would be warranted.

The locations of samples collected more recently by the Geological Survey are also shown on Fig. VIII-2 and some details of mineral contents are given in Table VIII-2;

Table VIII–1. Heavy mineral constituents of beach sands in southern Viet-Nam: compiled from Isnard (1957, 1962) and from unpublished data.

MINERALS SEPARATED	Cam-Ranh	Port Dayot	Cap Saint Jacques	Lagune d'Hoi Loc, Qui-Nhon	Bai-Bang, Qui-Nhon	Bo-Ngua, Sông-Cau	Go-Cong
	weight, 112 gm	weight, 192 gm	weight, 97 gm	weight, 76.65 gm	weight, 723 gm	weight, 616 gm	weight, 72.5 gm
	% in sample	% in sample	% in sample	% in sample	% in sample	% in sample	% in sample
Ilmenite	78.0	85.0	92.0	94.0	46.5	72.5	quite rare
Magnetite	1.5	0.1	1.5	0.03	0.07	0.9	rare
Monazite	3.0	2.0	0.25	0.4	0.1	0.5	very rare
Zircon	4.0	7.0	3.0	2.4	2.2	2.0	very rare
Rutile	0.5	0.5	0.5	2.0	1.0	1.5	very rare
Quartz	12.0	4.5	2.0	0.55	49.5	19.5	99.3
Calcite	rare	nil	rare	–	–	–	–
Kyanite	very rare	nil	very rare	rare	very rare	very rare	–
Hematite, brown	rare	very rare	rare	very rare	–	rare	very rare
Hematite, red	–	–	very rare	very rare	very rare	very rare	rare
Biotite	–	–	very rare	–	–	–	rare
Hornblende, green	0.3	0 5	rare	–	–	–	–
Diopside	–	very rare	very rare	rare	–	–	–
Ouwarowite	rare	rare	very rare	–	–	–	–
Epidote	–	very rare	rare	very rare	very rare	rare	quite common
Staurolite	very rare	rare	very rare	very rare	very rare	very rare	very rare
Tourmaline	quite rare	quite rare	rare	quite rare	0.1	1.0	very rare
Sillimanite	0.7	0.4	0.25	0.4	0.3	0.9	–
Andalusite	very rare	very rare	very rare	–	rare	very rare	–
Muscovite	–	–	–	–	–	–	quite rare
Spinel	–	–	–	very rare	rare	rare	–
Corundum	–	–	–	–	rare	rare	–
Titanite	–	–	–	rare	–	–	–
Garnet	–	–	–	very rare	very rare	rare	very rare
Apatite	–	–	–	–	very rare	–	–

Table VIII-2. Heavy mineral contents of beach sands in the Republic of Viet-Nam; analyses by Geological Survey of Malaysia (see report of sixth session of CCOP, doc. 9, p. 103, 104).

Name of beach and sample no.		Value per cubic metre in US cents[1]	Heavy mineral contents in original sands (g/m³)		
			Zircon	Rutile	Ilmenite
Thuan-An	1	45	1,823	3,199	15,537
(Eagle Beach)	2	46	1,641	3,692	13,537
	3	09	1,145	327	2,943
	4	21	2,377	648	7,566
	5	06	346	461	1,615
	6	12	1,707	142	4,410
Da-Nang	1	–	–	48	478
	2	–	50	–	301
	3	–	50	–	198
	4	–	–	–	189
Son-Tra		–	–	–	–
Nam-O		–	24	60	192
Nha-Trang		03	138	138	1,240
Thuy-Trieu	1	–	10	10	296
	2	–	35	20	151
Vung-Tau		–	–	–	32
Long-Hai	1	02	90	75	993
	2	05	230	184	2,625
	3	03	290	75	1,831

– Indicates nil or negligible content.

1: Value based on assumption of 85 per cent recovery of heavy mineral content and selling prices for zircon, rutile and ilmenite at US$44, $88 and $11 per ton, respectively.

these samples, analyzed by the Geological Survey of Malaysia (see report of sixth session of CCOP, doc. 9, p. 103, 104), were shallow samples collected at random from the beaches and would appear to have little significance in regard to overall grade.

CONCLUSIONS

Information available at this stage certainly suggests that the coast of southern Viet-Nam from Hue to the Mekong Delta is a mineral sand province supplied with ilmenite, zircon, rutile and monazite and that deposits of these minerals of significant grade are likely to occur where longshore currents, wave action and coastal morphology have combined to trap heavy minerals. The recent reconnaissance near Hue has indicated one such deposit and the earlier work of Isnard suggests other localities worthy of more detailed prospecting.

REFERENCES

Isnard, P., 1957, Etude de sables titanés du Viet Nam Meridional: *Archives Géologiques du Viet Nam,* No. 4. Service Geologique du Viet-Nam, Saigon.

————, 1962, Sables titanés du centre Viet-Nam: *Travaux de Géologique,* No. 1. Faculté des Sciences de Hue.

Macdonald, E. H., 1968, Manual of Beach Mining Practice-Exploration and Evaluation. Department of External Affairs, Canberra.

Appendix 1

A SEMI-QUANTITATIVE MINERALOGICAL STUDY OF BEACH SAND SAMPLES FROM THE VICINITY OF HUE, REPUBLIC OF VIET-NAM

By

M. J. W. Larrett

Australian Mineral Development Laboratories, Adelaide, Australia

(with tables VIII-3 and VIII-4)

INTRODUCTION

Thirty-three samples of beach sand were submitted for heavy mineral separation and subsequent mineralogical examination of the heavy constituents to determine species present and their relative abundances. The separations were made by D. Campbell and the work was carried out by M. J. W. Larrett under the direction of Dr. K. J. Henley, officer-in-charge, Mineralogy and Petrology Section.

Table VIII-3. Content of heavy minerals (per cent by weight) in samples of beach sands collected in the vicinity of Hue, Republic of Viet-Nam; separated by tetrabromoethane, S.G. 2.96.

Sample No.	Depth (metres)	Per cent by weight	Sample No.	Depth (metres)	Per cent by weight
0–0	0 – 0.9	6.64	N8–0–E10	0 – 0.8	6.99
0–E4	0 – 0.7	5.23	N8–0–E11	0 – 0.8	1.23
0–E8	0 – 0.75	6.49	N8–0–E12	0 – 0.7	10.37
0–E10	0 – 1.0	6.81	N8–0–E13	0 – 0.75	4.55
0–E10	1 – 1.8	8.95	N8–0–E14	0 – 0.75	2.61
0–E12	0 – 1.0	11.76	N8–0–E15	0 – 0.6	1.65
0–E12	1 – 1.8	6.73			
0–E13	0 – 1.0	10.57	N8–W4	0 – 0.8	1.12
0–E13	1 – 1.8	5.48	R1	–	0.14
0–E14	0 – 1.0	3.54	R2	1 – 1.5	0.31
0–E14	0.5 – 1.5	3.88	R3	0 – 3	1.70
			R3 (Foredune)	3 – 6	1.99
0–W4	0 – 0.7	3.70	R4	0 – 3	0.30
0–W8	0 – 0.9	0.12	R6	–	6.66
N8–0–0	0 – 0.8	6.03	HC–1	1 – 3	3.76
N8–0–E4	0 – 0.7	3.52	HC–2	0.08	0.38
N8–0–E8	0 – 0.7	5.54	HC–3	0.84	0.71

METHODS

Initially the wet sand samples were washed to remove residual salt and oven-dried. The dry samples were then riffled to obtain representative samples suitable for separation, and heavy mineral separations were carried out, using tetrabromoethane (S. G., 2.96) as the separating medium. Results are shown in Table VIII-3, expressed as percentages by weight.

Representative portions of each of the heavy fractions were obtained by riffling and examined in transmitted light by means of standard refractive index oil mounts to identify the non-opague phases present. A further portion of each was mounted as a polished briquette and examined optically using reflected light techniques, in order to identify the abundant opaque minerals present.

Table VIII-4. Mineralogical composition of heavy mineral fraction of samples listed in table VIII-3; per cent by grain count.

Sample No.	P.S. No.	Zircon	Rutile	Monazite	Ilmenite 1	Ilmenite 2	Leucoxene	Chromite	Others
0–0	14098	27	4	3	38	18	3	3	4
0–E4	14099	35	4	3	29	20	3	2	4
0–E8	14100	32	3	4	27	24	4	2	4
0–E10	14101	32	2	4	25	26	4	2	5
0–E10	14102	26	3	2	30	27	2	3	7
0–E12	14103	19	2	1	33	31	3	1	10
0–E12	14104	28	3	5	19	32	4	2	7
0–E13	14105	18	2	2	28	37	4	1	8
0–E13	14106	27	5	2	25	31	3	1	6
0–E14	14107	15	2	2	26	30	6	1	18
0–E14	14108	21	2	1	30	20	4	1	21
0–W4	14109	33	2	2	30	19	2	Tr	12
0–W8	14110	20	3	1	20	25	7	2	22
N8–0–0	14111	30	3	2	28	22	2	1	12
N8–0–E4	14112	27	2	2	31	14	2	1	21
N8–0–E8	14113	28	4	2	34	22	3	1	6
N8–0–E10	14114	34	4	3	30	18	4	1	6
N8–0–E11	14115	9	2	Tr	39	24	4	1	21
N8–0–E12	14116	20	3	3	26	29	11	–	8
N8–0–E13	14117	32	3	4	27	24	3	1	6
N8–0–E14	14118	13	3	1	37	30	5	4	7
N8–0–E15	14119	22	3	3	26	22	3	1	20
N8–W4	14120	21	4	1	26	24	4	1	19
R1	14121	16	1	1	29	28	4	–	21
R2	14122	27	3	3	24	17	8	1	17
R3	14123	12	1	1	43	23	2	1	17
R3(Foredune)	14124	12	2	1	38	23	4	2	18
R4	14125	16	1	1	24	26	9	1	22
R6	14127	34	2	3	26	22	3	1	9
HC–1	14128	23	1	1	25	23	5	1	21
HC–2	14129	26	3	2	23	21	7	1	17
HC–3	14130	9	1	Tr	15	13	4	1	57

Semi-quantitative grain counts were carried out on a minimum of 300 grains in each case, and the relative proportions of the constituent minerals are shown in Table VIII-4. The accuracy of these values may be taken as ± 10 per cent.

MINERALOGICAL NOTES

All heavy fractions examined are quite similar mineralogically and they contain zircon and opaque minerals as the dominant constituents; in most cases they also contain practically identical suites of accessory minerals, even in the samples from different localities.

It should be noted that discrete grains of partially oxidised magnetite were observed in trace amounts in only a few of the heavy fractions and were not present as major constituents of the samples. The near presence of a hand-magnet was found to evoke very little response from any of the heavy fractions.

The samples all contain ilmenite as the dominant constituent and this has been arbitrarily subdivided into three groups, namely: "Ilmenite 1", which consists of fresh to partially altered material; "Ilmenite 2", which consists of partially to extensively altered material (amorphous iron titanium oxides), and "Leucoxene" which represents the final stage in the weathering of ilmenite.

The progressive alteration of ilmenite is accompanied by a change in its magnetic susceptibility and thus the values given for these three groupings may be of use, should these sands be considered for treatment by magnetic separation. One grain of gold was noted in PS 14125 and, in addition to ilmenite, some silicates contain inclusions of sulphides, probably pyrrhotite and/or chalcopyrite.

DESCRIPTIONS OF MINERALS

Zircon

Zircon occurs as sub-rounded to subhedral (and more rarely euhedral) grains, the majority of which are colourless and contain abundant inclusions. A few purplish grains are present in most of the heavy fractions and they are generally of a larger grain size than the colourless variety. Many of the inclusions are opaque and these are mainly magnetite and ilmenite.

Rutile

Rutile occurs as red to red-brown sub-rounded to ovoid grains sometimes containing opaque inclusions. In some of the grains the colour is so dark as to render the grains almost opaque.

Monazite

This mineral is present in all the heavy fractions in very minor amounts, as very pale yellow, well rounded and ovoid grains, which in most cases can be distinguished by their peculiar 'pocked' or 'frosted' appearance.

Ilmenite 1

This consists of discrete, homogeneous, pinkish brown, subangular to sub-rounded grains, of relatively fresh to partially altered ilmenite. The majority of grains are strongly anisotropic and some contain minor oriented exsolution lamellae of hematite whilst oxidation to hematite and alteration to leucoxene is common at the edges of the grains and along fractures and cleavage planes.

Ilmenite 2

This type of ilmenite consists of discrete, sub-rounded to well-rounded grains with a rather porous texture and weak anisotropism, grading into brownish, porous, amorphous iron/titanium oxides.

Leucoxene

Leucoxene, the end product of the weathering of ilmenite, occurs as discrete well-rounded grains of a creamy white to orange brown colour, with a 'sugary' texture and a resinous lustre. Some grains appear to have recrystallised to fine-grained rutile, and others contain isolated ilmenite residuals.

Chromite

Chromite is present in most samples, in very minor amounts, as discrete, isotropic, greyish-brown grains, generally sub-rounded but sometimes octahedral. A few grains show oxidation rims of magnetite.

Other minerals

These consist of accessory to trace amounts of goethite, oxidized magnetite, hematite, tourmaline, kyanite, staurolite, epidote, green and brown spinel, pyroxene, garnet, sphene, (?) xenotime, sillimanite, andalusite and green amphibole; however, all are not necessarily present in any one heavy fraction.

ANALYSIS OF ILMENITE CONCENTRATE

A request was received later for the preparation and subsequent analysis of an ilmenite concentrate from the series of heavy mineral concentrates obtained from the beach sands.

The heavy mineral concentrates from samples prefixed 0 and N (23 samples) were halved by means of a microsplitter, and one half of each was combined to give a composite sample. This composite of the 23 heavy fractions was then magnetically separated, using a Frantz Isodynamic Separator at a setting of 0.2 amps, to produce an ilmenite concentrate. The purity of the concentrate was checked by means of a polished briquette, and it was then submitted for chemical analysis.

The ilmenite concentrate was analyzed for titanium, chromium, vanadium and ferric and ferrous iron; the percentages of these components were as follows: TiO_2, 51.9; Cr_2O_3, 0.70; V_2O_5, 0.20; Fe_2O_3, 17.5; and FeO, 26.3 (total 96.6%).

The results indicate a good quality ilmenite except that the value for chromium is anomalous. This high chromium value is probably attributable to the presence of rare chromite grains in the concentrate, and may be difficult to remove due to the similar magnetic properties of ilmenite and chromite. The analyses total 96.60 per cent, indicating that certain other elements such as magnesium and/or manganese may be present.

An important point in the utilization of ilmenite is that ilmenite is soluble in sulphuric acid, and that stronger acid is needed to attack those ilmenites higher in TiO_2 and lower in ferrous oxide.

Conventional methods would probably suit this material and this would entail the removal of quartz, etc., by wet gravity methods and magnetic separation of the ilmenite from the mixture of heavy minerals by high tension separators.

IX. SEISMIC INVESTIGATIONS ON THE NORTHERN PART OF THE SUNDA SHELF SOUTH AND EAST OF GREAT NATUNA ISLAND

(Projects CCOP-1A/UNEC. 1 and UNEC. 5)

By

B. P. Dash, C. M. Shepstone, S. Dayal[1], S. Guru, B. L. A. Hains, G. A. King and G. A. Ricketts

Department of Geophysics, Imperial College of Science and Technology, London. S. W. 7 2BP, England

(With figures IX-1 to IX-18)

ABSTRACT

A total of 1,160 line-km of continuous seismic profiling were made during April 1969 and March to May 1971 on the northern part of the Sunda Shelf to the south and east of Great Natuna Island. Basins, ridge-like features and some faulting were identified, and the evidence suggests the existence of a swell extending between mainland Asia and Borneo. A low-frequency high-velocity layer which may be of Mesozoic age was identified, as well as a sequence of tilted strata which may be a time equivalent of the Natuna Sandstone. Relict Pleistocene drainage patterns are also evident.

INTRODUCTION

During March to May 1971, seismic investigations were carried out over the following three areas on the northern part of the Sunda Shelf with the Indonesian research vessel R. I. Jalanidhi (Dash, 1971): (a) Southeast, south and east of Great Natuna Island between longitudes 107°E and 110°E, and latitudes 2°30'N and 4°10'N; (b) east and southeast of Tioman Island between 104°10'E and 104°50'E, and 2°15'N and 3°N; and (c) the offshore area east of western Malaysia between 103°40'E and 104°10'E, and 3°40'N and 4°N. The investigation was largely an extension of the work conducted with the Malaysian Navy vessels Mahamiru and Kerambit (Dash, 1971) and the R. I. Jalanidhi (Dash and Sano, 1969). This paper incorporates and extends the information

1: Guest scientist from R. D. and D. J. College, University of Bhagalpur, Monghyr, India.

presented by Dash and Sano (1969) and deals with the data obtained in 1971 from the area east and south of Great Natuna Island.

The area under discussion comprises part of the shallow marine shelf lying south of the Indochina Peninsula, east of the Malay Peninsula, to the north of the Sunda Islands and west of Borneo. It forms part of the Eurasian crustal block as defined by Le Pichon (1968) but its regional tectonic setting is rather complex owing to the proximity of both the Indo-Australian block, south of the Java trench, and the Pacific block to the east of the area. In addition there are a number of smaller blocks termed 'intermediate' by Le Pichon, such as the Philippine block, northeast of the Philippine trench. Nevertheless, the northern part of the Sunda Shelf, from where few earthquakes have been recorded, is considered to be relatively stable.

Different ideas have been expressed recently concerning the relationship between

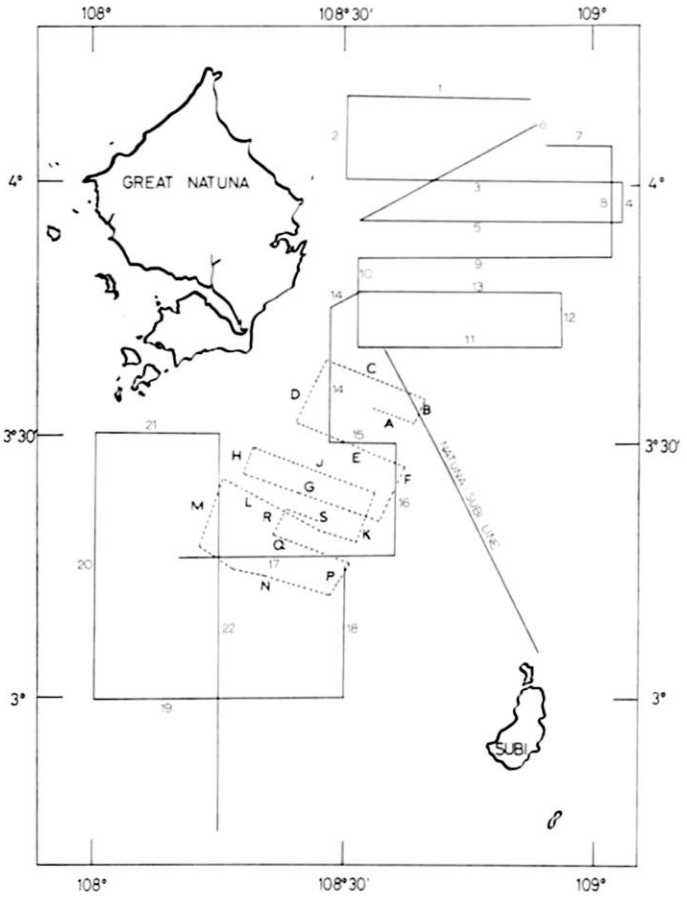

Figure IX-1. Track chart of seismic profiles in vicinity of Great Natuna Island, South China Sea; Traverses A to S made in April 1969, 1–22 and Natuna-Subi Line in April 1971, all by R/V R. I. Jalanidhi.

southeast Asia and the rest of mainland Asia during the break-up of Gondwanaland. Dietz and Holden (1970) suggest that southeast Asia remained attached to the mainland during the period of drifting, whereas Ridd (1971) and Burton (1970) suggest that southeast Asia was a part of Gondwanaland fitting between India and Australia.

The Paleozoic period in this region was characterized by the thick accumulation of sediments in a geosyncline. The Caledonian orogeny in middle Paleozoic times gave rise to the sequence of rocks termed 'Tonkinides' by Fromaget and Saurin (1952); these are highly metamorphosed limestones and quartzites. The Hercynian orogeny late in Paleozoic time caused considerable folding in the east and, in addition, a minor orogeny is thought to have occurred at about Tournaisian-Visean times. The rocks affected by late Paleozoic folding were largely Devonian and Carboniferous limestones which Fromaget termed the "Annamides"; unlike the Tonkinides, they did not undergo much regional metamorphism.

Outcrops of Paleozoic rocks are found throughout the Indochina-Malay Peninsula, but the Annamides and Tonkinides are found typically on the Kontum Block and the Annamitic chain, both in the eastern part of Indochina. The Permian limestone is thick in northern Thailand and it forms hills protruding through the Quaternary sediments in the valley of the Chao Phraya River in Thailand. A well drilled at Ayuthaya, about 80 km north of Bangkok, was reported to have penetrated shale and limestone, probably of Permian age, at 1,838 m (Kaufmann, 1961). Aeromagnetic survey data were interpreted as indicating a thickness of more than 3,000 m of Quaternary sediments in the area near the mouth of the Chao Phraya River but seismic surveys and drilling conducted later showed the thickness to be substantially less than had been inferred.

Between late Triassic and late Liassic times the Indosinian orogeny, which may actually have been a series of orogenic events, affected the western part of the geosyncline: the rocks of the Malay Peninsula south of the Isthmus of Kra were folded approximately along a north-south alignment, and granites were also intruded, while folding also took place in the Khorat Plateau region. The rock sequence arising from this event, known as "Indosinides", consists generally of Permian limestone which is overlain by sandstone and shale except on the swells of the northern part of the Sunda Shelf, from where it was probably eroded later. The Triassic and Liassic rocks of the Indochina-Malay Peninsula consist of an alternation of marine shales and sandstones grading upwards into a continental facies and 'red beds'. From early Mesozoic times onwards the sea gradually retreated from the present land areas. Igneous activity is believed to have occurred, and some of the granite intrusives have a probable age of Cretaceous or Paleogene.

The only Tertiary sediments known on the Indochina-Malay Peninsula are in a belt of intermontane lacustrine basins containing thicknesses of possibly more than 1,000 m of grey shales and sands, including some lignite beds and oil shales; they extend along the west flank of the Indochina-Malay Peninsula from Burma southwards through Thailand to Sumatra.

Tertiary basins are known below the sea bottom in the northern part of the Sunda Shelf. The thick deposits of Natuna Sandstone on Great Natuna Island, which display cross-bedding (Haile, 1970), are thought to be present in some places beneath the sea on the northern part of the Sunda Shelf. Geophysical evidence obtained on a previous

expedition (project CCOP-I/MAL. 3) off the eastern coast of West Malaysia (Dash, 1970) shows a series of layers which are thought to be of Tertiary age and may be contemporaneous with the Natuna Sandstone. The interpretation of the reflection seismic data obtained to south and east of Natuna Island, discussed below, supports this suggestion.

Seismic surveys have indicated the presence of three main basinal areas, separated by a swell, in the vicinity of the Natuna Islands. The Northwest Borneo Geosyncline, to the northeast of Great Natuna Island, extends southeast towards Borneo and also farther to the west; several faults found along the edge of the geosyncline have a similar parallel trend. To the northwest of the Natuna Islands and north of the Anambas Islands is another basin which has been termed the West Natuna basin by Koesoemadinata and Pulunggono (1971); step faulting at the eastern edge of this basin trends northeast-southwest. A third basin-like feature appears to be present south of the Anambas Islands.

FIELD OPERATIONS

Continuous seismic profiles (Figs. IX-3 to 12) were obtained using an E. G. & G. 8,000-joule, 3.6 kilovolt system (Fig. IX-2). The capacitor banks were triggered at intervals of four seconds through three single electrode, sea-return 'spark array' systems trailed 30 m behind the ship. Reflected signals were received by two types of hydrophone streamer cable. Lines 1 to 15 were recorded by an E. G. & G. streamer with four

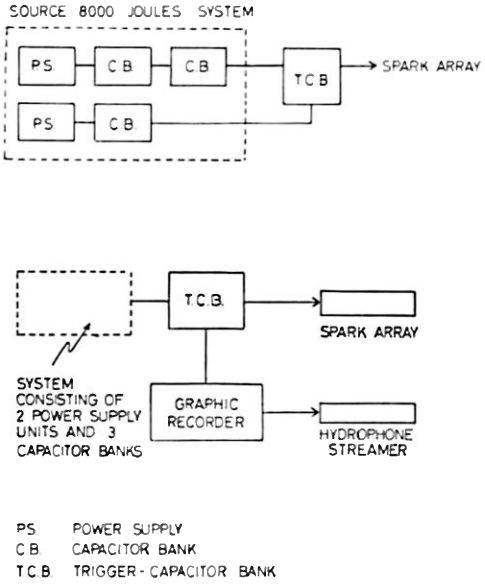

Figure IX-2. Schematic diagram of sparker system used for seismic profiling in vicinity of Great Natuna Island, South China Sea, April 1971.

active sections each 5 m long, incorporating four built-in preamplifiers; individual outputs were summed prior to the final amplification. The summing circuit was designed so that when one section became noisy, the overall signal-to-noise ratio of the summed output became very low. Unfortunately this cable later broke down and a second one, loaned to the survey party by Western Geophysical Company through Continental Oil Company of Indonesia, was used and Lines 15 to 23 were recorded with the latter; this streamer, about 35 m long, had a transformer coupling between individual hydrophone groups and it was towed 25 m behind the ship.

The energy source and the hydrophones were both kept at a depth of about 5 m and the buoyancy of the oil in the hydrophone array was counterbalanced by taping lengths of chain to the array. The seismic signals were filtered between 80 and 200 Hz and were plotted with an E. G. & G. recorder on wet paper 27 inches wide. The recorder sweep was maintained at four seconds and, with the ship's speed at 6 knots, one data point was recorded at an average distance of each 12 m along the traverses.

A total of 845 line-km of reflection data was obtained with depths of penetration ranging from 500 milliseconds (msec) to 1.5 seconds. Assuming an acoustic velocity of 1.5 km per second in water and 2.0 km per second in the sediments at shallow depths below the sea floor, the recorded profiles show a vertical exaggeration of either 12 to 1 or 18 to 1, as marked. The bathymetry was measured precisely on board with a Kelvin-Hughes echo sounder. The PDR record together with the sparker profiles provided a detailed picture of the topography of the sea floor along the lines traversed. Interference from multiple reflections between the water surface and the sea bottom, as well as from interbedded multiples in the sediments below the sea floor, was troublesome over the whole area, especially where the water was shallow and where there was only a thin sedimentary cover over the bedrock. Reduction of the power level from about 8,000 to 4,000 joules made no difference to the apparent penetration, nor to the intensity of the reflections or the number of multiples.

Navigation was by radar supplemented by visual fixes on various islands when the ship was beyond radar range of land. The weather during the period of the survey was very calm and noise levels were therefore usually low.

RESULTS

As the area under investigation is in an area being explored by a major oil company under contract with the Indonesian Government, only shallow reflection surveys were permitted and the investigations were limited to the superficial sediments and bedrock to shallow depths below the sea floor. Figures IX-4 to 7 illustrate the attitude of the upper part of the bedrock as well as the subsequent infilling. Figures IX-3 to 11 and IX-14 to 18 show a marked unconformity between the superficial sediments and the underlying bedrock. Despite the presence of multiple reflections from the sea floor as well as within the underlying sedimentary section, they did not hamper the interpretation to any great extent.

Parts of the traverses where the structure is most clearly shown in the profile records below the sea floor are illustrated in Figs. IX-4 to 7, together with a structural interpreta-

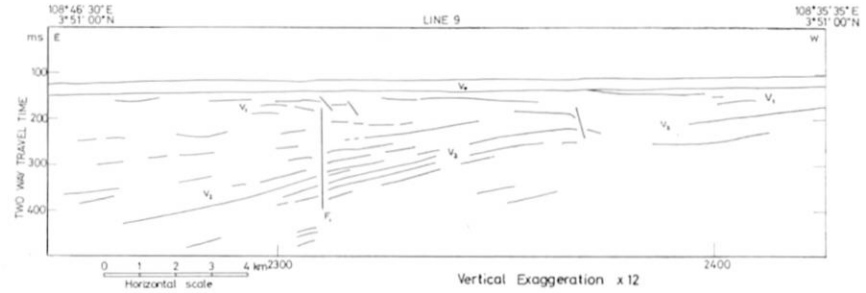

Figure IX-3. Interpretation of seismic profile along western part of Line 9, Fig. IX-1.

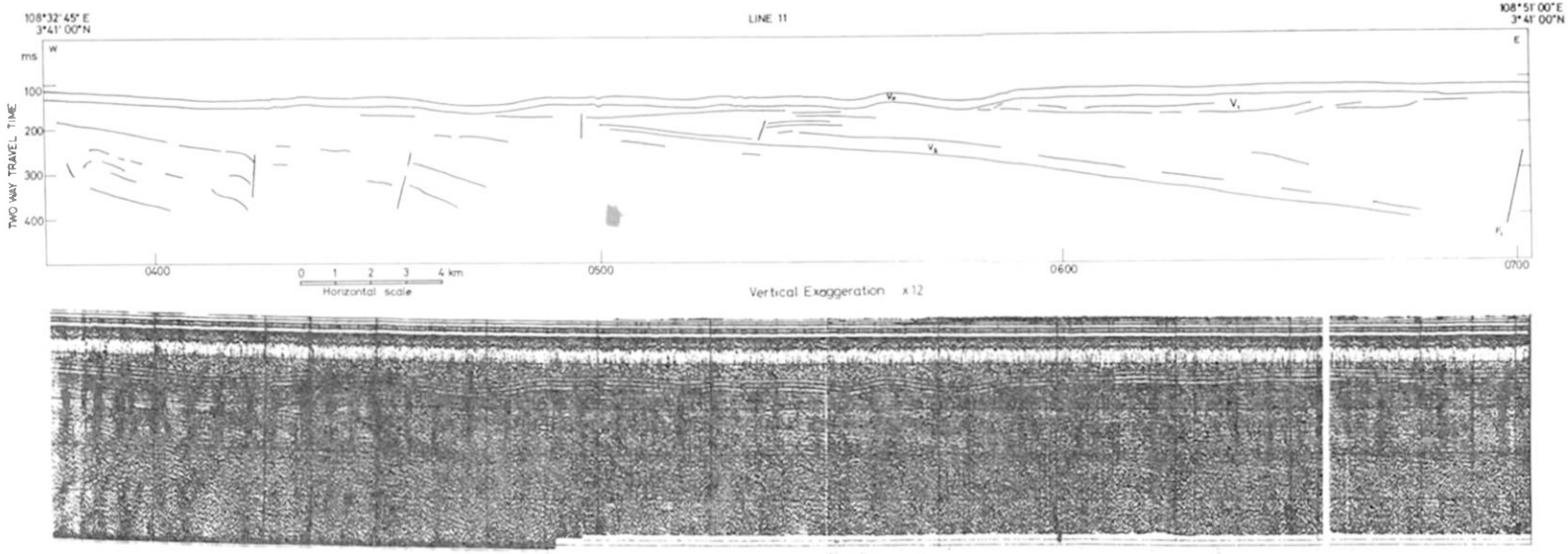

Figure IX-4. Original record and interpretation of seismic profile along Line 11, Fig. IX-1. Note fault F_1 at eastern end.

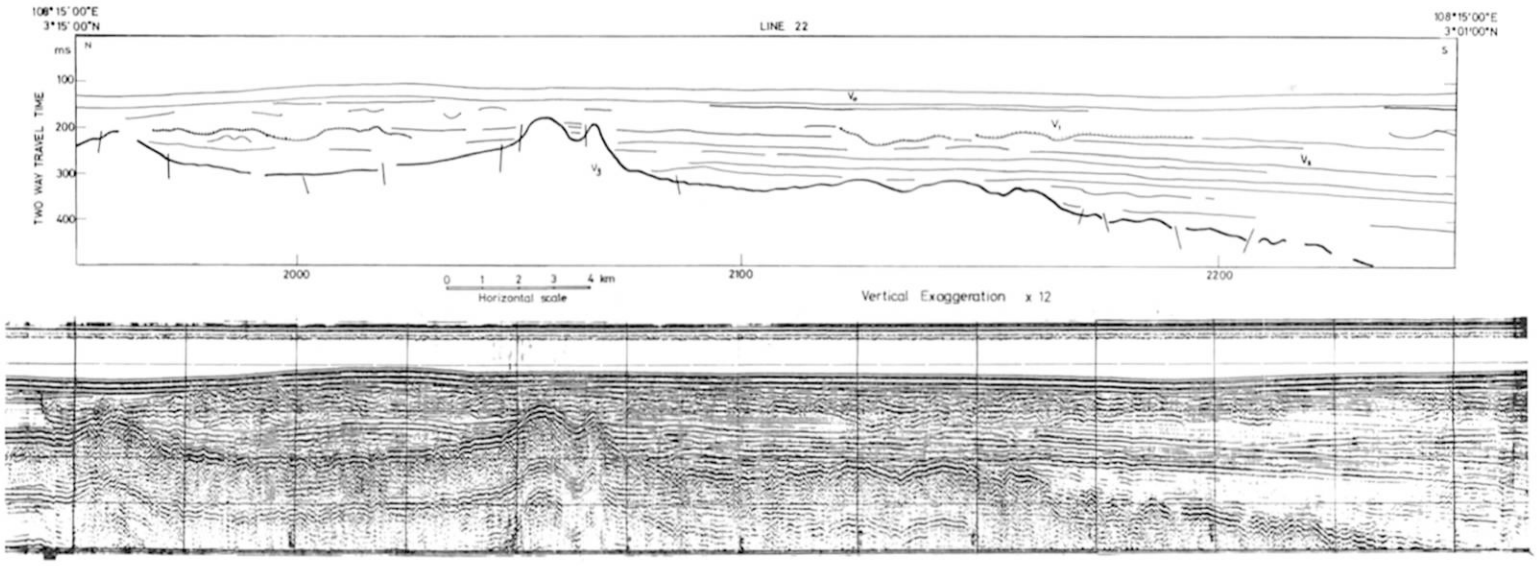

Figure IX-5. Original record and interpretation of seismic profile along middle part of Line 22, Fig. IX-1. Note acoustic basement surface with prominent ridge and structural pattern of overlying sediments.

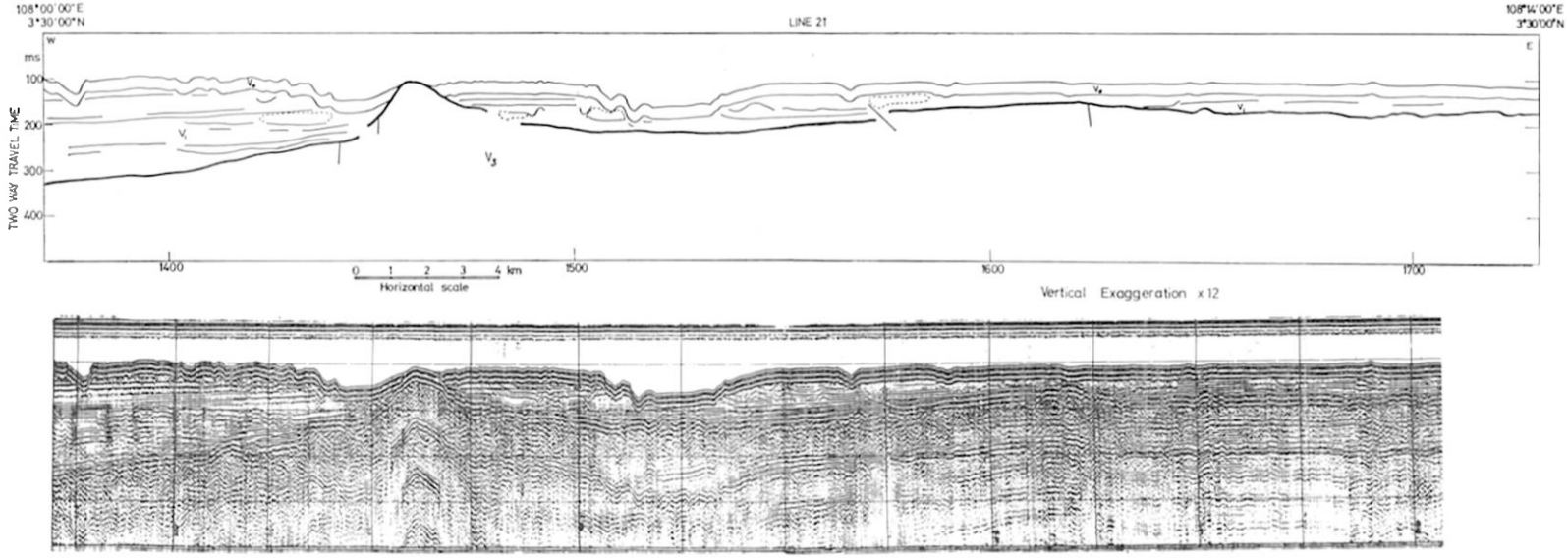

Figure IX-6. Original record and interpretation of seismic profile along Line 21, Fig. IX-1. Note subsea outcrop of acoustic basement and channels in sea floor.

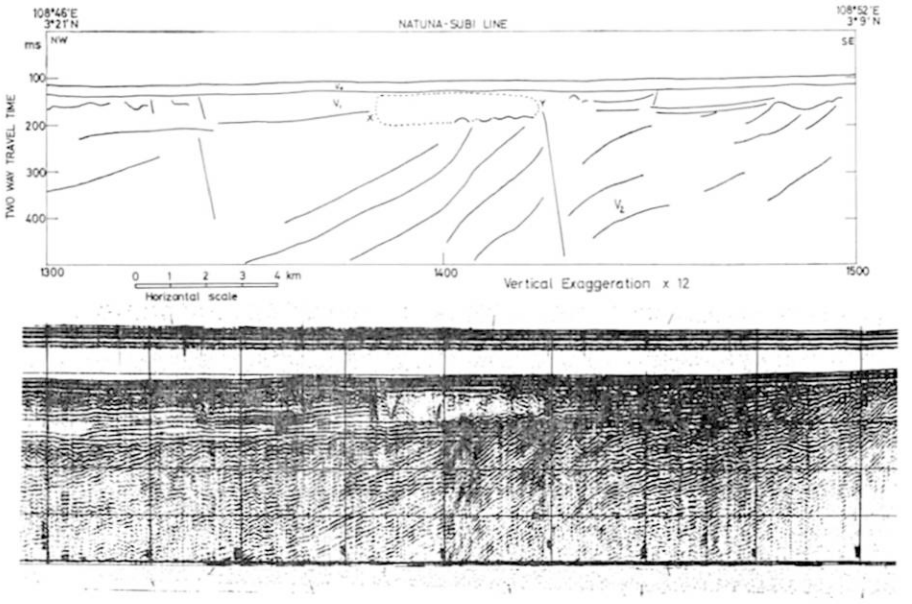

Figure IX-7. Original record and interpretation of seismic profile along southern part of Natuna-Subi Line, Fig. IX-1. Note the faulting and tilting of the sedimentary section in the V_2 layer and its effect on the V_1 layer; also the transparent zone, X-Y.

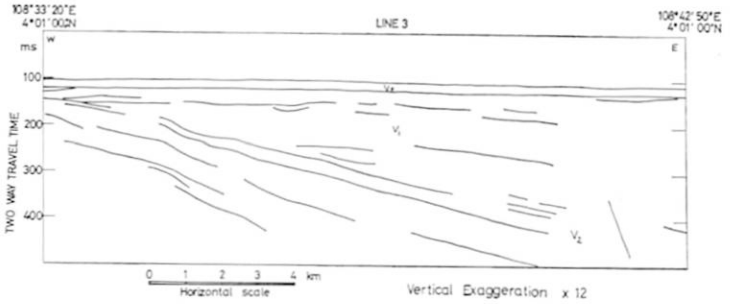

Figure IX-8. Interpretation of seismic profile along western part of Line 3, Fig. IX-1. Note the tilting and thickening of the sediments of the V_2 layer towards the east.

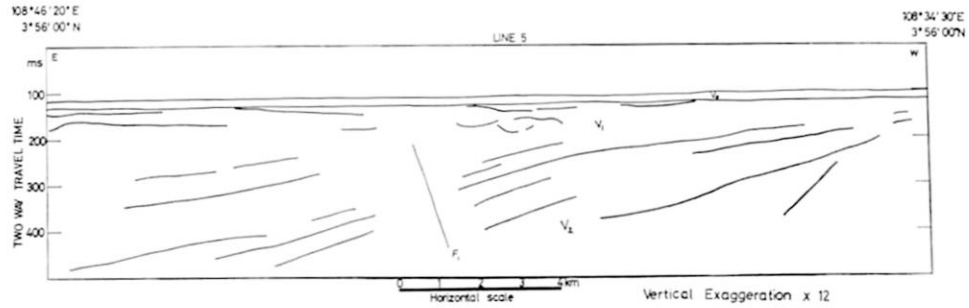

Figure IX-9. Interpretation of seismic profile along western part of Line 5, Fig. IX-1. Note features similar to Fig. IX-8 and the position of the fault, F_1.

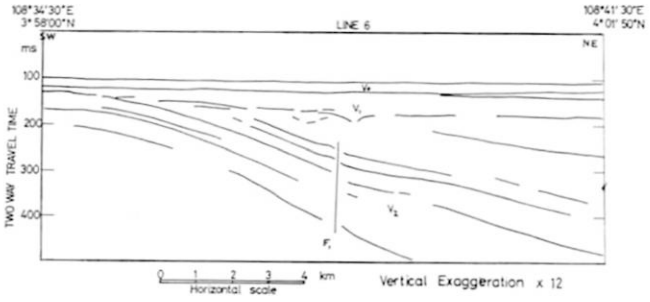

Figure IX-10. Interpretation of seismic profile along southwestern part of Line 6, Fig. IX-1. Note features similar to Figs. IX-8 and 9, and the position of the fault, F_1.

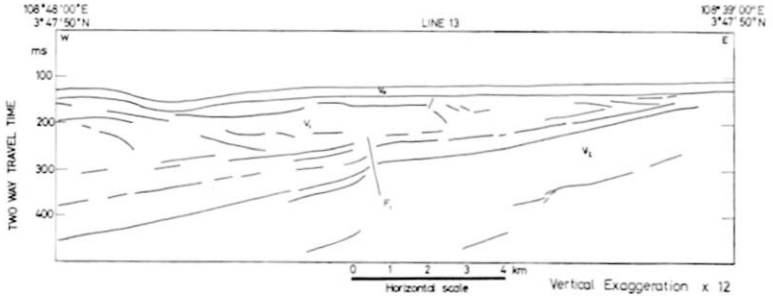

Figure IX-11. Interpretation of seismic profile along middle part of Line 13, Fig. IX-1. Note discordances in the V_1 layer and the position of the fault, F_1.

tion of them. On Lines 21 (Fig. IX-6) and 22 (Fig. IX-5) a basal layer beyond which there is no transmission of acoustic energy is clearly shown, which causes up to three multiples within the section. This basal layer has an irregular surface topography with some features of high topographic relief and there is evidence of faulting in some places. The remarkably irregular topography of the sea floor along Line 21 (Fig. IX-6) may be due to present day submarine processes of erosion. Fig. IX-7 shows the disturbed zone in the bedrock along the Natuna-Subi line; this line is parallel to the general trend of the faults in the area to the east of Great Natuna Island. On this section also, discrete absorption of energy quite close to the sea bed is evident in the V_1 layer between points X and Y; this feature is seen elsewhere in the region consistently at the same level. The profile along Line 11 (Fig. IX-4) is similar to that of the other east–west lines to the east of Great Natuna Island (Lines 1, 3, 5, 9, 13 on Fig. IX-1). Multiples are not so pronounced and the bedrock sediments dip towards the east and become thicker in that direction. In some places along the east–west lines the bedrock sediments are displaced by faults of unknown displacement which trend generally NNW–SSE.

The following velocity layers have been identified:

V_0, consisting of soft surface sediments thinly and uniformly distributed over the whole of the area surveyed.

V_1, consisting of sediments generally flat-lying or incompetently folded in places and filling depressions in the underlying surface. Where this can be identified with some certainty as an erosional feature (Figs. IX-5 and 7) it is marked with a dotted line.

V_2, consisting of well-consolidated sediments dipping northeastwards. This layer can be correlated with the Natuna Sandstone or a time equivalent thereof; it is probably thickest in the northeast part of the area surveyed and it appears to be absent in the south.

V_3, consisting of strongly faulted and/or folded rocks; these could be correlated with Mesozoic chert, siliceous shale and granite, exposed in parts of Great Natuna Island. This layer is found in the south and west of the area surveyed.

DISCUSSION

In the area between Great Natuna and Subi islands a channel with depths of 100 m or more extends SW–NE across the sea floor and becomes deeper and narrower towards the northeast (Fig. IX-12); it is generally 30–40 m deeper than the adjacent sea bed and varies in width from about 5–10 miles in the northeast to about 15 miles in the southwest. This channel forms part of the system termed the Sunda River by Molengraaf (1921). Kuenen (1950) and Molengraaf attribute the formation of the channel system to river action following glacial lowering of the sea level and exposure of the Sunda Shelf during the Pleistocene Ice Age. Another possible channel immediately southwest of Great Natuna Island is separated from the main channel by a swell or ridge trending SW–NE.

The traverses to the east of Great Natuna Island (Fig. IX-1) provide evidence of a faulted zone in this area. A major fault trending NNW–SSE, which can be correlated between Lines 6, 5, 9 and 13, is shown as F_1 on Figs. IX-10, 9, 3 and 11, respectively. Support for this correlation has been provided by other seismic surveys made to the

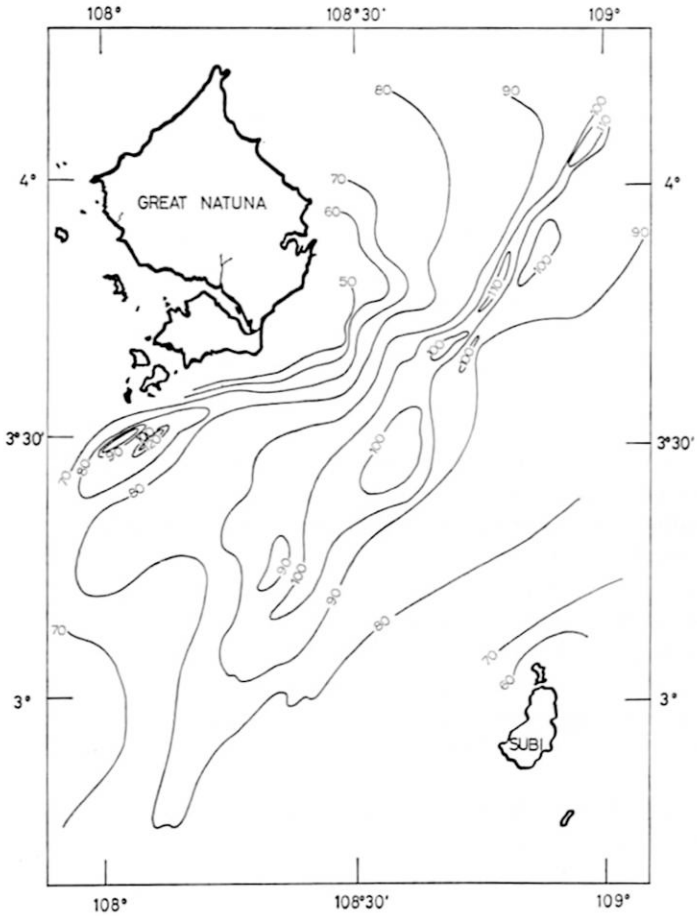

Figure IX-12. Bathymetric contours (in metres) on the sea floor between Great Natuna and Subi islands, South China Sea.

south of this area. In his regional map of the northern part of the Sunda Shelf, Mainguy (1968, map 1) shows a fault zone trending WNW–ESE extending seawards from Kuching, on the northwest coast of Borneo, which could be connected with fault F_1, as shown on Fig. IX-13. On the same figure, further north two fault zones have been defined. One, described by Dash *et al.* (1970) lies in the centre of the mouth of Gulf of Thailand and the other at the southern part of South Viet-Nam. While acknowledging that it is possible to connect F_1 with the fault system in South Viet-Nam, unpublished sources suggest that it may veer towards the west and subsequently connect with the fault in the Gulf of Thailand.

Koesoemadinata and Pulunggono (1971) recognize two main basinal areas on either side of a ridge termed by them the Natuna Ridge, which is here considered to be an extention of the Khorat-Kchol-Con Son Swell of Mainguy (1968), and is shown on Fig. IX-13 as the Khorat-Natuna Swell. These basins are the West Natuna Basin, the southern

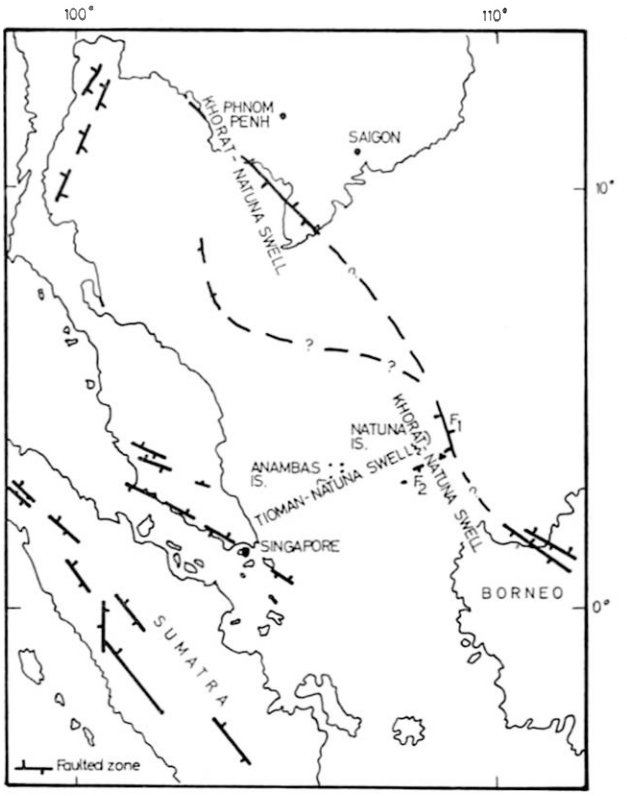

Figure IX-13. Regional structure in the northern part of the Sunda Shelf (data partly from map by Mainguy, "Tertiary Basins of Eastern Asia and their Offshore Extensions", revised April 1971).

boundary of which is marked by the Anambas Swell, and the Northwest Borneo Geosyncline which they suggest is terminated by a series of faults east of Great Natuna Island. The findings of the present survey generally support the existence of these two basins.

Preliminary results from seismic sections west of Great Natuna Island (Dash, 1971), however, show that the Anambas Swell proposed by Koesoemadinata and Pulunggono may in fact extend westwards to Tioman Island and eastwards to Great Natuna Island; this would then form the southern boundary of the West Natuna Basin. It is also felt that the Khorat-Natuna Swell may continue SSE from Natuna Island into southwestern Kalimantan, as shown on Fig. IX-13. Seismic sections from a previous cruise (Dash and Sano, 1969), some results of which are also presented here (Figs. IX-14 to 18, lines C, G, J, L and M), indicate the presence of a folded and faulted zone trending SW–NE between the islands of Great Natuna and Subi, shown as F_2 on Figs. IX-13, 15, 16 and 17, which may form part of the Khorat-Natuna Swell.

The islands off the southwest tip of Great Natuna Island are composed of Mesozoic chert, or gabbro, diorite and norite (Haile, 1970). Part of Lines 21, 22 and M pass close to these islands and, in this area, the basal layer, V_3, is mostly at shallow depth

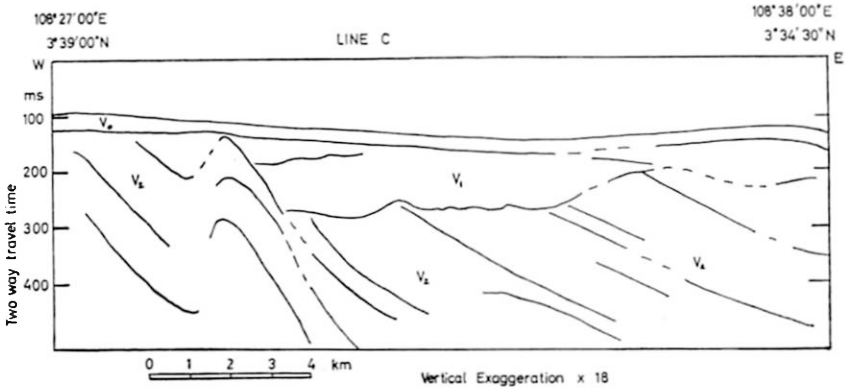

Figure IX-14. Interpretation of seismic profile along Line C, Fig. IX-1. Note the tilting of the sedimentary section in the V_2 layer towards the east and deformation by folding and/or faulting at the western end, and the erosional feature in the V_1 layer.

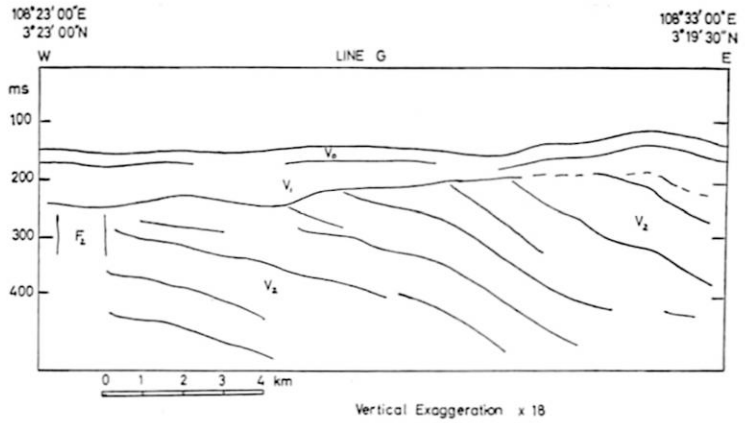

Figure IX-15. Interpretation of seismic profile along Line G, Fig. IX-1. Note features similar to those on Fig. IX-14 and the fault zone, F_2.

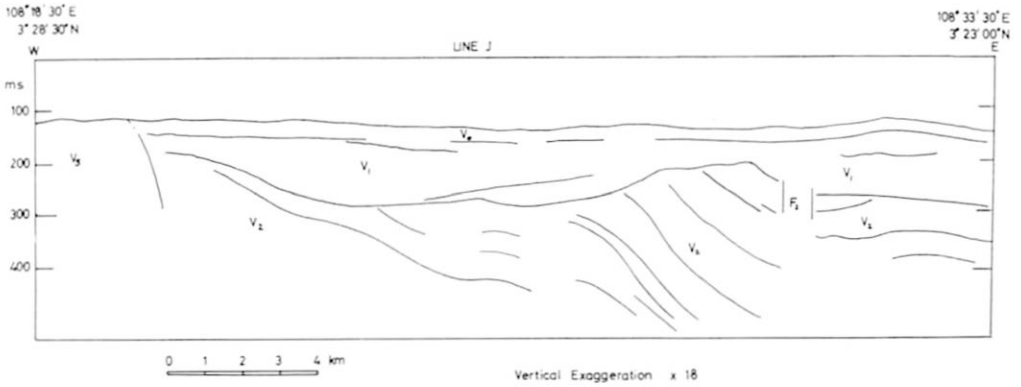

Figure IX-16. Interpretation of seismic profile along Line J, Fig. IX-1. Note features similar to those on Figs. IX-14 and 15, the fault zone, F_2, and the possible outcrop of acoustic basement, V_3, at the western end of the profile.

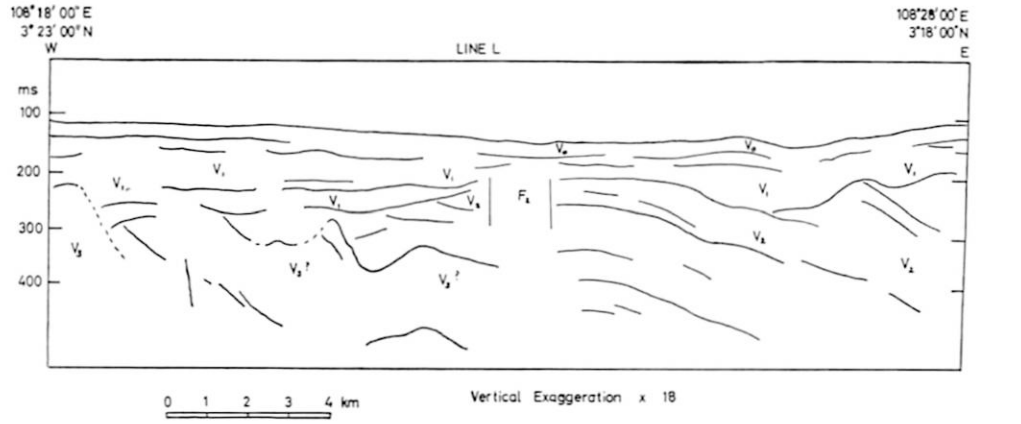

Figure IX-17. Interpretation of seismic profile along Line L, Fig. IX-1. Note features similar to those on Figs. IX-14 to 16, the position of the fault zone, F_2, and the presence of probable acoustic basement at depth.

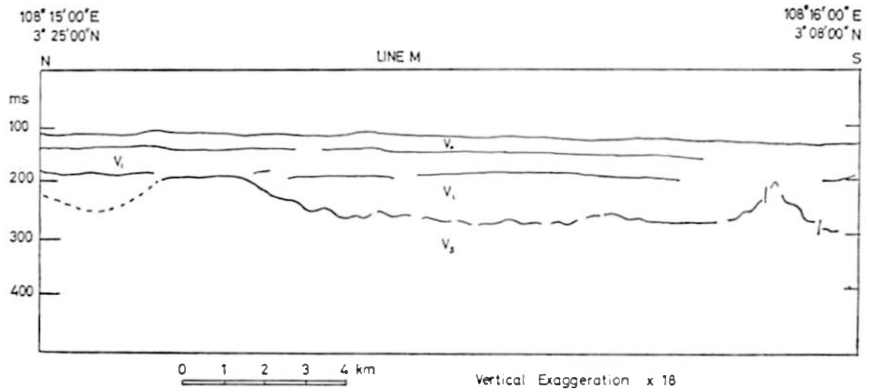

Figure IX-18. Interpretation of seismic profile along Line M, Fig. IX-1. Note the acoustic basement, V_3, at depth with ridge-like features, unconformably overlain by sediments of the V_1 and V_0 layers.

below the overlying sediments (Figs. IX-5, 6 and 18) and actually crops out at one point on Line 21 (Fig. IX-6). The top of the basal layer, which is considered to represent the surface of basement rocks similar to those exposed on the small islands southwest of Great Natuna, plunges to the south. A specimen of granite from Ranai, on the east coast of Great Natuna Island, has been assigned an age of 73 plus or minus 2 million years, which would date the emplacement as late Cretaceous (Harle, 1970).

The Natuna Sandstone, of probable Tertiary age, lies unconformably over the Mesozoic basement rocks; the largest exposure is in the northern part of Great Natuna Island, where it dips gently in a northerly direction (Haile, 1970), and its thickness appears to be at least 1,000 m. The sequence continues into the offshore area where it thickens and may grade into marine facies.

Gravitational slumping, fault movements and the dip of 8–10 degrees of the Natuna sediments in the eastern part of the area surveyed suggest that the Mesozoic basement has either been uplifted in the west or downthrown in the east since the time the Natuna sediments began to be deposited. It is likely therefore that the basin containing the Natuna Sandstone is quite deep, especially in the northeastern part of the area surveyed, and this may be connected with the transverse faulting on the Khorat-Natuna Swell.

In the V_1 layer, there are a number of channel-like incisions apparently cut by a river system flowing across the northern part of the Sunda Shelf at times of emergence during the Pleistocene Ice Ages; these have been subsequently infilled by incompetently folded and slumped beds.

SUMMARY

Basinal and ridge-like features can be distinguished in the area surveyed on the basis of the seismic profiles below the sea floor. The Khorat-Natuna Swell may be linked with both mainland Asia and Kalimantan as shown in Figure IX-13; this swell is crossed

by faulting to the north and south of Great Natuna Island and its eastern edge is marked by a fault zone which probably steps down into the Northwest Borneo Geosyncline. It is suggested that another swell extends from Tioman Island, off the east coast of West Malaysia, through the Anambas Islands to Great Natuna Island, forming a divide between basins to the north and south.

The deepest layer (V_3) recorded in the surveys is a low frequency, high velocity layer of probable Mesozoic age which is related in some way to the swells. The V_2 layer, represented by a thick sequence of sediments, can probably be correlated with the Natuna Sandstone, as described by Haile (1970). These layers were subsequently dissected by Pleistocene rivers during periods of emergence and infilling of the channels by younger sediments can be seen in places. The sea bottom topography shows the trend of the major channels eroded by the Sunda River which flowed from southwest to northeast between Great Natuna and Subi islands.

ACKNOWLEDGMENTS

This investigation was partly supported by the Overseas Development Administration of the British Government. Some of the equipment used was on loan from the Natural Environment Research Council of Great Britain. The research vessel R. I. Jalanidhi was provided for these investigations jointly by the Ministry of Mines, the Indonesian Institute of Sciences and the Naval Hydrographic Office of the Republic of Indonesia. Scientists from Indonesia and Malaysia also took part in the expedition. The Technical Secretariat of CCOP assisted with the preparations for the project. This project could not have been successfully carried out without the co-operation of the above-mentioned organizations for which the authors wish to express their appreciation. Our grateful thanks are due to Cdr. Ch. Melontige, captain of the Jalanidhi, and his crew for their help. Thanks are also due to the Continental Oil Company of Indonesia and Western Geophysical Co. of Singapore for rendering effective help when it was most needed.

REFERENCES

Burton, C. K., 1970, The palaeotectonic status of the Malay Peninsula: *Palaeogeography, Palaeoclimatology, Palaeoecology*, vol. 7, no. 1, p. 51.

Dash, B. P. and Sano, S., 1969, Preliminary note on sparker profiling on the Sunda Shelf: United Nations ECAFE, *Report of sixth session of CCOP*, p. 75–77, fig. 3–1.

————, Ahmed, K. O., and Hubral, P., 1970, Seismic investigation in the region of Poulo Panjang, offshore from southwestern Viet-Nam: United Nations ECAFE, *CCOP Tech. Bull.*, vol. 3, p. 37–54, figs. III-1 to 10, tables III-1 to 4.

————, 1970, Preliminary report on basic geologic and geophysical research in the eastern offshore area of West Malaysia: United Nations ECAFE, *Report of seventh session of CCOP*, p. 85–87, fig. 10–1.

————, Guru, S. and Tooms, J. S., 1972, Preliminary report of seismic refraction survey

southeast of Natuna Islands and seismic profiling in the vicinity of the Natuna and Tioman Islands on the Sunda Shelf: United Nations ECAFE, *report of eighth session of CCOP*, doc. 13 (in press).

Dash, B. P., 1972, Preliminary report on seismic refraction survey southeast of Natuna Islands and seismic profiling in the vicinity of the Natuna and Tioman Islands on the Sunda Shelf: United Nations ECAFE, *Report of eighth session of CCOP*, doc. 13 (in press).

Dietz, R. S. and Holden, J. C., 1970, Reconstruction of Pangaea: Breakup and dispersion of continents, Permian to Present: *Journ. Geophys. Res.*, vol. 75 (26), p. 4939–4956.

Emery, K. O. and Niino, H., 1963, Sediments of the Gulf of Thailand and adjacent continental shelf: *Geol. Soc. Am. Bull.*, vol. 74, p. 541–554.

Fromaget, J. and Saurin, E., 1952, Carte geologique, Viet-nam, Cambodge, Laos.

Haile, N. S., 1970, Notes on the geology of the Tambelan, Annambas and Bunguran (Natuna) Islands, Sunda Shelf, Indonesia, including radiometric age determinations: United Nations ECAFE, *CCOP Tech. Bull.*, vol. 3, p. 55–89, figs. IV-1 to IV-6, tables IV-1 to IV-3, pls. IV-1 to IV-10.

Kaufmann, G. F., 1961, Petroleum developments in Far East during 1960: *Am. Assoc. Petroleum Geologists Bull.*, vol. 45, p. 1224–1243.

Koesoemadinata, R. P. and Pulunggono, A., 1971, Offshore Tertiary sedimentary basins in Indonesia: Paper presented at 12th Pacific Science Congress, Canberra (unpublished).

Kuenen, P. H., 1950, Marine geology: John Wiley & Sons, Inc., New York, London.

Le Pichon, X., 1968, Sea floor spreading and continental drift: *Journ. Geophys. Res.*, vol. 73, no. 12, p. 3661–3697.

Mainguy, M., 1968, Regional geology and prospects for mineral resources on the northern part of the Sunda Shelf: United Nations ECAFE, *CCOP Tech. Bull.*, vol. 1, p. 129–142, maps 1, 2.

———, 1970, Regional geology and petroleum prospects of the marine shelves of eastern Asia: United Nations ECAFE, *CCOP Tech. Bull.*, vol. 3, p. 91–107, maps V-1 and 2.

Molengraaf, G. A. F., 1921, Modern deep-sea research in the East-Indian Archipelago: *Geog. Journ.*, vol. 57, p. 95.

Parke, M. L., Emery, K. O., *et al.*, 1970, Structural framework of the continental margin in the South China Sea. United Nations ECAFE, *CCOP Tech. Bull.*, vol. 4, p. 103–142, figs. VI-1 to 20, table VI-1.

Ridd, M. F., 1971, S. E. Asia as a part of Gondwanaland: *Nature*, vol. 234, p. 531.

X. GEOLOGICAL STRUCTURE AND SOME WATER CHARACTERISTICS OF THE JAVA SEA AND ADJACENT CONTINENTAL SHELF[1]

(Project CCOP-1/IND. 1)

By

K. O. Emery[2], Elazar Uchupi[2], John Sunderland[3], H. L. Uktolseja[4], and E. M. Young[2]

(with figures X-1 to X-18)

ABSTRACT

About 7,400 km of geophysical traverses were made in the Java Sea and adjacent continental shelf during June and July 1971 aboard the Woods Hole Oceanographic Institution's research vessel CHAIN as a contribution to the ECAFE—CCOP program. In addition to the geophysical measurements of seismic reflection and refraction, magnetics, gravity, and bathymetry, data were obtained on surface water temperature, salinity, color, content of suspended sediment, and wave direction and period.

Extrapolation from well data both onshore and offshore indicates that two types of basement are delineated by the seismic reflection profiles. One type, an irregular surface in the profiles, consists of pre-Tertiary igneous and metamorphic rocks. The other, a smoother surface, is probably the top of a lower Miocene limestone whose acoustical impedence masks the real basement, particularly where the latter is deep. North of Bangka and Belitung islands the igneous and metamorphic basement is very shallow, forming a broad platform. In the Java Sea farther southeast this basement takes the form of a series of ridges and basins or troughs that trend northeasterly from Sumatera and Java to Kalimantan (Borneo), and it is part of the East Indian tectonic ridge complex that has been studied by many authors. Drill hole data and gravity measurements obtained aboard CHAIN indicate that the total sediment above the igneous and metamorphic basement may reach thicknesses of 3 km in the basins and troughs between the ridges. Folds, faults, and pinch outs in the basin sediments justify widespread expectation that the Java Sea may be a major oil and gas region.

High frequency (3.5 kHz) acoustic profiling shows the presence of many cut-and-fill structures in the uppermost 50 m of the sea-floor sediments. These are attributed to subaerial

1: Contribution No. 2727 of the Woods Hole Oceanographic Institution
2: Woods Hole Oceanographic Institution, Woods Hole, Mass., U.S.A.
3: Institute of Geological Sciences, London, England
4: Indonesian Naval Hydrographic Office, Djakarta, Indonesia

erosion of the region during Pleistocene stages of glacially lowered sea level. The drainage pattern postulated long ago by Molengraaff on the basis of topography alone is supported reasonably well by the new data of CHAIN.

The cruise occurred during the season of the southeast monsoon which produced currents and swells that moved westward and northward around Kalimantan. The water became warmed as it flowed over the shallow sea floor, and it became less saline along the shores through dilution by runoff from Java, Sumatera, and Kalimantan. The same runoff contributed quantities of suspended sediments that caused the blue water of the open sea to become greenish near shore. Large plankton blooms were observed in the western part of the sea and shelf. Similar plankton blooms and contributions of fine-grained sediments during the past contributed to the basin fillings and helped to produce their oil-rich character.

ICHTISAR[5]

Djarak penjelidikan laut Geofisika sepandjang kira2 7400 km telah dilalui di Laut Djawa dan paparan benua disekitarnja selama bulan2 Djuni dan Djuli 1971, oleh kapal penjelidik R. V. Chain milik Woods Hole Oceanographic Institution, sebagai salah satu atjara progamma hasil kerdjasama ECAFE-CCOP.

Disamping pengukuran2 geofisika laut jang berupa-seismic reflection and refraction, magnetics, gravity, dan bathymetry; djuga dilakukan penelitian terhadap-temperatur permukaan air laut, salinitas, warna air laut, banjaknja zat jang me-lajang2 didalam air laut (content of suspended sediment) dan arah/perioda dari gelombang/ombak.

Ekstrapolasi dari data2 jang didapat baik dari daratan maupun lautan menund-jukkan bahwa-dua matjam basement telah dibentuk oleh profil2 seismik (seismic profiles).

Matjam pertama-suatu permukaan jang tak teratur pada profil2, jang terdiri dari batu2an pre-Tertiar dan batu2an metamorphic; dan jang lainnja-matjam kedua- suatu permukaan jang lebih teratur, jang mungkin adalah permulaan dari lower Miocene limestone jang mempunjai tjiri2 acoustical impedence menjerupai basement sebenarnja, teristimewa dapat dilihat pada bagian2 dari matjam kedua jang lebih dalam letaknja.

Disebelah Utara pulau2 Banka dan Biliton igneous dan metamorphic basement-nja sangat dekat kepermukaan laut atau terdapat pada kedalaman2 jang ketjil, jang membentuk suatu platform jang luas/lebar. Dilaut Djawa dan perpandjangannja kearah tenggara, basement tersebut mempunjai bentuk jang terdiri dari seri2 Ridges dan Basins jang berasal atau merupakan perpandjangan arah ke timur laut dari Sumatera dan Djawa ke Kalimantan, dan hal ini adalah bagian dari East Indian tectonic ridge complex jang telah dipeladjari/diketahui oleh banjak pengarang2 sebelumnja.

Hasil pengeboran dan pengukuran2 gravity jang dilakukan R. V. Chain menundjukkan bahwa-sedimen jang terdapat diatas igneous dan metamorphic basement, dapat mentjapai suatu lapisan setebal 3 km pada basin2 diantara ridges. Lipatan2, patahan2/retakan2 dan tondjolan2 pada sedimen2 dari basin menundjukkan/membuktikan besarnja kemungkinan, bahwa laut Djawa adalah suatu daerah minjak dan gas jang besar.

High frequency (3.5 kHz) acoustic profiling menundjukkan adanja banjak struktur2 "cut-and-fill" (cut-and-fill structures) pada lapisan2 atas setebal 50 m dari sedimen2 dasar laut. Struktur2

5: Abstract in the Indonesian language.

ini terdapat pada subaerial erosion dari daerah tersebut selama masa Pleistocene pada djaman glasial penurunan permukaan laut.
Pendapat2 terdahulu jang telah dirintis pada waktu2 jang silam oleh Molengraaff dengan tjara dasar topografisnja memberikan suatu perpaduan hasil jang baik dengan data2 jang baru dari R. V. Chain.
Pelajaran R. V. Chain tersebut berada dibawah pengaruh musim Tenggara, jang mana arus dan gelombang ombak pada saat itu bergerak kearah Barat dan Utara mengelilingi Kalimantan. Keadaan air laut mendjadi panas (temperatur air naik) ketika mengalir melalui laut jang dangkal, dan salinitasnja mengetjil sepandjang pantai Djawa, Sumatera dan Kalimantan jang disebabkanoleh pengaruh sungai jang bermuara dilaut.
Air sungai jang bermuara dilaut itu djuga, dengan banjaknja zat2 jang melajang2 didalamnja (suspended sediment), menjebabkan perubahan warna dari-biru pada laut jang terbuka, mendjadi-hidjau didekat pantai. Bunga2 plankton (plankton blooms) jang ter-apung2 djuga diketemukan pada daerah2 disebelah Barat dari paparan tersebut.
Bunga2 plankton sematjam itu pada djaman sekarang dan hasil contribusi dari sedimen2 jang halus (contributions of fine-grained sediments) pada masa2 silam, menghasilkan pengisian basin dasar laut dengan sifat2 untuk pembentukan minjak setjara kimiawi-organis.

INTRODUCTION

The United Nation's Economic Commission for Asia and the Far East established a Committee for Co-ordination of Offshore Prospecting (CCOP) in 1966 in order to learn something of the geological structure and general economic potential of the continental margin off eastern Asia. A contribution to the success of the program was made by R/V F. V. HUNT (a civilian geophysical survey ship on contract to the U.S. Naval Oceanographic Office), aboard which a reconnaissance study was made of the structure of the East China Sea and the Yellow Sea during 1968 (Emery *et al.*, 1969; Wageman, Hilde, and Emery, 1970). The shipboard work was supplemented by special airborne magnetic measurements of Project MAGNET of the U.S. Naval Oceanographic Office. During 1969 R/V HUNT extended the reconnaissance geophysical work into the South China Sea and Gulf of Thailand as far south as Singapore (Parke, *et al.*, 1971).

Changes in priorities of the U.S. Naval Oceanographic Office ended the cruises of R/V HUNT on behalf of ECAFE-CCOP. However, one of the ships of the Woods Hole Oceanographic Institution, R/V CHAIN (Fig. 1), was scheduled to be in the southeast Asian region as part of a round-the-world scientific cruise. Her presence gave an opportunity to continue southeastward the studies made aboard R/V HUNT. Funding for this work was provided by National Science Foundation (Grant GA-27449). Most of the geophysical equipment aboard CHAIN had been accumulated during many years of support by the Office of Naval Research (Contracts NOOO14-66-CO241 and NONR-4029-00) and National Science Foundation (Grants GA-1209, GA-279, GA-283, GA-12204, GA-1454, and GA-28193). The air compressor for the air guns and the filter arrangement for suspended sediments was kindly lent by the U.S. Geological Survey at Woods Hole.

Shipboard participation by Sunderland and Lo was permitted by travel funds from

their governments and by Uktolseja and Noer from UNESCO. The cruise began 22 June at Singapore and ended 14 July at Darwin, Australia, traversing the broad continental shelf north of Bangka and Belitung islands, the Java Sea south and east of these islands, and the Java Trench south of Lombok. It is referred to as R/V CHAIN Cruise 100, Leg 7 and is included in the work program of CCOP as project CCOP-1/IND. 1. Microfilm copies of the records have been transmitted to the National Geophysical Data Center, ECAFE headquarters in Bangkok, and Pertamina in Djakarta.

Much has been learned about the geology of the Indonesian islands by Netherland scientists (Umbgrove, 1938; van Bemmelen, 1949). Studies of marine gravity (Vening Meinesz, 1932–1934) and of bathymetry in the region (Kuenen, 1935) led to considerable speculation about the composition, structure, and origin of the Indonesian Island Arc and adjacent regions. All of this marine work preceded the development of modern techniques for seismic reflection and refraction, magnetics, and gravity from surface ships. Subsequently, many geophysical studies have been made in the region by oil companies or their contractors (Humphrey, 1970, 1971; Petroleum News South East

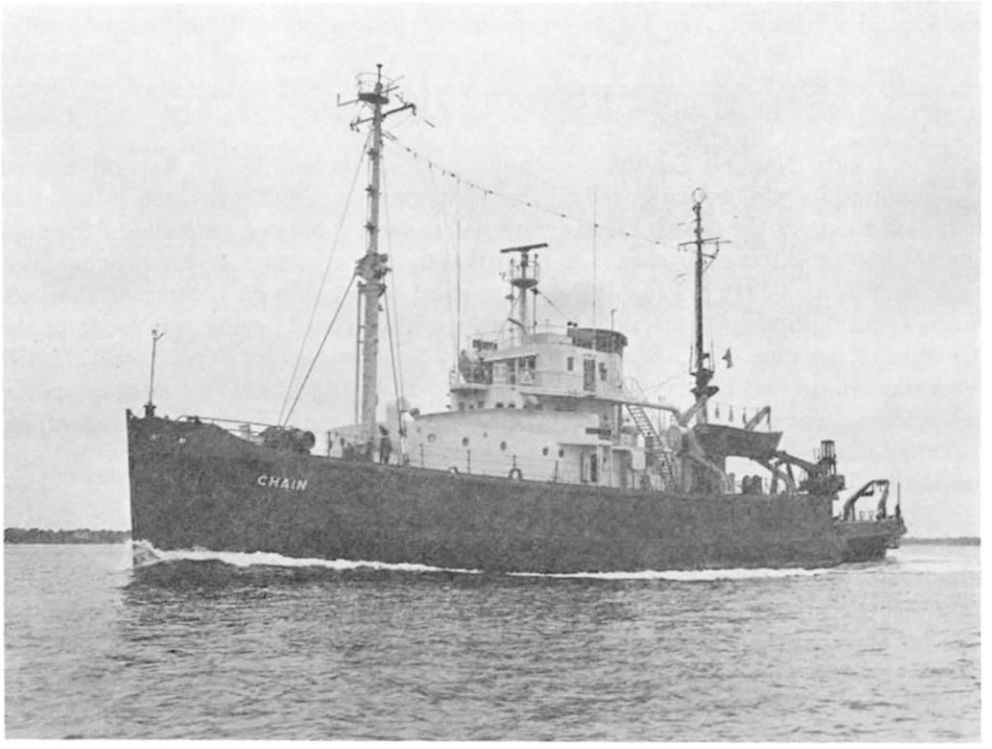

Figure X-1. R/V CHAIN, a former U. S. Navy salvage ship converted for oceanographic work in 1958 and assigned to the Woods Hole Oceanographic Institution. She has a length of 67 m and a displacement of 2,100 tons, with accomodations for 33 crew and 25 scientists. Laboratories and equipment are easily modified or exchanged for different missions. For geophysics she is able to do seismic reflection and refraction, magnetics, gravity, and heat flow; for geology—coring, dredging, photography, bathymetry, and other work as required. Navigation is by satellite, loran, radar, and celestial methods.

Asia, 1970, 1971), but the results are proprietary and not available for a synthesis of regional geology that was the object of the R/V CHAIN cruise.

The shipboard measurements were possible only through the cooperation of a fine group of technicians from the Woods Hole Oceanographic Institution: J. W. Mahoney, Jr., C. B. Morehouse, and W. Schmidt (laboratory watch chiefs), Bruce Simon (gravimeter), Don E. Woods and N. D. Gamble (satellite navigation and computer center), and P. A. Jezek (geological assistant). The watches were aided by Jen-Chu Lo (Chinese Petroleum Corporation, Taipei, Republic of China) and Hafny M. Noer (Geological Survey of Indonesia, Bandung, Indonesia), both of whom were particularly interested in the geophysical techniques employed aboard R/V CHAIN. Especial appreciation is due Captain Michael Palmieri and his officers and crew for their close cooperation in achieving the results of the cruise.

Primary effort in the interpretation of the data aboard ship was as follows: magnetics, 3.5 kHz profiles, and general synthesis—Emery, continuous seismic reflection profiles—Uchupi, gravity and seismic refraction—Sunderland, and water characteristics —Uktolseja; the adjustment and proper operation of the geophysical systems was handled by Young. The authors prepared this report aboard ship except correcting for the drift of the gravimeter, weighing of suspended sediments, final drafting of the illustrations, and slight modification of the text on the basis of a few publications that were not available aboard ship. This method assured that a summary of the cruise could be given by Emery near the end of the ECAFE-CCOP meeting at Manila (6 to 16 July 1971).

TOPOGRAPHY AND BOTTOM MATERIALS

The Java Sea is the southeastern part of the great Sunda Shelf that extends in a broad sweep from the Gulf of Thailand around the western and southern sides of Kalimantan (formerly Borneo). This study is restricted to the part of the shelf that lies southeast of Singapore, an area of nearly 770,000 sq. km bordered by Kalimantan on one side and by Sumatera and Java on the other (Fig. X-2). Its length is about 1,700 km and its average width is 450 km.

Lands that border the Java Sea and adjacent shelf have considerable relief and rise as high as 4,000 m above sea level. Even the small islands that rise above the shallows commonly reach elevations of more than 100 m. Most large and small islands consist of Cenozoic sedimentary rock resting on Paleozoic and Mesozoic sedimentary, igneous, and metamorphic rocks. Separating the Java Sea from the open ocean is the Indonesian Island Arc and beyond that the Java Trench with depths in excess of 6,500 m. The island chain and trench are the sites of numerous earthquakes, whose hypocenters lie near a plane sloping northward to depths of 300 to 600 km below sea level (Fitch, 1970; Fitch and Molnar, 1970). Rising above the hypocenters that are at a depth of 100 to 200 km are the many volcanoes of the island arc. In contrast, the Java Sea and adjacent continental shelf are almost free of earthquakes and volcanoes.

Depths of the Java Sea and shelf in the area of Figure 2 average about 30 m, with a maximum of 90 m just north of Madura, about the same as the depth of the shelf-

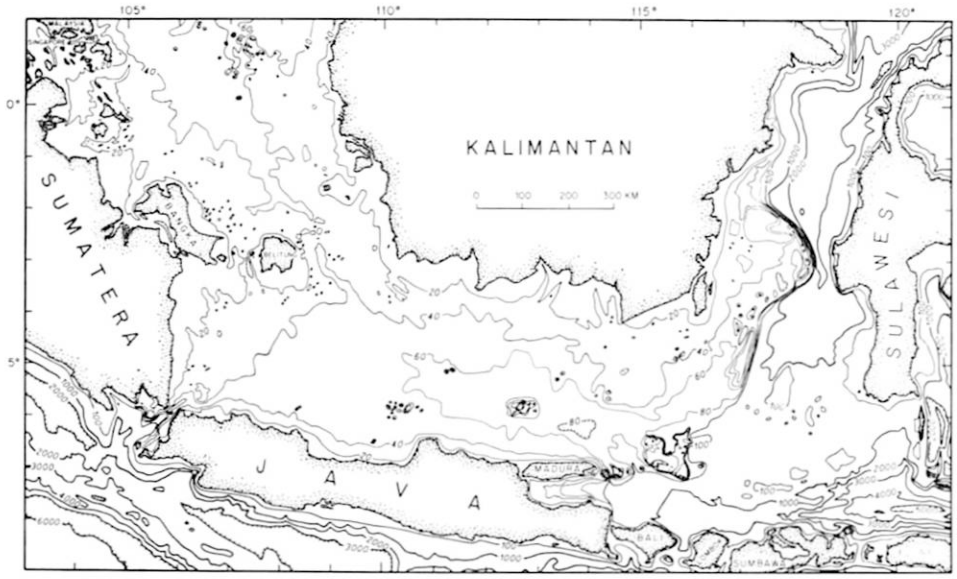

Figure X-2. Generalized bathymetry is areas shallower than 100 m was compiled from lead-line soundings given by U. S. Navy Hydrographic Office navigational charts 1170 and 3001 plus acoustic soundings from R/V CHAIN; bathymetry in deep water is from contours drawn by Fisher (1968).

break between Madura and Kalimantan. The topography of some areas shallower than about 30 m is irregular owing to rock outcrops and locally to the growth of algal and coral reefs. Other shallow areas and ones of greater depth are relatively smooth and flat, evidently the result of deposition of detrital sediments derived by streams and currents from Kalimantan, Sumatera, and Java. The dominant effect of these terrigenous sediments upon the bottom topography is suggested by the restriction of the greater depths to areas farthest from the sources. Some land-derived sediment also is contributed in the form of large floating islands of trees, underbrush, and grass washed out by the rivers of Kalimantan and carrying masses of sediment and rocks (U. S. Navy Hydrographic Office, 1951, p. 153, 170). A relatively minor amount of sediment is brought into the region from the Australian desert by the southeast monsoon winds (U. S. Navy Hydrographic Office, 1951, p. 11). This dust produces much haze during the summer, and most of the dust must settle to the ocean surface. In addition, suspended sediment in the surface water northeast of Singapore contains volcanic glass shards brought by the northerly-flowing currents from the Java Sea, probably through resuspension from the sea floor (Parke *et al.*, 1971).

The distribution pattern of bottom sediments on the shelf and sea floor was compiled from the 33,000 notations on original sounding charts (Emery, 1969). *Mud* is the chief sediment, covering about 58 per cent of the floor. Areas of *sand* surround outcrops of *rock* and patches of *coral* and *gravel*. Commonly, the areas of sand and those of mud are separated by belts of *mud-and-sand* that were combined with *mud* in the simplified version of Figure X-3.

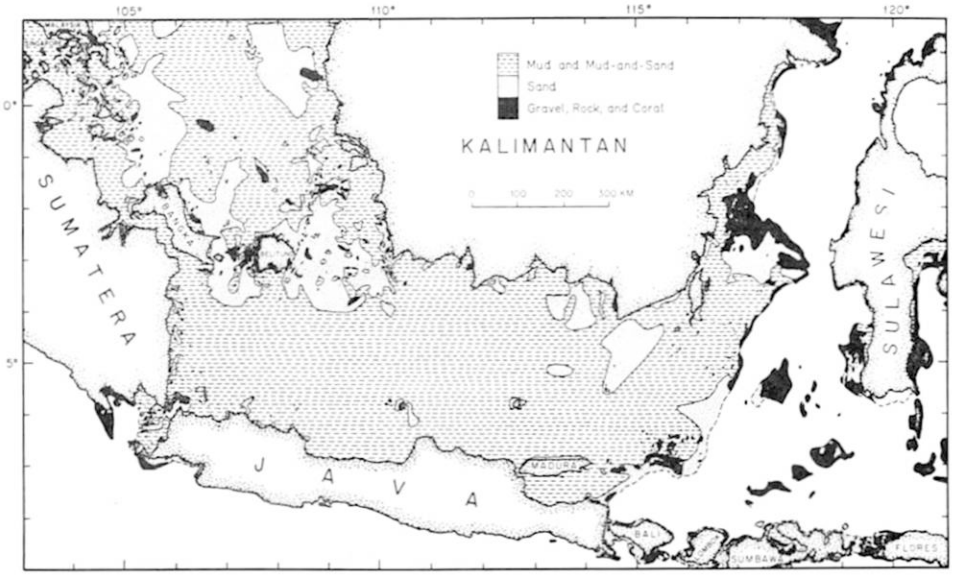

Figure X-3. Sediment map showing the distribution of *mud*, plus *mud-and-sand*, and *sand*, and *gravel* plus *rock* plus *coral* simplified from a chart by Emery (1969) that is based upon 33,000 bottom notations from original lead-line sounding charts.

METHODS

The spacing and direction of the geophysical traverses were chosen to provide the greatest amount of information about regional structure during the available time for ship work. Positions along the traverses were determined mainly by satellite navigation with occasional checks by dawn and dusk star fixes and by radar ranges and bearings off the steep-sided islands. All positions were checked for consistency with ship course and speed and plotted in chart form by the on-board computer (Hewlett-Packard 2116A with Extender 2150A and Cal Comp 563 and 564). Similarly, the computer converted time to distance along the traverses and merged the distance with the magnetic, gravity, and bathymetry data in the form of continuous profiles. Ship speed ranged from as slow as 6 km/hour for the recording of radiosonobuoy data to as fast as 16 km/hour for seismic profiles over shallow basement. A total of 6,000 km of seismic profiles and 7,400 km of bathymetry, magnetics, and gravity were recorded during the CHAIN cruise from Singapore to Lombok plus the approach to Singapore during the previous leg. Forty radiosonobuoys were used.

Bathymetry was obtained from 3.5 kHz returns from a hull-mounted transducer continuously recorded on a Precision Graphic Recorder. The recordings provided shallow (to 50-m penetration) structure beneath the bottom, mainly cut-and-fill features probably dating from Pleistocene times of glacially lowered sea level.

Continuous seismic reflection profiles were based upon two different sound sources

that were used both separately and together at various times in a search for the combination that provided the best data. One source was a spark discharge of 85,000 to 95,000 joules of stored energy released at 10-second intervals from single or 11-electrode units trailed about 10 m astern of the ship and at 10-m depth. The other source was an air gun of 40, 120, or 300 cubic-inch volume at a pressure of 1,800 pounds per sq. inch and discharged at 10- to 40-second intervals. Best results in the shallow sea were obtained with the spark source alone. Echoes from the bottom and sub-bottom reflectors were received on two 30-m streamers towed one from each quarter of the ship with the leading ends about 70 m astern and about 7 m deep; each streamer contained 200 pressure-sensitive detectors. The signals from the two streamers were amplified, algebraically added to reduce noise relative to signal, band-pass filtered generally between 20 and 50 Hz and recorded on three Precision Graphic Recorders, one having a 5-second sweep rate and the other two a 2.5-second rate. Recording was only in analog form, which of course allowed multiple bottom reflections to partly obscure the sub-bottom reflections. In addition, about two-thirds of the traverses (particularly where acoustic basement was deep) were recorded unfiltered on magnetic tape for possible more elaborate processing and printing at Woods Hole. Aboard ship, the 48-cm wide paper recordings were overlaid by sheets of clear plastic on which were traced the chief subbottom reflecting horizons. These tracings were reduced visually to fit the computer-adjusted bathymetry on profiles drawn at a distance scale of 1 cm = 4 km and a vertical scale of 26.7 times greater.

One to four radiosonobuoys were cast overside each day for the recording of wide-angle reflection and refraction data. Signals from the spark and/or air gun source were received by the buoy as the ship moved away from it at usually about 7 km/hour. These signals were transmitted back to the ship by FM radio telemetry, amplified, and recorded on a Precision Graphic Recorder and on magnetic tape. Preliminary analysis aboard ship provided information on the approximate depth of the acoustic basement, the velocity of sound within it, and the velocity of sound at various depths within the overlying sediments. For this report the average sound velocity was assumed to be 1.5 km/second in the water and 2.0 km/second in the sediment above acoustic basement, the latter being consistent with the radiosonobuoy results. These velocities were used in converting the time scale of the seismic profiles to a depth scale.

Continuous total-field magnetic intensity was recorded with a Varian proton precession magnetometer, whose sensor was towed 100 to 150 m astern to avoid magnetic effects of the ship. Digitized values at five-minute intervals were compared with the regional field based upon the reference field of Cain *et al.* (1968) reduced by 150 gammas to provide a better fit to the observed data. The anomaly between the observed and the adjusted regional values was printed as a continuous curve both on the scale of the base map (1 cm = 25 km) and as expanded profiles (1 cm = 4 km) for comparison with the interpretations of seismic reflections. Corrections were not made for diurnal variations nor magnetic storms.

Gravity was measured continuously with a vibrating-string gravimeter (Wing, 1969). The digital readout at five-minute intervals was adjusted for the Eötvos acceleration caused by the ship's east-west velocity, compared with the International Gravity Reference Field, and the anomaly was plotted by the computer for use on the expanded

profiles. Plots of free-air and simple Bouguer anomalies were quite similar, owing to the shallow bottom depths along all traverses in the Java Sea and adjacent shelf, so only the profiles for free-air anomalies are presented.

Several kinds of oceanographic observations were recorded for surface waters. At two-hour intervals (210 positions) throughout the cruise surface temperatures were measured with a special bucket thermometer, and water samples were collected for later determination of salinity using the shipboard salinometer. Also, at two-hour intervals 1-to 3-liter samples of surface water obtained with a plastic bucket and line were filtered through 0.45-micron tared Millipore® filters. Later, in the laboratory at Woods Hole the filters were dried, weighed, and the concentration of suspended sediment was calculated. For comparison, the color of the sea was measured during daylight hours using standard Forel color vials. Also during daylight hours notes were made of the wind direction and Beaufort wind force, the directions and periods of the swell and wind waves, and the presence of oil and of plankton slicks.

WATER CHARACTERISTICS

The dominant control over the waves and currents in the Java Sea and adjacent continental shelf is the monsoon, which blows steadily from the southeast between April and November and from the northwest during the rest of the year (Düing, 1970). The winds observed aboard CHAIN (Fig. X-4) fit this regional pattern except locally

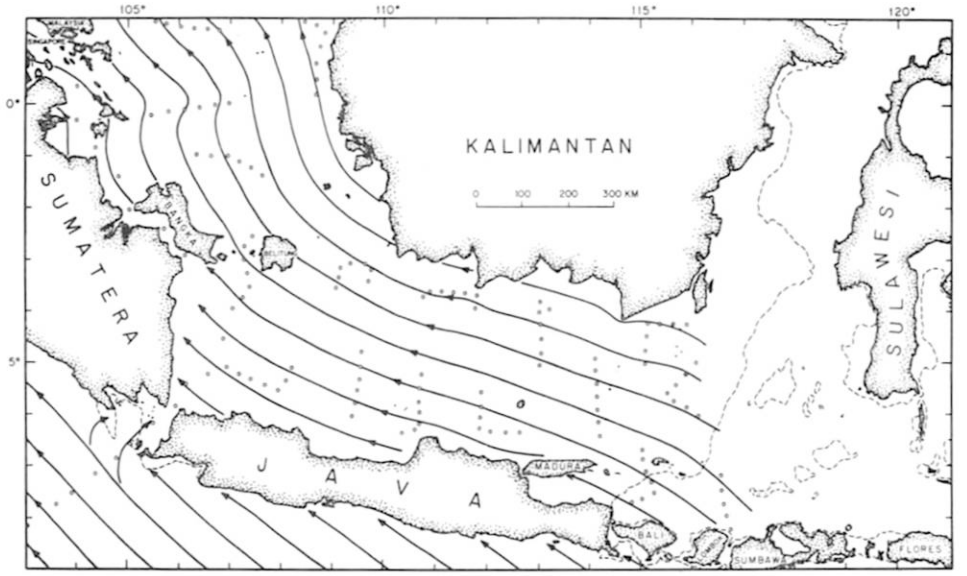

Figure X-4. Wind streamlines inferred from wind measurements aboard R/V CHAIN during 7 June to 10 July. Observations south of Sumatera and along the northeastern coast of Sumatera on Figures X-4, 5, 6, 9, 10, and 16 were made prior to 22 June when CHAIN was en route to Singapore.

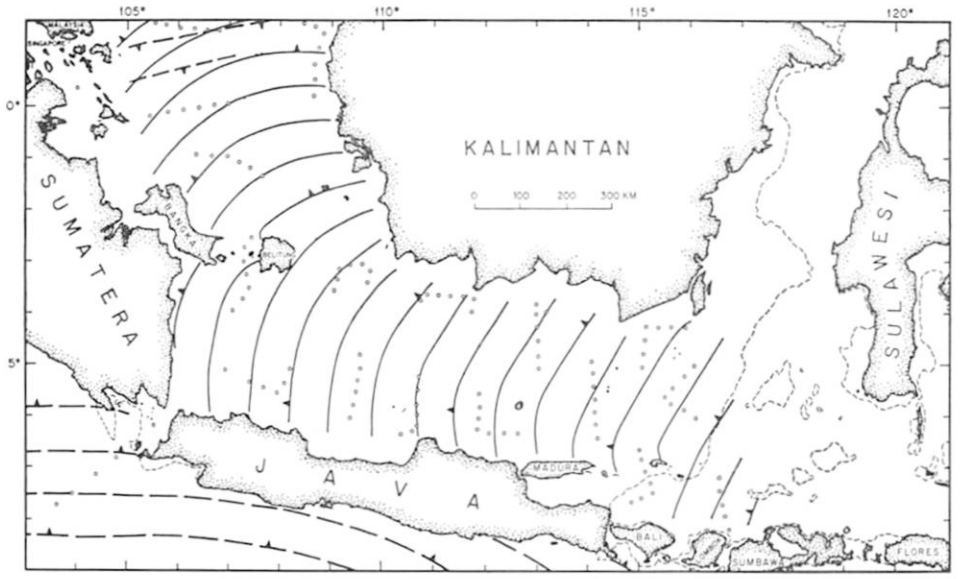

Figure X-5. Generalized pattern of swells produced by monsoon winds shows movement westward and northward around Kalimantan. Other swells near Singapore and south of Sumatera and Java are from the open Pacific Ocean and from near Antarctica, respectively.

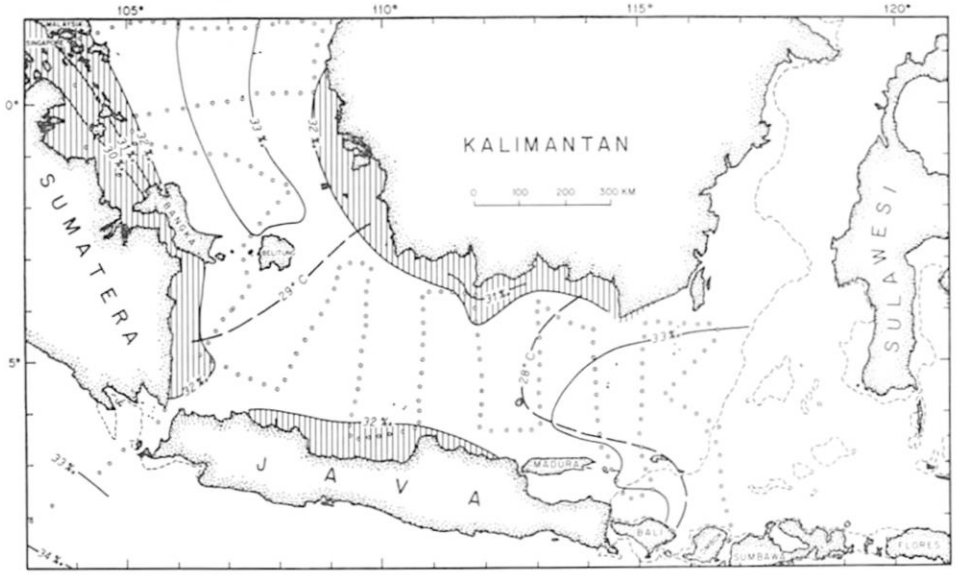

Figure X-6. Salinity and temperature of surface waters for the period 7 June to 10 July. Vertical hatching denotes areas of water diluted by runoff from the land.

near Sumatera and Java where landsea breezes were evident. The dominant southeast monsoon winds were effective in producing currents that flowed westward and then northward around Kalimantan. Local irregularities due to tidal or other currents were noted. Offsets of the ship amounted to as much as 2 km/hour especially in the area north of Bangka and Belitung islands, somewhat more than is indicated by the long-term averages shown by the pilot charts of the U. S. Naval Oceanographic Office (1962). Probably this current plus the slight rise in sea level caused by fresh water from runoff also accounts for a continuous southward flow through Sunda Strait. The monsoon winds also are responsible for the larger waves in the region, the swell that sweeps around Kalimantan (Fig. X-5) with a period of 4 to 8 seconds. Just east of Singapore is an opposing swell—one from the western North Pacific Ocean, and south of Sumatera and Java is a southerly one of about 22-second period from the Antarctic region. Smaller wind waves, or seas, mostly of 2 to 4 second period, were superimposed on the swells but were not mapped because of their minor and locally varying character. The sea and swell pattern is within the range of the averages mapped by U.S. Navy Hydrographic Office (1948).

Surface water temperature was found to exhibit a general decrease from about 30° C near Singapore to 29° C just south of Belitung Island to 28° C north of the eastern end of Java to less than 27° C in the Indian Ocean south of Lombok (Fig. X-6). This pattern is similar to the mean for the past century according to average charts of the U. S. Naval Oceanographic Office (1967), and probably it owes its origin to heating of the water as it is driven across the shallow sea floor by the southeast monsoon. Of interest is the effect of diurnal insolation in producing temperatures that were 0.3 to 1.0° C higher between the hours of 0700 and 2400 than between 0000 and 0700 local time.

A belt of water having salinity of 32.7 to 33.6 ‰ follows the axis of the Java Sea and the adjacent shelf, with values as low as 29 ‰ near the shores of Sumatera and nearly as low near Kalimantan and Java (Fig. X-6) due to local dilution by runoff. In contrast, typical salinities for the surface waters of the open Indian Ocean are about 34 ‰ (Wyrtki, 1957, 1961). The runoff from the islands plus wave erosion in shallow nearshore areas puts enough fine-grained sediments into suspension to make the water green, in contrast with the blue of waters far from shore in the Java Sea and the adjacent shelf. Measurements aboard CHAIN showed the color in terms of Forel standard vials to be more than 20 per cent yellow within a few tens of km of shore and less than 10 per cent yellow farther offshore (Fig. X-7). The actual concentration of total suspended sediment (both inorganic and organic in origin) is closely related to the color of the sea. Concentrations of more than 0.50 mg/liter (Fig. X-8) are typical of water having a color of more than 20 per cent yellow and a salinity of less than 32 ‰. In the open Java Sea the concentrations are mainly less than 0.25 mg/liter.

A plankton bloom that formed a brown-red surface discoloration along the parallel wind slicks was observed at all daytime stations south of Latitude 1° S. and west of Longitude 108° (Fig. X-7). Nowhere else in the region were concentrations noted; however, the navigational charts carry many notations of discolored water probably due to similar plankton blooms. Oil slicks also were recorded only north of Latitude 1° S. and west of Longitude 108° E., with special concentration along traverse 1; presumably they resulted from discharges by tankers approaching or departing Singapore.

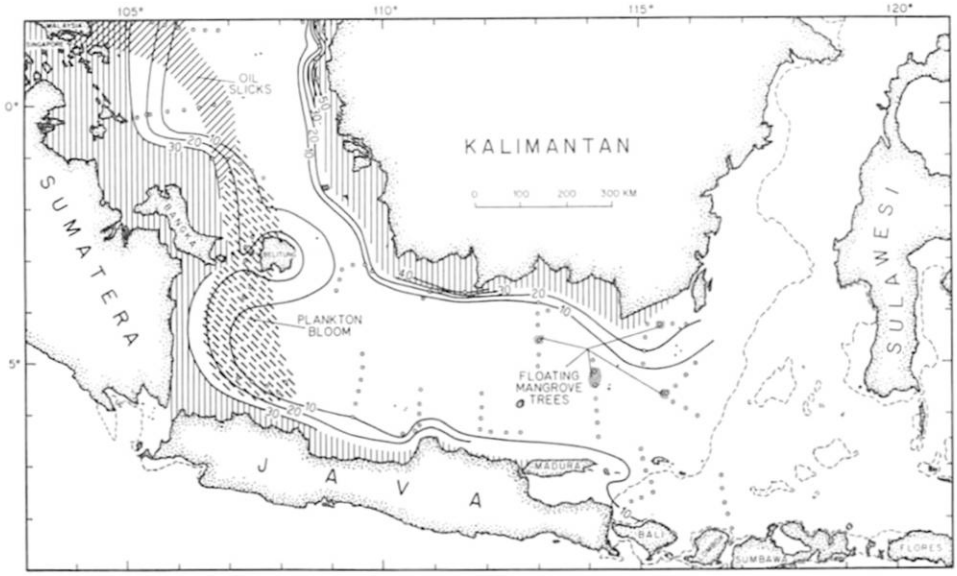

Figure X-7. Color of the sea in percentage yellow based upon Forel standard color vials. Also indicated are masses of floating mangroves and areas of intense plankton blooms and oil slicks.

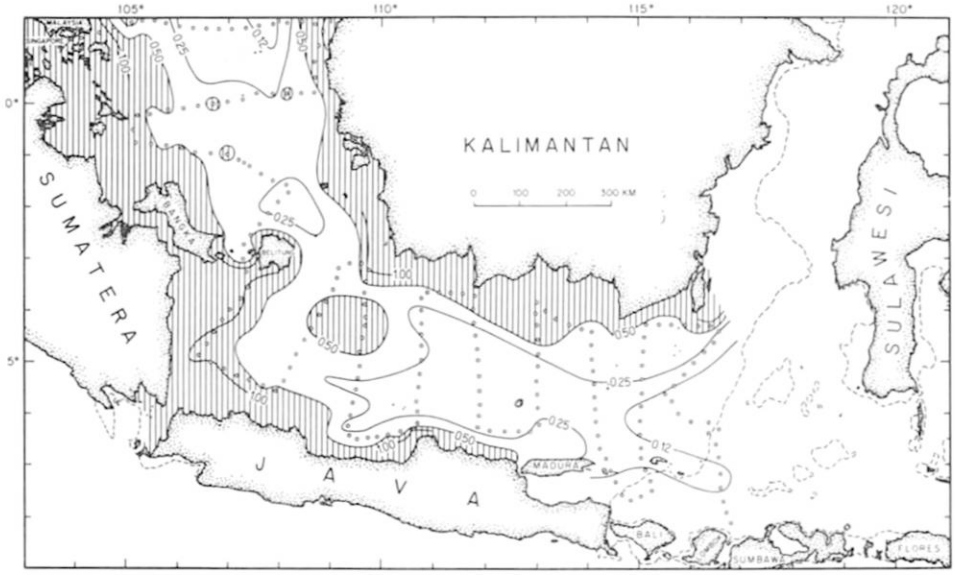

Figure X-8. Concentrations of total suspended sediment in surface water expressed as mg/liter.

A nearly continuous arc of floating debris was recorded aboard CHAIN on the way to Singapore outside the strait between Sumatera and Java, where it marks the convergence between continuously southward-flowing water from the Java Sea and the surface water of the open Indian Ocean. During the cruise small floating clusters of mangroves were noted at four stations in the eastern end of the Java Sea (Fig. X-7), where they had floated probably from the large compound delta in southeastern Kalimantan.

PLEISTOCENE CUT-AND-FILL FEATURES

The broad shallow platform of the Java Sea and adjacent shelf is so shallow that it must have been exposed to subaerial erosion and deposition during each of the four or five glacial lowerings of sea level of the Pleistocene Epoch. On the basis of topography alone, Molengraaff (1921) and later Kuenen (1950, p. 482) sketched a possible former stream drainage system extending throughout the region. Knowledge about these now-submerged and largely filled channels has practical value in the mining of alluvial tin deposits near Belitung and Sumatera. As a result, some shallow-penetration seismic surveys have been made in order to locate and map the channels (Untung, 1967; van Overeem, 1969).

During the cruise of R/V CHAIN the 3.5 kHz profiler was operated continuously for both bathymetry and shallow structure. The profiles (Fig. X-9) show many channels that presumably were cut by subaerial streams and then were largely filled by sediments during a later part of the glacial stage or the next interglacial stage of high sea

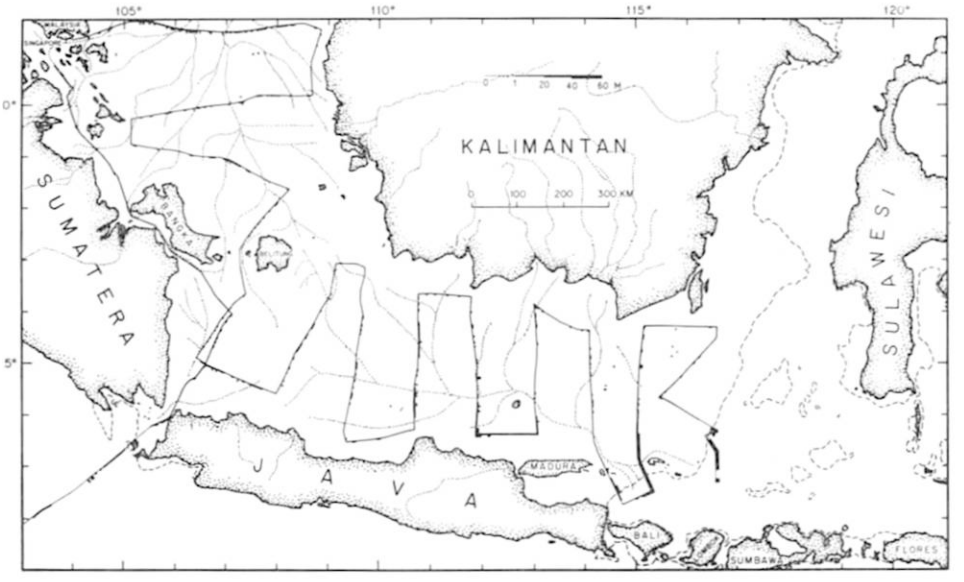

Figure X-9. Generalized pattern of 3.5 kHz penetration of the bottom sediments. Many of the filled channels are related to the slightly indented topography on the basis of which Molengraaff (1921) and Kuenen (1950, p. 482) described the Sunda river system (dots).

level. Next time the sea level was low a new channel was cut in the vicinity; thus the top 20 to 50 meters of sediment has a complicated structure. The cuts are deepest below the general level of the shelf in the downstream portions, particularly on the shelf east of Singapore and near Madura. While the new profiler data are far more complete than the simple soundings that were available to Molengraaff and Kuenen, the very great number of cut-and-fill structures and their differing ages render unreliable any attempt to improve upon the general pattern that previously was summarized. A far closer grid of 3.5 kHz profiles is needed before one can correlate single channels from profile to profile with any degree of confidence.

Fill within the channels is well bedded, and that in the smaller ones generally dips inward from both banks. However, the fill in the widest channels mainly dips away from the nearest large land mass (Sumatera, Java, or Kalimantan); this could be steep down-channel bedding but it may also be sheet-flood deposits across the shelf from the major sources of detrital sediments. In either case, the fill would appear to be non-marine in origin, with only slight re-working of the topmost layers by marine currents.

Comparison of Figures X-3 and 9 reveal no correlation between the type of bottom sediment and the depth of 3.5-kHz reflectors. This implies that the sediments at the surface probably are thin and not necessarily like those at even a few meters depth. Presumably, much of the sand consists of comminuted shells deposited atop thicker *mud* or *mud-and-sand*.

TERTIARY PLATFORM AND BASIN SEDIMENTS

The continental shelf between Singapore and Belitung Island is underlain by only thin acoustically transparent sediments, according to the seismic profiles (Figs. X-10, 11, and 15). The sediments are less than 100 m thick along the coasts of the Malay Peninsula, Sumatera, Bangka, Belitung, and Kalimantan. A few small areas nearer the middle of the shelf, particularly along the traverse east of Singapore, also have less than 100 m of sediments. Slightly more than 500 m were noted in two troughs that appear to be elongate northwest-southeast. The greatest thickness was 840 m in the Bangka Trough (new name) north of Bangka Island.

Considerably thicker sediments were measured in the western Java Sea (Figs. X-10, 11, 12, and 15), an area that has been extensively drilled (Humphrey, 1970, 1971). Four main basins are indicated: South Sumatera (on land), Sunda, West Java (partly on land), and Belitung, according to the nomenclature of Todd and Pulunggono (1971). These authors also presented drill logs and cross-sections that reveal metamorphic and igneous basement to be as deep as 3.0 km in the Sunda Basin and 2.5 km in the offshore part of the West Java Basin. Basement in the Belitung Basin on traverse 12 (Fig. X-12) may be at least as deep. In the basins is a lower Miocene formation, the Batu Radja, which consists of "reefoid limestone and thin dolomites." Its top is at a depth of about 1,800 m in the middle of the South Sumatera Basin, 1,500 m in the Sunda Basin, and 1,400 m in the West Java Basin. This limestone may be the acoustic basement seen on R/V CHAIN's unprocessed analog seismic profiles. Thus the profiles penetrated only about half of the total sediment section in the basins but virtually all of it on the high areas

surrounding and separating the basins. The general outline of the basins shown by Figure X-15 corresponds well with the outlines presented by Todd and Pulunggono on the basis of drill holes and detailed seismic coverage. Little help in estimating the thickness of basin sediments is provided by magnetic anomalies, because the wave lengths and amplitudes of the anomalies appear to be more a function of the varied lithology of basement rocks than of their depth, unlike in the previous studies of the East China Sea and the South China Sea. For example, traverse 6 (Fig. X-11) exhibits an almost smooth curve of magnetic anomaly where sediments are thick in the Sunda Basin at the left end of the traverse. The basin fill that is recorded has a general southward dip, and the up-dip ends of the strata are truncated by the bottom of the Java Sea, either because the strata have prograded toward the south or because they have been beveled by erosion. Few prominent folds are present, small ones overlie basement hills and probably are the result of differential compaction. Most faults in the sediments appear to be concentrated along the sides of the Karimundjara Arch (see especially traverse 12 of Figure X-12), where they may be due to compaction, but others are more probably diastrophic in origin. The relatively steep dips and possible unconformities in the strata at the south side of the arch in traverse 14 may also indicate uplift of the arch during the period of basin filling.

In the eastern Java Sea (Figs. X-10, 13, and 15) the thickness of sediments measured by seismic reflection was limited as in the western Java Sea by a strong acoustic reflector

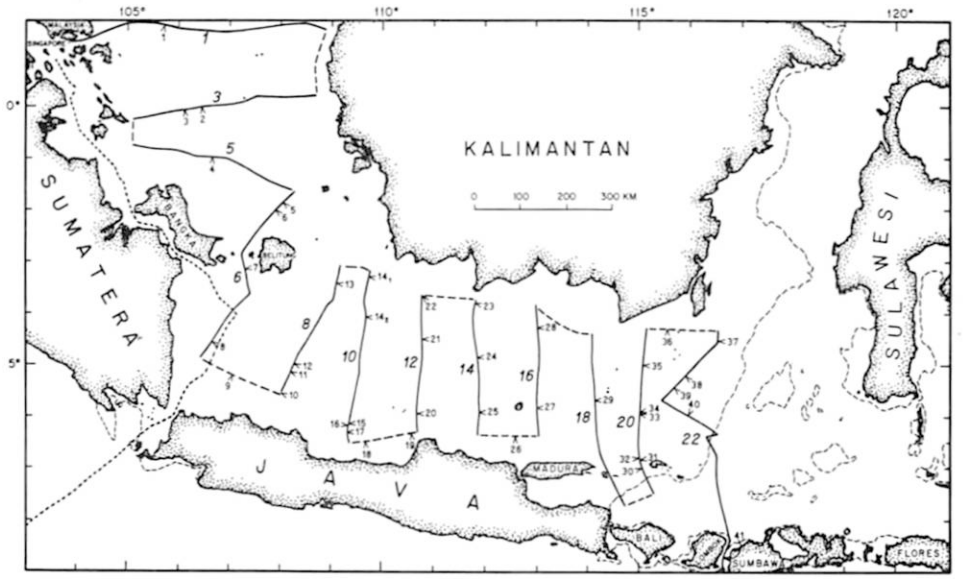

Figure X-10. Traverses along which geophysical measurements were made between 22 June and 10 July 1971. The large numbers identify the traverses that were interpreted and illustrated in subsequent figures grouped for the continental shelf, western Java Sea, and eastern Java Sea. Dashed lines show connecting traverses. The small numbers indicate the positions of radiosonobuoys that were used for measuring seismic velocities. The wide dashed line near Sumatera shows the route followed by CHAIN en route to Singapore between 6 and 10 June.

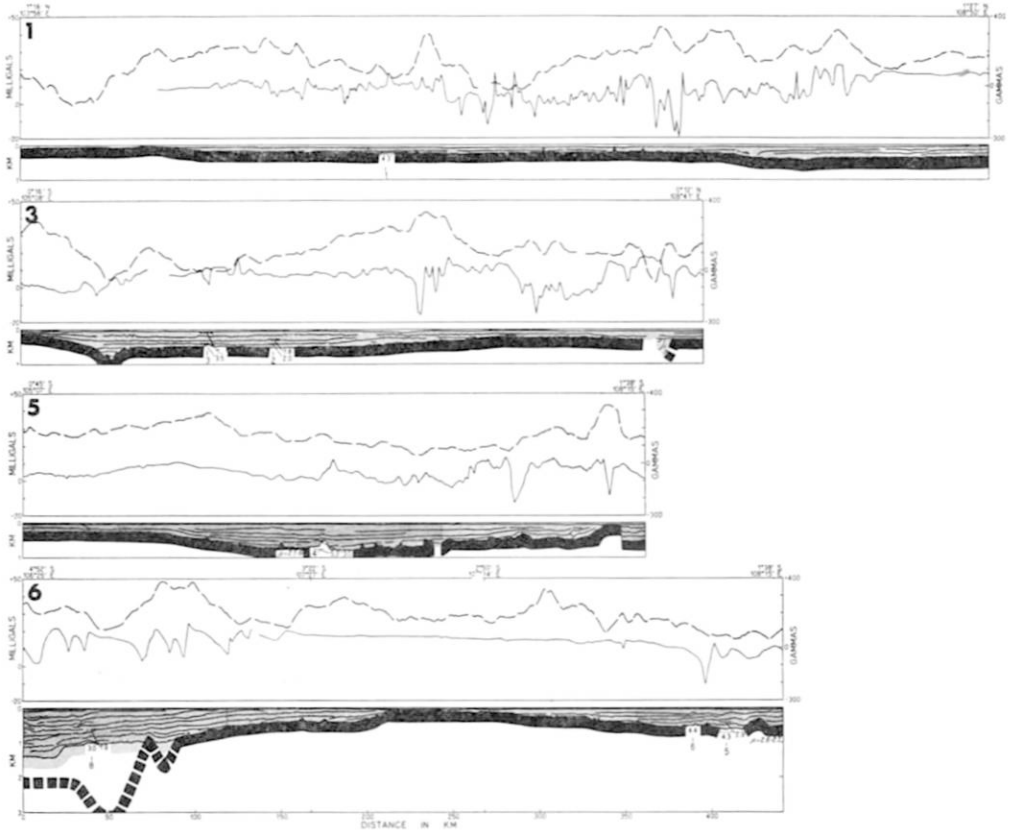

Figure X-11. Interpretation of geophysical traverses 1, 3, 5, and 6 across the continental shelf between Singapore and Belitung Island.

Top:—Wide dashed line shows free-air gravity anomalies; continuous line—magnetic anomalies.

Bottom:—Line drawing interpretation of continuous seismic reflection profiles. The black area indicates acoustic basement where we believe it to be igneous or metamorphic rock; coarse dotted pattern designates acoustic basement where it may be a lower Miocene reef limestone. The seismic velocity and depth information derived from the radiosonobuoy stations are shown; depths to the refractors are approximate (<150 m) and may change after more detailed analysis. Computed densities of acoustic basement are shown in italics.

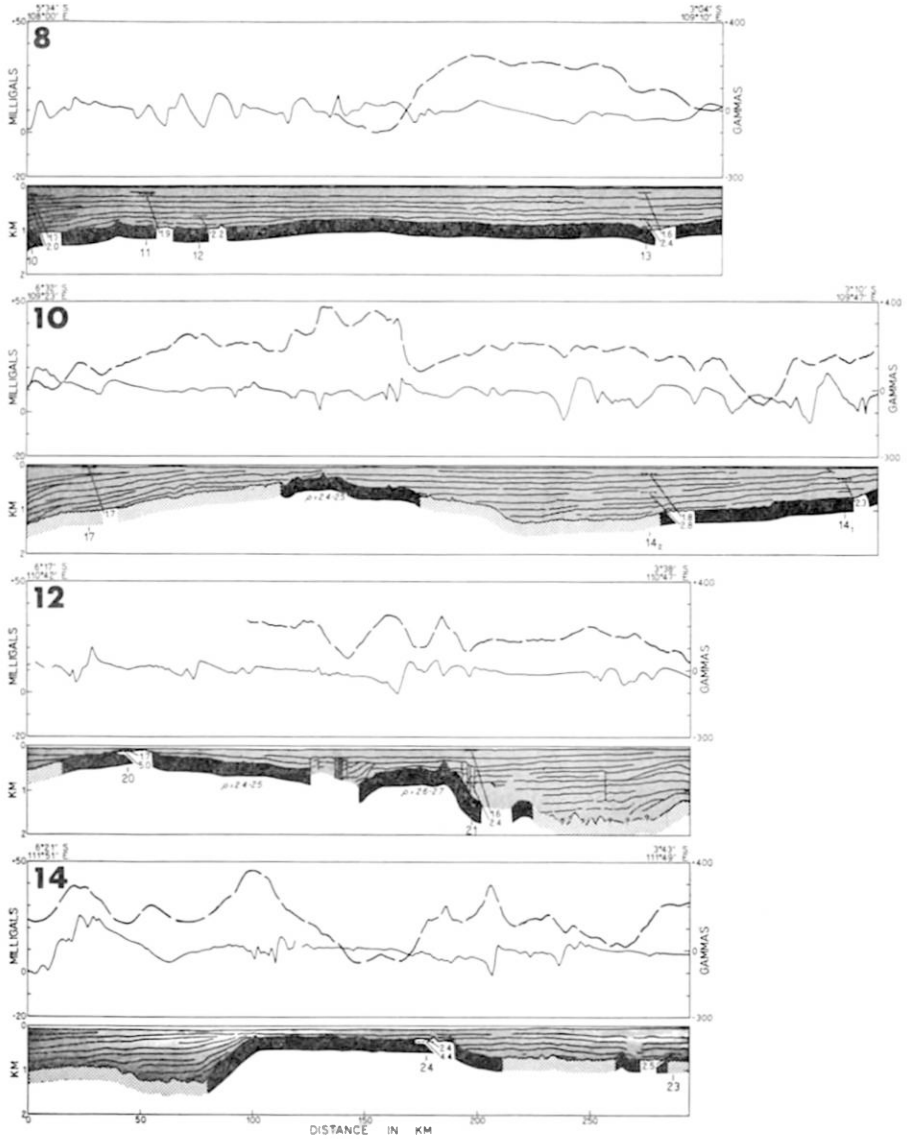

Figure X-12. Interpretation of geophysical traverses 8, 10, 12, and 14 across the western Java Sea. Symbols are the same as for Figure X-11.

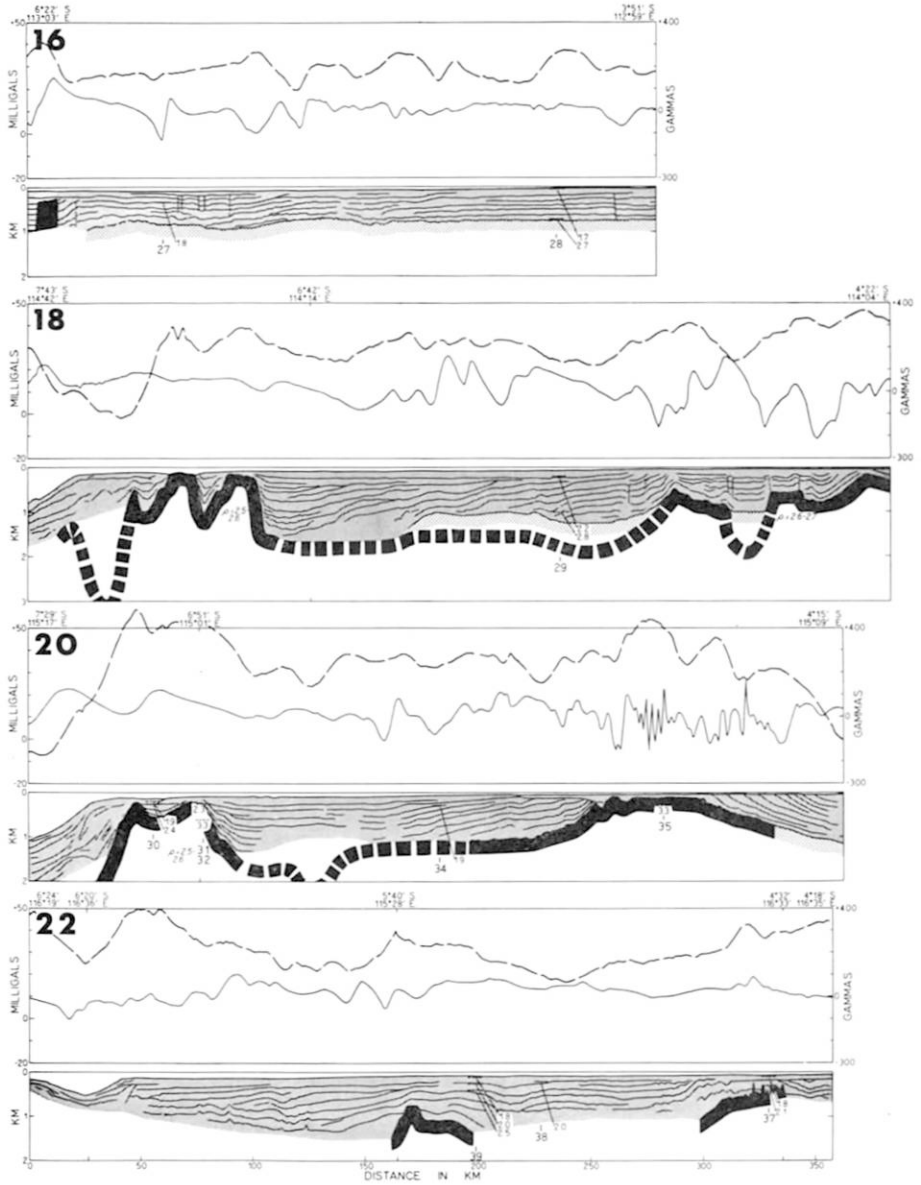

Figure X-13. Interpretation of geophysical traverses 16, 18, 20, and 22 across the eastern Java Sea. Symbols are the same as for Figure X-11.

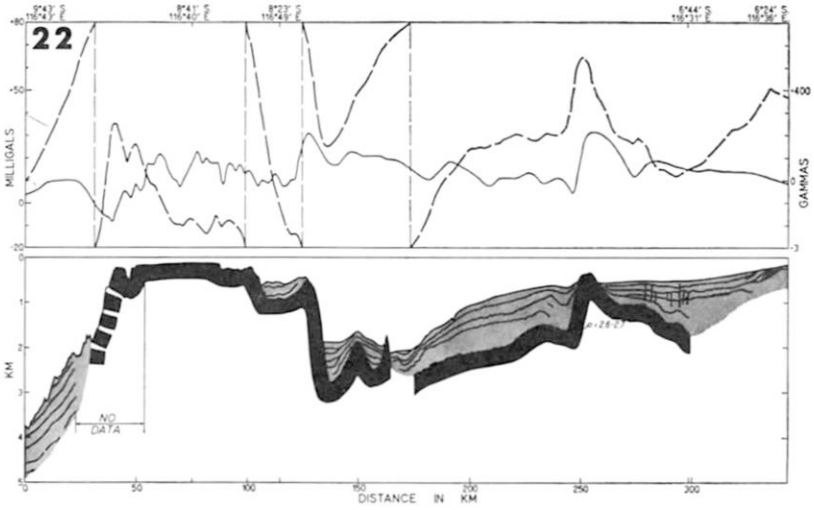

Figure X-14. Interpretation of geophysical traverse 22 when it crosses deep water between the Java Sea and Lombok. Symbols are the same as for Figure X-11.

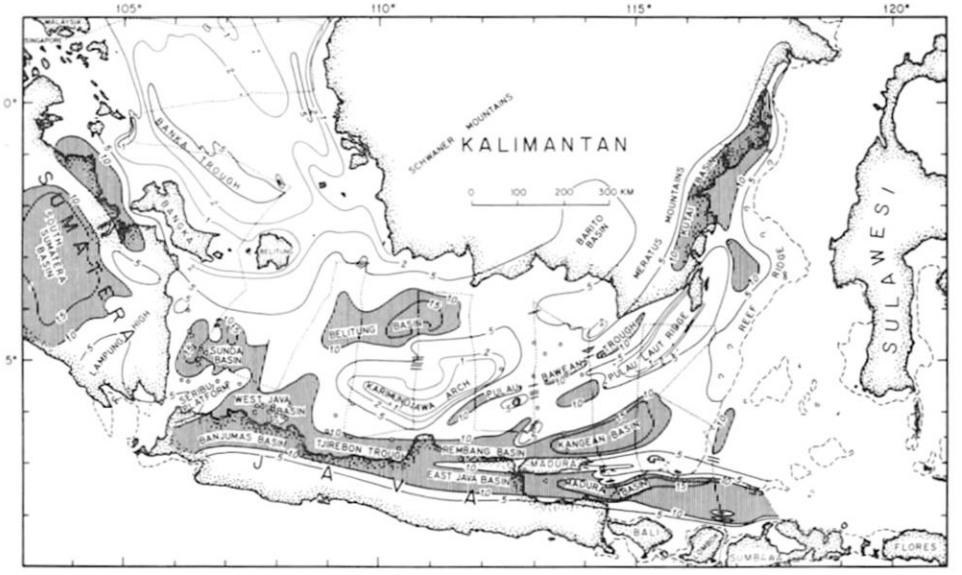

Figure X-15. Isopach map of sediments above acoustic basement. Compiled from data of Figures X-11, 12, 13, and 14, and of connecting traverses. Well data are from Todd and Pulunggone (1971) and Humphrey (1970, 1971). Vertical hatching designates basin areas that contain more than 1 km of sediments above acoustic basement.

located well above true lithologic basement. Nevertheless, the shapes of the basins shown by Figure X-15 probably are approximately correct. The data show that the Belitung Basin extends northeastward onto Kalimantan to connect with the Barito Basin —the site of an oil field. Bordering the south side of the Karimundjawa Arch is a long narrow trough, here named the Pulau Bawean Trough for the nearby island of that name. This trough reaches from the middle part of the north coast of Java northeasterly to the east coast of Kalimantan where it probably is continuous with the Kutai Basin, in which are several offshore oil fields. The series of oil-bearing basins that extends eastward from Sumatera (Fig. X-15) divides into two branches just west of Madura. One branch trends northeasterly to join in some unknown fashion with the Palau Laut Ridge. The main branch extends from Rembang Basin to the possibly deeper Kangean Basin (named for the island south of it). The Kangean Basin may continue northeastward beyond traverse 22, the limit of the present study. Lastly, the deeply-filled Madura Basin trends eastward from the East Java Basin through the reentrant between Madura and Java. These five elongate basins and troughs open to the east like the fingers of a hand. Depths to acoustic basement in the fingers appear to be progressively deeper from north to south. Strata in these basins and troughs of the eastern Java Sea are much more deformed than are those in basins farther west. They have many broad folds whose axes probably are parallel to the trends of the main troughs.

The water between the shelf and Lombok (traverse 22, Fig. X-14) reaches depths of 2,200 m. The seismic profile reveals three basement ridges, the largest of which is the one that carries Bali, Lombok, and Sumbawa. Between the ridges are troughs that contain more than 1,000 m of sediments. Probably all of the ridges and troughs trend east-west parallel to the island arc, but details are lacking.

STRUCTURES AT AND BELOW ACOUSTIC BASEMENT

The structure of the rocks below a depth of about 1 km could not be determined by the seismic profiling system because of its limited penetration. However, areas of "hard" rock or true basement as opposed to impenetrable sediments could be identified from the character of the acoustic basement (Figs. X-11, 12, 13, and 17). Additional information relating to the acoustic basement comes from the seismic refraction measurements of sound velocity and from the gravity and magnetic profiles.

All refraction velocity measurements relate either to the acoustic basement or to the overlying sediments. The 14 measurements for acoustic basement shown in Fig. X-17 seem to fall into four groups. North of Belitung Island are five measurements on true basement that range from 3.5 to 5.3 km/sec with a mean of 4.4 km/sec. This wide range suggests considerable variation in rock types, perhaps due to different degrees of metamorphism. Between Java and Kalimantan true basement appears to yield two groups of velocities, one of 4.4 to 5.0 km/sec near the center of the Java Sea and one of 3.3 to 3.5 km/sec off the southeastern coast of Kalimantan. Where acoustic basement appears to be a lower Miocene limestone rather than igneous and metamorphic rocks, three measurements yielded velocities of 2.7 to 3.0 km/sec, much lower than expected for a reefoid limestone.

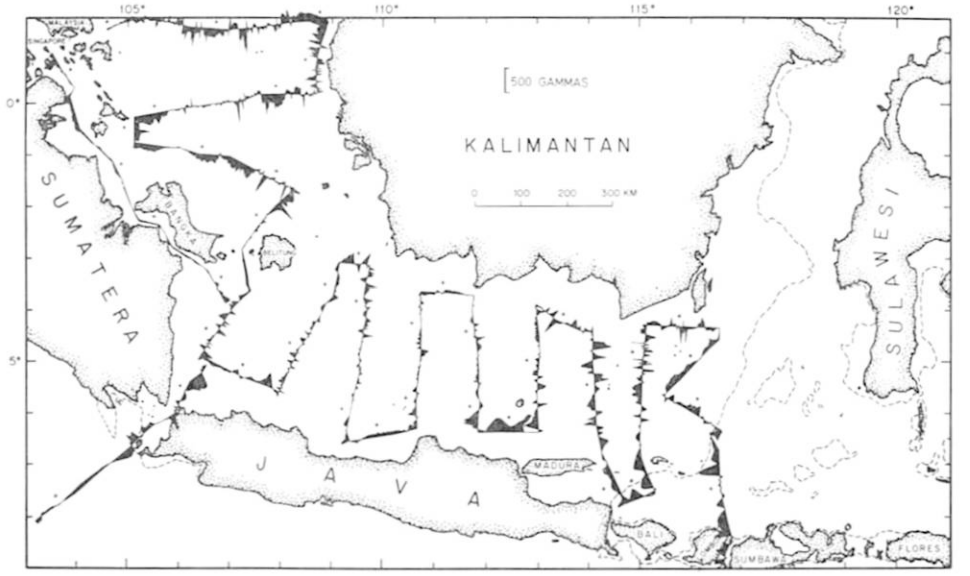

Figure X-16. Geomagnetic profiles plotted along all traverses. The traverse lines correspond to zero anomaly. The anomaly was derived from the regional field of Cain *et al.* (1964) minus 150 gammas.

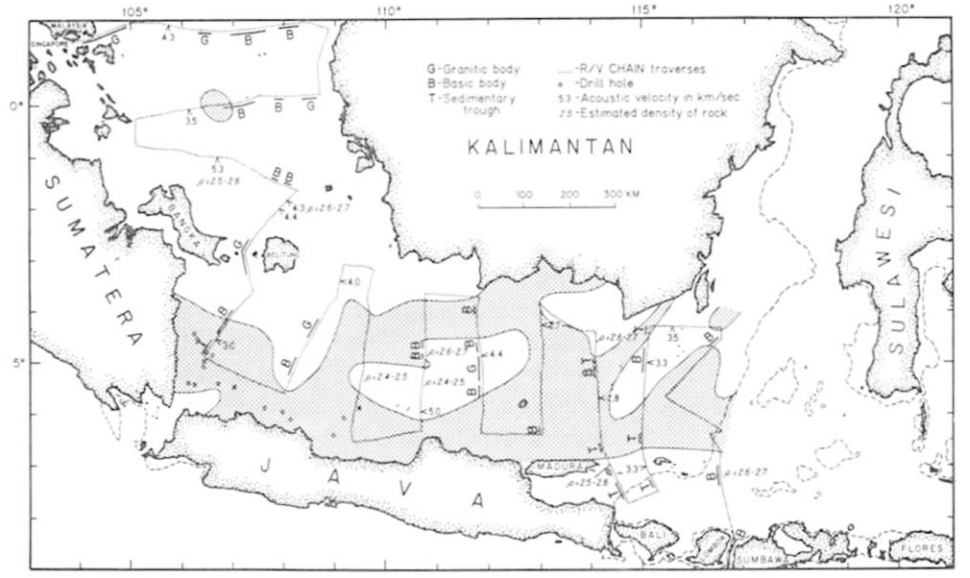

Figure X-17. Velocity and density measurements for acoustic basement. These data plus information from seismic reflection profiles, outcrops, and some offshore drill holes serve as the basis for the map of the type of acoustic basement (of pre-Tertiary igneous or metamorphic rocks-plain, and of lower Miocene reefoid limestone-coarsely dotted pattern).

The gravity profiles were used to estimate the density of the acoustic basement as an aid both to identification and to estimation of the depth of the basement. Wherever a change in observed gravity corresponds to a known change in depth to acoustic basement it was assumed that the two are causally related. This permits an estimate to be made of the density of the acoustic basement provided that the density of the immediately overlying sediments is known. The latter was estimated from the measured velocity of sound in the overlying sediments combined with the velocity/density curve of Nafe and Drake (1963); at all sites the deduced density was 2.2 ± 0.1 gm/cc. The derived densities for the underlying acoustic basement are shown on the profiles and also on Figure X-17; the 8 estimates range from 2.4 to 2.7 gm/cc and yield an average of 2.57 ± 0.1 gm/cc, a value representive of Carboniferous and Devonian rocks.

The main potential of the gravity measurements is in the information they can give about the structures beneath the acoustic basement, in particular the configuration of the true basement beneath a deep sedimentary basin. For the application of the method the density difference between the true and the acoustic basement must be known or estimated. At the south end of traverse 6 a steep drop in gravity of 15 mgals was observed near the northern margin of the Sunda Basin. Oil company drill holes (Todd and Pulunggono, 1971) indicate a difference of 1.25 km in depth to true basement, corresponding to this gravity change. This is consistent with a density of 2.6 for the true basement, 2.35 gm/cc for the acoustic basement and 2.2 for the material above acoustic basement. Using these values the probable trend of true basement shown on traverse 6 was deduced. A similar application of this method was made on traverses 18 and 20. The limits of the deeper parts of these basins are marked on Figure X-17 and labeled T (Sedimentary Trough).

On traverses 1, 3, 6, 8, and 14 (Figs. X-11, and 12) low gravity occurs over considerable distances in areas where the acoustic basement is thought to be true basement, i.e. areas where deep sedimentary basins cannot be present. The only possible explanation for such features are that, either the basement there has a lower density or that it is intruded by low-density rocks. In the latter case relatively steep gravity gradients can be expected (> 1 mgal/km) at the edges of the body. Several but not all of the gravity lows fit this latter description. Such "lows" usually are associated with granitic bodies, granite usually having a lower density than metamorphic rocks. It is therefore suggested that at least some of the gravity lows are caused by granitic bodies at or within the acoustic basement. The limits of these suggested granitic bodies are shown in Figure X-17 by the letter G. Granites often are associated with a smooth magnetic field; this was observed for the known granite between Bangka and Belitung islands (traverse 6, Fig. X-11) and also for a probable granite on traverse 14 (Fig. X-12).

Equally noticeable on the gravity profiles are numerous gravity highs, usually having steep gradients associated with depth changes in true basement and almost invariably associated with magnetic anomalies. These probably are caused by basic intrusions which normally are both dense and highly magnetized. Positions of these bodies are indicated on Figure X-17 by the letter B. In some instances the shape of the anomaly shows that it is caused directly by the basement. In others the shape is not related in any direct way with the shape of the basement, and the intrusive clearly is buried. An upper limit for the depth of the body can be deduced from the formula,

$$\text{Maximum Depth} = \frac{\text{Maximum Gravity Effect} \times 0.65}{\text{Maximum Gravity Gradient}}$$

given by Bott and Smith (1958). For most of the anomalies the maximum depth is less than 6 km, indicating a shallow origin. The wave length of the magnetic anomalies usually indicates a shallower source than do the gravity anomalies, often less than 4 km, suggesting that they are associated with thin dikes. If the same source body causes both the gravity and the magnetic anomalies, the source of most anomalies is shallower than 4 km.

DISCUSSION

The geophysical results of the R/V CHAIN cruise combined with geological data from outcrops on land and drill holes on land and sea floor reveal a series of ridges separated by sediment-filled basins and troughs in the Java Sea and adjacent shelf. The areal geology of the region (Roe, 1962; Sigit, 1965; Director-General, 1971), field studies by van Bemmelen (1949), and shipboard surveys by Parke *et al.* (1971) and by this cruise of R/V CHAIN show that the oldest of the ridges is the one that extends along the Malay Peninsula through Bangka and Belitung islands to the Schwaner Mountains of Kalimantan. It contains only pre-Cretaceous igneous, metamorphic, and sedimentary rocks and dates from probably Late Jurassic time. The adjacent ridge to the north, the Khorat-Semitau Ridge and the Karimundjara Arch—Meratus Mountains contain deformed Cretaceous sediments, and both ridges are believed to date from Late Cretaceous time. At still greater distance on either side of the Malay-Bangka-Belitung-Schwaner Ridge are the Peripheral Ridge to the north (Parke, *et al.*, 1971) and the Pelau Laut Ridge, Madura Ridge, and the long volcanic ridge that constitutes the main Indonesian Island Arc. All of these ridges appear to date from within the Tertiary Period, the later ones progressively farther from Kalimantan.

The basement ridges obviously are parts of a larger system, one that has been studied by many workers whose interests are in regional tectonics. The earlier studies received their impetus from the Snellius Expedition mainly in the Molucca Islands east of the Java Sea and from the pendulum gravity measurements of Vening Meinesz throughout the region. Most hypotheses involved tectogenes, as summarized by Kuenen (1950, p. 175–195), Umbgrove (1949), and Yanshin (1966). More recent studies are related to sea-floor spreading and the interactions between crustal plates (Isacks, Oliver, and Sykes, 1968; Fitch, 1970). The data of Figure X-15, based mainly upon the use of geophysics for tracing the ridges beneath their cover of shelf sediments, has been extended regionally through the use of modern deep-sea bathymetry (Fisher, 1968) for tracing the ridges at depth. The new chart of the ridges (Fig. X-18) differs from older ones only in certain details. Although the problems of the regional tectonics and the origin of the ridge system are related to the structure and stratigraphy of the Java Sea, their study is not part of this report.

The later structures of the Java Sea and adjacent continental shelf are illustrated by the various profiles and charts of the foregoing text. Basement is shallow and

sediments are thin beneath the continental shelf between Singapore and Belitung Island. In contrast, the Java Sea contains basins and troughs having thick sediments. These basins and troughs lie between members of the ridge complex, and both basins and ridges extend northeasterly from Sumatera and Java to Kalimantan. Seismic profiles in the basins and troughs are limited in depth of penetration by the presence of a lower Miocene reefoid limestone, but they do serve to outline the shapes of the basins and troughs. Total thicknesses to metamorphic and igneous basement reach 3 km, judging from the logs and total depth figures of scattered drill holes and the interpretations of gravity anomalies. Many structural traps (folds, faults, and pinch outs) are present in the basin fill, particularly in the eastern Java Sea. Altogether the volume of Neogene sediments above acoustic basement is about 400,000 cu. km. Perhaps another 80,000 cu. km is present beneath acoustic basement and above lithologic basement (pre-Tertiary igneous and metamorphic rocks). The large size of the basins and the characteristics of their strata warrant considerable optimism (Delegation, 1970; Mainguy; King, 1971) for the oil potential of the region. Oil and gas fields have been established in both land and sea-floor portions of the basins and troughs. Areas of the sea floor having thick accumulations of probable Neogene sediments that have not yet been tested by the drill occur in the eastern parts of the Belitung, Kangean, and Madura basins.

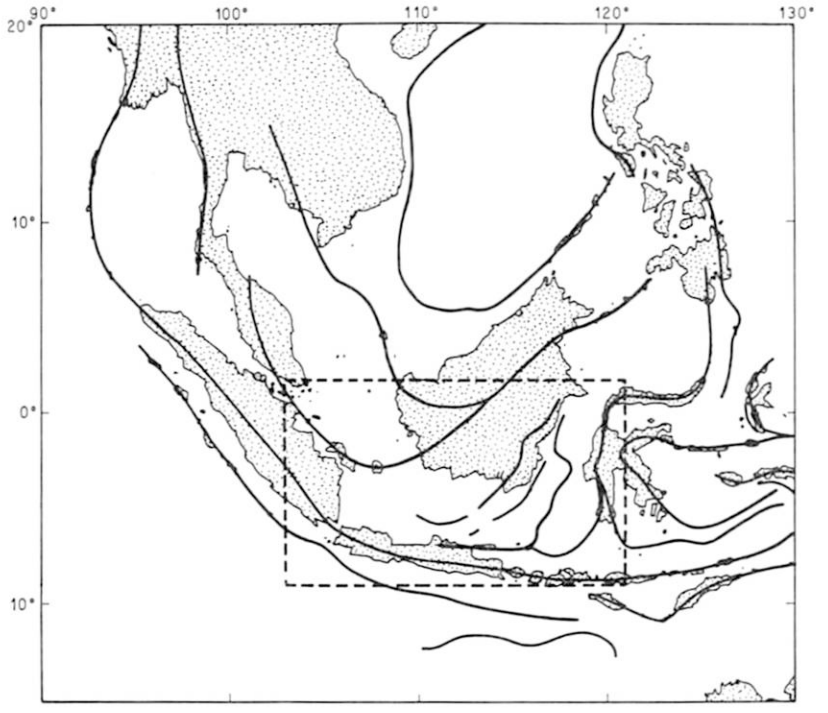

Figure X-18. Structural ridges of the Sunda Shelf inferred from geophysical results of this cruise and of Parke *et al.* (1971) compared with those of surrounding regions from other authors (Kuenen, 1950, p. 175–195) modified by up-dated knowledge of deep-sea topography (Fisher, 1968). The rectangle denotes the boundary of the area studied aboard R/V CHAIN.

Tin is mined on Bangka and Belitung islands, and it probably also occurs in the late Pleistocene stream channels that cross nearby submarine outcrops of granite. Whether or not economic concentrations and quantities are present east of Belitung Island remains to be tested by more detailed geophysical surveys and by test drilling. Economic concentrations more than a few km north or south of Belitung Island seem unlikely in view of the short distance that tin is moved by streams (Emery and Noakes, 1968) and the burial of granitic source rocks on the sea floor by sediments (Fig. X-15).

REFERENCES

Bott, M. H. P., and R. A. Smith, 1958, The estimation of the limiting depth of gravitating bodies: *Geophys. Prospect.*, vol. 6, p. 1–10.

Cain, J. C., S. Hendricks, W. E. Daniels, and D. C. Jensen, 1968, Computation of the main geomagnetic field from spherical harmonic expressions: Data Users Note NSSDC 68–11, NASA Data Center, 46 pp.

Delegation, Republic of Indonesia, 1970, The status of offshore petroleum exploration in Indonesia as of February 1970 and a brief analysis of potential areas: *ECAFE, CCOP Rept. of the 7th Session, Saigon*, p. 91–98.

Director-General, Geological Survey of India, 1971, Geological Map of Asia and the Far East, 2nd ed.: Bangkok, U. N. ECAFE, Comm. Geol. Map World, scale 1:5,000,000, 4 sheets.

Düing, Walter, 1970, The Monsoon Regime of the Currents in the Indian Ocean: Honolulu, East-West Center Press, 68 pp.

Emery, K. O., 1969, Distribution pattern of sediments on the continental shelves of western Indonesia: United Nations ECAFE, *CCOP Tech. Bull.*, vol. 2, p. 79–82.

Emery, K. O., Y. Hayashi, T. W. C. Hilde, K. Kobayashi, Ja Hak Koo, C. Y. Meng, H. Niino, J. H. Osterhagen, L. M. Reynolds, J. M. Wageman, C. S. Wang, and S. J. Yang, 1969, Geological structure and some water characteristics of the East China Sea and the Yellow Sea: United Nations ECAFE, *CCOP Tech. Bull.*, vol. 2, p. 3–43.

Emery, K. O., and L. C. Noakes, 1968, Economic placer deposits of the continental shelf: United Nations ECAFE, *CCOP Tech. Bull.*, vol. 1, p. 95–111.

Fisher, R. L,, 1968, Bathymetry of the eastern Indian Ocean: Scripps Inst. Oceanog., scale 1:2,000,000.

Fitch, T. J., 1970, Earthquake mechanisms and island arc tectonics in the Indonesian-Philippine region: *Bull. Seismol. Soc. America*, vol. 60, p. 565–591.

Fitch, T. J., and P. Molnar, 1970, Focal mechanisms along inclined earthquake zones in the Indonesian-Philippine region: *Jour. Geophys. Research*, vol. 75, p. 1431–1444.

Humphrey, Wilson, 1970, Petroleum developments in Far East in 1969: *Bull. Amer. Assoc. Petroleum Geologists*, vol. 54, p. 1551–1566.

Humphrey, Wilson, 1971, Petroleum developments in Far East in 1970: *Bull. Amer. Assoc. Petroleum Geologists*, vol. 55, p. 1634–1661.

Isacks, B., J. Oliver, and L. R. Sykes, 1968, Seismology and the new global tectonics: *Jour. Geophys. Research*, vol. 73, p. 5855–5899.

King, R. E., 1971, The East Asian shelves—a new exploration region with high potential: United Nations ECAFE, *CCOP Tech. Bull.*, vol. 4, p. 153–163.

Kuenen, P. H., 1935, Geological Results, The Snellius Expedition: vol. 5, Part 1, 124 pp.

Kuenen, P. H., 1950, Marine Geology, New York, John Wiley & Sons, Inc., 568 pp.

Mainguy, M., 1970, Regional geology and petroleum prospects of the marine shelves of eastern Asia: United Nations ECAFE, *CCOP Tech. Bull.*, vol. 3, p. 91–107.

Molengraaff, G. A. F., 1921, Modern deep-sea research in the East Indian Archipelago: *Geogr. Jour.*, vol. 57, pp. 95–121.

Nafe, J. E., and C. L. Drake, 1963, Physical properties of marine sediments: *in* M. N. Hill (ed.) The Sea, Ideas and Observations on Progress in the Study of the Seas, vol. 3, New York, Interscience Publ., pp. 794–815.

Parke, M. L., Jr., K. O. Emery, Raymond Szymankiewicz, and L. M. Reynolds, 1971, Structural framework of the continental margin in the South China Sea: *Bull. Amer. Assoc. Petroleum Geologists*, vol. 55, pp. 723–751; also in United Nations ECAFE, *CCOP Tech. Bull.*, vol. 4, p. 103–142.

Petroleum News South East Asia, 1970, 1971, Monthly summaries: Hong Kong.

Roe, F. W., coordinator, 1962, Oil and Natural Gas Map of Asia and the Far East: Bangkok, U. N. ECAFE, scale 1:5,000,000, 4 sheets.

Sigit, Soetarjo, 1965, Geologic Map of Indonesia: U. S. Geol. Survey Miscl. Geol. Investig. Map I-414, scale 1:2,000,000, 2 sheets.

Todd, D. F., and A. Pulunggono, 1971, The Sunda Basinal Area, an important new Indonesian oil province: Amer. Assoc. Petroleum Geologists, Ann. Mtg., Houston, 30 March.

Umbgrove, J. H. F., 1938, Geological history of the East Indies: *Bull. Amer. Assoc. Petroleum Geologists*, vol. 22, pp. 1–70.

Umbgrove, J. H. F., 1949, Structural History of the East Indies: Cambridge, England, Univ. Press, 63 pp.

U. S. Naval Oceanographic Office, 1962, Atlas of pilot charts, South Pacific and Indian Oceans: Washington, D. C., Hydrographic Office Publ. No. 107, 16 charts.

U. S. Naval Oceanographic Office, 1967, Monthly charts of mean, minimum, and maximum sea surface temperature of the Indian Ocean: Washington, D. C. Oceanographic Office Spec. Publ., 99, 48 pp.

U. S. Navy Hydrographic Office, 1948, Atlas of Sea and Swell Charts, Indian Ocean: Washington, D. C., Hydrographic Office Publ. No. 799G, 12 charts.

U. S. Navy Hydrographic Office, 1951, Sailing directions for Soenda Strait and the western and northwest coasts of Borneo and offlying islands: Washington, D. C., U. S. Gov't. Printing Office, 363 pp.

Untung, Mohamad, 1967, Results of a sparker survey for tin ore off Bangka and Belitung islands, Indonesia: ECAFE—CCOP Rept. of 4th Session, Taipei, pp. 61–67.

van Bemmelen, R. W., 1949, The Geology of Indonesia: The Hague, Martinus Nijhoff, 177 pp.

van Overeem, A. J. A., 1969, Sonia continuous profiler: *Offshore Technology Conf., May 18–21, Houston, Texas*, vol. II, p. 213–216.

Vening Meinesz, F. A., 1932–1934, Gravity expeditions at sea: vol. I, The expeditions, the computations and the results: vol. 33, The interpretation of the results (with the collaboration of J. H. F. Umbgrove and P. H. Kuenen), Delft, Ed. Waltman.

Wageman, J. M., T. W. C. Hilde, and K. O. Emery, 1970, Structural framework of East China Sea and Yellow Sea: *Bull. Amer. Assoc. Petroleum Geologists*, vol. 54, p. 1611–1643.

Wing, C. G., 1969, The MIT vibrating string surface-ship gravimeter: *Jour. Geophys. Research*, vol. 74, p. 5882–5894.

Wyrtki, Klaus, 1957, Die Zirkulation an der Oberfläche der südostasiatischen Gewässer: *Deut. Hydrog. Zeitschrift*, vol. 10, no. 1, p. 1–13.

Wyrtki, Klaus, 1961, Physical oceanography of the southeast Asian waters: Sci. Results of Marine Investig. South China Sea and Gulf of Thailand 1959–1961, Scripps Inst. of Oceanogr., NAGA Rept., vol. 2, 195 pp.

Yanshin, A. L., chief ed., 1966, Tectonic map of Eurasia: Akad. Nauk SSSR, 22nd Internat. Geol. Cong., India, Comm. Geol. Map World, Sci. Commun., pp. 103–109. Ministerstvo Geologii, scale 1:5,000,000, 12 sheets.

Blank page

Page blanche

XI. EXPLANATORY NOTE TO ACCOMPANY THE MAP, "TERTIARY BASINS OF EASTERN ASIA AND THEIR OFFSHORE EXTENSIONS (Revised, April 1971)"

By

Technical Secretariat of CCOP

(with map XI-1, in envelope on back cover)

INTRODUCTION

The explanatory notes given below were prepared by Mr. M. Mainguy to accompany the map, "Tertiary basins of eastern Asia and their offshore extensions, revised edition, April 1971", which was submitted for discussion at the eighth session of CCOP.

The first edition was presented at the Fourth Symposium on the Development of Petroleum Resources of Asia and the Far East, held at Canberra, Australia, in October-November 1969, and was later published, with slight amendments, in the CCOP Technical Bulletin, volume 3, issued in May 1970. A great amount of new data have been obtained since that time and a revision of the map was undertaken by Dr. Yoshiaki Sato, of the Technical Secretariat of CCOP, and Mr. Maurice Mainguy, Special Adviser to CCOP; the data shown on this revised edition, possibly with some later amendments, will be included in the second edition of the ECAFE Oil and Natural Gas Map, now in process of revision. It should be pointed out that the main purpose of the latter is to draw attention to future prospects and potentials, particularly those which might have been overlooked; consequently, the most optimistic outlook has been consistently followed.

STRUCTURAL FRAMEWORK

A new tectonic map of Asia and the Far East, based on the "plate" concepts of global tectonics is currently being prepared. No attempt has been made to make use of these concepts in preparing the present map and the structural framework adopted for the description of the area is still based on the older concepts. The so-called "faults" shown on the map may be dip-slip or strike-slip faults, or only undefined "fracture zones" or "lineations" based on morphological evidence.

TERTIARY BASINS

To facilitate the use of this map for preparing the offshore part of the ECAFE Oil

and Natural Gas Map, an attempt has been made to draw contours on the base of the Tertiary plus Quaternary sequence at zero metres, 1,000 metres and 3,000 metres below sea level, without differentiating the areas covered only by a few hundred metres of alluvium, except in the area of the lower Mekong River, where knobs of older formations (granites, Permian limestone or pre-Hercynian metamorphic rocks) protrude through a very thin cover of alluvium; this allows the delineation of a basin in the lowermost part of the delta, in which Tertiary sediments might well be developed.

Very little is known concerning the age and facies of the Tertiary basins defined on this map. They are probably filled with Neogene sediments, mostly marine or deltaic. In the more isolated basins, such as the Yellow Sea and the Gulf of Thailand, subcontinental facies may be developed. Paleogene sediments are known in several basins.

PRE-TERTIARY BASINS

It has become evident that unmetamorphosed pre-Tertiary sediments are present in several basins of eastern Asia. Their existence may explain some discrepancies between magnetic and seismic results. Pre-Tertiary sedimentary sequences around the Australian shield are not metamorphosed or intruded by igneous rocks and they have good prospects for oil and gas (Cretaceous gas in Papua, Permo-Triassic gas on the Sahul Shelf, possible Mesozoic oil on Ceram and in the Vogelkop area).

On the Sunda Shelf, however, plugs of acid or intermediate composition are known to have intruded even the youngest parts of the Mesozoic sequence. The date of intrusion of these plugs is an important problem of the geology of the area which, as yet, has only been partly solved. Even though the main events took place during or immediately after the Hercynian orogeny, it becomes increasingly evident that renewals of intrusive activity occurred at intervals throughout Mesozoic time and particularly near the end of Cretaceous time.

In the areas where the Mesozoic is not intruded by igneous plugs—and these areas may be quite extensive —, the Mesozoic sediments do not give rise to magnetic anomalies, and they cannot be differentiated from the overlying Tertiary sediments. Most probably, the first marker to be identified by seismic refraction would be the Permian limestone, or the metamorphic rocks of Devonian and Carboniferous age. This may happen in the Gulf of Kuantan and in the Mekong delta.

The prospects of the pre-Tertiary rocks of northern Borneo have never been evaluated, but they may form a part of the sedimentary section inferred from airborne magnetometer surveys. In the Philippines, to the north of Palawan Island and on the Cuyo Shelf, a well developed Jurassic flysch, probably covered to the northeast by the Cretaceous of southwestern Mindoro which does not give rise to any magnetic anomaly, has been identified as a basin by the Project MAGNET survey of Region III of the Philippines, but the Tertiary is probably absent over most of this area.

OIL AND GAS PROSPECTS

Little can be added to the economic developments reported in the article accom-

panying the first edition of the map (CCOP Tech. Bull., vol. 3, Article V). The results of exploration on the Sunda Shelf, off West Malaysia, East Malaysia, Sumatra, Java and eastern Kalimantan are only partially known and few details have been released. Several oil discoveries have been made to the north of Java, and another, probably of major importance, has been reported to the east of Kalimantan.

ACKNOWLEDGMENTS

The revised map has been discussed with Prof. K.F.G. Hosking of the University of Malaya, Dr. Johannas of the Geological Survey of Indonesia, Mr. Pulunggono of the State Oil Company Pertamina, Prof. J. Katili of the Indonesian Institute of Sciences, Mr. Felipe Francisco and Mr. Juanito Fernandez of the Bureau of Mines of the Philippines, and Dr. C. Y. Meng of the Chinese Petroleum Corporation, to all of whom thanks are due for their suggestions.

Blank page

Page blanche

CORRECTION TO PAPER BY TUNYOW HUANG, "FORAMINIFERAL TRENDS IN THE SURFACE SEDIMENTS OF TAIWAN STRAIT"

Tunyow Huang
Chinese Petroleum Corporation, Miaoli, Taiwan, China
and National Taiwan University, Taipei, Taiwan, China

In title, page 23 of CCOP Technical Bulletin, Volume 4, THE SERFACE SEDIMENTS should read THE SURFACE SEDIMENTS.

Figure II-1, page 25 should be interchanged with Figure II-35, page 53, but the captions of these pages are correct.

Figure II-12, page 37 should be interchanged with Figure II-17, page 42, but the captions on these pages are correct.

Figure II-22, page 45 is upside down.

Blank page

Page blanche

CONTENTS OF TECHNICAL BULLETINS, VOLUMES 1 ~ 5

TECHNICAL BULLETIN, volume 1, issued June 1968

CONTENTS

TECHNICAL BULLETIN, volume 2, issued May 1969

CONTENTS

TECHNICAL BULLETIN, volume 3, issued May 1970

CONTENTS

TECHNICAL BULLETIN, volume 4, issued June 1971

CONTENTS

TECHNICAL BULLETIN, volume 5, issued June 1972

(Special volume—Detrital Heavy Minerals)

CONTENTS

Blank page

Page blanche

SUGGESTIONS FOR CONTRIBUTORS TO THE CCOP TECHNICAL BULLETINS

Language: Every paper must be written in English.

Title and Author's affiliation: Titles of papers should be carefully phrased to include only the key words. Example for style:

STRATIGRAPHY AND PETROLEUM PROSPECTS
OF KOREA STRAIT AND THE EAST CHINA SEA

By
K. O. Emery
Woods Hole Oceanographic Institution, Woods Hole, Massachusetts, U.S.A.
and Hiroshi Niino
Tokyo University of Fisheries, Tokyo, Japan

If the authors wish, the following style is also acceptable:

REPORT ON THE SEISMIC REFRACTION SURVEY
ON LAND IN THE WESTERN PART OF TAIWAN,
REPUBLIC OF CHINA

By
K. Sato[1], C. Y. Meng[2], J. Suyama[1], S. Kurihara[3]
S. Kamata[1], H. Obayashi[3], E. Inouye[1], and P. T. Hsiao[2]

(foot note)
1: Geological Survey of Japan, Kawasaki, Japan
2: Chinese Petroleum Corporation, Miaoli, China
3: Ube Industries Ltd., Ube, Japan

Unit of measurements: Use of the metric system is highly desirable.

Abstract: Every paper must have an English abstract. The abstract should, in a single paragraph, state the nature of the investigation and summarize the important conclusions. It should be suitable for separate publication and be adequate for indexing purposes. It should not be in the form of a list of contents and no references should be cited in it.

In addition, an abstract written in the author's native language or in the official language of the country is also acceptable. It will be printed at the end of the paper unless the author requests otherwise, with an appropriate reason.

Footnotes: Because text footnotes are distracting and generally unnecessary, this type of information should be incorporated in the text wherever possible.

Tables: Tables must be numbered in the order of their text citations. The column headings should be arranged so that their relation to the data is clear. The caption should be placed at the head of the table and should be concise and fully explanatory.

Illustrations: All illustrations must be cited in the text. All pertinent explanations should be given in the caption and not on the figure. The caption should be placed at the foot of the figure and should be concise and fully explanatory of the contents of the figure. Coloured illustrations are acceptable only if they are essential.

The illustrations submitted to the editor must be either original drawings or sharply focused glossy prints. The smallest letters or symbols in the printed illustration, after reduction where necessary, should be at least 1 mm, but preferably 1.5 mm.

A graphic scale, preferably in kilometers, must be shown on all maps and it is advisable that at least two meridians and two parallels of latitude are shown and identified.

If it is necessary to subdivide figures into parts, each part must be clearly identified and a brief title should accompany each figure or each part of a figure.

References: A complete and accurate list of references is of major importance. Text citations in the Bulletin are by the author's name and year of publication, e.g.: (Menard, 1964). If the author's name is part of the text, only the year is bracketed: Menard (1964). In a citation to a publication by three or more authors, *et al.* should be substituted for the names of the co-authors if no confusion will result. Two or more publications by the same author in the same year are distinguished by *a*, *b*, etc., after the year. Names of journals should either be written out in full or be abbreviated as shown in samples below.

References to abstracts only should be indicated by placing "abstract" in parentheses following the title. A parenthetical notation of the language of publication is also required after a translated title. If a translated version of a foreign journal was used, "English Transl." should appear after the journal name. For government, company and laboratory reports, the sponsoring agency or the place where the report may be obtained should be included.

Personal communications and unpublished data are not included in the reference list. Such information may be cited in the text within parentheses.

The references should be listed, without numbers, alphabetically by author's names. Examples:

Emery, K. O., 1968, Relict sediments on continental shelves of the world: *Bull. Amer. Assoc. Petroleum Geologists*, vol. 52, p. 445–464.

Geological Survey of Japan, 1964, Geological Map of Japan: Scale 1 : 2,000,000, one sheet.

Menard, H. W., 1964, *Marine geology of Pacific*: McGraw-Hill, New York, U.S.A., 271 pp.

Meng, C. Y., 1968, Geologic concepts relating to the petroleum prospects of Taiwan Strait: United Nations ECAFE, *CCOP Tech. Bull.*, vol. 1, p. 143–153.

Murauchi, S., and H. Hotta, 1968, Studies of the continental slope off the Sanriku Coast by seismic profiler survey (in Japanese): *Natl. Sci. Musium. Mem.*, no. 1, p. 37–40.

———*et al.*, 1968, Crustal structure of the Philippine Sea: *Jour. Geophys. Research*, vol. 73, p. 3143–3171.

Review and submission of paper: It is recommended that the author should have his paper reviewed critically by his colleagues for scientific accuracy, presentation, and correct use of English before it is submitted to the editor. The paper should be submitted to the designated editor-in-chief at the Geological Survey of Japan. Papers may be accepted at any time. However, the dead-line date for submission of papers for a regular volume will be decided at the preceding session of CCOP.

Reprints: Reprints of articles will be available on request from the author, at the author's expense. The author must inform the editor of the number of reprints required and the address to which the account should be forwarded for payment.

PREPARING ILLUSTRATIONS FOR REPRODUCTION

In the course of editing Volume 6, it was found that illustrations submitted by several contributors were not adequate for reproduction and some of them had to be redrafted. On the other hand, increasing number of articles contributed to one volume has exerted pressure on the editorial staff in completing the printing in a limited period. In view of this, the contributors to future volumes are requested to pay attention to the following notes in addition to "SUGGESTION FOR CONTRIBUTORS" enumerated in the preceding pages.

Printed illustrations should be smaller than 14 cm × 20 cm including the space for caption. These dimensions and the fact that reduction at a scale of one half to two-thirds is most appropriate, should be kept in mind when the drawings are planned. Thickness of lines, and size of letters and symbols should be carefully determined taking the printed dimensions into account.

Larger illustrations inserted between text pages or occupying two facing pages are not acceptable in principle.

Original figures drafted or printed on transparent plastic sheets are preferable in order to avoid damages during transport.

Editor-in-Chief

Annexed 1 Map (Figure VII–3)
to
AEROMAGNETIC SURVEY OF THE PALAWAN-SULU
OFFSHORE AREA OF THE PHILIPPINES
By
W. Bosum, J. C. Fernandez, E. G. Kind and C. F. Teodoro
Bundesanstalt für Bodenforschung
and Bureau of Mines, Philippines

Map XI–1
TERTIARY BASINS OF EASTERN ASIA
AND THEIR OFFSHORE EXTENSIONS
(Revised, April 1971)
By
M. Mainguy
ELF-R. E.